

Investigation of the Groundwater Hydrogeochemistry Characteristics in Beaufort West, South Africa

Ligavha-Mbelengwa Lufuno

Submitted in fulfilment of the requirements in respect of the
Master's Degree qualification

Master of Science (Geohydrology)

at the
Institute for Groundwater Studies
in the
Faculty of Natural and Agricultural Sciences
at the
University of the Free State

Supervisor: Dr Modreck Gomo

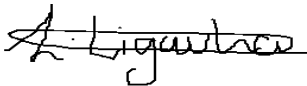
January 2017

Declaration

I, Ligavha-Mbelengwa Lufuno, declare that the master's degree dissertation that I herewith submit for the Master's Degree qualification *Master of Science (Geohydrology)* at the University of the Free State is my independent work, and that I have not previously submitted it for a qualification at another institution of higher education.

I, Ligavha-Mbelengwa Lufuno, hereby declare that I am aware that the copyright is vested in the University of the Free State.

I, Ligavha-Mbelengwa Lufuno, hereby declare that all royalties as regards intellectual property that was developed during the course of and/or in connection with the study at the University of the Free State will accrue to the University.



.....

Ligavha-Mbelengwa Lufuno

January 2017

Acknowledgements

I would like to express my sincere gratitude to my academic supervisor, Dr Gomo M, for his academic guidance, support and motivation in the completion of this study.

Special thanks also go to the Council for Geoscience colleagues (Dr Malumbazo N, Muvhuso Musetsho, Kate Robey, Bantu Hanise, Thato Kgari, Khayaletu Madikizela and Connie Setladi) for providing me with an opportunity to work with them. Their assistance, support, guidance and encouragement throughout the completion of this study are highly appreciated. Again, I would like to thank them for providing me with the best training during the field visits for sample collection.

My gratitude is also extended to Mr Koorzen J, my technical field assistant, and the Beaufort West Municipality staff, for going an extra mile to assist me whenever I needed them.

I would also like to send many thanks to Prof Van Heerden E, Dr Erasmus M, Jou-An Chen, Chris Van Vuuren and Elizabeth Ojo for their great training in the field and laboratory, and their assistance and support towards the completion of this study. The opportunity they granted me to work with them and to use their equipment, both in the field and laboratory, is highly appreciated.

Special thanks are also extended to my parents, Mr MH and Mrs MM Ligavha-Mbelengwa, who always encouraged me to persevere and carry on whenever I called them to complain; their support was great. This goes without forgetting my best friend Dominic Komape who played a major role in encouraging, supporting and assisting me throughout this study. His input is greatly valued. I would also like to thank my siblings Mutshinyani and Maanda Ligavha-Mbelengwa for always acting quicker whenever I needed their assistance with a laptop and mouse, which they never hesitated to lend me at any time.

Many thanks also to my friends for their support and encouragement. I would also like to thank everyone else who believed in me.

Last but not least; I would like to thank the Almighty God for guiding me throughout conducting this research. It is through His help and guidance that I've reached where I am today.

Abstract

This study was conducted to investigate hydrogeochemical processes controlling the evolution of groundwater chemistry and their influence on water quality in the Beaufort West town. Beaufort West is located in a dry and arid part of South Africa and thus groundwater is an important source of water for the town. The study further assessed the quality of the groundwater to determine its suitability for domestic and agricultural uses. Groundwater sampling was done for three seasons (spring, summer and autumn). Twenty samples were collected for both spring and summer seasons, whereas twelve samples were collected for autumn. Identification of the hydrogeochemical processes controlling the evolution of the groundwater quality and chemistry was done using various complementary tools. These tools are: classification of the main water types, evaluation of water-rock interaction by means of stoichiometry analysis and bivariate correlation plots, inverse geochemical modelling and statistical analysis (hierarchical cluster analysis and principal component analysis).

The main water types that were found at the area are calcium bicarbonate, sodium chloride and mixed water. Similar hydrogeochemical processes were found to be occurring in the groundwater system for different seasons. However, certain processes were dominating specific areas, whereas others were happening randomly at different areas. The main hydrogeochemical processes that were inferred to be influencing the groundwater chemistry and quality are ion exchange, reverse ion exchange, silicate weathering, carbonate dissolution, gypsum dissolution, and to some extent evaporation. Other processes that took place though were not dominant, are dissolution of halite and sylvite. Anthropogenic sources releasing nitrate and ammonia to the groundwater were also identified to play a role in negatively impacting the groundwater quality.

Assessment of the groundwater quality showed that the water is suitable for irrigation purposes, although some of the water samples should be used only to crops less sensitive to salt load. Furthermore, not all the samples were recommended for drinking water. Only water samples that showed hydrogeochemical characteristics of recent recharge were suitable for drinking. Conversely, all the samples were suitable for use by livestock. The calculated total hardness showed that the water at this area was hard to very hard. The findings of this study indicated the importance of hydrogeochemical processes in changing the water chemistry and quality from good to poor along the flow paths. The study also demonstrated the value of utilising various assessment tools as complementary techniques to improve the understanding of hydrogeochemical processes, and its influence on evolution of groundwater chemistry and quality.

Keywords: Geochemical modelling, Groundwater chemistry, Groundwater-rock interaction, Groundwater quality, Hydrogeochemical processes, Principal component analysis, Water types.

Opsomming

Hierdie studie is uitgevoer om die hidrochemiese prosesse te ondersoek wat die evolusie van chemiese prosesse in grondwater beheer, en om die invloed daarvan op die kwaliteit van water in Beaufort-Wes te ondersoek. Beaufort-Wes is geleë in 'n dor en droë deel van Suid-Afrika en dus is grondwater 'n belangrike bron van water vir die dorp. Die studie is gedoen om die kwaliteit van die grondwater te evalueer om die geskiktheid van die grondwater vir huishoudelike en landbougebruik te bepaal. 'n Grondwatersteekproefneming is oor drie seisoene (lente, somer en herfs) gedoen. Twintig monsters is ingesamel vir beide die lente- en somerseisoene, terwyl twaalf monsters vir die herfsseisoen ingesamel is. Identifisering van die hidrochemiese prosesse wat die evolusie van die gehalte van grondwater en chemie beheer, is gedoen met behulp van verskeie aanvullende instrumente, naamlik klassifikasie van die belangrikste watertipes, evaluering van water:rots-interaksie deur middel van stoïgiometrie-ontleding en tweeveranderlike korrelasie 'plots', omgekeerde geochemiese modellering en statistiese ontleding (hiërargiese 'cluster'-analise en hoofkomponent-analise).

Die hooftipes water wat in die gebied gevind is, is kalsiumbikarbonaat, natriumchloried en gemengde water. Soortgelyke hidrochemiese prosesse is vir die verskillende seisoene in die grondwaterstelsel gevind. Sekere prosesse oorheers spesifieke gebiede, terwyl ander lukraak op verskillende gebiede gebeur. Die belangrikste hidrochemiese prosesse wat uit die grondwaterchemie en gehalte afgelei kon word, is ionuitruiling, omgekeerde ionuitruiling, silikaatverwering, karbonaatontbinding, gipsontbinding, en tot 'n mate verdamping. Ander prosesse wat plaasgevind het, al was dit nie dominant nie, is ontbinding van haliet en silvite. Antropogeniese bronne wat nitraat en ammoniak in die grondwater vrystel, is geïdentifiseer as bydraende faktore wat 'n negatiewe impak op die gehalte van grondwater het.

Assessering van die grondwatergehalte het getoon dat die water geskik is vir besproeiingsdoeleindes, hoewel sommige van die watermonsters slegs gebruik behoort te word op gewasse wat minder sensitief is vir soutladings. Nie al die monsters is aanbeveel vir drinkwater nie. Slegs watermonsters wat hidrochemiese eienskappe van onlangse herlaaide water getoon het, is as geskik beskou vir drinkwater. Aan die ander kant, al die monsters was geskik vir gebruik deur vee. Die berekende totale hardheid het getoon dat die water in hierdie gebied hard tot baie hard was. Die bevindinge van hierdie studie het aangedui hoe belangrik hidrochemiese prosesse in die verandering van die waterchemie en gehalte van goed na swak langs die vloeipaaie is. Die studie het ook die waarde van die gebruik van verskillende assesseringsinstrumente beklemtoon wat gebruik kan word as aanvullende tegnieke om die begrip van hidrochemiese prosesse te verbeter, en die invloed daarvan op die evolusie van grondwaterchemie en kwaliteit.

Slutelwoorde: Geochemiese Modellering, Grondwater chemie, Grondwater-rots interaksie, Gehalte grondwater, Hidrochemiese prosesse, Hoofkomponent-ontleding, Watertipes.

Table of Contents

Declaration	ii
Acknowledgements.....	iii
Abstract	iv
Opsomming	v
Table of Contents.....	vi
List of Figures	xi
List of Tables	xiii
List of Abbreviations and Acronyms.....	xv
List of Chemical Symbols	xvi
List of Units.....	xvii
Chapter 1 Introduction.....	1
1.1 Background	1
1.2 Research Aims and Objectives	3
1.2.1 Aims.....	3
1.2.2 Objectives	3
1.3 Outline of the Dissertation	3
Chapter 2 Literature Review	5
2.1 Introduction.....	5
2.2 Previous Groundwater Studies in Beaufort West	5
2.2.1 Hydrological properties	5
2.2.2 Hydrogeochemical analysis	7
2.2.2.1 Total dissolved solids, electrical conductivity and pH	7
2.2.2.2 Chemical characteristics.....	8
2.2.2.3 Groundwater types	10
2.2.2.4 Hydrogeochemical processes.....	11
2.2.2.5 Groundwater suitability for use	13
2.3 Hydrogeochemical Characterisation Tools.....	13
2.3.1 Stoichiometric analysis	13
2.3.1.1 Bivariate correlation plots.....	14
2.3.2 Hydrochemical facies plots	15
2.3.2.1 Piper diagrams.....	15
2.3.2.2 Expanded Durov diagrams	16
2.3.3 Multiple component plots	17
2.3.3.1 Stiff diagrams.....	17
2.3.3.2 Pie diagrams.....	18
2.3.3.3 Bar diagrams	19
2.3.4 Geochemical modelling.....	20

2.3.4.1	Inverse modelling.....	20
2.3.4.1.1	Speciation modelling.....	20
2.3.4.1.2	Mass-balance modelling.....	22
2.3.4.2	Forward modelling.....	23
2.3.4.2.1	Reaction-path modelling.....	23
2.3.4.2.2	Reaction-transport modelling.....	24
2.3.5	Statistical methods.....	25
2.3.5.1	Principal component analysis.....	25
2.3.5.2	Distribution analysis.....	26
2.3.5.2.1	Hierarchical cluster analysis.....	26
2.3.5.2.2	Histogram.....	27
2.3.5.2.3	Box and whisker plots.....	28
2.4	Conclusion.....	29
	Chapter 3 Study Area.....	30
3.1	Introduction.....	30
3.2	Site description.....	30
3.3	Climate.....	30
3.3.1	Rainfall.....	30
3.3.2	Temperature.....	33
3.3.3	Vegetation.....	33
3.4	General Geology.....	34
3.5	Hydrology.....	36
3.6	Groundwater Recharge.....	37
3.7	Elevation Maps.....	38
3.8	Water Levels and Flow Direction.....	42
3.9	Groundwater Uses.....	44
3.9.1	Borehole usage and depths.....	44
3.9.2	Current groundwater use.....	46
3.10	Conclusion.....	46
	Chapter 4 Methods and Materials.....	47
4.1	Introduction.....	47
4.2	Field Data Collection.....	47
4.2.1	Hydrocensus.....	47
4.2.2	Groundwater sampling.....	48
4.2.3	Sample storage and transport for chemical analysis.....	50
4.3	Laboratory Analysis.....	50
4.4	Data Quality and Reliability Check.....	50
4.5	Water Type Classification.....	50
4.6	Water-Rock Interaction.....	51
4.6.1	Stoichiometric analysis.....	51
4.6.2	Bivariate plots analysis.....	53
4.7	Geochemical Modelling.....	55

4.7.1	Mineral saturation indices	55
4.7.2	Mass-balance modelling	55
4.8	Statistical Analysis.....	56
4.8.1	Statistical characteristics.....	57
4.8.2	Hierarchical cluster analysis	57
4.8.3	Principal component analysis	57
4.9	Assessment of Groundwater Quality	58
4.9.1	Groundwater quality assessment for irrigation use	58
4.9.2	Groundwater quality assessment for domestic use	59
4.9.3	Groundwater quality assessment for livestock use	60
4.10	Conclusion.....	60
	Chapter 5 Results and Discussions	61
5.1	Introduction.....	61
5.2	Data analysis and quality checks	62
5.2.1	Ion balance error	62
5.3	Assessment of Water Types and Hydrogeochemical Processes	63
5.3.1	Groundwater chemistry data	64
5.3.1.1	Spring season.....	64
5.3.1.2	Summer season.....	66
5.3.1.3	Autumn season.....	67
5.3.2	Hydrochemical (water type) classification	68
5.3.2.1	Spring season.....	68
5.3.2.2	Summer season.....	69
5.3.2.3	Autumn season.....	71
5.3.2.4	Summary on hydrogeochemical (water type) classifications	72
5.3.3	Stiff Diagrams	72
5.4	Water-rock interaction	72
5.4.1	Stoichiometric analysis	72
5.4.1.1	Weathering	75
5.4.1.2	Carbonate weathering	75
5.4.1.3	Silicate weathering.....	76
5.4.1.4	Calcium and sulphate	77
5.4.1.5	Sodium and chloride	78
5.4.1.6	Silica	79
5.4.2	Analysis of the bivariate correlation plots.....	79
5.4.2.1	Calcium + magnesium versus bicarbonate.....	80
5.4.2.2	Calcium versus alkalinity	82
5.4.2.3	Calcium versus magnesium.....	83
5.4.2.4	Calcium versus sulphate.....	83
5.4.2.5	Calcium + magnesium-sulphate-bicarbonate versus sodium + potassium-chloride	84

5.4.2.6	Pottasium versus chlorine.....	85
5.4.2.7	Calcium + magnesium versus bicarbonate + sulphate	86
5.4.2.8	Sodium versus chloride	87
5.4.2.9	Sodium/chlorine versus electrical conductivity.....	89
5.4.2.10	Summary on water-rock interaction	90
5.5	Hierarchical cluster analysis	91
5.5.1	Spring season	91
5.5.2	Summer season.....	93
5.5.3	Autumn season	94
5.5.4	Summary on cluster analysis	95
5.6	Geochemical modelling	96
5.6.1	Mineral saturation indices	96
5.6.1.1	Spring season.....	96
5.6.1.2	Summer season.....	98
5.6.1.3	Autumn season.....	99
5.6.1.4	Summary on saturation indices.....	99
5.6.2	Mass-balance modelling	100
5.6.2.1	Mole transfer between Period 1 (spring to summer) and Period 2 (summer to autumn).....	100
5.6.2.1.1	Evolution from Solution 1 (spring) to Solution 2 (B55H).....	101
5.6.2.1.2	Evolution from Solution 1 (B55H) to Solution 2 (B10H)	102
5.6.2.1.3	Evolution from Solution 1 (B10H) to Solution 2 (B58H)	104
5.6.2.1.4	Evolution from Solution 1 (B58H) to Solution 2 (B25H)	105
5.6.2.1.5	Evolution from Solution 1 (B25H) to Solution 2 (B22H)	106
5.6.2.2	Summary on inverse geochemical modelling	107
5.7	Statistical analysis	108
5.7.1	Statistical data summary	108
5.7.1.1	Spring season.....	108
5.7.1.2	Summer season.....	109
5.7.1.3	Autumn season.....	110
5.7.2	Principal component analysis	111
5.7.2.1	Spring season.....	111
5.7.2.2	Summer season.....	114
5.7.2.3	Autumn season.....	117
5.7.2.4	Summary on statistical analysis.....	119
5.8	Groundwater Quality Assessment.....	120
5.8.1	Groundwater suitability for irrigation purposes.....	120
5.8.1.1	Sodium adsorption ratio	122
5.8.1.2	Total salinity	125
5.8.1.3	Residual sodium carbonate	126
5.8.1.4	Sodium percentage.....	126
5.8.1.5	Magnesium hazard	127
5.8.2	Groundwater suitability for domestic purposes	127

5.8.2.1	pH	129
5.8.2.2	Total dissolved solids	130
5.8.2.3	Total hardness	131
5.8.2.4	Sodium.....	132
5.8.2.5	Potassium	133
5.8.2.6	Bicarbonate.....	133
5.8.2.7	Chloride	133
5.8.2.8	Sulphate.....	133
5.8.2.9	Nitrate	134
5.8.2.10	Ammonia.....	135
5.8.2.11	Fluoride.....	135
5.8.2.12	Iron.....	136
5.8.2.13	Manganese	136
5.8.3	Groundwater suitability for use by livestock	136
5.9	Conclusion.....	137
Chapter 6 Conclusions and Recommendations		138
6.1	Conclusions.....	138
6.1.1	Main water types	138
6.1.2	Main hydrogeochemical processes and their influence on groundwater chemistry	138
6.1.3	Anthropogenic sources	140
6.1.4	Seasonal variations.....	140
6.1.5	Groundwater quality characteristics	141
6.2	Recommendations	142
References		143
Appendix 1 Hydrochemical Classification (Stiff Diagrams)		154
Appendix 2 Water-Rock Interaction Calculations		156
Appendix 3 Bivariate Correlation Plots		159
Appendix 4 Mineral Saturation Indices		161

List of Figures

Figure 1.1:	A map indicating South African provinces and the study area which is Beaufort West.....	2
Figure 2.1:	Water quality variation as indicated by electrical conductivity in the Gouritz water management area.....	8
Figure 2.2:	Expanded Durov diagram example.....	16
Figure 2.3:	Pie chat example.....	18
Figure 2.4:	Bar diagram example.....	19
Figure 3.1:	Gouritz water management area map showing different catchments and their respective Quaternary catchments.....	31
Figure 3.2:	Rainfall map of part of the Western Cape Province indicating the mean annual rainfall in millimetre.....	32
Figure 3.3:	Graph indicating the average rainfall for Beaufort West area in months.....	32
Figure 3.4:	Temperature variation along the Beaufort West region throughout the year showing minimum, average and maximum temperatures for every month.....	33
Figure 3.5:	Geology of the Gouritz water management area, Western Cape.....	35
Figure 3.6:	Aquifer types of the Gouritz water management area and their yielding capacities.....	37
Figure 3.7:	Gouritz water management area recharge map for Quaternary catchments and variations in their recharge.....	38
Figure 3.8:	Elevation contour map around the study area.....	40
Figure 3.9:	Cross sections for the study area with lines cutting through the contour maps showing the variations in elevation.....	41
Figure 3.10:	A three-dimensional map showing how boreholes are sited with respect to the surface elevation.....	42
Figure 3.11:	A graph showing elevation and hydraulic heads for some of the boreholes in Quaternary catchment J21A for the data that was collected in summer 2016.....	44
Figure 4.1:	Field pictures showing an overview of some sites visited as well as the sampling methods used.....	49
Figure 5.1:	A Google Earth map displaying the distribution of the boreholes at the study area.....	63
Figure 5.2:	Piper diagram showing water types for spring results as plotted for 18 samples.....	68
Figure 5.3:	Piper diagram showing water types for summer results as plotted for 20 samples.....	70
Figure 5.4:	Piper diagram showing water types for autumn results as plotted for 9 samples.....	71
Figure 5.5:	Linear correlation plots for calcium versus alkalinity for spring (A), summer (B) and autumn (C) seasons.....	82

Figure 5.6:	Linear correlation plots for calcium versus sulphate for spring (A), summer (B) and autumn (C).....	84
Figure 5.7:	Linear correlation plot for calcium + magnesium + sulphate + bicarbonate versus sodium + potassium - chlorine for spring (A), summer (B) and autumn (C)	85
Figure 5.8:	Linear correlation plots for calcium + magnesium versus bicarbonate + sulphate for spring (A), summer (B) and autumn (C) seasons.....	86
Figure 5.9:	Linear correlation plot for sodium versus chlorine for spring (A), summer (B) and autumn (C).....	88
Figure 5.10:	Scatter plot of sodium/chlorine versus electrical conductivity for spring (A), summer (B) and autumn (C)	90
Figure 5.11:	Dendrogram indicating the relationship between water samples in groups for spring data.....	92
Figure 5.12:	Dendrogram indicating the relationship between water samples in groups for summer data.....	93
Figure 5.13:	Dendrogram indicating the relationship between water samples in groups for autumn data	95
Figure 5.14:	Google Earth map displaying the selection of the flow paths considered for mass transfer.....	101
Figure 5.15:	Component plot in rotated space for component loadings of spring season .	112
Figure 5.16:	Component plot in rotated space for component loadings of summer season	116
Figure 5.17:	Component plot in rotated space for component loadings of autumn season	118
Figure 5.18:	Beaufort West indicating the activities and facilities around town.....	120
Figure 5.19:	SAR diagrams classifying water for irrigation purposes for spring (A), summer (B) and autumn (C)	124

List of Tables

Table 2.1:	General hydrochemistry for the Central Karoo aquifers.....	9
Table 3.1:	Geographic coordinates of the boreholes measured in metre above mean sea level.....	39
Table 3.2:	Static water level, elevations and hydraulic heads for 20 boreholes from the summer season.....	43
Table 3.3:	Site names and their respective depths in metre below ground level	45
Table 5.1:	Ion balance error for spring, summer and autumn seasons.....	62
Table 5.2:	Major ions and other important parameters displayed with electrical conductivity for spring results.....	64
Table 5.3:	Major ions and other important parameters displayed with electrical conductivity for summer results.....	66
Table 5.4:	Major ions and other important parameters displayed with electrical conductivity for autumn results.....	67
Table 5.5:	Major ions, silica, total dissolved solids and electrical conductivity for spring results.....	73
Table 5.6:	Major ions, silica, total dissolved solids and electrical conductivity for summer results.....	74
Table 5.7:	Major ions, silica, total dissolved solids and electrical conductivity for autumn results.....	75
Table 5.8:	Guildford's rule of thumb showing variation in correlation coefficients	79
Table 5.9:	Correlation coefficients for the bivariate plots for spring, summer and autumn seasons	80
Table 5.10:	Saturation indices for all the boreholes in the spring season.....	97
Table 5.11:	Inverse modelling results obtained from PHREEQC showing the mole transfer from one water type to the next (springtoB55H)	102
Table 5.12:	Inverse modelling results obtained from PHREEQC showing the mole transfer from one water type to the next (B55H to B10H)	103
Table 5.13:	Inverse modelling results obtained from PHREEQC showing the mole transfer from one water type to the next (B10H to B58H)	104
Table 5.14:	Inverse modelling results obtained from PHREEQC showing the mole transfer from one water type to the next (B58H to B25H)	105
Table 5.15:	Inverse modelling results obtained from PHREEQC, showing the mole transfer from one water type to the next (B25H to B22H)	107
Table 5.16:	Hydrochemical parameters indicating statistical characteristics as calculated for spring season samples	109

Table 5.17:	Hydrochemical parameters indicating statistical characteristics as calculated for the summer season samples	110
Table 5.18:	Hydrochemical parameters indicating statistical characteristics as calculated for the autumn season samples	110
Table 5.19:	Principal component analysis results after Varimax rotation as generated for spring	111
Table 5.20:	Principal component analysis results after Varimax rotation as generated for summer	115
Table 5.21:	Principal component analysis results after Varimax rotation as generated for autumn	117
Table 5.22:	Criteria for testing the suitability of water for irrigation purposes as applied over three seasons	121
Table 5.23:	Groundwater classification for irrigation purposes by following the different criteria	122
Table 5.24:	Standards as described in the South African National Standards (SANS) and World Health Organization (WHO)	128
Table 5.25:	Depth, calculated total hardness for all seasons, as well as the average of fluoride, ammonia, iron and manganese for each borehole	129
Table 5.26:	Water quality description for total dissolved solids as well as the samples that fall under the respective categories	130
Table 5.27:	Hardness of water expressed as calcium carbonate	132
Table 5.28:	Parameters and their respective range for suitability for livestock watering ..	137

List of Abbreviations and Acronyms

DEADP	Department of Environmental Affairs and Development Planning
DO	Dissolved Oxygen
DOC	Dissolved Organic Carbon
DWS	Department of Water Affairs and Sanitation
EC	Electrical Conductivity
EPA	Environmental Protection Agency
GPS	Global Positioning System
HCA	Hierarchical Cluster Analysis
IBE	Ion Balance Error
IWRM	Integrated Water Resource Management
K_{sp}	Solubility product
log IAP	log of the ion activity product
log K_T	log of the solubility constant
ORP	Oxidation-Reduction Potential
PCA	Principal Component Analysis
pe	Reduction potential
pH	Power of hydrogen
PHREEQC	pH Reaction Equilibrium Calculation
r	Correlation coefficient
RSC	Residual Sodium Carbonate
SANS	South African National Standards
SAR	Sodium Adsorption Ratio
SAWQG	South African Water Quality Guidelines
SI	Saturation Indices
TDS	Total Dissolved Solids
TH	Total Hardness
TLC	Temperature Level Conductivity metre probe
WHO	World Health Organisation
WISH	Windows Interpretation System for Hydrologists
WMA	Water Management Area

List of Chemical Symbols

Al	Aluminium
Ca	Calcium
CaCl ₂	Calcium chloride
CaHCO ₃	Calcium bicarbonate
CaSO ₄	Calcium sulphate
Cl	Chlorine
F	Fluoride
Fe	Iron
HCO ₃	Bicarbonate
K	Potassium
meq/l	Milliequivalents per litre
Mg	Magnesium
Mn	Manganese
Na	Sodium
NaCl	Sodium chloride
NaHCO ₃	Sodium bicarbonate
NaSO ₄	Sodium sulphate
NH ₃	Ammonia
NO ₃	Nitrate
NO ₃ -N	Nitrate as nitrogen
Si	Silicon
SiO ₂	Silica
SO ₄	Sulphate

List of Units

d	days
km	kilometre
l/s	litre per second
m	metre
m ² /d	square metre per day
mamsl	metre above mean sea level
mbgl	metre below ground level
mmol/l	millimole per litre
meq/l	milliequivalents per litre
mg/l	milligram per litre
mm/a	millimetre per annum
Mm ³	cubic mega meter
m/s	metres per second
mS/m	millisiemens per metre
s	seconds
µg/l	microgram per litre

Chapter 1

Introduction

1.1 Background

Groundwater chemistry and quality is generally altered by natural and anthropogenic factors. These factors make groundwater not always safe to drink since its quality can change from good to poor water that is sometimes unsuitable for certain uses. Naturally, groundwater quality is mainly influenced by processes such as water-rock interaction, anthropogenic sources and the geochemical reactions that take place along the flow path as the water moves from recharge to discharge areas (Chidambaram *et al.*, 2013; Van Camp and Walraevens, 2008). These hydrogeochemical processes may therefore result to different groundwater types within the same aquifer, depending on the most dominant processes along the flow path.

As a result of different aquifer mineralogy, geochemistry, recharge variations, differences in flow paths and the nature of the aquifer; the hydrogeochemical properties in two areas will rarely be the same (Van Camp and Walraevens, 2008). Although the majority of the aquifers may indicate the occurrence of various hydrogeochemical processes at the same time, they take place at different rates and environments resulting in a change in groundwater quality.

It was therefore important to conduct this research in order to understand the hydrogeochemical processes that control the evolution of groundwater chemistry and its quality in Beaufort West. Accordingly, groundwater is an important resource and knowledge on its quality is thus vital. The study also assessed the evolution of groundwater chemistry and quality from one season to another. The seasonal changes of the groundwater chemistry may be influenced by recharge variations. Recharge can lead to dilution of the groundwater, whereas less recharge can result in the increase of dissolved salts through processes such as dissolution and evaporation.

Beaufort West is located in the Western Cape Province of South Africa (Figure 1.1). The quaternary catchment is characterised by semi-arid conditions.

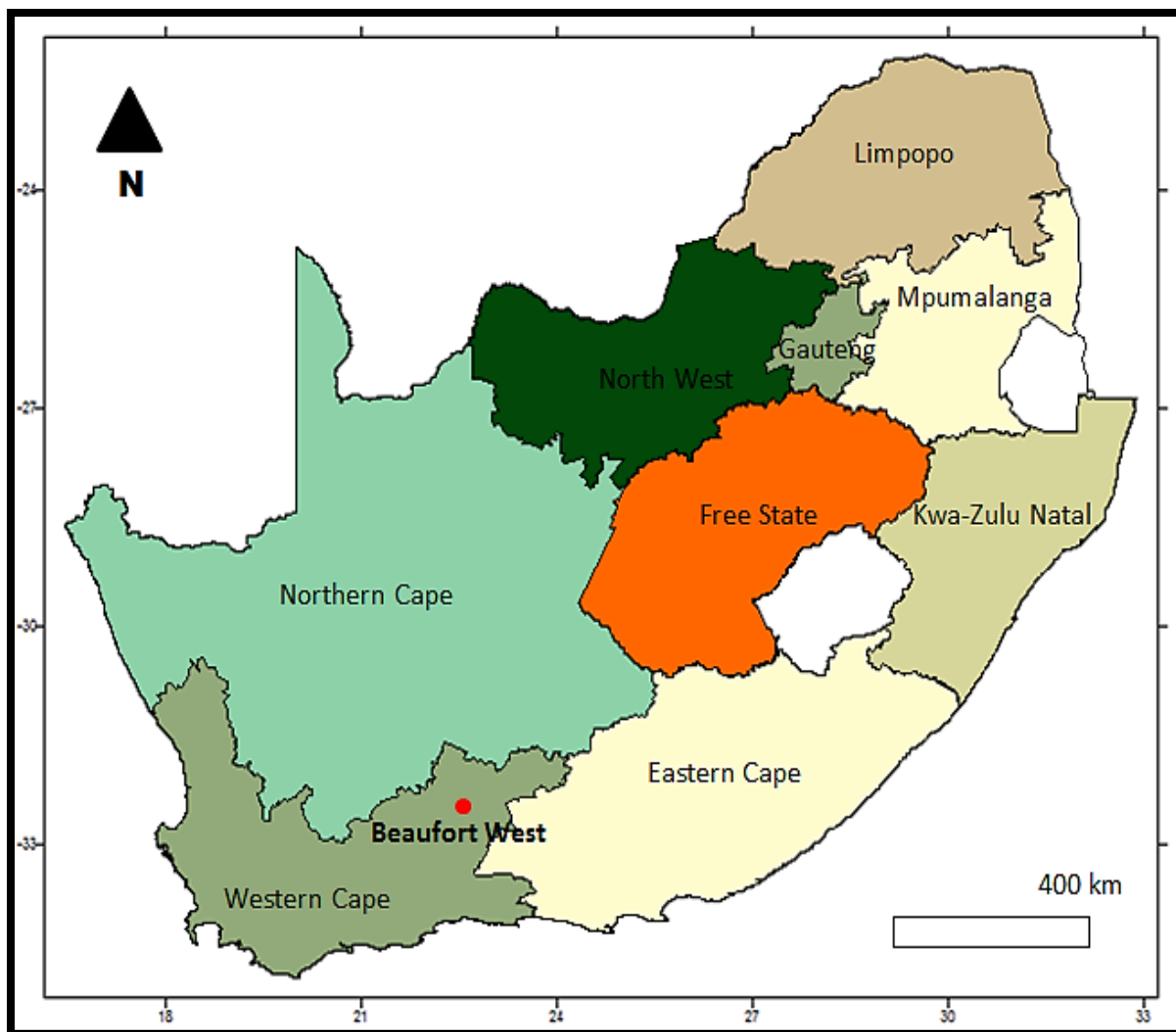


Figure 1.1: A map indicating South African provinces and the study area which is Beaufort West

Studies to investigate various aspects of groundwater resources have been previously conducted in Beaufort West. These studies include investigation of groundwater resource occurrence (Pike, 1948; Campbell, 1980); hydrochemistry (Adams *et al.*, 2001); groundwater resource development (Rose and Conrad 2007); contamination (Gomo 2009) and mass-transport properties (Van Wyk and Witthueser, 2011). While these studies have improved the knowledge about groundwater resources in Beaufort West, limited emphasis had been placed on comprehensive investigation of the hydrogeochemical processes and its influence on the groundwater chemistry and resultant quality. This was noted throughout the literature review of the above-mentioned studies which led to an interest towards researching about this aspect. Additionally, less research on the usage of various tools to identify the hydrogeochemical processes has been done. The use of various techniques at the same time is an advantage since one tool has its own strengths and limitations.

As part of this study, a comprehensive hydrocensus was initially conducted to identify potential groundwater sampling boreholes. Groundwater sampling was then conducted for three seasons (spring, summer and autumn). To identify and describe the hydrogeochemical processes controlling the groundwater chemistry evolution and its quality, a variety of complementary tools were used to analyse and interpret the data collected during the three seasons. The approaches that were used included; characterisation of the ions, description of the main water types and source rocks using Piper and Stiff diagrams, respectively. Additionally, evaluation of water-rock interaction was done by means of a stoichiometry analysis and bivariate correlation plots; inverse geochemical modelling and statistical analysis were also used.

1.2 Research Aims and Objectives

1.2.1 Aims

- ❖ To understand the main hydrogeochemical processes and their influence on the evolution of groundwater chemistry and quality.
- ❖ To assess groundwater quality to determine its suitability for use.

1.2.2 Objectives

- ❖ To conduct a literature review to provide background understanding.
- ❖ To conduct a hydrocensus to identify the groundwater sampling boreholes.
- ❖ To collect the groundwater samples.
- ❖ To analyse the samples for the inorganic chemistry at the laboratory.
- ❖ To use the complementary tools to determine the main hydrogeochemical processes and assessing the groundwater quality.

1.3 Outline of the Dissertation

Chapter 1 introduces the research topic giving the background, research aims and objectives.

Chapter 2 reviews the literature by explaining the findings from previous conducted studies and characterising the hydrogeochemical tools.

Chapter 3 describes the study area.

Chapter 4 provides the methodology followed throughout conducting the research.

Chapter 5 presents the results and discusses the main findings from the results obtained.

Chapter 6 concludes the entire study with the main findings being mentioned and also provides recommendations to what other researchers can do to improve the findings.

Chapter 2

Literature Review

2.1 Introduction

Chapter 2 focuses on discussing various groundwater studies that were previously conducted by different researchers in the Beaufort West area. This chapter is therefore divided into two sections: the first section reviews previous groundwater studies at Beaufort West and expands to look at the hydrological properties and hydrogeochemical analysis (groundwater parameters, water types, hydrogeochemical processes) based on the studies that were conducted in this area. The chapter further characterises various complementary hydrogeochemical tools that were used to analyse and interpret the groundwater data that was collected.

2.2 Previous Groundwater Studies in Beaufort West

Various studies have been conducted in the Beaufort West area, as well as in the entire Karoo basin on different aspects; however, only the findings linked to the hydrology, geology and hydrogeochemistry investigations are discussed in this section. The reason for considering only these fields is because they are closely related to research theme of the current investigation.

The oldest studies that were done on groundwater at Beaufort West were performed by Pike (1948) as cited by Campbell (1980); however, the main investigation on the conditions of groundwater in this area was carried out in 1959 where the geophysics of the area was also included. Most of the early studies as indicated by Campbell (1980) focused mainly on the north and north-east of Beaufort West town.

2.2.1 Hydrological properties

The study conducted by Campbell (1980) stated that the aquifers at Beaufort West town and the surrounding areas are semi-confined and unconfined. Furthermore, Woodford and Chevalier (2002) as well as Van Wyk and Witthueser (2011) indicated that Beaufort West is covered mostly by fractured rock aquifers. However, a combination of fractured and intergranular rock aquifers is also present due to alluvial processes and deeply weathered Beaufort sediments overlying the young Karoo sediments.

Around the period between 1975 and 1977, a study on the transmissivities of Beaufort West boreholes (Quaternary catchments J21A and L11F) was conducted by Campbell (1980). The findings indicated that the transmissivities varied from 90 m²/d to 900 m²/d. Years later, Rose and Conrad (2007) also conducted a study on the borehole transmissivities and yields at boreholes mostly situated towards the north of Beaufort West town. Their results showed that the transmissivity values ranged between <10 m²/d and 400 m²/d at various areas. In the study that was conducted by Gomo (2009), the pump test results for the formation at Beaufort West town gave a transmissivity ranging between 3.4 m²/d and 15.4 m²/d. The variation in the transmissivities for these studies could be that although the studies were conducted in the same area, different boreholes were tested for transmissivity. Some of the boreholes tested could have been sited on fractured rock aquifers, whereas some were located on intergranular rock aquifers. Additionally, the period through which the borehole had been used since its drilling, could also have had a huge influence. Gomo (2009) stated that a certain borehole that had been abstracting groundwater since 2002 had a higher transmissivity compared to the newly drilled boreholes because this specific borehole was fully developed.

The study conducted by Rose and Conrad (2007) at Beaufort West further described that the borehole yields ranged between 2 l/s and 18 l/s. This disparity was observed at different areas. Dolerite dykes at this area had a huge impact on the borehole yields such that boreholes drilled closer to these structures displayed higher yields. Furthermore, fractured rock aquifers at the study area produced yields of about 5 l/s. There are also aquifers with dual porosities such that their yields were low (0.1-0.5 l/s) (Rose and Conrad, 2007; Van Wyk and Witthueser, 2011). Furthermore, the Karoo Groundwater Expert Group (2013) stated that aquifers in the eastern Karoo have high recharge and yields and their water quality is improved as compared to aquifers in the western Karoo. The higher aquifer characteristics such as the borehole yields at Beaufort West ensured that the aquifer could act as a future reliable source of water supply to the community of Beaufort West (Van Wyk and Witthueser, 2011).

The tracer tests that were performed in the fractured rock aquifer and the intergranular fractured rock aquifer at the north of Beaufort West showed that the flow of the groundwater follows various flow paths. Nevertheless, the main flow direction of the groundwater is from north to south (Van Wyk and Witthueser, 2011).

2.2.2 Hydrogeochemical analysis

2.2.2.1 Total dissolved solids, electrical conductivity and pH

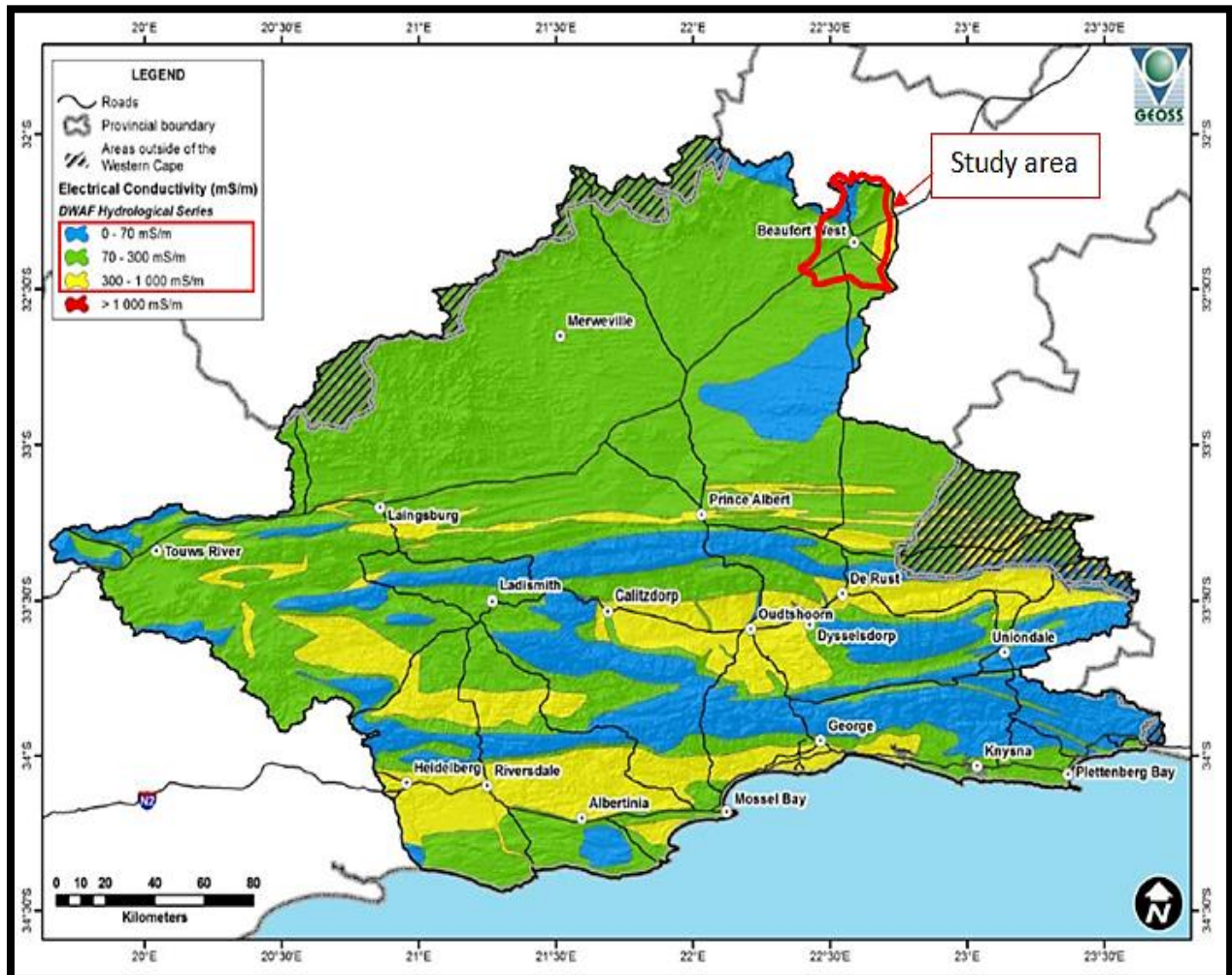
Studies on the general hydrochemistry of Beaufort West and the central Karoo at large have been conducted. The major part of the Karoo basin was classified to have total dissolved solids (TDS) ranging from 450 mg/l to 1 000 mg/l. Nonetheless, higher TDS could be measured in the southern and western basin due to less recharge and mixing of groundwater with connate water (Woodford and Chevalier, 2002). Additionally, a study based at the Brandwag farm (approximately 17 km north-east of Beaufort West town) as conducted by Campbell (1980), described twelve boreholes in this area. The TDS range for the boreholes was between 357 mg/l and 2 146 mg/l. The study carried out by Gomo (2009) indicated that the TDS values that were measured in the boreholes at the town ranged from 195.8 mg/l to 1 090.8 mg/l. The TDS as given by these authors indicated both fresh, less mineralised water and brackish, highly mineralised water.

The electrical conductivity (EC) measurements, on the other hand, were carried out by Campbell (1980) at Rhenosterkop farm (approximately 21 km north-east of Beaufort West town). The values ranged in depth with shallow aquifer levels (15-16 m) giving conductivities between 400 mS/m and 500 mS/m, whereas EC at >30 m depths were found to be around 250 mS/m. An explanation for these findings was that the aquifers with shallow depth could be influenced by local leaching and surface infiltrations (Campbell, 1980).

The Gouritz WMA report (DEADP, 2011) indicated that the EC at Beaufort West might be as low as <70 mS/m and could rise to 1 000 mS/m (Figure 2.1). Groundwater quality becomes poorer with increase in salinity towards the south of Beaufort West (Great Karoo basin) as compared to the north where the Nuweveld Mountains are situated and to the escarpment (Campbell, 1980).

General pH that was measured for groundwater in the Karoo aquifers indicated a pH of 8.0-8.5. However, the northern and eastern parts (higher rainfall areas) of the basin displayed a pH of less than 7.5 (Woodford and Chevalier, 2002). Furthermore, the pH of the groundwater in Beaufort West town and the surrounding farms ranged between 7.0 and 8.0 (Campbell, 1980). While the pH in the town boreholes as indicated by Gomo (2009) varied between 6.8 and 8.07. On the contrary, the study that was carried out by Van Wyk and Witthueser (2011) on boreholes at Beaufort West north showed that groundwater in the fractures had a pH greater than that of water in the matrix. It was therefore stated that the high pH in

fractures caused carbonates to precipitate, leading to groundwater chemistry in fractures to become alkaline.



Source: Modified from DEADP (2011).

Figure 2.1: Water quality variation as indicated by electrical conductivity in the Gouritz water management area

2.2.2.2 Chemical characteristics

Calcium and bicarbonate dominate the recharge water in the hydrological cycle. The report for the Karoo basin written by Woodford and Chevalier (2002) indicated that Ca^{2+} ranged from 30 mg/l to 150 mg/l at the central Karoo (Beaufort West included). Magnesium, on the other hand, ranged between 30 mg/l and 70 mg/l (Table 2.1). Magnesium is normally not as abundant in the water as calcium because the magnesium containing minerals do not dissolve easily. The average Ca/Mg ratio calculated for most of the Karoo samples ranged between 1.0 and 4.0. The ratios that appeared as 1.0 indicated dolomite dissolution, whereas the ratios of >1.0 indicated calcite dissolution (Maya and Loucks, 1995).

Sodium ranged between 20 mg/l and 200 mg/l (Table 2.1) at Beaufort West and it may have resulted from the exchange of ions (Gomo, 2009; Woodford and Chevalier, 2002) such that in areas where ion exchange does not take place, the Na/Cl ratio equal 1, indicating meteoric sources (Woodford and Chevalier, 2002). Furthermore, the Na/Cl concentration along the central Karoo was within the 1.1 to 2 ratios showing the release of Na⁺ by silicate weathering (Meyback, 1987). Thus, there was less carbonate weathering and ion exchange as compared to silicate weathering. Conversely, the chloride concentration fell between 200 mg/l and 600 mg/l. Increased chloride may have resulted from low recharge in some parts of the central Karoo (Woodford and Chevalier, 2002), and also the result of mixing with connate water (Zaidi *et al.*, 2015).

Total alkalinity in the water represents the concentration of bicarbonate and carbonate ions. These ions were also abundant in the central Karoo groundwater since they fell between 100 mg/l and 300 mg/l (Woodford and Chevalier, 2002). The ions initially form through recharge of the aquifer when CO₂ interacts with rainwater to form H₂CO₃ (Gomo *et al.*, 2013). They may also originate from carbonate dissolution or silicate weathering.

Gomo (2009) indicated that the sulphate concentrations that were measured ranged from 5.84 mg/l to 315 mg/l with the highest concentrations in the municipal boreholes.

Potassium in the central Karoo water was stated not to be important. On the other hand, the highest concentration of silica measured was 20 mg/l (Campbell, 1980; Gomo, 2009). Silica in the groundwater resulted from silicate weathering of minerals like albite, anorthite and K-feldspar (Woodford and Chevalier, 2002).

TABLE 2.1: GENERAL HYDROCHEMISTRY FOR THE CENTRAL KAROO AQUIFERS

Parameters	Range (mg/l)
Calcium	30 - 150
Magnesium	30 - 70
Sodium	20 - 200
Potassium	10 - 20
Total alkalinity	100 - 300
Chloride	200 - 600
Sulphate	100 - 400
Nitrate (as Nitrogen)	2 - 4
Fluoride	0.7 - 1
Silica	15 - 25

Source: Woodford and Chevalier (2002).

Nitrate (as N) was one of the minor ions that were found in some groundwater samples at the central Karoo (2-4 mg/l, Table 2.1). General descriptions for the central Karoo, stated by Woodford and Chevalier (2002), indicated that nitrate in the groundwater may be influenced by redox controlled reactions. Nitrate was also measured to be lower than 10 mg/l in the Beaufort West town, except in the municipal borehole that had a nitrate concentration of 18.4 mg/l (Gomo, 2009). On the other hand, in a study conducted by Campbell in 1980 based at Beaufort West, the nitrate measurements ranged between 45 mg/l and 113 mg/l. The outcomes of Campbell's study showed that it could be nitrate from sewage effluent and inorganic nitrogenous fertilisers that were applied to irrigation soil. Nitrate was also explained to have originated from the soil through nitrogen fixing bacteria.

Lastly, high nitrate values were measured in boreholes at the north-east of Beaufort West that had a brackish to fresh water quality. Comparing the findings from the 1970s and 2000s, the concentration of nitrate in the water has dropped tremendously. This could be that between these years there was an increase in rainfall that could have diluted the groundwater. Again, it could be that less nitrogenous fertilisers are used at the present time as compared to the 1970s. It might also be that there was high leaking of sewage matter into the groundwater, leading to high nitrate concentrations.

Fluoride was also one of the minor ions that were measured in the groundwater. Higher fluoride in the water was found in samples that displayed high salinity. Woodford and Chevalier (2002) stated that high fluoride in the central Karoo groundwater aquifers is a result of long residence times and evaporation. Fluoride was also measured near Beaufort West at the Brandwag farm. This is indicated in the study that was conducted by Campbell (1980) whereby concentrations as high as 4.7 mg/l were measured.

2.2.2.3 Groundwater types

Groundwater quality tests for Beaufort West town and its surrounding farms were done thoroughly by Campbell (1980). The groundwater quality at Brandwag and Rhenosterkop farms showed poor quality stagnant water that was enriched in chloride and sulphate (Campbell, 1980).

Campbell (1980) also performed sampling on boreholes between Beaufort West and Kuilspoor (Quaternary catchment J21A). The findings indicated that the same ions showed an increase in mineralisation down-gradient. The groundwater composition showed that the samples that were collected at the margin of the Brandwag/Kuilspoor dyke had a CaHCO_3 water type; although in the Kuilspoor mudstone flats, water appeared as a mixed type.

Samples collected at some of the farms surrounding Beaufort West (Kuilspoot flats, Speelma's Kuil and south of Lemoenfontein) were dominated by Cl^- ions. This water was classified to be brackish due to high chloride content. Conversely, samples from the Gamka River channel at the northern side of Beaufort West indicated a CaHCO_3 water type. This showed that the permeability and recharge in this area were high as compared to recharge at the flat area (Campbell, 1980).

The study that was conducted by Gomo (2009) at the heart of Beaufort West town showed that the groundwater classification was $\text{Ca}-(\text{Na}+\text{K})-\text{HCO}_3$. This was the classification because municipality boreholes were characterised by old groundwater, whereas the rest of the sampled boreholes had recent recharged groundwater at the time of the investigation.

The groundwater composition as sampled at Vetkuil south of Beaufort West and the lower catchment of Platdorings River was described to be stagnant due to its high salinity and NaClSO_4 composition. A connection in some boreholes was observed since the boreholes indicated simultaneous changes in chemical compositions throughout the flow. Some areas displayed a change of the groundwater chemistry from CaHCO_3 to mixed type, then to NaSO_4 and then to NaCl water type (Campbell, 1980).

Additionally, the general quality of the groundwater in the central Karoo was described to be mixed water (CaMgClSO_4 and $\text{CaMg}(\text{HCO}_3)_2$) (Woodford *et al.*, 2013). In a study conducted by Adams *et al.* (2001) at Sutherland in the western Karoo it was found that the main water types at this area were CaHCO_3 , CaSO_4 , NaSO_4 , NaHCO_3 , NaCl and CaCl_2 .

2.2.2.4 Hydrogeochemical processes

The process of silicate weathering, stated in Woodford and Chevalier (2002), falls amongst the main hydrogeochemical processes that take place in the main Karoo basin. During silicate weathering, bicarbonate is released in the groundwater and leads to high concentrations of this ion. This happens mostly in the eastern Karoo basin due to wet conditions. Furthermore, the weathering of plagioclase leads to increased calcium and sodium in the groundwater.

Ion exchange was also experienced in the Karoo basin whereby calcium in solutions is exchanged for sodium (Adams *et al.*, 2001; Woodford and Chevalier, 2002). This process has been experienced in areas where there are sodium rich minerals. The process of calcite dissolution, on the other hand, is influenced more by the exchange capacity of clay minerals. Likewise, exchange capacity mobilises sodium into solution, resulting in solutions that are alkaline (Woodford and Chevalier, 2002).

Evaporation also happens in the Karoo basin, more especially in the western part. Woodford and Chevalier (2002) indicated that the groundwater type and ionic concentrations in the eastern and western parts of the Karoo basin are different from one another. This is caused by varying climatic conditions in these areas. The eastern Karoo, since it receives higher amounts of rainfall than the western part, experience dilution in its groundwater leading to a low concentration of ions and other constituents in the water. The study further states that groundwater in most parts of this basin is undersaturated in the majority of minerals because of constant dilution.

On the contrary, as a result of low rainfall in the western Karoo basin, the groundwater is highly concentrated in various constituents (Adams *et al.*, 2001; Woodford and Chevalier, 2002). This is because there is less recharge in these areas, leading to less or no dilution in some parts of the basin. Moreover, the groundwater is forced to experience long residence time in the aquifer. Consequently, the increased salt concentrations in this water results from long residence times and evaporation as a result of low rainfall (Woodford and Chevalier, 2002). The processes of dissolution and precipitation as stated in Adams *et al.* (2001) may also take place in the Western Karoo.

Oxidation of pyrite in the Karoo rocks falls amongst the important hydrogeochemical processes. This process is experienced along the pyrite mineralised rocks whereby the pH of the water becomes acidic with increased sulphate as a result of oxygenated water interacting with these rocks (Adams *et al.*, 2001). However, this is the process that is experienced in the northern Karoo basin where there are coal and gold mines and also in the western Karoo (Woodford and Chevalier, 2002). Opposite to the addition of sulphate from pyrite oxidation in the western Karoo, it was also shown that sulphate reduction was one of the processes changing the groundwater composition (Adams *et al.*, 2001).

The groundwater quality variations in both high and low recharge areas of the Karoo basin mostly depend on the availability of carbon dioxide (CO₂) and dissolved oxygen (DO), as well as the climatic patterns (Woodford and Chevalier, 2002). The reduction of carbon dioxide from groundwater leads to the formation of clay minerals and iron oxides. The type of clay minerals that is formed during these conditions depends on the climatic conditions. Clay montmorillonite will form in arid conditions that mostly prevail in the western Karoo. On the other hand, clay kaolinite will form in wet conditions in the eastern Karoo (Woodford and Chevalier, 2002).

2.2.2.5 Groundwater suitability for use

The report by Campbell (1980) indicated that within the 10 km radius of Beaufort West town there is about eight boreholes that could be used for municipal water supply to the community. Furthermore, it is indicated that the groundwater quality is brackish and poor for boreholes located between 10 km and 20 km north and east of Beaufort West town. Thus, this could be water samples with EC ranging between 150 mS/m and 300 mS/m (Freeze and Cherry, 1979). Again, saline water with an EC of >300 mS/m was found at the Rhenosterkop floodplain at the south of the main dolerite sill to Speelma's Kuil and at the lower Plaatdoorns. Lastly, at a distance beyond a 20 km radius from Beaufort West town, the groundwater could be considered for supply since this water is potable.

The general groundwater quality of the central Karoo is good; however, variations in this water occur depending on the geology of an area such that some water may be considered not suitable for domestic or irrigation use (DEADP, 2011).

Finally, the total hardness (TH) as calculated for calcium and magnesium ions were between 240 mg/l and 790 mg/l for the Beaufort West town boreholes, showing hard groundwater (Gomo, 2009). Furthermore, the general TH showed very soft to soft groundwater for the eastern and northern Karoo samples, whereas samples on the western edge of the basin appeared as very hard to extremely hard. On the other hand, the central Karoo displayed hard to very hard groundwater (Woodford and Chevalier, 2002).

2.3 Hydrogeochemical Characterisation Tools

Various tools may be applied in identification of the possible hydrogeochemical processes taking place in the groundwater aquifer system leading to the evolution of the groundwater chemistry. The tools may also be used to characterise the reactions responsible for changing the chemistry and also altering the aquifer geology. Therefore, it is significant to consider applying more than one of these tools in a study to be confident about the results obtained. Application of these tools gives a better understanding of the hydrogeochemistry of the study area. This section provides a review of different tools that may be used in hydrogeochemistry investigations.

2.3.1 Stoichiometric analysis

Stoichiometry of reaction gives the relationship between reactants and products in a balanced chemical reaction. It is therefore applied in doing calculations for chemical reactions; however, an understanding on how the reactants and products are related is

important before performing the calculations (Petrucci *et al.*, 2007). Stoichiometric reactions are therefore the principal control of the water chemistry evolution because without groundwater reactions there would not be any hydrogeochemical processes taking place. Furthermore, the groundwater chemistry would not change unless in cases where there are atmospheric inputs. The groundwater composition may be altered by several processes such as rock weathering and evaporation that are led by reactions producing different minerals. This occurs as the groundwater at recharge areas moves down-gradient to the discharge area (Hounslow, 1995).

Stoichiometric reactions are therefore useful during assumptions of the reactions that could have taken place in changing the composition of the initial water. Thus, it indicates the possible origin of the groundwater (Hounslow, 1995). The stoichiometry of a balanced equation defines the number of products in a reaction (Petrucci *et al.*, 2007). The relationship in these reactions can also be reflected on bivariate correlation plots.

2.3.1.1 Bivariate correlation plots

Bivariate correlation is a measure of the relationship between two variables (example: Section 5.4.2) whereby the strength of their relationship is indicated by a correlation value between 0 and ± 1 (Acock, 2008). These scatter plots are considered the simplest plots when it comes to understanding hydrochemical data (Hounslow, 1995) and they can give a better understanding of the groundwater system (Van Camp and Walraevens, 2008). The reason is that two variables (x and y) are plotted against each other; or rather, the sum for two or more ions is plotted on one axis and the other ions on another axis (US EPA, 2006).

The strong relationship on these plots is indicated by a straight line as well as a high correlation coefficient ($r = \pm 1$) value (Jenn *et al.*, 2007). A correlation of 0.1 shows a weak relationship, $r=0.3$ shows a moderate relationship and $r=0.5$ shows a strong relationship (Acock, 2008). The linear shape that represents the correlation is primarily known as the 1:1 line; however, a 1:2 or 1:4 line may also be defined depending on the reactions that resulted in the respective ions (Kozłowski and Komisarek, 2016). An example is given in cases where Ca^{2+} and HCO_3^- entered the solution through calcite weathering, a ratio of 1:2 for $\text{Ca}^{2+}:\text{HCO}_3^-$ will be obtained. Conversely, if the source of these ions is dolomite weathering, a ratio of 1:4 will result (Garrels and Mackenzie, 1971).

Bivariate correlation plots may be used to indicate various groundwater types, mixing of the water together with ion exchange (Van Camp and Walraevens, 2008). The correlation plots easily show the outliers in the data and these reduce the relationship between the plotted

variables. If outliers are removed from the data, a correlation higher than the one that was obtained prior to its removal will be developed (Garrels and Mackenzie, 1971).

According to The United States Environmental Protection Agency (US EPA, 2006), a weakness of the bivariate correlation is that if there is less data plotted, non-linear relationships may appear linear, thus wrong results will be generated. Therefore, a large data set would be required to perform these plots for accurate results.

2.3.2 Hydrochemical facies plots

2.3.2.1 Piper diagrams

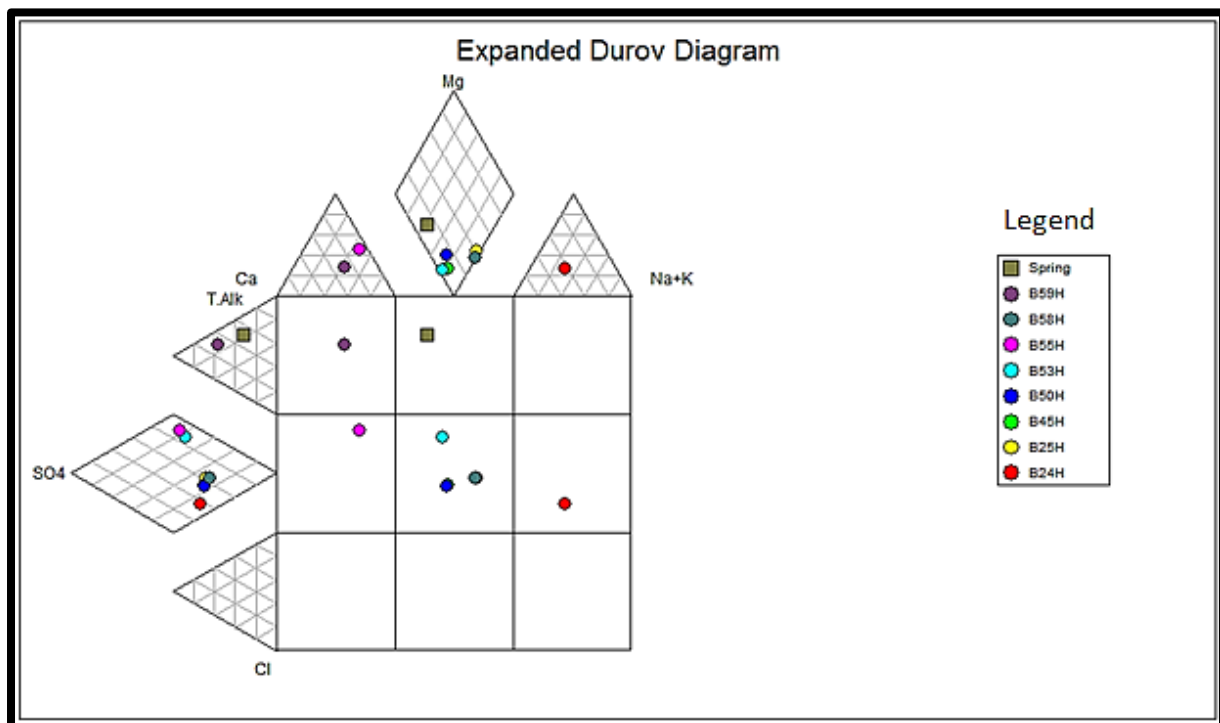
A piper diagram is a graphical presentation of groundwater that categorises the samples in terms of how concentrated they are with specific major ions (Bredenhann and Hodgson, 1998; Hounslow, 1995). This diagram is normally considered first when working with water samples in order to understand the groundwater evolution (El-Manharawy and Hafez, 2003). The Piper diagram is made up of two ternary diagrams as well as a central diamond diagram (an example is indicated by Figure 5.2). One ternary represents major cations (calcium, magnesium and sodium, plus potassium) and the other is major anions (sulphate, chloride and bicarbonate, plus carbonate ions) that are labelled on the apices. Each apex represents 100% of a labelled component (Appelo and Postma, 2005; Hounslow, 1995).

Results presented on the Piper diagram plots the sample on the cation and anion ternaries. The points are therefore extended by means of a line to the diamond, and their meeting point defines the main water type for a respective sample (Bredenhann and Hodgson, 1998). A diamond gives a better understanding on the resulting water type, as well as assumptions on the water origin (El-Manharawy and Hafez, 2003).

Besides an indication of the main water types, other processes such as mixing, ion exchange and chemical evolution may also be noted on these diagrams (Bredenhann and Hodgson, 1998; Hounslow, 1995; Van Camp and Walraevens, 2008). However, for the above-mentioned processes to be observed on the Piper diagram, linear trends must be formed. Again, samples must plot on the connecting line of two points because if there is no trend, nothing will be indicated except for the water types (Bredenhann and Hodgson, 1998). A Piper diagram is capable of plotting many types of water analysis on one diagram. A drawback of the Piper diagram is that concentrations are renormalized. It also plots relative concentrations; for example, water of the element concentrations of similar ratios will fall on the same position regardless of whether the water is diluted or saline (Bredenhann and Hodgson, 1998). Thus, it cannot accommodate water easily where other ions are important.

2.3.2.2 Expanded Durov diagrams

Durov or expanded Durov diagrams is a graphical representation that is used to classify various groundwater hydrochemical facies (Younger, 2007). This diagram has a more or less similar form and properties as the Piper diagram. The difference is that the expanded Durov indicates six trilinear diagrams with three displaying cations and three displaying anions with each ion plotted on separate triangles (Bredenhann and Hodgson, 1998). The expanded Durov diagram also has a square with nine fields that displays various water types (Figure 2.2) or predominant facies (Lloyd and Heathcote, 1985). Younger (2007) explained the main difference between the Piper and expanded Durov to be the way the calculations of ions are done. The preparation of an expanded Durov plot requires percentages of total ions (major ions), whereas Piper plots involve percentages of major cations and major anions, separately. The Durov diagram, on the other hand, is similar to the expanded Durov diagram, except that it does not display the nine areas that explain the water types in detail (Zaporozec, 1972). Furthermore, apart from the chemical compositions for major ions, the Durov diagram also displays the total dissolved solids or EC, as well as the water pH.



Source: Author's own (2016).

Figure 2.2: Expanded Durov diagram example

The expanded Durov diagram gives clear deductions on the processes that are involved in evolving the chemistry of the groundwater (Lloyd and Heathcote, 1985). The limitation of

expanded Durov diagrams is that if there is sewage or liquid waste polluting the groundwater, it may lead to samples plotting on uncommon areas on the diagram (Bredenhann and Hodgson, 1998). Therefore, this will result in wrong interpretations. Again, both Piper and Durov diagrams do not offer enough differentiation in certain groundwater types like saline water such that alternative sources are not indicated (Younger, 2007).

2.3.3 Multiple component plots

Multiple component plots consist in a variety of diagrams. These are stiff diagrams, pie diagrams, bar diagrams, vector diagrams, and radial diagrams. The component plots display trends for various parameters, mostly the major components. All these plots may be plotted in meq/l units. However, others such as radial diagrams may also use % meq/l as the units. The plots therefore show the main components of the chemical compositions of groundwater (Appelo and Postma, 2005). Below are the discussions on multiple component plots; however, only plots that are mostly used in groundwater data interpretation are discussed.

2.3.3.1 Stiff diagrams

A Stiff diagram is a polygon that results by connecting the dots that correspond to the concentration of respective major ions displayed in meq/l (Younger, 2007). Stiff diagram plots the parameters in pairs, thus a cation on the left against an anion on the right (Appendix 1). Sodium is plotted adjacent to chloride; calcium adjacent to bicarbonate; magnesium alongside sulphate; and lastly but rarely displayed, is iron and carbonate (Zaporozec, 1972). These components are plotted on parallel horizontal lines of which the points are connected once all the parameters are plotted. The connection of all the points results in a polygon (Appelo and Postma, 2005; Hounslow, 1995).

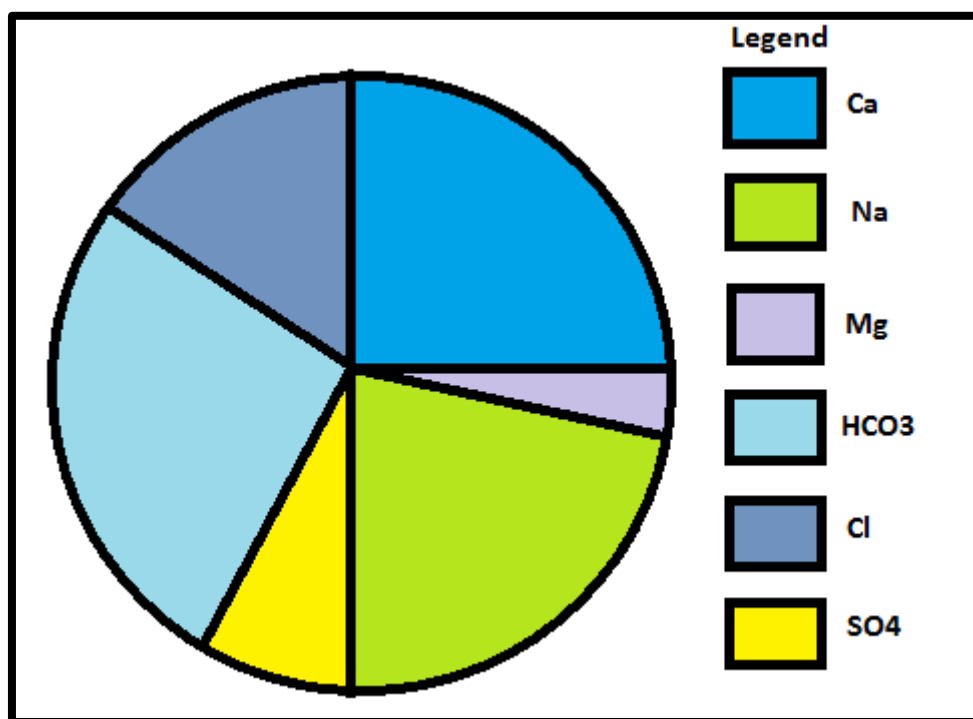
Various patterns or polygons as displayed by stiff diagrams indicate water types (Zaporozec, 1972). Likewise, the horizontal line for Na-Cl indicates the possibility of a marine source owing to dominance of NaCl in the seawater. The next horizontal line of Ca-HCO₃ shows carbonate dissolution, whereas the next or last line (Mg-SO₄) in some studies displays the remaining major components (Appelo and Postma, 2005). The last pair is not indicated in most of the interpretations, therefore its use depends on the study that is being carried out.

A stiff diagram, as indicated by Zaporozec (1972), is referred to as a sophisticated tool in presenting vertical changes in the chemical composition of water. It is one of the methods that may be used to deduce the source-rock. Stiff diagrams are also significant because they visualise differences in the way cations and anions are distributed relative to their varying patterns (Singhal and Gupta, 2010). Its limitation is that each analysis requires a separate

diagram, thus not all samples can be plotted simultaneously on the same diagram (Singhal and Gupta, 2010).

2.3.3.2 Pie diagrams

A pie diagram is a circle that is divided into slices representing various components (Norris *et al.*, 2014; Sharma *et al.*, 2009). The slices form two semi-circles whereby one half represents the cations, whereas the other half represents the anions (Figure 2.3) if there is a balance between cations and anions (Appelo and Postma, 2005; Younger, 2007). Zaporozec (1972) stated that each half represents 100% of the respective total ion concentration. Additionally, the circles' diameters or its size is a representative of total dissolved constituents (Appelo and Postma, 2005; Hounslow, 1995; Younger, 2007). When constructing a pie diagram, it is best to convert the concentrations into percentages. Each percentage concentration therefore needs to be multiplied by 3.6 to obtain an angle of a slice for the respective ion because a circle forms 360 degrees (Norris *et al.*, 2014).



Source: Author's own (2016).

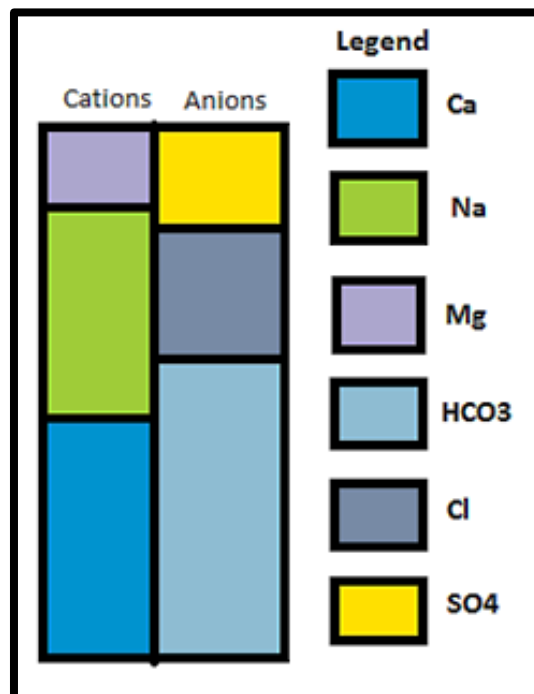
Figure 2.3: Pie chat example

Pie diagrams are among the simplest and most quickly understood diagrams and they are normally used to represent concentrations on maps (Younger, 2007; Zaporozec, 1972). Pie diagrams further give a quick visualisation of the dominant ions (Sharma, 2005). Conversely, their primary use on maps may be a disadvantage because if many sampling points are

indicated, the map may end up being complex or difficult to read. Again, smaller pie diagrams will not be options because they will not be clear (Zaporozec, 1972). This leads to the use of these diagrams as not an option at all times. Furthermore, pie diagrams may be less effective compared to bar diagrams in terms of accurate reading. This is seen mostly where the series is divided into a large component number (more than 6 components) or when there is a small difference between the components (Sharma, 2005).

2.3.3.3 Bar diagrams

Bar diagrams are defined as inline columns that indicate the size of a category (Norris *et al.*, 2014; Sharma, 2005), with the heights of the bars showing trends in the data (Norris *et al.*, 2014). The displayed inline columns are two (Appelo and Postma, 2005; Younger, 2007) and they draw the sum of cations (left column) and anions (right column) normally at equal height (see Figure 2.4). These show the total concentration of each ion group (cations and anions) if there are no errors in the data (Hounslow, 1995; Zaporozec, 1972). The ions concentrations for anions or cations appear stacked, regardless of which ion contributes more in the groundwater sample (Appelo and Postma, 2005).



Source: Author's own (2016).

Figure 2.4: Bar diagram example

Bar diagrams are considered a significant method of displaying data because errors in the results may easily be indicated (Bredenhann and Hodgson, 1998). Furthermore, they are

easily understandable because they fall among the simplest and easiest diagrams. Unlike other diagrams such as pie diagrams, bar diagrams may be used to compare a large number of components (Sharma, 2005). One of the limitations of bar diagrams is that one sample of data is represented by each bar. Additionally, it can only be used when there is a small difference between the values to be plotted (Sharma *et al.*, 2009).

2.3.4 Geochemical modelling

Geochemical models are defined as the tools that are useful in interpretation of the geochemical reactions in the groundwater (Parkhurst and Plummer, 1993). They can further be used for other applications such as approximating the groundwater flow. Parkhurst and Plummer (1993) stated that geochemical modelling is divided into inverse and forward modelling. The pH Reaction Equilibrium Calculation (PHREEQC) hydrogeochemical program (Parkhurst and Appelo, 1999) is used to perform water calculations for geochemical modelling.

2.3.4.1 Inverse modelling

Inverse modelling is defined as the mole transfer between phases in the groundwater that leads to chemical changes through the movement of water along the flow paths (Plummer *et al.*, 1994). The purpose of inverse modelling is to determine all chemical reactions that lead to chemical and isotopic compositions of the groundwater. This approach uses the measured groundwater compositions to assume the possible geochemical reactions (Parkhurst and Plummer, 1993). Besides the groundwater chemistry data, the input data also requires the potential reactive mineral phases along the flow path. Inverse modelling calculations normally require the solution or solution spread, the data blocks of the phases and inverse modelling keyword data block (Parkhurst and Appelo, 1999). Inverse modelling is a combination of speciation modelling and mass-balance modelling that are discussed below.

2.3.4.1.1 Speciation modelling

Speciation modelling calculates the distribution of species and saturation indices (SI) of phases by using a water chemical analysis (Parkhurst and Appelo, 1999). Besides calculating the distribution of species and SI; speciation modelling may also generate results for description of solutions (Lollar, 2005; Parkhurst and Plummer, 1993). However, from these results, SI for minerals is most significant and it is therefore discussed. During data input, speciation calculations require the solution data block that incorporates pH, temperature and concentrations of elements in order for results to be generated (Parkhurst *et al.*, 1980). The mg/l or ppm units are considered as default in performing the calculations (Parkhurst and

Appelo, 1999; Parkhurst and Appelo, 2012). Therefore, because ppm is a mass unit rather than a mole unit the program converts all concentrations into molal units (Parkhurst and Appelo, 1999).

The advantage of this approach is that the model can be modified easily such that new elements can be included (Parkhurst *et al.*, 1980). Additionally, it is theoretically suitable to solutions of any ionic strength. The limitation of speciation modelling by specific interaction is that its applicability is more focused on elements that form strong electrolytes (Parkhurst and Plummer, 1993). Lastly, this approach does not include spatial and temporal information like reaction-transport modelling (Zhu and Anderson, 2002).

2.3.4.1.1.1 Saturation indices analysis

According to Merkel and Planer-Friedrich (2008), the saturation index can be defined as the logarithm of the proportion of the ion-activity product (IAP) and solubility product (K_{SP}). Saturation indices (SI) for minerals are obtained from the PHREEQC program (Parkhurst and Appelo, 1999). PHREEQC calculates the SI for all the possible minerals that can be formed given the components (for example, Ca^{2+} , SO_4^{2-} , CO_3^{2-}) in the solution. These indices are important because they show how certain phases are saturated with respect to the solution within which they are found (Parkhurst and Appelo, 2012; Peikam and Jalali, 2016). Furthermore, it indicates how the solution changed from its equilibrium phase relative to the phases that were dissolved (Jalali, 2007). Calculating the equilibrium of minerals for SI is significant in determining minerals that reacted in the groundwater system (Deutsch, 1997).

Under SI speciation, all the minerals that are applicable for the given input data are listed in alphabetical order as generated for the output. The output further gives the phases, SI, log of ion activity product (log IAP), log of the solubility constant (log K_T) as well as the chemical formulas for the respective minerals (Parkhurst and Appelo, 1999).

Interpretation of SI results indicates that if minerals are saturated (equilibrium conditions) in the water, their obtained SI should give a value of 0. Moreover, if the mineral is supersaturated or oversaturated, the $SI > 0$; and lastly, minerals are undersaturated within the solution if the $SI < 0$. In SI, undersaturation of mineral phases suggests that dissolution of that mineral can still occur (Van Camp and Walraevens, 2008). However, Merkel and Planer-Friedrich (2008) stated that in practice it is only if the SI is between -0.05 to +0.05 that a solution can be assumed as being in equilibrium relative to that mineral.

The advantage of this approach is similar to the one specified for speciation modelling that it can easily be modified. The drawback of SI is that it only shows what should happen dynamically instead of the rate of the reaction (Parkhurst and Plummer, 1993).

2.3.4.1.2 Mass-balance modelling

Mass-balance modelling can be defined as the transfer of moles during the groundwater flow in the aquifer leading to a different groundwater composition (Plummer *et al.*, 1994). This approach attempts to indicate the nature and extent of geochemical reactions by defining the minerals that are reacting in the groundwater system, indicating the ones precipitating or dissolving (Parkhurst and Plummer, 1993; Zhu and Anderson, 2002). Precipitation or dissolution of phases between two solutions (initial and final) can simply be explained by the difference in the chemical concentrations of the ions present (Plummer and Back, 1980).

During mass-balance modelling, two wells are normally considered. Thus, water samples collected up-gradient is referred to as initial water, whereas water samples collected down-gradient is final water that evolved from the initial water; however, on the same flow path as assumed (Parkhurst and Plummer, 1993). Therefore, a steady state situation relative to the flow of groundwater and chemical compositions is predicted (Parkhurst and Plummer, 1993; Plummer and Back, 1980). The data collected from those wells is used to generate the mass-balance between them along the flow path in order to predict the chemical reaction(s) that took place between those wells (Parkhurst and Plummer, 1993). Mixing of two initial water samples may also take place resulting in final water (Plummer and Back, 1980; Zhu and Anderson, 2002). In cases where the selected wells are at different flow lines, incorrect mass-balance results will be obtained.

Mass-balance may indicate different redox states of certain elements as part of the reaction; this may be an indication that there might be redox processes taking place (Parkhurst and Plummer, 1993). Additionally, it can define geochemical reactions that played a role in changing the groundwater chemistry (Parkhurst and Appelo, 1999). The difficult part in using mass-balance modelling comes when all the possible reacting phases (minerals and gases) are to be stated. However, background knowledge on the geology and mineralogy of the area will be useful. The weakness of mass-balance approach is that for models to be calculated, the analytical data input should include uncertainty limits (Parkhurst and Appelo, 1999). Because of this weakness, it cannot be easily applied to trace elements data. Therefore, this approach is more effective when applied to elements that predominate in solutions (Zhu and Anderson, 2002).

2.3.4.2 Forward modelling

Forward modelling is defined as the calculation of water composition from the assumed or specified geochemical reactions (Parkhurst and Appelo, 1999). This tool is normally applied in cases where there is no chemical data present (Parkhurst and Plummer, 1993). This approach depends on the aqueous solutions and mineral phases to generate the solution composition. Forward modelling can simulate advection, dispersion, spatial and temporal distribution of groundwater composition and minerals (Parkhurst and Appelo, 1999; 2012). It can therefore be used in verifying the thermodynamic consistency in the mass-balance results. This can only be done if a flow path does not precipitate a product from an undersaturated solution and does not dissolve a reactant in a supersaturated solution (Parkhurst and Plummer, 1993). Forward modelling is divided into reaction-path and reaction-transport modelling.

2.3.4.2.1 Reaction-path modelling

A reaction path model can be defined as the assumption of the water chemical composition as the water undergoes reversible (occurring close to equilibrium) and irreversible (not at equilibrium) geochemical reactions in the aquifer system (Wolery and Daveler, 1992). The principal use of reaction-path modelling is to identify the solubility of certain minerals in solution and identifying the groundwater composition if geochemical reactions took place (Parkhurst and Plummer, 1993). The reaction-path model is related to the speciation model because they both involve the mass-balance equations for individual elements (Parkhurst and Plummer, 1993; Wolery and Daveler, 1992). Nonetheless, reaction-path modelling also contains mass action equations for equilibrium phases. Again, unlike in the speciation calculations, the pH, redox conditions and mass of the water are calculated by the program from the additional equations that are included (Parkhurst and Plummer, 1993).

Parkhurst and Plummer (1993) stated that uncertainties in the results may be caused by the selected aqueous species, thermodynamic data for aqueous species and uncertainties in theoretical data. In order to calculate the reaction-path model, starting water compositions, as well as the reversible and irreversible reactions, are required (Wolery and Daveler, 1992; Parkhurst and Plummer, 1993). The mass action phase equilibrium equation also forms part of the calculations (Parkhurst and Plummer, 1993).

The strength of this approach is that problems can be defined with more than one irreversible reaction happening at the same time. On the other hand, limitations of reaction-path modelling is that it cannot calculate the spatially and temporary chemical compositions of the

groundwater on its own (Zhu and Anderson, 2002). It is also not capable of modelling the advection and dispersion mechanisms (Parkhurst and Plummer, 1993).

2.3.4.2.2 Reaction-transport modelling

The reaction-transport model is defined as the groundwater flow and transport model joint to the chemical reaction model (Bethke and Yeakel, 2013). This approach calculates the flow of the groundwater and the species it dissolves through its movement in the aquifer (Bethke and Yeakel, 2013; Parkhurst and Plummer, 1993). Unlike the reaction-path modelling, it also models the dispersion and advection mechanisms. Correspondingly to reaction-path modelling and speciation modelling, this model involves the aqueous model and thermodynamic data of solid phases (Parkhurst and Plummer, 1993). In order to conduct the reaction-transport model, hydraulic parameters of the aquifer, groundwater composition, assessment of the distribution and composition of minerals and estimates of the irreversible reactions in the aquifer are all required (Parkhurst and Appelo, 2012). This approach is fast for one-dimensional calculations (Appelo and Willemssen, 1987) and it can be used to investigate geochemical reactions in dynamic groundwater systems because it is flexible (Parkhurst and Plummer, 1993).

Reaction-transport modelling can be done for advective-transport and advective-dispersive transport models (Parkhurst and Appelo, 1999). Advective-transport calculations imitate chemical reaction and advection when the water flows through a one-dimensional column that is divided into n^{th} number of cells, depending on what the user chooses (Parkhurst and Plummer, 1993). Each cell should contain a solution that is numbered according to the cell numbering and they may also comprise other reactants (Parkhurst and Appelo, 1999). The cells may also define reversible or irreversible reactants. In addition, the solution composition needs a solution spread data block (Parkhurst and Appelo, 2012).

In advective-dispersive transport models, a dispersion or diffusion coefficient is used for all chemical species. Similar to the advective transport, the number of cells is defined with an addition of dispersion-diffusion parameters such as cell lengths, direction of flow, boundary conditions and time steps (Parkhurst and Appelo, 1999). The transport data block can model advective transport, advective-dispersive one-dimensional and diffusive two-dimensional or three-dimensional transport (Parkhurst and Appelo, 2012).

Reaction-transport model in general can model complicated processes. This approach is unique because it can simulate the transport of fluids by dispersion and advection; whereas inverse modelling is not capable of this simulation (Parkhurst and Plummer, 1993).

Furthermore, the chemical composition of groundwater can be calculated spatially and temporary of which cannot be performed by reaction-path modelling on its own (Zhu and Anderson, 2002). A drawback of this tool is that since the explicit finite difference algorithm is included in calculating the one-dimensional transport models, it may display numerical dispersion when the grid is coarse. Furthermore, the size of numerical dispersion is reliable on the modelled reactions. Therefore, modelling of reaction transport requires a step by step approach (Parkhurst and Appelo, 2012).

2.3.5 Statistical methods

2.3.5.1 Principal component analysis

Principal component analysis (PCA) is defined as a multivariate statistical analysis technique that displays data on the basis of how they are related. Thus, it can classify the patterns in the data (Villegas *et al.*, 2013). Dragon (2006) stated that the primary purpose of using this technique is to generate components of related variables as obtained from initial data. Villegas *et al.* (2013) explained that the analysed variables equal the number of components generated; however, only a few of all the components are meaningful and cover up the variance. One extracted component can be used to explain one or numerous hydrochemical processes taking place (Suk and Lee, 1999).

According to Jenn *et al.* (2007), loadings are values that display the correlation between a variable and a component relative to this variable (concentrations of ions or other parameters) (Dragon, 2006). These values are obtained after the generation of principal components. High loadings (close to ± 1) for each component indicate that their respective variables contributed the most in altering the groundwater chemistry (Dragon, 2006; Jenn *et al.*, 2007). Since this study is mainly focused on reviewing the hydrogeochemical processes that influence the groundwater quality, the first components will explain the main processes (Villegas *et al.*, 2013; Gajbhiye, Sharma and Awashi, 2015). Norman and Streiner (2008) explained that component loadings that are low (about 0.3 or 0.4) can be ignored during the interpretation of the results.

Communality is explained as the total influence by the variables related to a specific parameter for the extracted components. This is obtained by squaring all the component loadings that associates with a variable and summing them all together (Dragon, 2006). Communality indicates the way in which components describe the variance of variables. Additional to the extracted components of PCA, rotation of the component loadings is also performed by the varimax rotation technique as described by Davis (1973). This is

considered as a simple orthogonal structure and is used in most interpretations. Varimax rotation is generated to display variables that plot next to 1 as obtained in one component and closer to zero for other components (Villegas *et al.*, 2013).

Contingent with the units that the initial data is presented, Dragon (2006) indicated that before performing the analysis the initial data should be standardised; this is done if the parameter units are different (for example, mg/l and mS/m). The generation of principal component analysis is performed using the statistics software program (IBM SPSS).

PCA is considered as accurate and therefore decreases the statistical noise by reducing a large variable set to a few components (Jenn *et al.*, 2007). It places the principal components in a way that the ones contributing most in the evolution of the solution are classified as the first and the ones that contribute less are taken as the last principal components (Jenn *et al.*, 2007; Kumar *et al.*, 2011; Kura *et al.*, 2013). PCA also extracts factors relative to variances, co-variances of the variables and communalities. Furthermore, it generates eigenvalues and loadings for correlation matrix (Kumar *et al.*, 2011).

Gajbhiye *et al.* (2015) mentioned that PCA is considered as more dependable with no assumptions unlike factor analysis (FA). Nevertheless, its limitation as discussed by Olmez *et al.* (1994) is that it cannot differentiate between hydrogeochemical processes that resulted in the same variation of groundwater chemistry. Hence, it is considered very useful to apply other hydrogeochemical tools before working on PCA. This helps to have a background understanding on which hydrogeochemical processes are expected in the study area.

2.3.5.2 Distribution analysis

Distribution analysis includes some of the statistical tools that may be used in interpreting the groundwater chemistry and processes. The analysis will include the hierarchical cluster plots, cross plots, histogram and distribution plots.

2.3.5.2.1 Hierarchical cluster analysis

Hierarchical cluster analysis (HCA) is a multivariate statistical technique that groups variables into clusters (Section 5.5) in terms of how closely related they are to each other and how different they are from the rest of the groups (Kura *et al.*, 2013; Van Camp and Walraevens, 2008). The clustering can be indicated by a dendrogram that links the clusters in similar pairs (Jenn *et al.*, 2007). Thus, the clustering for water quality data may indicate how borehole groundwater samples are concentrated in various ions (Jenn *et al.*, 2007).

Similar to PCA, the initial data must be standardised before generating the clusters; this is done if the parameters that are used have different units.

The methods of identifying the clusters on the dendrogram are different and these are explained in Einax *et al.* (1997); Jenn *et al.* (2007); Wasserman and Faust, (1994). A line known as a phenon line (cut-off line dividing dendrogram into different clusters) can be drawn from the dissimilarity axis (horizontal or vertical depending on the position of the dendrogram) through a dendrogram to separate the clusters from each other to form various groups. This helps in determining which groups are closely related. The generation of hierarchical cluster plots can be done by using a statistics software program.

The advantages of HCA are that it is a distinct method that clusters components into subsets. The clustering and interpretation is clear. The limitation of HCA is that there is no consistent way of identifying the number of groups or subsets from the generated clusters, thus the approach is random (Wasserman and Faust, 1994).

2.3.5.2.2 Histogram

A histogram is defined as a set of rectangles with areas being proportional to the frequency class (Sharma *et al.*, 2009). It is the graphical presentation of data visually such that the data is presented in vertical bars (Sharma, 2005; US EPA, 2006; Jenn *et al.*, 2007). The data is first organised into classes or bins (US EPA, 2006; Jenn *et al.*, 2007); for example, if there are 20 water samples with various concentrations of magnesium, concentrations that fall within 5 mg/l will be grouped together; between 5 and 10 mg/l will be grouped together. In order to obtain the range for grouping classes, a square root of sample number or size ($n=20$) can be done.

After the grouping of the data, the frequency is obtained indicating the number of samples that fall within a particular class. Lastly, the relative frequency is calculated by dividing the frequency with the sample size (US EPA, 2006). Thus, a histogram can be drawn using the concentration data in mg/l on the x-axis and the relative frequency on the y-axis (Sharma, 2005; US EPA, 2006).

A histogram is capable of resembling the underlying frequency distributions of the population (Jenn *et al.*, 2007; Acock, 2008) that can be seen by visualising the diagram (US EPA, 2006). Although data presentation indicates the main picture of the attained data, the drawbacks of histograms is that it does not display details in the data, it only shows the number of values in an interval. Again, these diagrams are used to plot numerical data only (Einax *et al.*, 1997).

A frequency curve and polygon can be derived from a histogram. A frequency polygon is defined as a graphical presentation of frequency distribution in the form of a polygon. This polygon can be derived from a histogram since it overlies the histogram (Sharma *et al.*, 2009). It is developed by placing points at the middle top of each histogram rectangle and joining those points with straight lines to form a polygon. The area of a polygon is similar to that of a histogram (Norris *et al.*, 2014; Sharma *et al.*, 2009). Additionally, a frequency curve is a smooth curve that develops from small intervals and a large number of observations (Acock, 2008; Jenn *et al.*, 2007; Sharma *et al.*, 2009; US EPA, 2006). It is attained by resembling a histogram whereby a smooth hand curve is made (Van Camp and Walraevens, 2008; Sharma *et al.*, 2009). An example of such a curve could be a normal or skewed distribution.

Histograms can be presented by normal and lognormal curves, indicating local or anthropogenic sources of pollution and natural concentration distribution, respectively (Wendland *et al.*, 2005). Furthermore, histograms may also be used to display water interceptions (Campbell, 1980).

2.3.5.2.3 Box and whisker plots

Box and whisker is a simple plot that portrays the distribution of the data and the underlying distribution, the shape, as well as the location just like the histogram (Black, 2009; US EPA, 2006). A box and whisker presents data in percentiles. These plots may occur as simple or complex box plots (EPA, 2006). However, in most data presentations a simple box plot that indicates the 0th (minimum value), 25th (lower percentile), 50th (median), 75th (upper percentile) and 100th (maximum value) percentiles are applied. The 25th and 50th percentiles will depend on the sample size.

Once all these values are obtained, a simple box plot can be drawn from the median, upper and lower quartiles. The upper and lower quartiles form the end points of the box, whereas the median cuts the box into halves (Black, 2009). The whiskers therefore extend from the 25th and 75th percentiles towards the minimum and maximum values, respectively (Black, 2009; Chidambaram *et al.*, 2013). This tool may also be used to indicate if data is distributed as normal or skewed. Thus, if the upper box and whisker are the same length as the lower box and whisker, the data is symmetrically distributed. However, if the box and whisker at either of the sides is longer than the other side then the distribution is skewed (US EPA, 2006).

Box and whisker diagrams may be used in groundwater to indicate the distribution of ions (Chidambaram *et al.*, 2013). They are capable of displaying large data in a summarised manner. Furthermore, they may be used to indicate outliers and also to show if there is skewness in the distribution (Black, 2009). Limitations of box and whisker plots is that it can only be used with numerical data and again it does not clearly show the original data; the mean and the mode from the statistical data cannot be seen directly from the diagram (Einax *et al.*, 1997).

2.4 Conclusion

This chapter examined the various water types and the hydrogeochemistry of Beaufort West at large as discussed by various researchers. It also described the complementary hydrogeochemical tools that may be used in describing the hydrogeochemical processes that are involved in evolving the groundwater chemistry. This chapter first looked at variations in the hydrochemistry at various sites of Beaufort West, including the water types. It then described the complementary tools that were used in analysing the groundwater chemistry results.

Chapter 3 **Study Area**

3.1 Introduction

This chapter provides a description of the study area which is Beaufort West town. The chapter is divided into eight sections and goes deeply into describing the climate, geology, hydrology, recharge and groundwater uses at this area. The catchment and elevation maps are also included to show the exact location of the study area and how topography varies from recharge to discharge areas.

3.2 Site description

The area under study is situated in Beaufort West town in the Western Cape Province, South Africa (Figure 1.1). Beaufort West is approximately 450 km northeast of Cape Town and is located along the N1 national route. The study area is specifically Quaternary Catchment J21A in the Gamka River Primary Catchment (J2). It falls under the Gouritz water management area (WMA) which is regarded as the largest WMA in the Western Cape, covering a surface area of 53 139 km² (DEADP, 2011) as indicated by Figure 3.1.

3.3 Climate

3.3.1 Rainfall

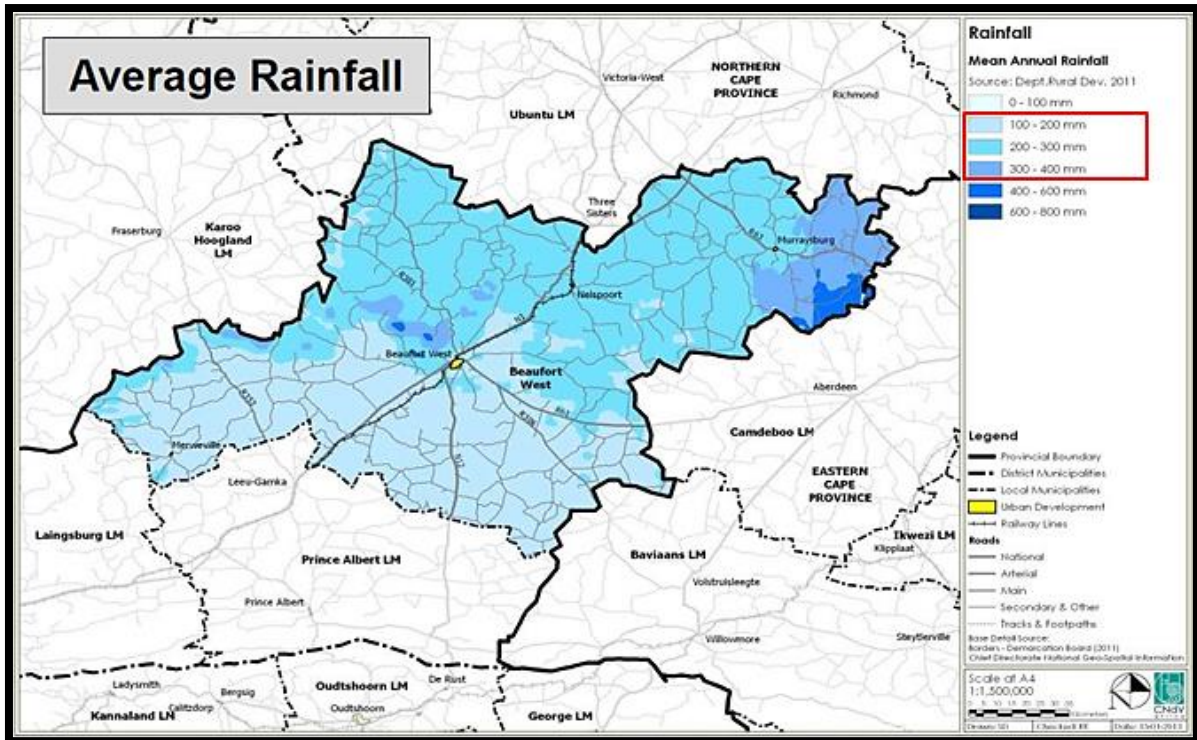
The climatic conditions at Beaufort West, as stated in Campbell (1980) and the Gouritz WMA report (DEADP, 2011), are arid to semi-arid with little or no rainfall. More rainfall may be experienced during summer months than during winter months. The Gouritz WMA report (DEADP, 2011) further stated that the average rainfall that can be experienced in this area is 225 mm/a with a surface water evaporation rate of 2 000 mm/a (Campbell, 1980). Figure 3.2 shows that the mean annual rainfall ranges between 100 mm and 400 mm at Beaufort West (Beaufort West Municipality, 2013).



Source: Modified from the Gouritz WMA report (DEADP, 2011).

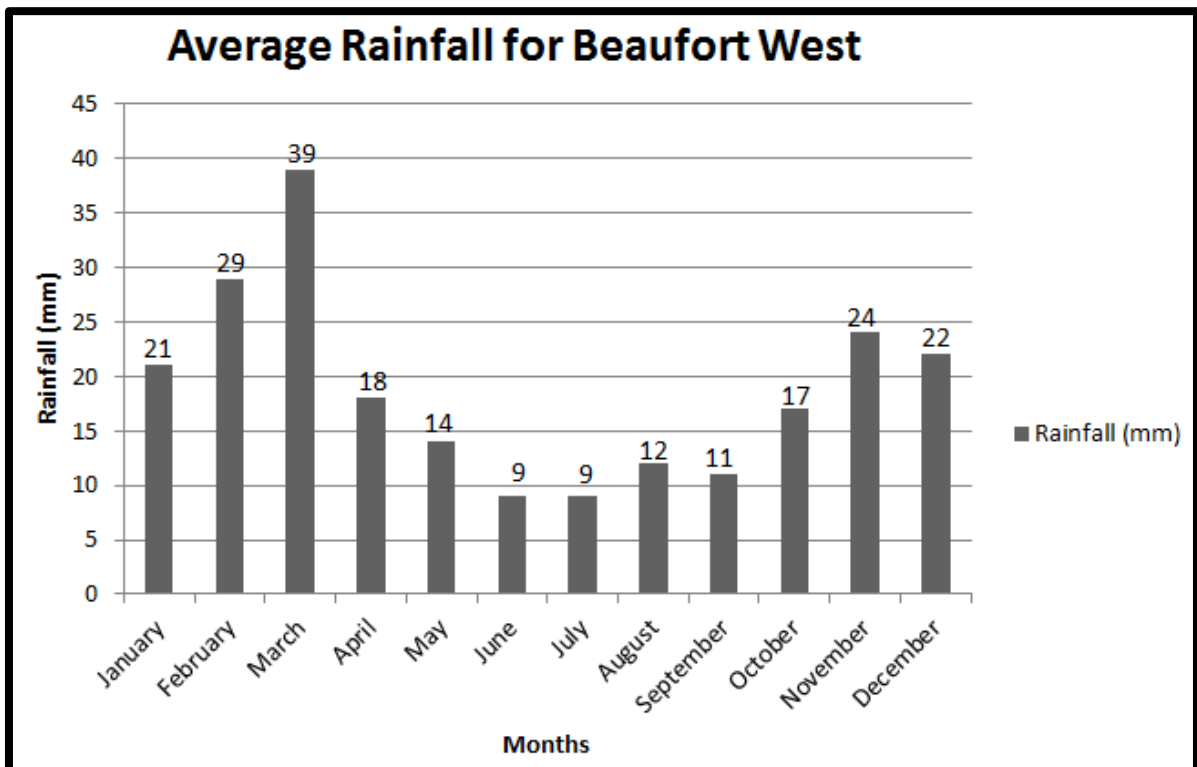
Figure 3.1: Gouritz water management area map showing different catchments and their respective Quaternary catchments

The variation in the annual rainfall at Beaufort West is indicated in Figure 3.3. The graph further shows that the lowest precipitation is normally experienced in June with an average of 9 mm (driest month), whereas the highest precipitation is experienced in March with an average of 39 mm (Campbell, 1980; ClimateData.org). The variation between the precipitation and evaporation rates per year simply indicates how dry the area can be throughout the year.



Source: Modified from Beaufort West Municipality (2012/2013).

Figure 3.2: Rainfall map of part of the Western Cape Province indicating the mean annual rainfall in millimetre

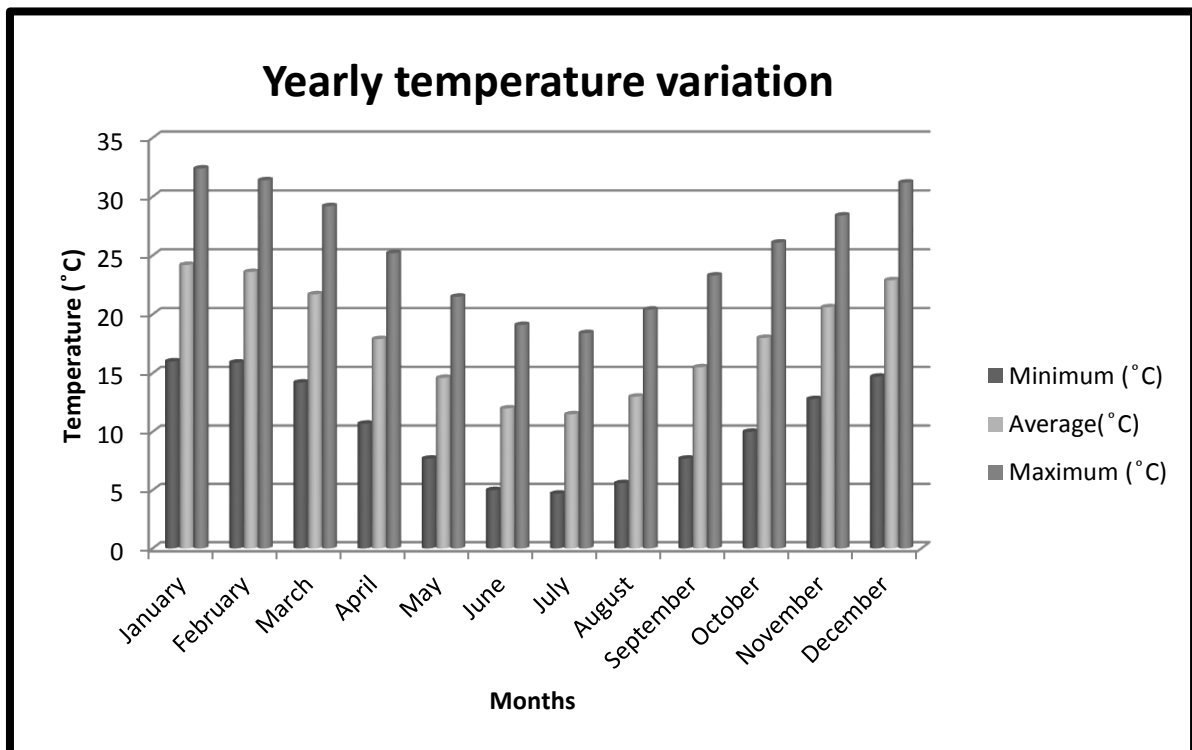


Source: Created from ClimateData.org.

Figure 3.3: Graph indicating the average rainfall for Beaufort West area in months

3.3.2 Temperature

Figure 3.4 shows the variation in temperatures throughout the year at Beaufort West. The summer months can be extremely hot in a way that during the hottest month (January) the temperature can rise up to $\pm 40^{\circ}\text{C}$. Additionally, during the coldest month (July) temperature can drop to 0°C , or rather freezing point, with snow mostly covering the Nuweveld Mountains north of Beaufort West (Campbell, 1980).



Source: Created from ClimateData.org.

Figure 3.4: Temperature variation along the Beaufort West region throughout the year showing minimum, average and maximum temperatures for every month

3.3.3 Vegetation

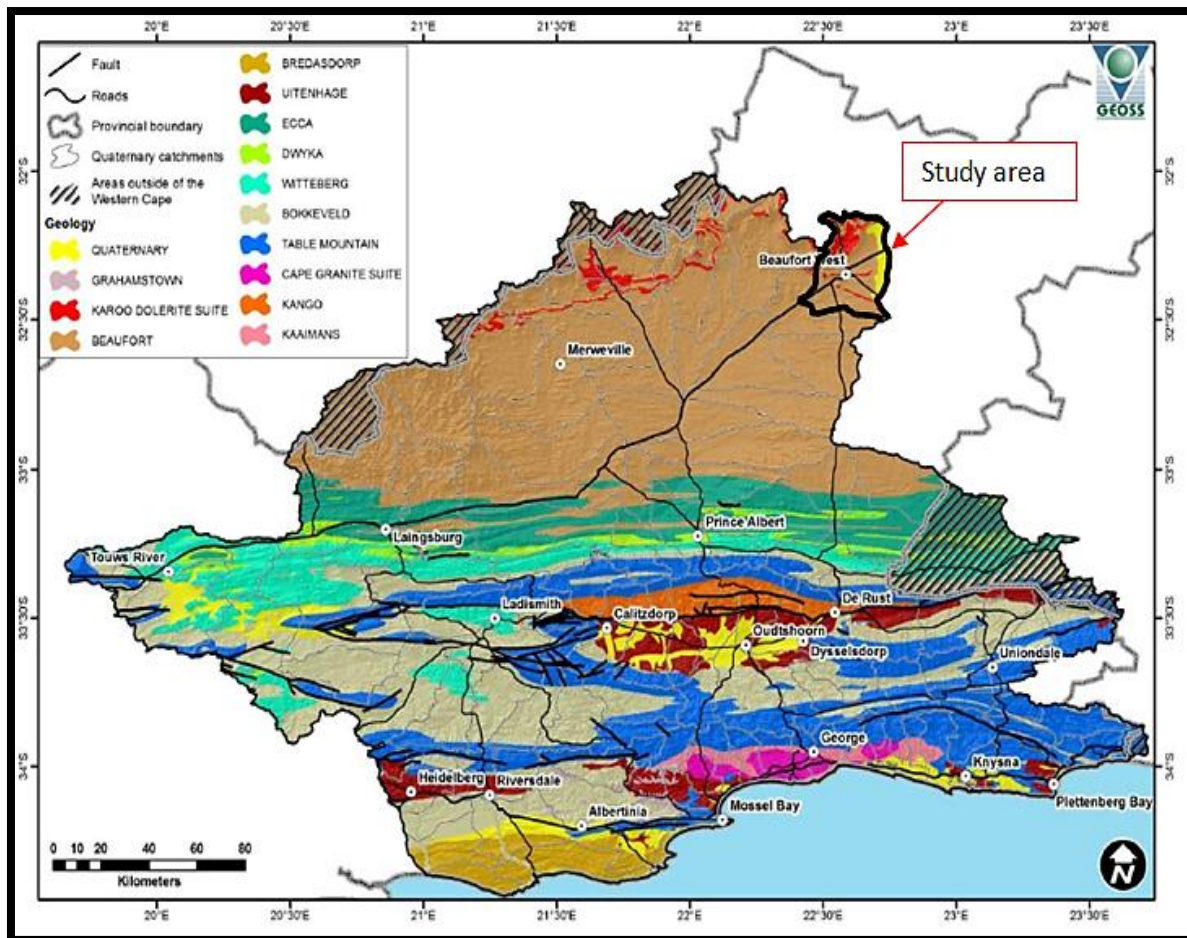
According to the Beaufort West Municipality Annual Review (2013), a total of nine vegetation types are found in the municipal area of Beaufort West. Moreover, the Karoo at large is highly characterised by mesembs ('vygies') and succulents as the main plant types. Hardy acacia as one of the plant types that may be found, is restricted to run-off channels. Amongst the vegetation, the white 'steekgras' (*Aristida congesta*) is the most common of the species in the Beaufort West area (Campbell, 1980).

3.4 General Geology

The Karoo Sequence consists of the Dwyka Group at the bottom, followed by the Eccca Group, Beaufort Group (Figure 3.5) and then Stormberg Group that is overlain by the Drakensberg lavas (Woodford and Chevalier, 2002). All these groups were deposited during different periods of the geological time scale. The deposition of the Dwyka Group occurred during the glacial conditions. The materials eroded by glaciers were deposited into the sea. After the deposition of the Dwyka Group, a basin formed as a result of quick subsidence and this is where dark muds of the Eccca Group were deposited (Praekelt and Nel, 2011; Woodford and Chevalier, 2002). The condition in which the Eccca Group material was deposited is marine. Turner (1981) as well as Woodford and Chevalier (2002) stated that after deposition of the Eccca sediments, the Beaufort Group was deposited during fluvial conditions. Both meandering and braided streams existed and they were characterised by finer argillaceous and arenaceous deposits, respectively.

The Stormberg Group consists of three formations known as the Molteno, Elliot and Clarens. Deposition of the Molteno Formation occurred while the conditions were still fluvial; however, deposition was mostly by braided streams. During the deposition of the Elliot Formation, the conditions had changed to strongly oxidising as a result of the arid climate. Since the climate continued to become more arid, the Clarens Formation was therefore deposited during the semi-desert to desert conditions (Praekelt and Nel, 2011; Woodford and Chevalier, 2002).

The geology of Beaufort West falls under the Beaufort Group of the Karoo Supergroup (Figure 3.5). The Beaufort sediments were third to be deposited under the Karoo basin as described above. They consist mostly of sedimentary rocks such as shale, mudstone, siltstone and sandstone (Turner, 1981; Woodford and Chevalier, 2002). The Beaufort Group is the middle part of the succession and it is the most visible unit along the Karoo basin (Turner, 1981). It is sub-divided into the Upper Tarkastad and Lower Adelaide subgroups of the Permian age within which the area of study falls (Van Wyk and Witthueser, 2011). The Adelaide subgroup consists of two formations, namely the lower Abrahamskraal and the upper Teekloof Formations (Woodford and Chevalier, 2002). These formations comprise of grey, very fine- to medium-grained sandstone and alternating bluish-grey mudstone, and have thicknesses of 1 500-2 000 m and $\pm 1\ 400$ m, respectively (Woodford and Chevalier, 2002).



Source: Modified from the Gouritz WMA report (DEADP, 2011).

Figure 3.5: Geology of the Gouritz water management area, Western Cape

The sediments (siltstone, mudstone and sandstone) are fractured and display major joints and they are mostly horizontal in their positioning. Campbell (1980) explained that these sedimentary facies have subordinate conglomerates. Calcrete (secondary limestone) is found to cover a bigger surface area north of Beaufort West, with alluvium also covering some portion of the surface. The sediments in the Adelaide sub-group are lithified by chlorite and sericite, with an addition of carbonates, iron oxides, feldspar (content >25% total composition) and quartz. Accessory minerals that may be found are biotite, muscovite, epidote and zircon (Campbell, 1980). Furthermore, the Karoo sequence primarily consists of sedimentary minerals such as calcite, pyrite, K-feldspar, quartz and minor amounts of Na-plagioclase and gypsum in arid soils (Woodford and Chevalier, 2002).

Figure 3.5 also indicates that the Beaufort Group on the far north of Beaufort West and the rest of its north-western direction was intruded by the Karoo Dolerite Suite. The Gouritz WMA report (DEADP, 2011) highlighted that the major dolerite dykes that outcropped in the north of Beaufort West determine the flow direction of groundwater. Dolerite dykes and sills

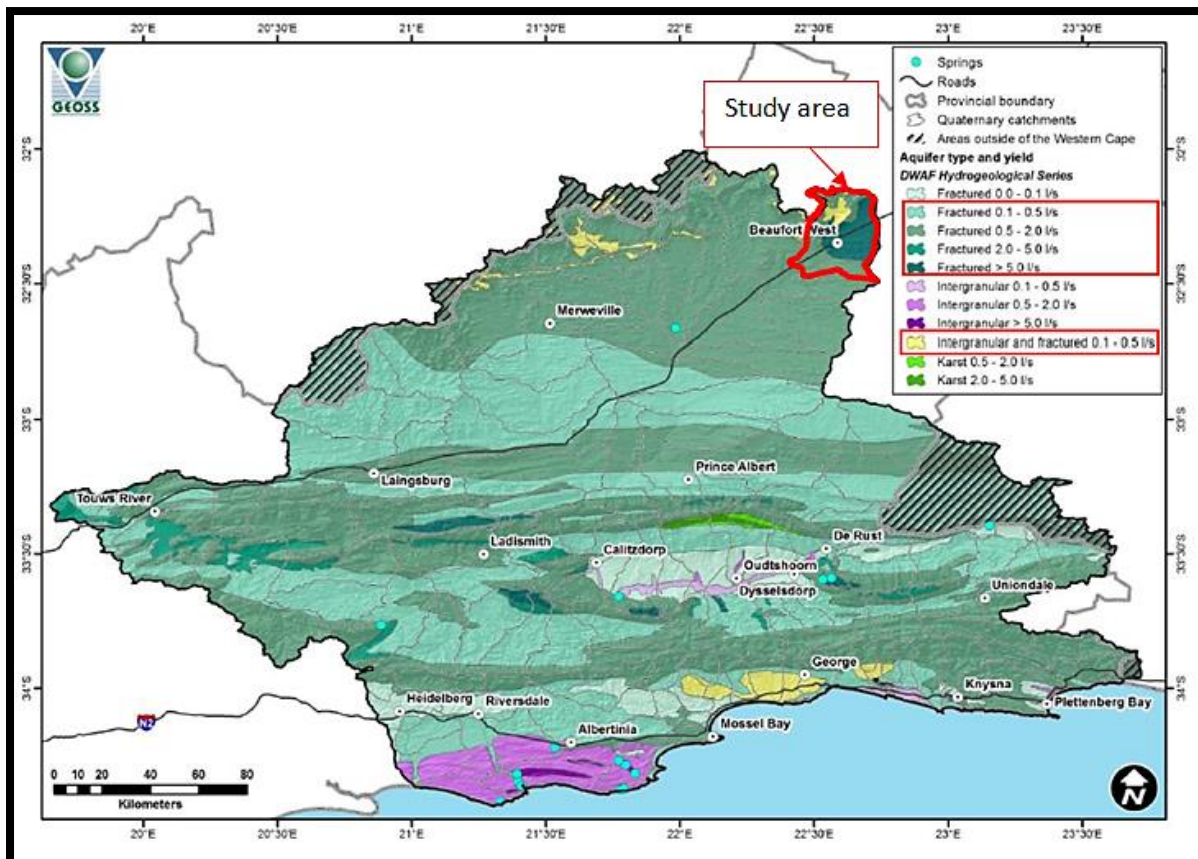
that intruded the area resulted in alteration of the geology since they are composed of clinopyroxene and more calcic plagioclase feldspar.

According to Van Wyk and Witthueser (2011), the three main dykes that are found at Beaufort West are, first, an east-west trending dyke that runs from the Nuweveld Mountains and cuts through the Brandwag, Rhenosterkop and Tweeling farms. The second dyke cuts through the town from east to west, and lastly, the Hansrivier trending dyke runs from northwest to southeast. Dolerite sills may be observed at the top of the Nuweveld Mountains acting as thick sheet caps.

3.5 Hydrology

The main aquifer type found in the Karoo is the Karoo fractured aquifer as indicated in Figure 3.6 (DEADP, 2011; Woodford and Chevalier, 2002). This type of aquifer allows preferential flow to fluids such as water and contaminants that may penetrate through soil into the groundwater systems. The highest yield that is normally experienced in the boreholes drilled through the fractured-rock aquifers is more than 5 l/s (Figure 3.6) in the aquifers towards the south and northeast of Beaufort West (DEADP, 2011). Although for those fractured aquifers with low porosities the yield is between 0.1 l/s and 0.5 l/s (Figure 3.6). The sedimentary units that are found here therefore have a very low primary porosity and permeability. The sediments decrease in their primary porosity with depth as a result of lithostatic pressures and temperature (Woodford and Chevalier, 2002).

Van Wyk and Witthueser (2011) defined another type of aquifer at Beaufort West area to be the intergranular and fractured rock aquifer. This aquifer type is indicated by Figure 3.6 to be at the northern part of Beaufort West, and it is characterised by a yielding capacity of 0.1-0.5 l/s (DEADP, 2011). Additionally, semi-unconfined and semi-confined aquifers were also discovered to be the two main aquifer types at Beaufort West (Campbell, 1980).



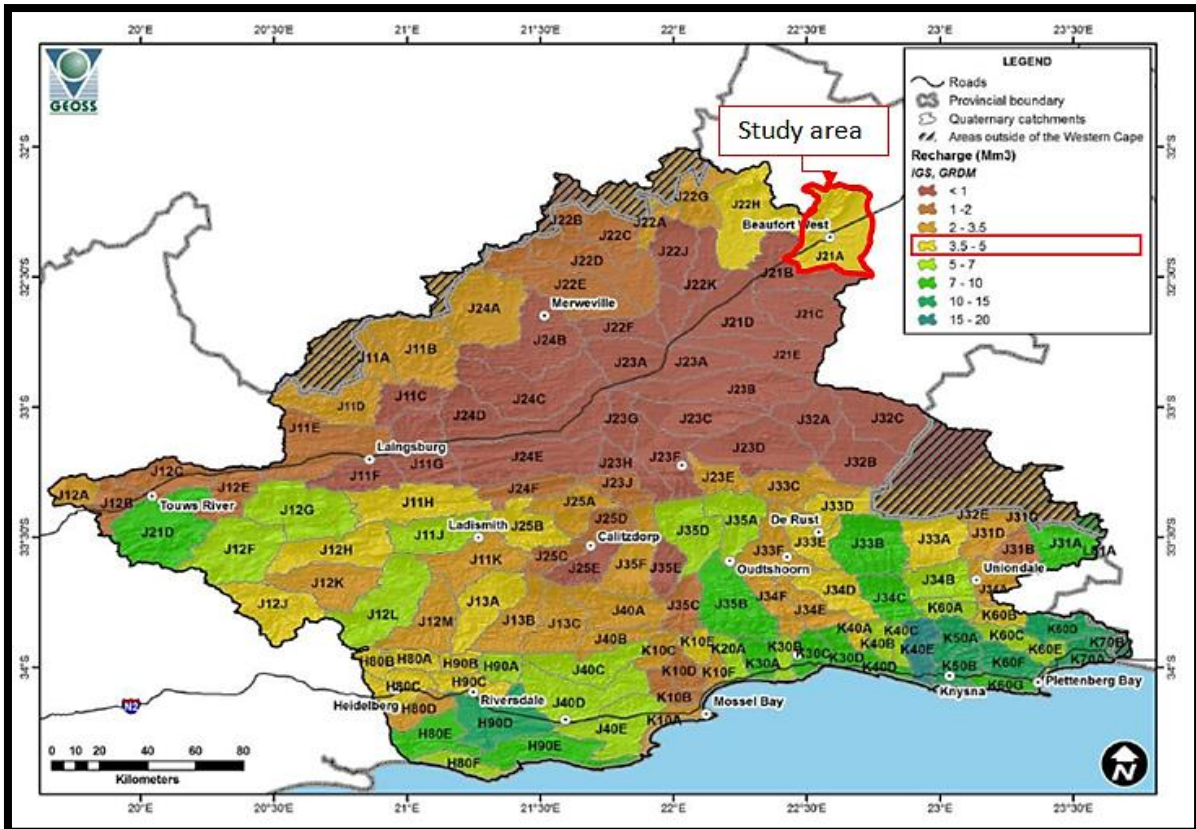
Source: Modified from the Gouritz WMA report (DEADP, 2011).

Figure 3.6: Aquifer types of the Gouritz water management area and their yielding capacities

As a result of weathering of rocks near the earth's surface, Van Wyk and Witthueser (2011) stated that the porosity of the Karoo sediments becomes high as compared to those at lower depths. Consequently, the storage capacity of formations is very limited because matrix stores water and acts as the supplier to the preferential pathways (Campbell, 1980). The recharge into the groundwater system appears to be very low as a result of the evaporation rate being higher than the precipitation rate in this area. Campbell (1980) mentioned that the highest groundwater levels in the Central Karoo are recorded in July, whereas the lowest are recorded in December.

3.6 Groundwater Recharge

Recharge into the groundwater system can be described looking at the volume of water that enters the groundwater system from different sources.



Source: Modified from the Gouritz WMA report (DEADP, 2011).

Figure 3.7: Gouritz water management area recharge map for Quaternary catchments and variations in their recharge

In Beaufort West, recharge occurs from rainfall along the drainage systems, from run-off that occurs on the edges of the Nuweveld Escarpment (Campbell, 1980) as well as run-off along the entire area. Figure 3.7 indicates recharge ranging volumes per Quaternary catchment in the Gouritz WMA (DEADP, 2011). Nevertheless, the focus for this research lies on Quaternary catchment J21A that has a recharge ranging from 3.5 Mm³ to 5 Mm³ (DEADP, 2011; Van Wyk and Witthueser, 2011). Recharge in this area is high at the northern mountainous side as compared to the lower topography areas.

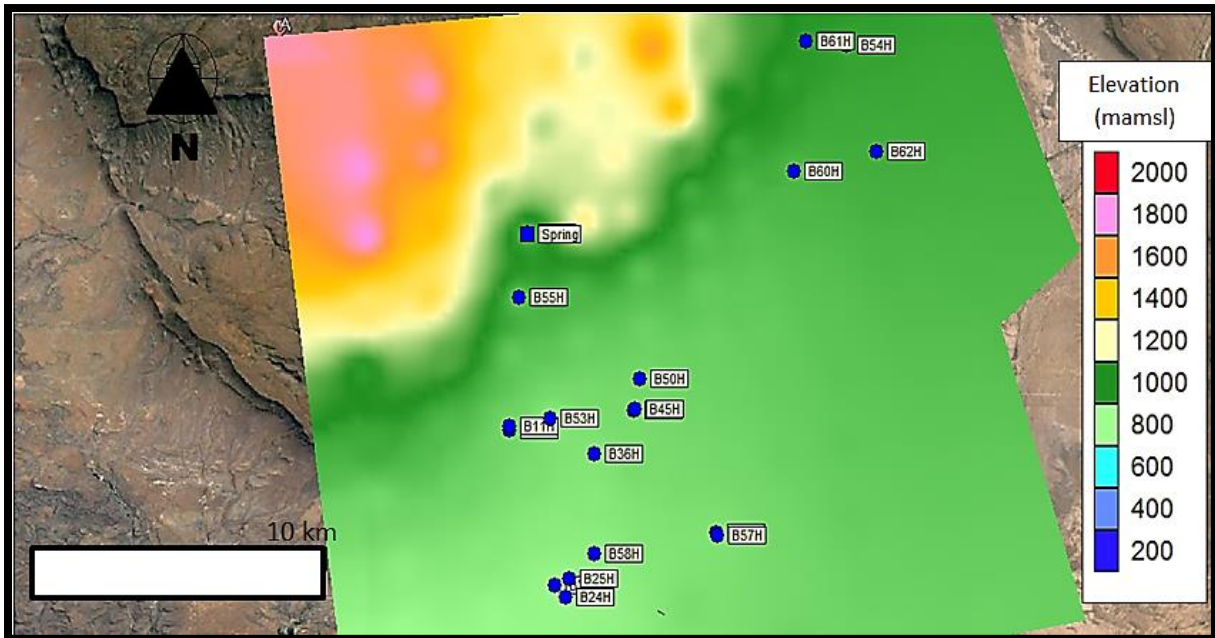
3.7 Elevation Maps

Table 3.1 shows the borehole names together with the respective Global Positioning System (GPS) coordinates. These include the X-, Y- and Z- (elevations) coordinates for each borehole. This is the information that was recorded during the hydrocensus.

TABLE 3.1: GEOGRAPHIC COORDINATES OF THE BOREHOLES MEASURED IN METRE ABOVE MEAN SEA LEVEL

Site Name	Y-coordinates	X-coordinates	Z-coordinates
B10H	-32.341520	22.552170	873
B11H	-32.339946	22.552315	867
B22H	-32.396890	22.566120	810
B24H	-32.401533	22.570283	810
B25H	-32.395250	22.572917	814
B36H	-32.352810	22.589290	843
B44H	-32.339060	22.608960	862
B45H	-32.338966	22.609396	860
B50H	-32.328600	22.612670	868
B53H	-32.338830	22.570800	832
B54H	-32.220317	22.719083	961
B55H	-32.295550	22.561520	911
B56H	-32.384835	22.641169	850
B57H	-32.385865	22.641121	848
B58H	-32.387600	22.585410	826
B59H	-32.273690	22.567750	939
B60H	-32.262170	22.690570	925
B61H	-32.217460	22.700730	979
B62H	-32.258130	22.728290	945
Spring	-32.273970	22.568170	947

The X- and Y-coordinates in Table 3.1 were used to locate the boreholes on a Google earth map (Figure 3.8). The map indicates the distribution of the boreholes in the study area and it only shows boreholes that are discussed in this study. Figure 3.8 further shows boreholes B61H and B54H to be located at the highest elevation as compared to the rest of the boreholes on the map. Conversely, B24H and B22H are situated at the lowest elevation. A legend indicates how the elevations decrease from the high topography to the flat area.

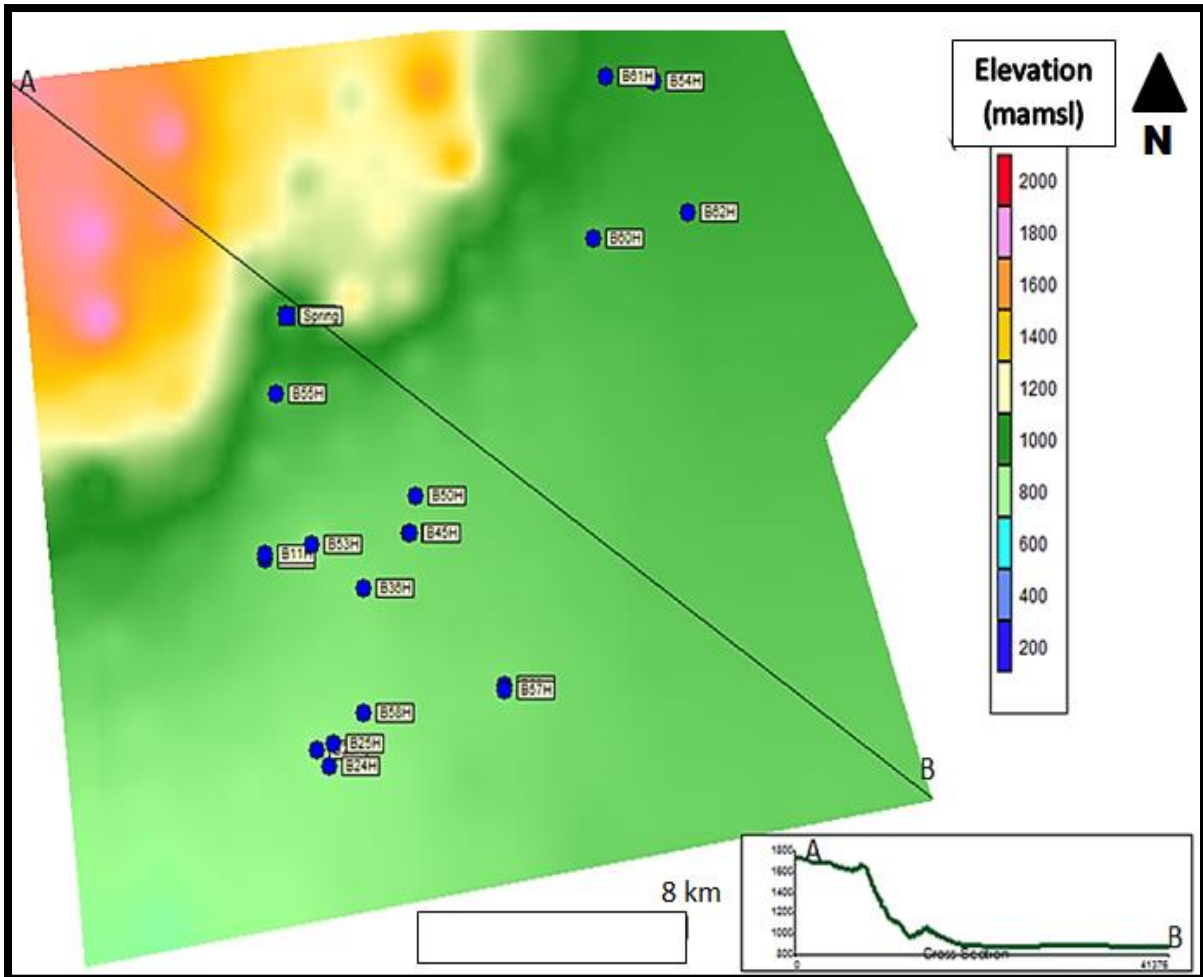


Source: Google earth (2016).

Figure 3.8: Elevation contour map around the study area

The following maps (Figure 3.9 and Figure 3.10) indicate the topography, elevation and cross section at the study area.

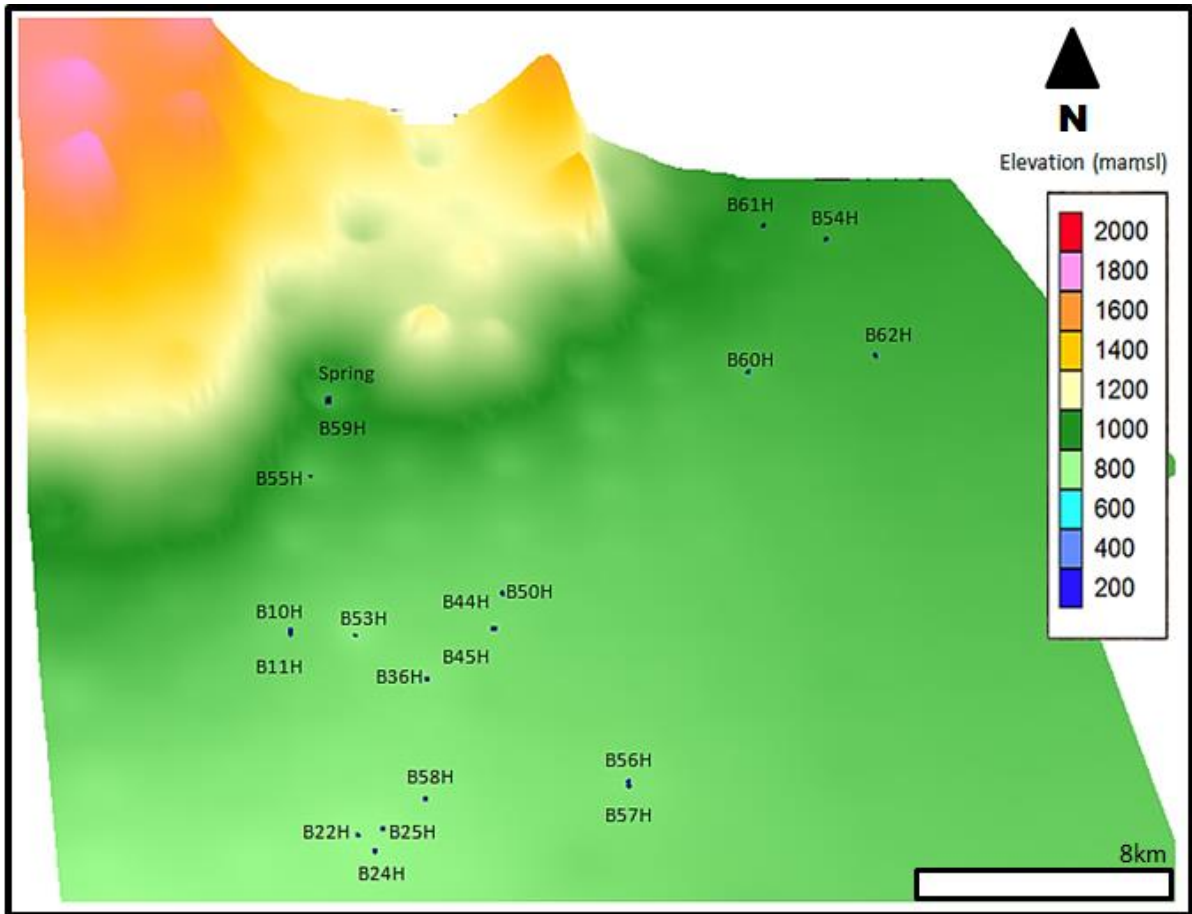
The elevation map may serve as an indication of certain geological features such as rivers, dams, valleys and mountains. It may also be used to indicate the source of recharge if features such as rivers and drainage systems are located. Lastly, at areas where the groundwater flow direction follows the topography, elevation may be used to infer the groundwater flow direction. Beaufort West town is highly characterised by a flat topography with an elevation ranging between 800 m to 900 m (green area, Figure 3.9). The mountainous area is indicated by a yellow-pink colour and has a higher elevation (1 200-1 900 mamsl). The cross-section is indicated in Figure 3.9 for the map. The polyline (A and B) that cuts through the map was used to generate the cross-section that is displayed on the map. The line was drawn to indicate the variation in elevation with topography from one point to another. Figure 3.9 shows that the elevation decreases from point A to point B.



Source: Author's own (2016).

Figure 3.9: Cross sections for the study area with lines cutting through the contour maps showing the variations in elevation

A three-dimensional image of the ground surface elevation of the study area is displayed in Figure 3.10. The mountains and flat area are outstanding on the map as clearly shown by the topography.



Source: Author's own (2016).

Figure 3.10: A three-dimensional map showing how boreholes are sited with respect to the surface elevation

3.8 Water Levels and Flow Direction

Water levels that were measured in the summer season and the elevation data for the respective boreholes were used to calculate the hydraulic heads to determine the groundwater flow direction (Table 3.2). The reason for specifically using the summer data is because during this season water levels were measured for many boreholes as compared to what was measured for the other seasons. A total of 20 borehole water levels were measured, whereas for other seasons less than 10 boreholes were measured. However, this water level data also includes the boreholes that are not considered as part of the discussions for this study because they were only sampled during one season.

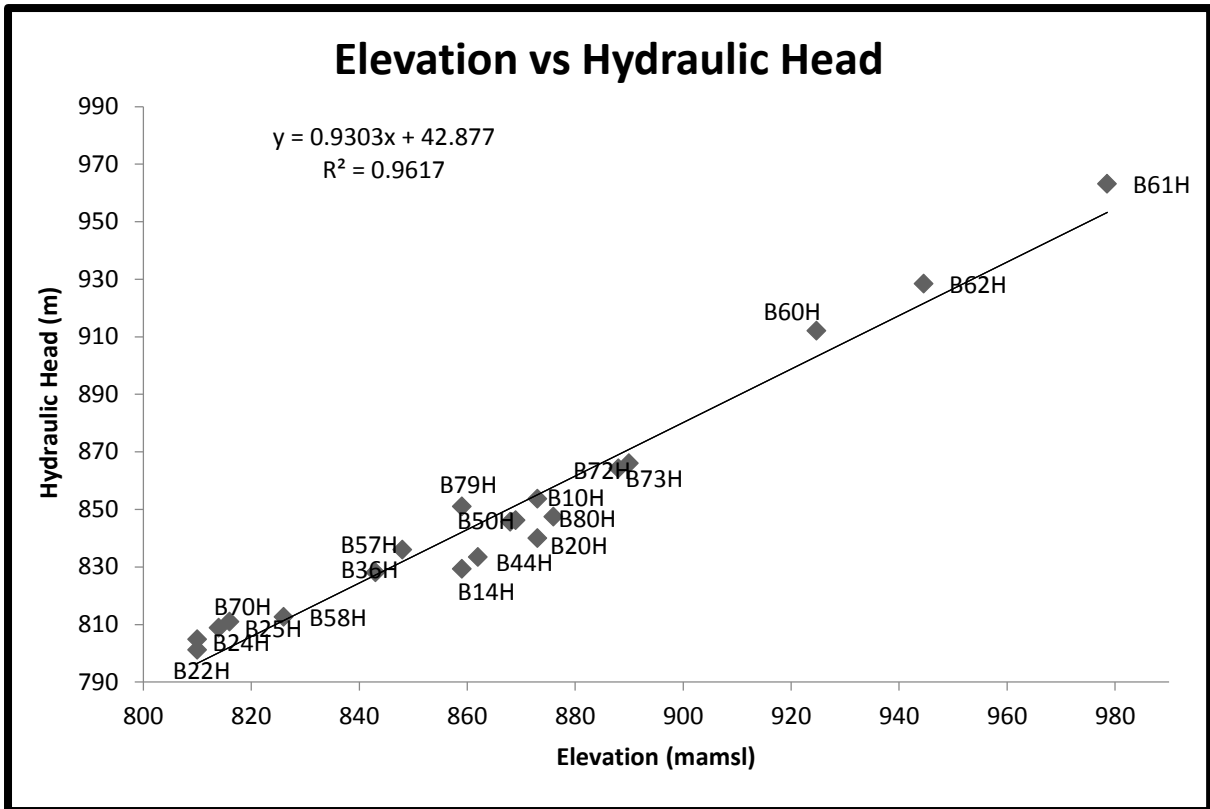
TABLE 3.2: STATIC WATER LEVEL, ELEVATIONS AND HYDRAULIC HEADS FOR 20 BOREHOLES FROM THE SUMMER SEASON

Site Name	Static water level (mbgl)	Elevation (mamsl)	Hydraulic Head (m)
B10H	19.37	873	853.63
B22H	8.92	810	801.09
B24H	5.20	810	804.80
B44H	28.64	862	833.36
B50H	22.35	868	845.66
B25H	5.19	814	808.81
B58H	13.43	826	812.57
B57H	12.04	848	835.96
B36H	15.00	843	828.00
B14H	29.71	859	829.29
B48H	22.89	869	846.11
B72H	24.00	890	866.00
B20H	33.05	873	839.95
B73H	23.86	888	864.14
B70H	5.13	816	810.87
B60H	12.70	925	912.04
B61H	15.46	979	963.08
B62H	16.12	945	928.42
B80H	28.61	876	847.39
B79H	8.00	859	851.00

Note: mbgl – metre below ground level; mamsl – metre above mean sea level; m – metre

Data from Table 3.2 was used to plot Figure 3.11. This is a correlation plot of hydraulic heads against the elevation. The graph shows a high linear correlation between hydraulic head and elevation ($r=0.98$). This high linear correlation between ground surface and topography shows that groundwater flow at the study site generally follows the topography. It will therefore be expected that groundwater would flow from the mountains towards the town.

Van Wyk and Witthueser (2011) also stated that the general groundwater flow at this area is from north to south, with higher water levels in the Nuweveld escarpment where higher recharge occurs as compared to the south. This is exactly what is indicated by the calculated hydraulic heads.



Source: Author's own (2016).

Figure 3.11: A graph showing elevation and hydraulic heads for some of the boreholes in Quaternary catchment J21A for the data that was collected in summer 2016

3.9 Groundwater Uses

3.9.1 Borehole usage and depths

Boreholes at the Beaufort West area have different purposes. They can either be for monitoring, production or abandoned when it is an old production or monitoring borehole. Other boreholes were drilled, but because there was no water strike intersected during drilling, the boreholes were of no use and were therefore closed. There are also boreholes that are blocked with rocks, thus they too are of no use.

Monitoring boreholes are either of the Beaufort West Municipality or the Department of Water Affairs and Sanitation (DWS). These are used to monitor the influence of contamination to the groundwater quality, and also to determine the water flow direction from measured water levels. Monitoring boreholes can also be used to check the position of main fractures in the aquifers, to determine the sustainable yield of certain boreholes by performing pump tests, and to monitor any change in the groundwater quality over time. The purposes of all the boreholes as well as the spring that were sampled for this study are indicated below:

- ❖ Boreholes B11H, B14H, B36H, B45H, B48H, B53H, B54H, B56H, B57H, B59H and B72H are active production boreholes that supply water to the Beaufort West community.
- ❖ Boreholes B25H and B58H are production boreholes; however, unlike the rest of the production boreholes, their water is chlorinated first before it can be supplied to the community.
- ❖ Boreholes B20H, B60H, B61H and B62H, B70H, B73H, B79H and B80H are DWS monitoring boreholes.
- ❖ Boreholes B10H, B24H and B44H are municipal monitoring boreholes.
- ❖ Borehole B50H is one of the abandoned active production boreholes.
- ❖ The spring is also abandoned.

Table 3.3 indicates the depth of the boreholes that were sampled. Depths at some boreholes were not measured due to circumstances beyond control of the samplers. These values are used to indicate the depth to which each borehole was drilled.

TABLE 3.3: SITE NAMES AND THEIR RESPECTIVE DEPTHS IN METRE BELOW GROUND LEVEL

Site Name	Depth (mbgl)
B10H	53.68
B11H	Depth not measured
B22H	62.01
B24H	62.01
B25H	62.20
B36H	Depth not measured
B44H	36.24
B45H	78.00
B50H	59.88
B53H	Depth not measured
B54H	110.00
B55H	85.00
B56H	130.00
B57H	108.00
B58H	75.00
B59H	91.44
B60H	56.90
B61H	85.19
B62H	88.94
Spring	Depth not applicable

3.9.2 Current groundwater use

Most of the information on the current groundwater use was provided by Mr Johan Koorzen who works for the Beaufort West Municipality, whereas some of the uses at various areas were known during the hydrocensus. Groundwater from the active production boreholes is supplied to the community of Beaufort West. This water is used for domestic purposes such as drinking, cooking, bathing, washing clothes and cleaning. Furthermore, groundwater is also used for agricultural purposes and recreation. The production borehole at the golf course (B53H) also supplies water to the community; however, the water is also used for watering the golf course. The production borehole at Bulkraal (B55H) inside the Karoo National Park supplies water to fill up the swimming pool, to water the garden and also supply water to the community and the National Park. Raw groundwater from some of the boreholes is first chlorinated before it is piped into the supply tank and then to the community for usage. This is because the water contains white suspensions even after purging.

3.10 Conclusion

This chapter focused on discussing the climate (including rainfall, temperature and vegetation) of Beaufort West town which is the area of focus for this study. It then looked at the general geology of the study area and the Karoo Supergroup. The chapter further described the hydrology of the study area as well as the recharge at various areas along the Gouritz WMA, including Quaternary catchment J21A, which was the main focus for this study. Elevation maps at this area and the inferred direction of the groundwater flow were discussed and were indicated on the maps. This chapter concluded by discussing the current groundwater uses.

Chapter 4

Methods and Materials

4.1 Introduction

This chapter focuses on the description of the methodology that was followed during analysis of the results. This chapter is divided into eight sections written in order of collection data in the field, laboratory analysis, checking the reliability of data by calculating the ion balance errors, classification of the water types, water-rock interaction, geochemical modelling, statistical analysis and assessing the quality of groundwater for certain uses. The methodology is described for all the hydrogeochemical tools applied and includes groundwater sampling.

4.2 Field Data Collection

Hydrocensus was conducted at the field whereby background information about all the sampling sites and boreholes was collected. The first groundwater samples were also collected at these boreholes during the same season that the hydrocensus was done. Sample collection for inorganic chemistry analysis started in November 2015 (spring season). The sampling was carried out seasonally such that the second sample collection was done in February 2016 (summer season) and the last one in May 2016 (autumn season)

4.2.1 Hydrocensus

A hydrocensus of the study area (Quaternary Catchment J21A of Gamka (J2) sub-basin 2 at Beaufort West, Western Cape) indicated in Figure 3.1, was carried out and information about the area was recorded. This was done during the first field visit that took place in November 2015. During hydrocensus, existing boreholes (accessible and non-accessible) and the spring were noted. Basic information about the areas that were visited was captured. This included geographic coordinates (recorded by a GPS), pictures, borehole description (depth, collar height, accessibility of borehole, production or monitoring, municipal, communal or DWS boreholes). A measuring tape was used to measure the depth and collar height of each borehole. In addition to the measuring tape, a rope hooked to a one-litre plastic bottle filled with soil was also used in measuring the depth of the boreholes. Basic information was recorded for each borehole within the catchment regardless of their distribution.

4.2.2 Groundwater sampling

Groundwater sampling and storage was done, following the sampling procedure suggested by Weaver *et al.* (2007). Representative samples were collected from accessible boreholes, as well as the spring in the study area. Sampling was conducted during three yearly seasons, namely spring, summer and autumn. A total of 27 boreholes and a spring were sampled during the first sampling that was conducted in the spring season. During the second sampling that was done in the summer season, a total of 38 boreholes with an addition of a spring, were sampled. Although 38 boreholes were sampled during this season, 9 boreholes were outside the study area in Quaternary catchment L11F. Lastly, during the autumn season only 13 boreholes were sampled together with the spring. Since some of the boreholes were sampled only once or during one season, they were not used for the analysis because they could not be compared with any results. Therefore, only boreholes that were sampled at least during two seasons were used for analysis of results. Due to circumstances beyond control, only 14 samples were collected during the autumn season. Out of the 14 samples, only 12 were collected from the boreholes that were already sampled in the spring and summer season.

During sample collection, the following parameters were measured and recorded from the samples: temperature, EC, TDS, dissolved oxygen (DO), oxidation-reduction potential (ORP) and pH. Water levels were also measured in boreholes that were accessible. The parameters were recorded using an In-Situ[®] Inc. smarTROLL Multiparameter Handheld meter. A flow-through cell was used for the measurement of these parameters after it was cleaned with water to be sampled. It was then filled with water and the handheld multiparameter was lowered inside. Before taking the recordings, the handheld multiparameter was always allowed sufficient time so that it could stabilise. This was done to ensure consistency in the results. After the measurements were recorded for each sample, the handheld multiparameter was cleaned with deionised water.

Prior to purging of boreholes which were accessible, static water levels were measured using a deep meter. The static water levels were used to calculate the hydraulic heads that helped in determining the general groundwater flow direction. Furthermore, purging was performed before a sample was collected at a particular borehole. This was accomplished to introduce water straight from the aquifer into the boreholes so that the collected samples were representatives of water from the aquifer. The removal of water was done differently depending on the condition of the borehole. Production boreholes were pumped for at least five minutes before samples were collected. Contrariwise, the open boreholes were purged

by either a low-flow bladder pump or a plastic bailer. Figure 4.1 indicates some of the sites that were visited for sampling.



Source: Author's own (2016).

Figure 4.1: Field pictures showing an overview of some sites visited as well as the sampling methods used

The sampling methods that were followed are also displayed in the pictures. Samples were collected from tap outlets (Figure 4.1A), using a bailer (Figure 4.1B) and using a low-flow bladder pump (Figure 4.1C). The 500 ml glass bottles and 350 ml polyethylene bottles were used to store the samples. Sample names were marked with a permanent marker on the sampling bottles. Prior to filling of the bottles, they were rinsed with deionised water and then with water to be sampled. Bottle caps were removed before collecting the water sample. The sampler used rubber gloves to avoid contamination to the sample. Immediately after filling the bottles they were closed and caps were tightened securely to guard the samples from atmospheric gases.

4.2.3 Sample storage and transport for chemical analysis

Immediately after sampling, the samples were placed in cooler boxes with ice packs to keep it cool; the cooler boxes also protected the samples from exposure to the sun. The samples were transported to the laboratory at least within 72 hours. Before they could be delivered to the laboratory, samples were kept in a refrigerator at temperatures below 4 °C.

4.3 Laboratory Analysis

All the groundwater samples collected in the field were transported to the laboratory where inorganic chemical analysis was done for different parameters. The laboratory that was used for sample analysis is the inorganic laboratory of the Council for Scientific and Industrial Research (CSIR) in Pretoria, South Africa. In the laboratory, analysis was done for 35 parameters which included the major and minor or trace ions, as well as TDS, EC and pH.

4.4 Data Quality and Reliability Check

The results that were received from the laboratory after analysis for inorganic chemistry were checked for their reliability and accuracy. Raw groundwater chemistry data from the laboratory was converted from mg/l to meq/l in order to substitute the values in Ratio 5.1. The Ion Balance Error (IBE) was then calculated for all three seasons. Samples that indicated an IBE of $\pm 5\%$ were considered acceptable or accurate. On the other hand, there were samples that had an IBE greater than 10% and these were regarded as unreliable.

4.5 Water Type Classification

The groundwater chemistry data was organised in a Microsoft Excel file into a Windows Interpretation System for Hydrogeologists (WISH) format. The WISH data file was loaded into the WISH windows program. Piper and Stiff diagrams were therefore automatically

generated by this program. The diagrams were used to interpret the water types displayed. Piper diagrams were used to group water samples in such a way that those that are closely related are grouped together, resembling the same water type. On the other hand, Stiff diagrams were used to deduce the source rocks in addition to the water types.

4.6 Water-Rock Interaction

4.6.1 Stoichiometric analysis

Since the concentrations of major ions are normally reported in mg/l units in the raw groundwater chemistry data from the laboratory, they were converted to milliequivalents per litre (meq/l) and silica to millimole per litre (mmol/l). The data was converted to make meaningful chemical combinations during the deductions of mineralogy and reactions along the area, as well as in water quality parameter calculations. As stated by David and Pyne (1995), this is done because meq/l units incorporate the charge together with the atomic mass units of all the calculated ions, thus normalisation by ionic charge is required. Furthermore, mmol/l places into account the atomic weight only. On the other hand, mg/l gives the total concentrations for specific ions relative to the solution.

Ratios 4.1 to 4.4 from Hounslow (1995) were used to come up with the deductions on the possible hydrogeochemical processes. The converted concentrations (meq/l) for each borehole of all the seasons were substituted in the expressions. The results obtained after substitution in Ratios 4.1 to 4.4 gave insight on the possible hydrogeochemical processes within the aquifer system. Again, since the calculations were done for each borehole, the location where the processes were taking place or dominating along the flow path was indicated.

The occurrence of silicate and/or carbonate weathering in the aquifer system was checked by Ratio 4.1. A general assumption on chemical weathering based on Ratio 4.1 as described by Hounslow (1995), explains that if carbonate weathering was taking place within the system, a ratio of >10 is obtained during the calculations. On the other hand, a ratio of <5 will be calculated if there was silicate weathering; and lastly, a ratio >5 and <10 will be calculated for further analysis.

$$\frac{\text{HCO}_3^-}{\text{SiO}_2} \quad (4.1)$$

The HCO_3^- and SiO_2 concentration values in meq/l and mmol/l, respectively, were substituted in Ratio 4.1, and the results indicated the occurrence of either carbonate or silicate

weathering. There were samples that gave the results that indicated neither carbonate nor silicate weathering and they were considered for further analysis.

Ratio 4.2 was applied to identify silicate weathering, although specifically for plagioclase minerals such as albite and anorthite. Hounslow (1995) stated that the explanation behind Ratio 4.2 is that if the calculated ratio is <0.2 or >0.8 it means it is rare that plagioclase weathering took place, whereas if the ratio is >0.2 and <0.8 , then there is a possibility that it did take place.

$$\frac{\text{Na}^+ + \text{K}^+ - \text{Cl}^-}{\text{Na}^+ + \text{K}^+ - \text{Cl}^- + \text{Ca}^{2+}} \quad (4.2)$$

The ion values of Na^+ , K^+ , Ca^{2+} and Cl^- in meq/l were substituted in Ratio 4.2. The results obtained after the use of this expression showed either the possibility of plagioclase weathering or no possibility within the aquifer system.

The examination of calcium and sulphate by Ratio 4.3 was to check the possible origin of these ions in solution. The occurrence of gypsum dissolution was also tested by this approach. Hounslow (1995) explained that ratios calculated after the application of Ratio 4.3 may show the following: A calculated ratio of 0.5 indicates the occurrence of gypsum dissolution and a ratio of <0.5 with a pH of <5.5 may show pyrite oxidation. Additionally, a ratio <0.5 and a neutral pH may show the removal of calcium by ion exchange or calcite precipitation; and a >0.5 ratio indicates calcium sources other than gypsum. The sources can be carbonates or silicates.

$$\frac{\text{Ca}^{2+}}{\text{Ca}^{2+} + \text{SO}_4^{2-}} \quad (4.3)$$

The converted concentrations (meq/l) of calcium and sulphate were substituted in Ratio 4.3. Some of the ratios calculated indicated the occurrence of gypsum dissolution, whereas some showed carbonates to be the source of calcium.

Ratio 4.4 was used to check whether the process of ion exchange and reverse ion exchange took place in changing the groundwater chemistry. Ratio 4.4 was taken from Hounslow (1995) and can be explained as follows: If the calculated ratio becomes 0, halite dissolution is assumed; whereas, if the ratio is <0.5 with TDS >500 mg/l it could be an indication of water from brines or connate sources where reverse ion exchange was experienced. Lastly, if the ratio is <0.5 with a TDS <50 mg/l it will be a good indication of rainwater. This is because rainwater does not have dissolved solids, except that it interacts with carbon dioxide in the

atmosphere making it acidic; hence, a <50 mg/l TDS (Alizadeh, Ghaneian and Motedayen, 2011).

$$\frac{\text{Na}^+}{\text{Na}^+ + \text{Cl}^-} \quad (4.4)$$

The concentrations of Na^+ and Cl^- in meq/l were substituted in Ratio 4.4, whereby the obtained ratios of $\text{Na}/\text{Na}+\text{Cl}$ indicated the occurrence of either ion or reverse ion exchange in the groundwater system.

Furthermore, the assumed hydrogeochemical processes when using Ratio 4.1 to Ratio 4.4 were used to come up with the hydrochemical reactions that have taken place to give out the respective ions in solution (Section 5.4.1). Nonetheless, additional tools such as bivariate correlation plots, geochemical modelling and principal component analysis were also used to confirm the hydrogeochemical processes that were assumed by stoichiometric analysis.

4.6.2 Bivariate plots analysis

The converted groundwater chemistry data (meq/l and mmol/l) was used to plot the bivariate graphs (Section 5.4.2). As the possible occurring minerals in the study area have been understood from literature, the ions that were involved during the formation of these minerals were correlated for all three seasons. These helped in understanding the possible processes that influenced the groundwater chemistry. Furthermore, the sources of the ions were also identified.

A linear correlation scatter plot was done for Ca versus alkalinity (Figure 5.5) to identify the source of calcium and bicarbonate. An explanation behind this correlation graph is that if the source is calcite dissolution, a ratio of 1:2 will be obtained; whereas, if the source is dolomite dissolution, a ratio of 1:4 will be calculated (Garrels and Mackenzie, 1971). Another linear correlation plot of Ca versus Mg (Appendix 3) was done to identify the dissolution of carbonates in solution. A Ca/Mg ratio was calculated such that a ratio of 1 indicated the dissolution of pure dolomite in the groundwater, whereas a Ca/Mg ratio of >1 and <2 indicates calcite dissolution (Maya and Loucks, 1995). Kozlowski and Komisarek (2016) stated that if the Ca/Mg ratio is more than two, dissolution of silicate minerals is taking place.

Plotting of Ca versus SO_4 (Figure 5.6) showing a linear trend was also done to identify the occurrence of gypsum dissolution in the groundwater system. This plot was also used to show if there were other sources of calcium besides gypsum dissolution. The graph shows that if the samples plot above the 1:1 line towards high SO_4^{2-} , the occurrence of gypsum dissolution is indicated. On the other hand, if the samples plot below the 1:1 line, other

sources of Ca^{2+} besides gypsum dissolution are indicated (Jalali, 2007). A correlation plot of $\text{Ca} + \text{Mg} + \text{SO}_4 + \text{HCO}_3$ versus $\text{Na} + \text{K} - \text{Cl}$ (Figure 5.7) was done to check whether dissolution processes of carbonates, gypsum, halite (Jalali, 2007) and cation exchange (Jalali, 2005) are the most important process involved in altering the groundwater chemistry. If these processes fall amongst the most significant ones, a linear plot with a -1 slope is generated.

The graph of K versus Cl was also plotted to check if there was sylvite weathering taking place in the aquifer system (Jalali, 2007). This plot showed a linear correlation between the ions. The occurrence of sylvite weathering was indicated by linear correlation plots with high coefficients ($r > 0.68$) between K and Cl

The occurrence of ion exchange and/or carbonate or silicate weathering and reverse ion exchange in the groundwater was shown by the linear correlation plots of $\text{Ca} + \text{Mg}$ versus $\text{SO}_4 + \text{HCO}_3$ (Figure 5.8). Additionally, dissolution of calcite, gypsum and dolomite may also be indicated on this plot by the samples that lie on the 1:1 equiline (Fisher and Mullican, 1997). The samples that plot above the 1:1 line next to $\text{Ca} + \text{Mg}$ indicate reverse ion exchange. Conversely, the samples that plotted below the 1:1 line next to $\text{SO}_4 + \text{HCO}_3$ indicated ion exchange, carbonate or silicate weathering (Belkhiri *et al.*, 2010). A linear correlation plot of Na versus Cl (Figure 5.9) was also done to further confirm the processes of cation/ion exchange or silicate weathering and to check the occurrence of halite dissolution in the groundwater system. Halite dissolution was indicated by samples that fell on the 1:1 line (Fisher and Mullican, 1997). The samples that plotted below the 1:1 line next to Na^+ represented ion exchange or silicate weathering in the system, while the samples that plotted above the 1:1 line next to Cl^- , showed the removal of sodium from solute by cation exchange (Jalali, 2009).

Lastly, a correlation plot of Na/Cl versus EC (Figure 5.10) was generated to identify if the process of evaporation was one of the main hydrogeochemical processes that took place. In order for evaporation to be assumed, the samples must indicate an increasing trend of EC, whereas the Na/Cl ratio is constant.

After plotting of all these correlations, the strength of the correlations was determined by reviewing the correlation coefficients as stated in Kura *et al.* (2013), who further explained that the correlation plots display the relationship between water variables. The equilines were also used to indicate the strength of the correlations.

4.7 Geochemical Modelling

PHREEQC geochemical modelling software (Parkhurst and Appelo, 1999) was used to calculate inverse geochemical models. These models are used to indicate geochemical reactions that might have taken place throughout the flow paths in the groundwater system, resulting in groundwater chemistry evolution (Belkhiri *et al.*, 2010).

4.7.1 Mineral saturation indices

Groundwater chemistry data for boreholes in all the seasons was entered into the PHREEQC program. This included concentrations for all major ions as well as Si, minor ions (Al, F, Fe and Mn), temperature, density and pH. The model generation was performed separately for each borehole and the output was also acquired for each borehole. The calculation of SI for separate boreholes was to see how the respective samples were saturated in certain minerals within the groundwater and again how the SI results related to results obtained from other tools. The SI output can be explained that if negative values are obtained, they show undersaturation; whereas positive values show oversaturation of minerals with respect to the solution within which they are found.

Appelo and Postma (1996) explained that the direction of the specific process taking place within the system is shown by the saturation state of minerals relative to the water. Thus, for all the minerals that show undersaturation with respect to water, their dissolution will be anticipated, whereas for those that are supersaturated, their precipitation will be expected. This can be noted from the results where some minerals were undersaturated initially and then were dissolved such that the end solution was supersaturated in these phases.

4.7.2 Mass-balance modelling

The mineral phases that were used to develop the mass-balance models are quartz, plagioclase, carbonates, gypsum, biotite and clay minerals (montmorillonite, kaolinite) as per the geology of the study area (Campbell, 1980), together with evaporites halite and sylvite. The following elements were selected to check the occurrence of ion exchange in the system: NaX and CaX₂ where X stands for the exchange site which can either be occupied by a divalent or two monovalent cations (Fisher and Mullican, 1997). Similar to speciation modelling, the input data requires concentrations of major and significant minor ions, pH and temperature in their respective units of measurement. However, for mass-balance modelling, the solutions to be modelled as well as the possible mineral phases are stated. Furthermore, when conducting mass-balance modelling, the uncertainty limits should be specified; otherwise the default limit is used. Uncertainty limit is a value that is specified during

modelling of the mass transfer and specifies that the concentration of each element in a respective stated solution (for example, Solution 1) can only vary up to the specified uncertainty limit. The uncertainty limits are important in PHREEQC since they perform the mole and charge balance for each element and solution respectively, in different simulations (Sharif *et al.*, 2008).

Mass-balance models were developed for various inferred groundwater flow paths whereby two wells were selected to represent Solution 1 and Solution 2. The well at a higher elevation was taken as Solution 1, whereas the well at a lower elevation was taken as Solution 2. An assumption was made that the selected wells were sited along the same flow paths. The uncertainty values used to develop the models, ranged between 2.5% and 18.5%.

The simulations along the inferred groundwater flow path were generated to determine how the water chemistry evolved with elevation. The samples collected at high elevation showed recently recharged water, whereas the chemistry changed as the elevation decreases along the flow paths. Thus, there were processes taking place resulting to this evolution. The selection of solutions was made based on the concept of flow direction. Water samples with a CaHCO₃ composition collected from the spring at high elevation was linked to boreholes towards the southern direction with the assumption that it was the main flow path. The consideration was based on the borehole distribution along the study area, as well as how their hydrochemistry changed. Furthermore, the boreholes that were selected are the ones that have groundwater chemistry data for all three seasons so that the simulations were developed for two periods (first, spring to summer; and second, summer to autumn). Therefore, all the flow paths that had a shortage of data from one season were not considered for these simulations.

The attained models are an indication of reactants and products that led to a chemical composition different from the previous one (for example, Solution 1 was different from Solution 2) (Belkhiri *et al.*, 2010). This output results showed the mole transfer between two waters and it can be interpreted as follows: If the obtained mole transfers for certain mineral phases are negative, precipitation of those minerals from solution is assumed. On the other hand, positive mole transfers indicate the process of dissolution of the respective minerals in solution.

4.8 Statistical Analysis

The IBM SPSS Software program was used to develop the hierarchical cluster plots as well as the PCA. Raw groundwater chemistry data for all the parameters was entered into the

program for each borehole. Prior to generating the cluster plots and principal component analysis, the groundwater chemistry data was standardised using the criterion explained in Davis (1973) as well as Okiongbo and Douglas (2014). Standardisation of the raw groundwater chemistry data was completed to avoid using data with different units, since this would give unreal results.

The groundwater chemistry data was first loaded into the IBM SPSS program and then analysing of the descriptive statistics data was done such that the raw groundwater data was converted to the 'Z-scores' that are regarded as the standardised values. To confirm if the variables have been standardised, the output data should give mean and standard deviation Z-scores of 0 and 1, respectively. Additionally, if the calculated Z-scores are negative, it is an indication that the loaded variables of the raw groundwater chemistry data were less than the mean of the raw groundwater chemistry data. On the other hand, if the calculated Z-score was positive, it indicates that the loaded variable from the raw groundwater chemistry data was bigger than the mean of that data.

4.8.1 Statistical characteristics

The SPSS software program was used to generate the univariate statistical values such as minimum, maximum, mean and standard deviation for all the parameters. The calculations indicated variations in the results, showing which parameters had the highest values or the lowest values in the datasets. The statistical characteristics were obtained for all the three seasons.

4.8.2 Hierarchical cluster analysis

Hierarchical cluster plots (Section 5.5) were developed using the SPSS program after standardising the data. The hierarchical plots generate groups of how samples from different boreholes are related according to the measured groundwater parameters (Kura *et al.*, 2013). The groups were linked to the distribution of samples on the piper diagrams. The relationship (grouping) indicated by the dendrogram always depend highly on the types of parameters used (Belkhiri *et al.*, 2010).

4.8.3 Principal component analysis

The IBS SPSS Software program was used to generate the PCA after standardising of data. A total of 17 parameters were used to generate the analysis such that 17 principal components (PCs) were accumulated after each run. Out of the 17, the PCs with >1 eigenvalue are the ones that were selected for data interpretation since they were

considered significant (Arslan, 2013). Kura *et al.* (2013) as well as Okiongbo and Douglas (2014), explained that these are important because they make a bigger contribution to the total variation. Total variation resulted from all the components that displayed a >1 eigenvalue, unlike a contribution given by a single variable. A Varimax rotation technique was used to calculate the loadings (Okiongbo and Douglas (2014). The loadings that were closer to 1 or -1 were used to understand the results since these indicate the stronger relationship (Dragon, 2006; Okiongbo and Douglas, 2014). Lastly a three-dimensional component plot in a rotated space (Section 5.7.2) was generated to show where the parameters were grouped for the different components axis.

4.9 Assessment of Groundwater Quality

4.9.1 Groundwater quality assessment for irrigation use

The suitability of groundwater for irrigation use was determined by several criteria that were followed to come up with a solid conclusion. Ratio 4.5 to 4.7 formed part of the criteria that were used, since concentrations of ions in meq/l were used for substitution in those expressions. Calculations were done using Microsoft Excel to get the results. Ratio 4.5 is a Sodium Adsorption Ratio (SAR) and it was used to determine the fitness of groundwater for irrigation (Wilcox, 1955). The values of Na⁺ to Ca²⁺ and Mg²⁺ were substituted into Ratio 4.5, and by doing it this way the results obtained indicated how suitable the water is for irrigation. The SAR diagrams were also generated by using the WISH program and these were used to classify the water samples in terms of the sodium and salinity hazards.

$$SAR = \frac{Na^+}{\sqrt{\frac{Ca^{2+} + Mg^{2+}}{2}}} \quad (4.5)$$

The explanation behind SAR is that if the calculated ratios fall between 0 and 10, the water samples are classified as excellent for irrigation use. A range from 10 to 18 represents good water; 18 to 26 show fair water and; lastly, values of >26 show water samples that are poor for irrigation use.

Expression 4.6, which is normally used to calculate the residual sodium carbonate (RSC), was also useful in classification of the water for irrigation (Nazzal *et al.*, 2014).

$$RSC = (HCO_3^- + CO_3^{2-}) - (Ca^{2+} + Mg^{2+}) \quad (4.6)$$

Residual sodium carbonate explains that samples with a value of <1.25 are good for irrigation; 1.25-2.5 are medium and >2.5 are bad for irrigation purposes.

The sodium percentage (%Na) was calculated, and this was done using Ratio 4.7 whereby the concentrations were converted to meq/l. Singh, Janardhana and Ramakrishna (2015) stated that the calculated percentage of sodium may serve as an indication to how suitable the groundwater is for irrigation purposes.

$$\text{Na}\% = \frac{(\text{Na} + \text{K})}{(\text{Ca} + \text{Mg} + \text{Na} + \text{K})} * 100 \% \quad (4.7)$$

A sodium percentage of 0-20 shows that the groundwater is excellent for use; 20-40 is good; 40-60 is permissible; 60-80 is doubtful and >80 is unsuitable.

The residual Mg/Ca ratio was also calculated using the meq/l units. The results of these calculations explain that if the ratio is <1.5, the groundwater is safe to use for irrigation; 1.5-3 shows moderate water; whereas a ratio of >3 shows that the water is unsafe to use for irrigation (Zaidi *et al.*, 2015). The decisions on the suitability of the groundwater for irrigation use were made based on the South African National Standards (SANS), South African Water Quality Guidelines (SAWQG) and the World Health Organization (WHO) standards relative to the results obtained during the calculations.

4.9.2 Groundwater quality assessment for domestic use

The groundwater was also tested for its suitability for domestic use. SANS, SAWQG and the WHO standards were used to conclude on the water suitability for drinking. Making use of the raw groundwater chemistry data in mg/l, the water was classified per parameter. The following parameters were discussed in conjunction with the groundwater standards as already mentioned: pH, TDS, sodium, potassium, bicarbonate, chloride, sulphate, nitrate, ammonia, fluoride, iron and manganese. Effects that may have resulted from unacceptable concentrations of any element were also described.

The TDS standards as stated by WHO (2011) helped in classifying if the water was fresh, brackish or saline. The TDS measured in the groundwater results were compared to the standards. The groundwater with TDS concentrations of <300 mg/l is excellent; 300-600 mg/l is good; 600-900 mg/l is fair; 900-1 200 mg/l is poor; and lastly, water samples with TDS >1 200 mg/l is regarded as unacceptable for domestic use.

In addition to the use of the given parameters, the total hardness (TH) was also calculated to determine if the groundwater was hard or soft. Expression 4.8 which indicates TH was used and this is expressed as CaCO₃ in mg/l.

$$\text{TH (mg CaCO}_3\text{/l)} = 2.497 \times [\text{mg Ca/l}] + 4.118 \times [\text{mg Mg/l}] \quad (4.8)$$

Description of TH for drinking water explains that a range from 0 mg/l to 50 mg/l shows soft water; 50 mg/l to 100 mg/l is moderately soft water and 100 mg/l to 150 mg/l is slightly hard water. Additionally, a range between 150 mg/l and 200 mg/l was moderately hard water; 200 mg/l and 300 mg/l was hard water; and water with a hardness of >300 mg/l is classified as very hard water and this is the water that would be unsuitable for drinking.

4.9.3 Groundwater quality assessment for livestock use

The suitability of groundwater for livestock use was also assessed. This was also completed with the SAWQG standards (SAWQG, 1996c) in mind, using the groundwater chemistry data in mg/l. All the elements that were tested for the suitability of groundwater for domestic use were also tested for the suitability for livestock use. The water suitability for livestock use varied in several ways, such as the livestock type, age, their food and habitats. However, the general permissible ranges are provided in Section 5.8.3.

4.10 Conclusion

This chapter focused on describing the detailed methodology that was followed at the field during the hydrocensus and also during groundwater sample collection and storage. This was followed by the description of the methods followed when applying the complementary hydrogeochemical tools.

Chapter 5

Results and Discussions

5.1 Introduction

This chapter presents and discusses results obtained for the groundwater chemistry. The meaning of the results and the conclusions are provided as part of the discussion. This chapter incorporates the description of hydrogeochemical characteristics, including the raw groundwater chemistry data and hydrochemical classification (water types). The hydrogeochemical processes were further described resulting in the conclusion of the main processes that led to the evolution of the water chemistry. Understanding the water types and the processes that took place helped in conducting the groundwater quality assessment for domestic and agricultural use (irrigation and livestock). Data analysis and quality check was applied as the first step to assess the accuracy and reliability of the data.

Descriptions on the possible types of rocks and minerals that are found in the study area were done based on general geological understanding. Knowledge of the geology of the study area was significant since this was the starting point in an attempt to deduce the main hydrogeochemical processes that may have been taking place in the groundwater system. Consequently, the interpretation of the results will make sense since the rocks and minerals through which the groundwater moves are known. The chemical characteristics were described after the data quality checks whereby the orders of abundance for major ions were indicated. This was followed by hydrochemical classifications indicating different water types, ion exchange and mixing (Hounslow, 1995). On the Piper diagrams, the samples were grouped according to the distribution of major ions in the groundwater.

Stoichiometric analysis followed which indicated the possible reactions that took place, leading to an excess of ions, or removal of certain ions in the groundwater system. Likewise, bivariate plots also displayed the correlation between ions providing a better insight of hydrogeochemical processes that led to the groundwater chemistry change. Cluster plots, inverse geochemical modelling and statistical analysis have been utilised to further explain the hydrogeochemical processes that took place leading to the evolution of the water chemistry.

5.2 Data analysis and quality checks

5.2.1 Ion balance error

Ion balance error (IBE) is calculated to check the accuracy and validity of the laboratory analysis for water quality data (De Moel *et al.*, 2013; Murray and Wade, 1996). It can also be used to identify the errors that could have occurred during the analysis. Water samples with a high concentration of cations relative to anions are represented by a positive IBE and the opposite is true for water quality that is highly concentrated in anions. The acceptable water analysis has an IBE of $\pm 5\%$ as described by Domenico and Schwartz (1990). This is taken as the adequate IBE because ion solutions are known to be electrically neutral and therefore the present positive charges should equal the negative charges (Hounslow, 1995). The IBE was calculated using Ratio 5.1 (Knödel *et al.*, 2007).

$$IBE = \frac{\sum \text{Cations} - \sum \text{Anions}}{\sum \text{Cations} + \sum \text{Anions}} * 100 \% \quad (5.1)$$

Table 5.1 shows that the obtained values from spring data collected in November 2015 falls within the $\pm 5\%$ range, except for B11H and B54H with an IBE of -20.93% and -60.92%, respectively. Furthermore, the autumn data that was collected in May 2016 shows an error for B10H, B11H and B22H with an IBE outside the $\pm 5\%$ range.

TABLE 5.1: ION BALANCE ERROR FOR SPRING, SUMMER AND AUTUMN SEASONS

Site Name	ION BALANCE ERROR		
	Spring	Summer	Autumn
B10H	-0.16	3.92	12.69
B11H	-20.93	3.74	11.24
B22H	-4.25	-3.04	16.67
B24H	-3.96	-2.52	-0.64
B25H	-0.28	-0.31	0.68
B36H	-4.14	0.96	No data collected
B44H	-1.82	-1.52	No data collected
B45H	-0.13	3.91	-1.16
B50H	0.18	-2.67	-1.05
B53H	1.60	-1.34	3.27
B54H	-60.92	-0.81	No data collected
B55H	1.41	0.26	-2.65
B56H	-2.37	0.57	No data collected
B57H	-1.80	2.57	No data collected
B58H	0.61	2.64	3.13
B59H	6.25	2.70	4.62
B60H	-0.34	7.27	No data collected
B61H	2.82	9.79	No data collected
B62H	-0.96	5.15	No data collected
Spring	-0.51	3.41	4.13

These values indicate a very huge potential error in the analysis issued from the laboratory. Therefore, the results that will be shown by these samples can be considered as unreliable and may not be useful in water quality conclusions (Hounslow, 1995; Zaidi *et al.*, 2015). On the other hand, all the obtained IBE from summer groundwater chemistry data as collected in February 2016 falls within the $\pm 5\%$ range. Knödel *et al.* (2007) indicated that an ion balance error may result from several factors due to errors during analysis or sampling. This includes metal hydrolysis, laboratory errors during analysis, OH^- in high pH water and H^+ in low pH water, unmeasured dissolved species such as major ions and the presence of matter like organic acids that were not considered during analysis (Murray and Wade, 1996).

5.3 Assessment of Water Types and Hydrogeochemical Processes

Figure 5.1 is used as a reference map for the distribution and location of all the boreholes that are discussed in this chapter.



Source: Google Earth (2016).

Figure 5.1: A Google Earth map displaying the distribution of the boreholes at the study area

Table 5.2 to Table 5.4 indicate the groundwater chemistry data for the measured parameters in mg/l. Sample B24H for different seasons have the highest concentrations in all parameters. This sample was therefore considered as an outlier and was not included in the application of some of the tools. The reason is that when this sample was incorporated, odd results were obtained. This was seen especially in the bivariate correlation plots where no

correlations were indicated by the trend lines and also the hierarchical cluster plots where all the samples appeared as one group, whereas B24H appeared as another group. Nonetheless, B24H was not totally excluded from the results. Discussions on what could have happened to result in this groundwater composition are presented in the sections to follow.

5.3.1 Groundwater chemistry data

Table 5.2 to Table 5.4 displays the raw groundwater chemistry data for ions (mg/l) and parameters measured during the spring, summer and autumn seasons. This data is used to determine most and least dominant ions in the groundwater.

5.3.1.1 Spring season

Table 5.2 is a representation of data measured during the spring season. It contains major ions, SiO₂, TDS, EC and pH for all the boreholes.

TABLE 5.2: MAJOR IONS AND OTHER IMPORTANT PARAMETERS DISPLAYED WITH ELECTRICAL CONDUCTIVITY FOR SPRING RESULTS

Site Name	pH	EC	TDS	Ca	Mg	Na	K	HCO ₃	Cl	SO ₄	NO ₃ -N	SiO ₂
		mS/m	mg/l									
B10H	6.58	55.30	384.00	66.00	16.00	20.00	1.90	240.00	15.00	40.00	5.00	25.16
B11H	-	-	-	-	-	-	-	-	-	-	-	-
B22H	6.73	128.00	888.00	105.00	32.00	107.00	3.60	297.00	135.00	224.00	5.60	25.16
B24H	7.30	575.00	4520.00	297.00	136.00	934.00	4.10	744.00	1248.00	1193.00	0.20	22.16
B25H	6.73	199.00	888.00	129.00	52.00	195.00	2.40	253.00	271.00	356.00	2.30	26.16
B36H	6.99	128.00	418.00	103.00	35.00	97.00	3.10	298.00	151.00	185.00	5.40	25.16
B44H	6.67	154.00	561.00	164.00	24.00	140.00	2.50	223.00	163.00	410.00	1.80	21.16
B45H	7.10	172.00	571.00	194.00	12.00	173.00	2.00	278.00	225.00	338.00	4.90	21.16
B50H	6.63	204.00	711.00	200.00	47.00	159.00	4.30	237.00	275.00	415.00	7.20	22.16
B53H	6.80	85.80	260.00	88.00	16.00	57.00	1.40	295.00	39.00	93.00	1.30	24.16
B54H	-	-	-	-	-	-	-	-	-	-	-	-
B55H	6.54	73.80	382.00	78.00	21.00	35.00	0.78	248.00	24.00	106.00	0.20	24.16
B56H	6.63	177.00	298.00	163.00	37.00	128.00	5.70	279.00	252.00	252.00	11.00	23.16
B57H	6.66	190.00	1050.00	176.00	39.00	149.00	5.80	291.00	279.00	296.00	7.00	23.16
B58H	6.88	244.00	1314.00	191.00	59.00	279.00	3.00	456.00	343.00	424.00	4.20	27.16
B59H	6.95	68.20	284.00	95.00	10.00	31.00	0.55	234.00	13.00	91.00	0.20	25.16
B60H	6.79	115.00	608.00	94.00	28.00	92.00	1.80	333.00	89.00	142.00	2.70	24.16
B61H	6.75	86.60	382.00	81.00	25.00	56.00	1.00	338.00	25.00	88.00	0.20	26.16
B62H	6.79	158.00	784.00	106.00	40.00	139.00	1.70	266.00	265.00	143.00	2.00	25.16
Spring	6.60	53.60	260.00	46.00	21.00	25.00	0.40	235.00	13.00	44.00	0.55	28.16
Average	6.78	208.89	809.06	132.00	36.11	156.44	1.38	308.05	212.50	268.89	6.78	24.38

Note: (-) = Samples with high IBE

Table 5.2 shows all the major ions together with silicon dioxide concentrations in the groundwater. The pH values (Table 5.2) for the water in all the boreholes ranged from 6.5 to

7.3 which are close to neutral, whereas the EC ranged from 53.6 mS/m as the lowest for the spring water and 575 mS/m as the highest for B24H water. The reason for variation of EC in the boreholes is that since the spring is located in a high mountainous area, it might have received high recharge by recent rainwater. Additionally, B24H is sited down-gradient at the lowest elevation and therefore is recharged by mineralised water.

The order of abundance for major ions is discussed below. The major cations displayed two categories of abundance: the first one for samples B22H, B24H, B25H, B58H and B62H indicates $\text{Na}^+ > \text{Ca}^{2+} > \text{Mg}^{2+} > \text{K}^+$. Conversely, the order of abundance moved from $\text{Ca}^{2+} > \text{Na}^+ > \text{Mg}^{2+} > \text{K}^+$ for the rest of the samples. The average order for cations showed $\text{Na}^+ > \text{Ca}^{2+} > \text{Mg}^{2+} > \text{K}^+$ with concentrations of 156.44 mg/l > 132 mg/l > 36.11 mg/l > 1.38 mg/l, respectively. Therefore, Ca^{2+} was the most dominant ion in some of the samples whereas Na^+ was also the most dominant ion in some of the samples. The least concentrated cation in all the samples was potassium. This might be because K^+ is found in sericite and accessory minerals such as biotite and muscovite in Beaufort West, as explained by Campbell (1980). Jalali (2007), as well as Peikam and Jalali (2016), stated that in the geology where there is clay, K^+ normally appears to be the least dominant ion because it gets attached to the clay minerals as it leaves none, or less K^+ , in solution. The same case is assumed to be occurring in the study area where the geology comprises mostly of shale and mudstone sediments that are rich in clay minerals.

The major anions did not show any consistent order of abundance. Thus, for some samples the abundance showed $\text{HCO}_3^- > \text{Cl}^- > \text{SO}_4^{2-} > \text{NO}_3^-$ (B62H and B56H); $\text{Cl}^- > \text{SO}_4^{2-} > \text{HCO}_3^- > \text{NO}_3^-$ (B24H); $\text{SO}_4^{2-} > \text{Cl}^- > \text{HCO}_3^- > \text{NO}_3^-$ (B25H and B50H); $\text{SO}_4^{2-} > \text{HCO}_3^- > \text{Cl}^- > \text{NO}_3^-$ (B44H, B45H and B57H); and lastly, $\text{HCO}_3^- > \text{SO}_4^{2-} > \text{Cl}^- > \text{NO}_3^-$ for the rest of the samples. It was assumed that the order was controlled by the hydrochemical processes taking place within the system. Therefore, order $\text{HCO}_3^- > \text{SO}_4^{2-} > \text{Cl}^- > \text{NO}_3^-$ was considered to be the most significant order at the study area since it comprised the majority of samples. Likewise, the average values for anions matched this order $\text{HCO}_3^- > \text{SO}_4^{2-} > \text{Cl}^- > \text{NO}_3^-$ with concentrations of 308.05 mg/l > 268.89 mg/l > 212.50 mg/l > 6.78 mg/l, respectively. Nevertheless, the least abundant anion remained to be NO_3^- in all the samples. Apart from the majors, silica was also considered to be important in the groundwater with its average of 24.38 mmol/l.

According to Peikam and Jalali (2016), the presence of HCO_3^- in abundance within the groundwater system enhances minerals to dissolve in solution. Values for Ca^{2+} , Na^+ , HCO_3^- , Cl^- and SO_4^{2-} were the highest, and this can be an indication of addition of these ions through the contact of water with the aquifer. Further discussions on the hydrogeochemical processes that took place resulting in high concentrations of certain ions are presented in the sections to follow.

5.3.1.2 Summer season

Major ions, SiO₂, pH, TDS and EC are presented in Table 5.3. These are the parameters that were measured in the samples that were collected during the summer season.

Table 5.3 indicates the summer dataset showing how the groundwater was dominant in certain ions after the data analysis for the summer season. The parameters displayed in Table 5.3 are similar to the ones displayed in Table 5.2, therefore only the difference between the datasets will be discussed. The pH in these water samples ranged between 6 and 7.4 and can therefore be classified as near neutral pH, to slightly alkaline.

TABLE 5.3: MAJOR IONS AND OTHER IMPORTANT PARAMETERS DISPLAYED WITH ELECTRICAL CONDUCTIVITY FOR SUMMER RESULTS

Site Name	pH	EC	TDS	Ca	Mg	Na	K	HCO ₃	Cl	SO ₄	NO ₃ -N	SiO ₂
		mS/m	mg/l									
B10H	6.83	59.00	394.00	75.00	16.00	27.00	1.90	281.00	14.00	34.00	1.40	26.16
B11H	6.16	64.00	398.00	89.00	9.00	43.00	1.00	316.00	17.00	43.00	0.20	25.16
B22H	6.2	196.00	1261.00	79.00	7.00	325.00	2.20	302.00	180.00	460.00	3.90	21.16
B24H	7.33	451.00	3676.00	308.00	77.00	790.00	3.80	427.00	872.00	1319.00	0.20	20.16
B25H	6.48	177.00	1102.00	113.00	51.00	207.00	2.40	336.00	244.00	304.00	4.20	25.16
B36H	6.48	128.00	804.00	115.00	41.00	109.00	3.60	285.00	161.00	194.00	6.00	25.16
B44H	6.19	170.00	1118.00	173.00	31.00	15.00	3.10	202.00	187.00	477.00	3.10	23.16
B45H	6.52	151.00	912.00	144.00	25.00	164.00	3.40	292.00	173.00	255.00	3.50	22.16
B50H	6.21	189.00	1192.00	170.00	46.00	157.00	4.60	269.00	291.00	338.00	8.60	24.16
B53H	6.54	99.00	634.00	97.00	15.00	86.00	1.50	271.00	47.00	206.00	0.91	24.16
B54H	6.46	123.00	912.00	120.00	27.00	131.00	1.70	294.00	148.00	245.00	1.20	23.16
B55H	6.22	81.00	528.00	100.00	23.00	51.00	0.90	235.00	29.00	211.00	0.20	25.16
B56H	6.41	156.00	900.00	138.00	35.00	128.00	5.90	268.00	216.00	194.00	11.00	22.16
B57H	6.43	180.00	1076.00	178.00	45.00	171.00	6.70	287.00	281.00	281.00	9.80	22.16
B58H	6.68	241.00	1592.00	178.00	62.00	310.00	3.20	453.00	342.00	414.00	6.20	25.16
B59H	6.48	65.00	430.00	91.00	11.00	36.00	0.66	242.00	16.00	107.00	0.20	28.16
B60H	6.38	109.00	704.00	107.00	32.00	119.00	2.00	323.00	99.00	146.00	4.00	23.16
B61H	6.47	81.00	514.00	91.00	29.00	70.00	1.20	329.00	29.00	92.00	1.30	24.16
B62H	6.42	153.00	978.00	117.00	47.00	176.00	2.10	262.00	286.00	147.00	4.00	23.16
Spring	6.12	57.00	358.00	63.00	17.00	37.00	0.31	243.00	18.00	60.00	0.20	30.16
Average	6.45	146.50	974.15	127.30	32.30	164.80	1.50	295.85	182.50	276.35	6.25	24.16

The ions give a similar explanation as the one above in many cases. The differences obtained are explained as follows: boreholes B45H, B54H, B60H showed the order of abundance as Na⁺ > Ca²⁺ > Mg²⁺ > K⁺ and not Ca²⁺ > Na⁺ > Mg²⁺ > K⁺ as before. The concentration of SiO₂ ranged between 20.16 mg/l and 30.16 mg/l at B24H and the spring, respectively.

The major anions, on the other hand, indicated $\text{HCO}_3^- > \text{Cl}^- > \text{SO}_4^{2-} > \text{NO}_3^-$ (B56H and B57H); $\text{SO}_4^{2-} > \text{Cl}^- > \text{HCO}_3^- > \text{NO}_3^-$ (B24H and B50H); $\text{SO}_4^{2-} > \text{HCO}_3^- > \text{Cl}^- > \text{NO}_3^-$ (B44H and B22H); and lastly, $\text{HCO}_3^- > \text{SO}_4^{2-} > \text{Cl}^- > \text{NO}_3^-$ for the rest of samples. The order of abundance of the anions followed $\text{HCO}_3^- > \text{SO}_4^{2-} > \text{Cl}^- > \text{NO}_3^-$, with 296 mg/l > 276 mg/l > 183 mg/l > 3.49 mg/l as the respective concentrations.

5.3.1.3 Autumn season

The groundwater chemistry data in Table 5.4 represents the autumn season. It consists of major ions, TDS, EC, pH and SiO_2 . The average of each measured parameter is also indicated in the table.

The difference in the order of ions in Table 5.4 as compared to Table 5.2 and Table 5.3 is discussed. There was an increase in the pH for samples that were collected in autumn with the values ranging from 6.2 to 8.2. The possible causes of the pH elevation are discussed in the next sections where the hydrochemical processes are explained. The highest total dissolved solids (TDS) of 3 787 mg/l were indicated by B24H as in the previous results; whereas the lowest TDS was shown by the spring with a concentration of 320 mg/l. The autumn results further indicated an increase in the SiO_2 values ranging between 25.16 mg/l and 34.16 mg/l.

TABLE 5.4: MAJOR IONS AND OTHER IMPORTANT PARAMETERS DISPLAYED WITH ELECTRICAL CONDUCTIVITY FOR AUTUMN RESULTS

Site Name	pH	EC	TDS	Ca	Mg	Na	K	HCO_3	Cl	SO_4	$\text{NO}_3\text{-N}$	SiO_2
		mS/m	mg/l									
B10H	-	-	-	-	-	-	-	-	-	-	-	-
B11H	-	-	-	-	-	-	-	-	-	-	-	-
B22H	-	-	-	-	-	-	-	-	-	-	-	-
B24H	8.04	431.00	3787.00	267.00	98.00	924.00	4.20	599.00	1019.00	1148.00	0.20	25.16
B25H	6.21	136.00	1227.00	114.00	52.00	212.00	2.50	309.00	244.00	327.00	3.30	27.16
B45H	7.99	163.00	1121.00	171.00	30.00	171.00	3.70	270.00	259.00	327.00	6.00	25.16
B50H	8.08	164.00	1177.00	169.00	47.00	161.00	4.50	274.00	271.00	338.00	9.20	26.16
B53H	6.18	83.80	652.00	107.00	17.00	96.00	1.60	238.00	49.00	235.00	1.20	25.16
B55H	7.09	68.70	523.00	94.00	24.00	48.00	0.88	225.00	30.00	226.00	0.20	27.16
B58H	6.36	196.00	1610.00	168.00	60.00	300.00	3.20	414.00	329.00	396.00	7.00	28.16
B59H	8.16	61.70	434.00	97.00	13.00	37.00	0.66	254.00	18.00	105.00	0.20	30.16
Spring	7.87	46.90	320.00	51.00	24.00	28.00	0.48	231.00	19.00	46.00	0.20	34.16
Average	7.33	242.52	1205.67	137.56	43.71	219.67	0.78	312.66	248.67	349.77	8.09	27.61

Note: (-) = Samples with high IBE

There was no difference obtained for the cations' order of abundance; however, a slight difference was observed for the anions. Samples B25H, B50H and B55H indicated the order

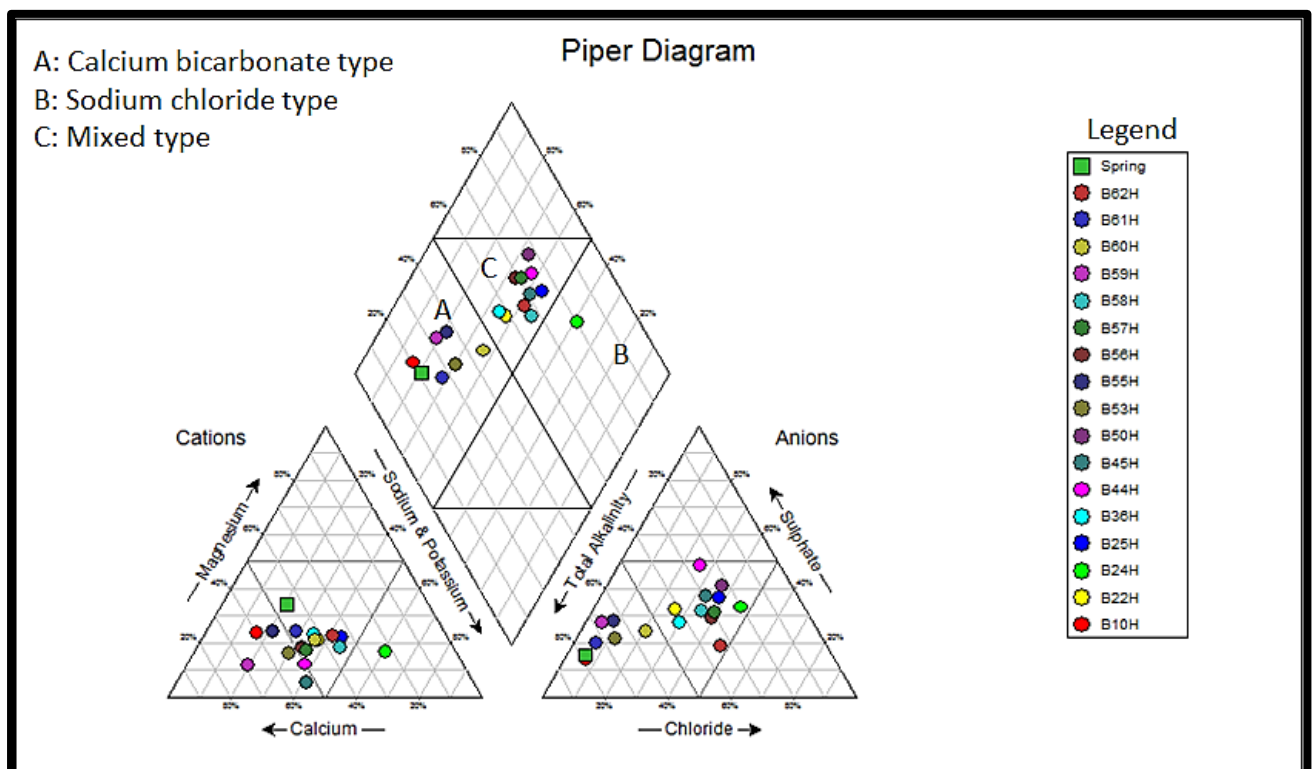
as $\text{SO}_4^{2-} > \text{HCO}_3^- > \text{Cl}^- > \text{NO}_3^-$, whereas for spring and summer they indicated a different order (see Sections 5.3.1.1 and 5.3.1.2). Moreover, the order of $\text{HCO}_3^- > \text{Cl}^- > \text{SO}_4^{2-} > \text{NO}_3^-$ was shown by B22H that also indicated a different order in the other seasons.

5.3.2 Hydrochemical (water type) classification

Piper diagrams (Figure 5.2 to Figure 5.4) were conducted using the groundwater chemistry data. These were done to determine the main water types at the study area relative to how certain ions were constituted in the water. Deductions on the water type were therefore made with the distribution of the samples on the Piper diagrams.

5.3.2.1 Spring season

Figure 5.2 displays the distribution of samples on the Piper diagram with the water types as labelled A to C.



Source: Author's own (2016).

Figure 5.2: Piper diagram showing water types for spring results as plotted for 18 samples

A. Calcium bicarbonate water type

Samples that indicated this water type were B10H, B53H, B55H, B59H, B60H, B61H and the spring. This water is known as recently recharged groundwater because of its high Ca^{2+} and HCO_3^- concentrations (Figure 5.2). Gomo *et al.* (2013) described that during recharge to the groundwater system water interacts with the carbonate minerals resulting in high Ca^{2+} , Mg^{2+}

and HCO_3^- in the system. This process is the first during recharge of the aquifer. Additionally, Jalali (2009) explained that during dissolution of carbonate rocks, Ca^{2+} and HCO_3^- are released into solution leading to CaHCO_3 water type.

B. Sodium chloride water

This water could be stagnant or old groundwater; there is a possibility of very low recharge if the water is contained in a semi-confined or leaky aquifer. However, Table 5.2 displays an excess of ions Ca^{2+} , Mg^{2+} , Na^+ , Cl^- , HCO_3^- , SO_4^{2-} and TDS in solution. Therefore, as the groundwater moved down-gradient in the aquifer it was enriched in these ions through mineralisation. The sodium chloride water was represented by sample B24H.

C. Mixed type

This is water from different sources after ions and minerals have been added and removed as the water flows in the groundwater system. Accordingly, after recharge as the water move through the flow paths down the gradient, many hydrogeochemical processes can take place leading to the evolution of the water quality. Consequently, this water was not enriched in any kind of specific ions, hence it was categorised as mixed type. This might be due to mixing of the stagnant groundwater and recharged water or interaction of water underground. The boreholes in which this water was collected were B22H, B25H, B36H, B44H, B45H, B50H, B56H, B57H, B58H and B62H. This water had a TDS ranging from > 298 mg/l to < 1315 mg/l, showing a high concentration of dissolved solids as a result of dissolution of minerals which is discussed in detail later.

5.3.2.2 Summer season

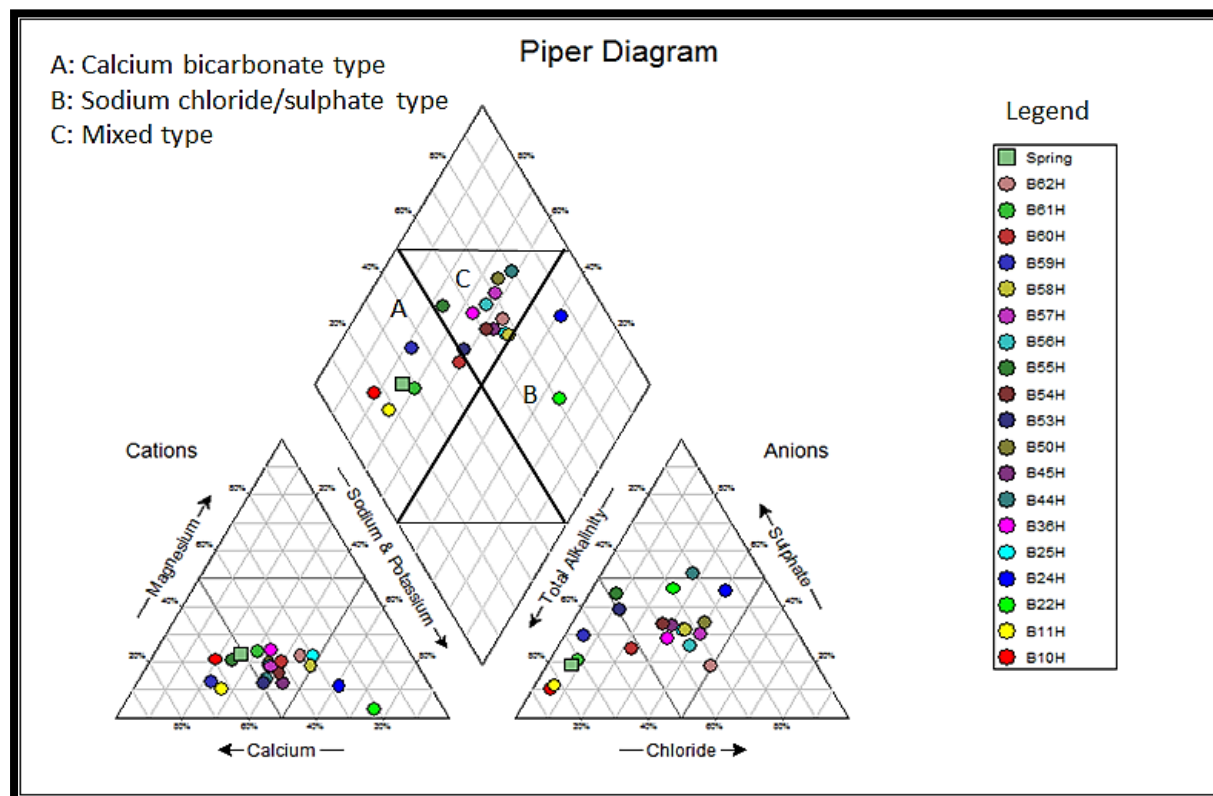
The results obtained for the summer season (Figure 5.3) showed more similarities with results that were obtained for the spring season. There were only minor differences displayed when comparing the two Piper diagrams and these are explained below under each water type.

A. Calcium bicarbonate water

Boreholes that had this water type were B10H, B11H, B59H, B60H, B61H and the spring, with the exception of B53H and B55H that indicated this water type in the spring season results. As already stated, this water is known as recently recharged groundwater (Figure 5.3).

Based on the results obtained from the spring and summer seasons, an elevation in all the major ions, except for HCO_3^- and NO_3^- , was observed. This included a slight change in Mg^{2+} and Ca^{2+} concentrations. The TDS in samples B53H and B55H changed from 260 mg/l and

382 mg/l to 634 mg/l and 528 mg/l, respectively. There was also an increase of Na^+ , Cl^- and SO_4^{2-} (Table 5.3) as compared to these concentrations in Table 5.2.



Source: Author's own (2016).

Figure 5.3: Piper diagram showing water types for summer results as plotted for 20 samples

B. Sodium chloride/sulphate water

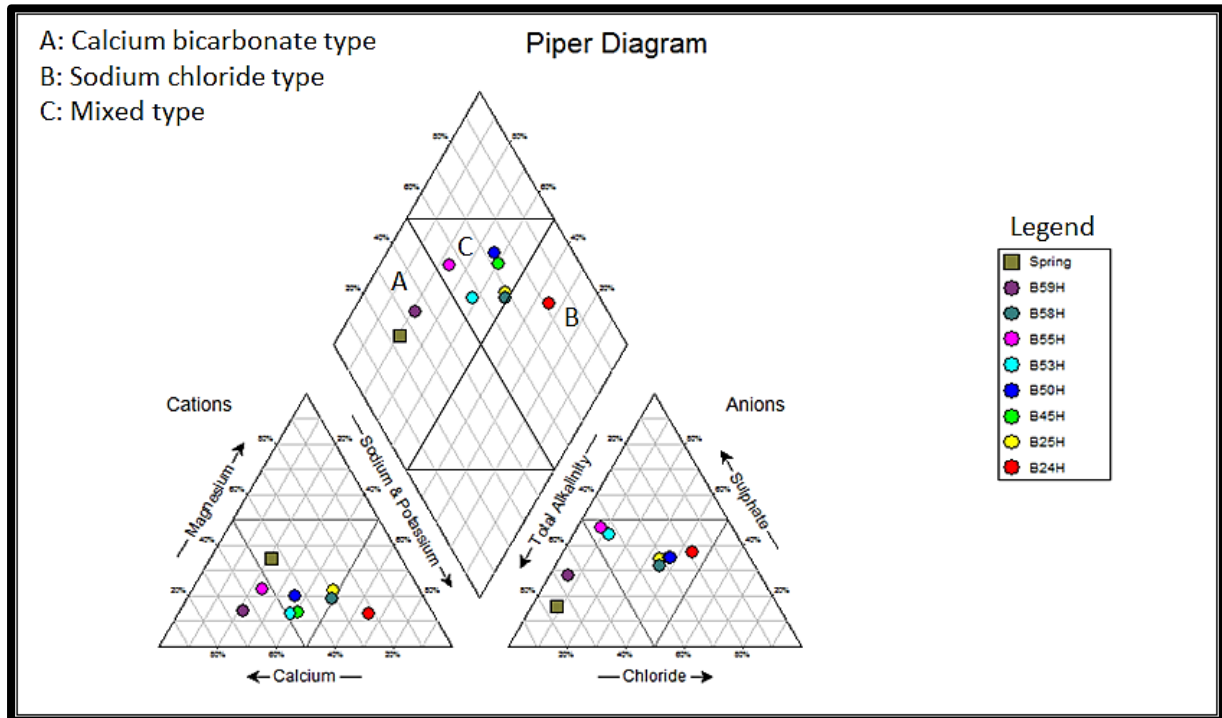
Boreholes B22H and B24H were classified in this water type. Sample B24H did not change in its water type from how it was classified during the spring season. However, sample B22H water type changed from a mixed water type to sodium chloride/sulphate water. This is an indication of possible hydrogeochemical processes that might be taking place along the flow path. The results from both seasons showed how the TDS for B22H increased dramatically from 888 mg/l in spring to 1 261 mg/l in summer. There was a decrease in Ca^{2+} and Mg^{2+} ions and explanations behind this are shown in the discussions of the processes that took place in the groundwater system.

C. Mixed water

The same samples that indicated mixed water in the spring season results were still indicating this water type. Only sample B53H and B55H were added since they indicated calcium bicarbonate water in the spring results and mixed water in the summer results. Clarifications on these have been done under CaHCO_3 water.

5.3.2.3 Autumn season

Figure 5.4 is a Piper diagram generated using the autumn season results. A total of 9 samples were plotted, excluding 3 samples that had a high IBE. The water types, as well as differences in the autumn results from the results obtained for the rest of the seasons, are discussed here.



Source: Author's own (2016).

Figure 5.4: Piper diagram showing water types for autumn results as plotted for 9 samples

A. Calcium bicarbonate water

The samples that displayed this water type were the same as in the summer season. There was an increase in the concentrations of calcium and magnesium for all the samples in this water except for the spring, and also a decrease in sulphate for all the samples as indicated by Table 5.4.

B. Sodium chloride water

Only B24H was classified in this water type as indicated by the results.

C. Mixed water

The same samples as the ones from the other seasons showed this water type. Therefore, the same explanation will apply.

5.3.2.4 Summary on hydrogeochemical (water type) classifications

The general conclusion on hydrogeochemical classifications indicated three main water types along the study area, namely: calcium bicarbonate, sodium chloride and mixed water types. The groundwater from one season to the other showed a drastic increase in TDS concentration from spring to summer and then to autumn. An increase of TDS concentrations from spring to summer occurred for all the samples, except B24H, whereas an increase for summer to autumn excluded B50H and the spring.

5.3.3 Stiff Diagrams

The generated stiff diagrams are presented in Appendix 1 for spring, summer and autumn results. The results obtained by these diagrams showed that there was an interaction of the groundwater with gypsum rock. This was shown by samples B44H and B50H for spring season and sample B44H from summer, as indicated in Appendix 1. This may be an indication of recharge water interacting with the gypsum deposits. Shale was also deduced to be one of the source rocks by using stiff diagrams (Hounslow, 1995). This was noticed from sample B24H for all three seasons. Other samples such as B10H, B11H, B53H, B55H, B59H, B60H, B61H and the spring for all seasons (Appendix 1), resembled a limestone and/or dolomite source rock. These were the water samples associated with recently recharged water and they were not dominated by the majority of ions (Appelo and Postma, 2005). There were other samples that showed no dominance in any specific ion and this included B25H, B36H, B45H, B54H, B56H, B57H and B62H (Appendix 1). These samples plotted in the mixed water types in the Piper diagrams and they may be indicating mixing of different water types and evaporation.

5.4 Water-rock interaction

5.4.1 Stoichiometric analysis

Subsequently, no geological/borehole logs or rock samples were collected for the study area. Several approaches were used to help in identification of hydrogeochemical processes that led to the water types at the study area. The measured ion concentrations and stoichiometry of reactions were used together to improve the understanding of the hydrogeochemistry process. Furthermore, the type of rocks and the linked mineralogy of aquifers were deduced from the literature review. Campbell (1980) described the following minerals as the ones linked to sandstone, shale, mudstone, limestone and dolerite along the study area, namely: carbonates, feldspars, quartz, gypsum, biotite, muscovite, chlorite and iron oxides. In addition, the presence of evaporites such as halite and sylvite, were assumed from the general geology and climatic conditions of Beaufort West. Schreiber and El Tabakh

(2000) stated that evaporites may form in sedimentary areas where evaporation is higher than the water inflow. The literature study has indicated that the climatic conditions at Beaufort West are arid. It is therefore expected that minerals that dominate the non-marine evaporites are gypsum or anhydrite and halite.

Twenty samples in total from different locations (Figure 5.1) were collected for chemical analysis during spring and summer and 12 during the autumn season. Although these samples were all collected from various boreholes, they were all from within the same study area. Samples that had high IBE were excluded from the interpretation and conclusion of results as stated earlier. Table 5.5 to Table 5.7 indicates major ions in meq/l as well as SiO₂ compound in mmol/l, TDS and EC, together with their respective site names.

SPRING SEASON

The meq/l calculations for ions are displayed in Table 5.5 with silicon dioxide included, since it indicates some contribution in the groundwater. TDS and EC are reported in mg/l and mS/m respectively.

TABLE 5.5: MAJOR IONS, SILICA, TOTAL DISSOLVED SOLIDS AND ELECTRICAL CONDUCTIVITY FOR SPRING RESULTS

Site Name	EC	TDS	Ca	Mg	Na	K	HCO ₃	Cl	SO ₄	NO ₃ -N	SiO ₂
	mS/m	mg/l	meq/l								mmol/l
B10H	55.30	384.00	3.29	1.32	0.87	0.05	3.93	0.42	0.83	0.36	0.42
B11H	-	-	-	-	-	-	-	-	-	-	-
B22H	128.00	888.00	5.24	2.63	4.65	0.09	4.87	3.81	4.66	0.40	0.42
B24H	575.00	4520.00	14.82	11.19	40.63	0.10	12.19	35.20	24.84	0.01	0.37
B25H	199.00	888.00	6.44	4.28	8.48	0.06	4.15	7.64	7.41	0.16	0.44
B36H	128.00	418.00	5.14	2.88	4.22	0.08	4.88	4.26	3.85	0.39	0.42
B44H	154.00	561.00	8.18	1.97	6.09	0.06	3.65	4.60	8.54	0.13	0.35
B45H	172.00	571.00	9.68	0.99	7.53	0.05	4.56	6.35	7.04	0.35	0.35
B50H	204.00	711.00	9.98	3.87	6.92	0.11	3.89	7.76	8.64	0.51	0.37
B53H	85.80	260.00	4.39	1.32	2.48	0.04	4.83	1.10	1.94	0.09	0.40
B54H	-	-	-	-	-	-	-	-	-	-	-
B55H	73.80	382.00	3.89	1.73	1.52	0.02	4.06	0.68	2.21	0.01	0.44
B56H	177.00	298.00	8.13	3.04	5.57	0.15	4.57	7.11	5.25	0.79	0.39
B57H	190.00	1050.00	8.78	3.21	6.48	0.15	4.78	7.87	6.16	0.50	0.39
B58H	244.00	1314.00	9.53	4.85	12.14	0.08	7.47	9.68	8.83	0.30	0.45
B59H	68.20	284.00	4.74	0.82	1.35	0.01	3.83	0.37	1.89	0.01	0.42
B60H	115.00	608.00	4.69	2.30	4.00	0.05	5.46	2.51	2.96	0.19	0.40
B61H	86.60	382.00	4.04	2.06	2.44	0.03	5.54	0.71	1.83	0.01	0.44
B62H	158.00	784.00	5.29	3.29	6.05	0.04	4.36	7.48	2.98	0.14	0.42
Spring	53.60	260.00	2.30	1.73	1.09	0.01	3.85	0.37	0.92	0.04	0.47

Note: (-) = Samples with high IBE

SUMMER SEASON

The same format as used for reporting the results in Table 5.5 was also used to report the results in Table 5.6. These were, however, the results of the groundwater chemistry data for the summer season.

TABLE 5.6: MAJOR IONS, SILICA, TOTAL DISSOLVED SOLIDS AND ELECTRICAL CONDUCTIVITY FOR SUMMER RESULTS

Site Name	EC	TDS	Ca	Mg	Na	K	HCO ₃	Cl	SO ₄	NO ₃ -N	SiO ₂
	mS/m	mg/l	meq/l								mmol/l
B10H	59.00	394.00	3.74	1.32	1.17	0.04	4.60	0.39	0.70	0.10	0.44
B11H	64.00	398.00	4.44	0.74	1.87	0.02	5.17	0.47	0.89	0.10	0.42
B22H	196.00	1261.00	3.94	0.58	14.13	0.05	4.94	5.07	9.57	0.28	0.36
B24H	451.00	3676.00	15.37	6.33	34.36	0.09	6.99	24.59	27.46	0.01	0.34
B25H	177.00	1102.00	5.64	4.19	9.00	0.06	5.50	6.88	6.32	0.30	0.42
B36H	128.00	804.00	5.74	3.37	4.74	0.09	4.67	4.54	4.03	0.43	0.42
B44H	170.00	1118.00	8.63	2.55	6.91	0.07	3.31	5.27	9.93	0.22	0.38
B45H	151.00	912.00	7.19	2.05	7.13	0.08	4.78	4.88	5.3	0.25	0.36
B50H	189.00	1192.00	8.48	3.78	6.82	0.11	4.40	8.20	7.03	0.61	0.40
B53H	99.00	634.00	4.84	1.23	3.74	0.03	4.44	1.32	4.28	0.06	0.40
B54H	123.00	912.00	5.99	2.22	5.69	0.04	4.81	4.17	5.10	0.09	0.39
B55H	81.00	528.00	4.99	1.89	2.21	0.02	3.85	0.81	4.39	0.01	0.42
B56H	156.00	900.00	6.89	2.87	5.56	0.15	4.39	6.09	4.03	0.79	0.38
B57H	180.00	1076.00	8.88	3.70	7.43	0.17	4.70	7.92	5.85	0.70	0.37
B58H	241.00	1592.00	8.88	5.10	13.48	0.08	7.42	9.64	8.61	0.44	0.42
B59H	65.00	430.00	4.54	0.90	1.56	0.01	3.96	0.45	2.22	0.01	0.47
B60H	109.00	704.00	5.34	2.63	5.17	0.05	5.29	2.79	3.03	0.29	0.38
B61H	81.00	514.00	4.54	2.38	3.04	0.03	5.39	0.81	1.91	0.09	0.40
B62H	153.00	978.00	5.84	3.86	7.65	0.05	4.29	8.06	3.06	0.29	0.38
Spring	57.00	358.00	3.14	1.39	1.60	0.01	3.98	0.50	1.24	0.01	0.50

AUTUMN SEASON

Table 5.7 displays various parameters converted to meq/l and mmol/l, as well as TDS and EC in mg/l and mS/m units, respectively. These were the results for the 9 samples that were collected during the autumn season.

Possible reactions that could have taken place in the groundwater leading to the dominance of certain ions in the water are discussed in this section. These are the reactions that were assumed to have played a major role in controlling the chemistry and quality of groundwater and they are shown as Equation 5.2 to Equation 5.9.

TABLE 5.7: MAJOR IONS, SILICA, TOTAL DISSOLVED SOLIDS AND ELECTRICAL CONDUCTIVITY FOR AUTUMN RESULTS

Site Name	EC	TDS	Ca	Mg	Na	K	HCO ₃	Cl	SO ₄	NO ₃ -N	SiO ₂
	mS/m	mg/l	meq/l								mmol/l
B10H	-	-	-	-	-	-	-	-	-	-	-
B11H	-	-	-	-	-	-	-	-	-	-	-
B22H	-	-	-	-	-	-	-	-	-	-	-
B25H	136.00	1227.00	5.69	4.28	9.22	0.06	5.06	6.88	6.81	0.24	0.45
B45H	163.00	1121.00	8.53	2.47	7.44	0.09	4.42	7.31	6.81	0.43	0.42
B50H	164.00	1177.00	8.43	3.87	7.00	0.12	4.49	7.64	7.04	0.66	0.44
B53H	83.80	652.00	5.34	1.40	4.18	0.04	3.90	1.38	4.89	0.09	0.42
B55H	68.70	523.00	4.69	1.97	2.09	0.02	3.69	0.85	4.71	0.01	0.45
B58H	196.00	1610.00	8.38	4.93	13.04	0.05	6.78	9.28	8.24	0.50	0.47
B59H	61.70	434.00	4.84	1.07	1.61	0.02	4.16	0.51	2.19	0.01	0.50
Spring	46.90	320.00	2.54	1.97	1.22	0.01	3.79	0.54	0.96	0.01	0.57

Note: (-) = Samples with high IBE

5.4.1.1 Weathering

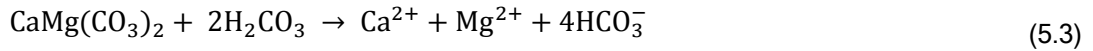
Weathering may occur in minerals at different rates whereby some minerals are weathered faster than others, depending on factors such as temperature and stability of minerals (Bowen, 1922). The potential influence of weathering of carbonates (calcite and dolomite), silicates (quartz, calcic and sodic plagioclase, micas (biotite, muscovite) and clay minerals is discussed in this section.

5.4.1.2 Carbonate weathering

Carbonate weathering of calcite and dolomite has been deduced to have occurred in the groundwater system, when substituting the converted concentrations (Table 5.5 to Table 5.7) in Ratio 4.1, whereby a >10 ratio was calculated for those samples (Appendix 2). The rationale behind this ratio was explained in Section 4.6.1. Equation 5.2 obtained from Earle (2015) and Gomo *et al.* (2013), indicates the dissolution of calcite. This process occurs in the presence of carbonic acid resulting in calcium and bicarbonate ions as the products.



Consequently, the process of dolomite dissolution is presented by Equation 5.3. Dolomite was dissolved by water enriched in carbon dioxide, resulting in the assemblage of calcium, magnesium and bicarbonate ions as the products in the groundwater (Zhang *et al.*, 2007).



The carbonic acid that reacted with calcite and dolomite forms as a result of carbon dioxide gas in the soil, interacting with rain water that percolates through the groundwater system.

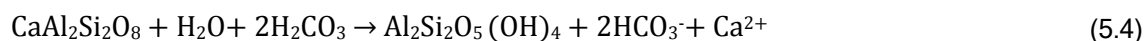
5.4.1.3 Silicate weathering

The process of silicate weathering is slow, such that its contribution in changing the groundwater chemistry is also very slow, as compared to that of carbonates (Appelo and Postma, 2005). The weathering order of the silicate minerals explained in Goldich (1938) shows that calcic plagioclase is weathered easily and can therefore alter the water chemistry more (Van Camp and Walraevens, 2008). This is followed by sodic plagioclase and biotite, then muscovite and the most resistant one, namely quartz (Goldich, 1938; Woodford and Chevalier, 2002). The dissolution of these silicate minerals leads to the formation of secondary clay minerals such as kaolinite and montmorillonite (Van Camp and Walraevens, 2008; Woodford and Chevalier, 2002). Silicate dissolution may also release cations such as Na^+ , Ca^{2+} , and K^+ , as well as silica, in the groundwater (Van Camp and Walraevens, 2008).

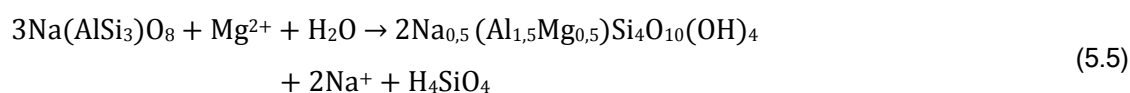
The occurrence of silicate weathering within the system was checked using several approaches, such as Ratios 4.1 and 4.2. The logic behind these expressions was explained in Section 4.6.1. Ratio 4.1 explains that if silicate weathering is assumed, the calculated ratio should be <5 . The use of this ratio indicated that no sample gave a ratio of <5 ; however, samples B10H, B25H, B55H, B59H and the spring gave a ratio of >5 and <10 (Appendix 2). Ratio 4.2 was then used to further investigate if silicate weathering took place in the groundwater system. This ratio, as explained in Hounslow (1995), is used to determine silicate weathering, specifically for plagioclase minerals. The rationale behind this ratio was described in Section 4.6.1. Plagioclase weathering was assumed after the application of Ratio 4.2, making use of the concentrations in Table 5.5, Table 5.6 and Table 5.7.

Samples B24H, B53H, B58H, B60H and B61H showed the possibility of plagioclase weathering taking place, where the calculated ratio was >0.2 and <0.8 (Appendix 2). The presence of plagioclase weathering was assumed to be of anorthite (Equation 5.4) and albite (Equation 5.5). The reason this assumption was made is because Campbell (1980) claimed these minerals to be amongst the ones forming the geology of the study area. The stoichiometric reactions displayed as Equation 5.4 to Equation 5.6 would therefore be the ones taking place with the assumption that both sodic and calcic plagioclase dissolutions occurred in this system.

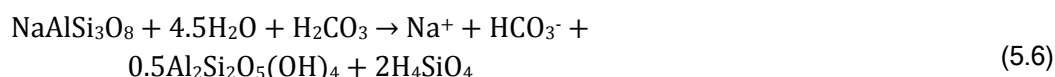
Hounslow (1995) indicated that if plagioclase anorthite weathering took place, silica will not be released in solution because this is low silica mineral (Bowen, 1922). This is shown by Equation 5.4 which indicates that anorthite reacted with carbonic acid and water to release clay kaolinite, bicarbonate and calcium ion in the solution (Clark, 2015).



The occurrence of albite weathering will lead to less bicarbonate concentration if not equal to that of silica (Hounslow, 1995). Equation 5.5 by Appelo and Postma (2005) and Equation 5.6 by Clark (2015), indicate the dissolution of albite. Equation 5.5 shows the dissolution of albite in water to give out clay montmorillonite, sodium ions and silicic acid in the system.



Meanwhile, Equation 5.6 indicates the dissolution of albite by water and carbonic acid to give out clay kaolinite, silicic acid, bicarbonate and sodium ions (Clark, 2015).



Appelo and Postma (2005) explained that montmorillonite clay forms in low rainfall, dry climate areas accompanied by longer residence time of the water underground, whereas the opposite is true for the formation of kaolinite. Therefore, both these secondary minerals were capable of forming at Beaufort West because both dry and wet conditions may prevail during different seasons.

5.4.1.4 Calcium and sulphate

Ratio 4.3 was used to check the possible origin of calcium and sulphate ions in solution and also to determine the occurrence of gypsum dissolution. Table 5.5 to Table 5.7 indicate that $\text{Ca}^{2+} > \text{SO}_4^{2-}$ (meq/l) in the majority of the samples. According to Hounslow (1995), in this case a calcium source can be assumed to be calcite, dolomite or rather plagioclase. This could be so because from Ratio 4.1, carbonate weathering has been deduced to be taking place in this system.

In contrast, there are other samples such as B24H, B25H and B44H for all seasons and B22H for summer, in which their calcium concentrations were less than that of sulphate ($\text{Ca}^{2+} < \text{SO}_4^{2-}$ in meq/l). The process that may have resulted to this is the removal of calcium by precipitation, or most probably ion exchange (Hounslow, 1995). In addition, gypsum

dissolution (Equation 5.7) from some of the samples such as B25H, B44H, B50H and B58H for all seasons, B22H for spring and B55H for summer and autumn, was deduced by the use of Ratio 4.3, where the calculated ratio was equal to 0.5 (Appendix 2).



The dissolution of gypsum in solution is explained by Freeze and Cherry (1979) as well as Li *et al.* (2010), whereby gypsum was dissolved to give calcium and sulphate ions; hence an increased SO_4^{2-} and Ca^{2+} in solution.

5.4.1.5 Sodium and chloride

The occurrence of ion exchange and reverse ion exchange in the groundwater system was checked by using Ratio. Ion exchange takes place when calcium ions are removed from the groundwater to replace the void spaces in the sediments. Reverse ion exchange, on the other hand, is experienced when cation exchange occurs with Na^+ being removed from solution and replaced by Ca^{2+} , leaving less concentration of Na^+ . This is the process called freshening, whereby CaHCO_3 water flushes out the salt in the water (Appelo and Postma, 2005). It may also be noticed by an increase in Cl^- concentration in the water over a Na^+ concentration (Zaidi *et al.*, 2015). Thus, water recharging the aquifer may be coming from other sources such as connate groundwater sources (Zaidi *et al.*, 2015).

The conversions made from the hydrochemistry data shown in Table 5.5, Table 5.6 and Table 5.7 indicate that Na^+ was greater than Cl^- in most of the samples. Moreover, when using Ratio 4.4, a ratio of >0.5 (Appendix 2) was obtained for some samples and it was concluded to be an indication of ion exchange in the solution (Hounslow, 1995). The source of the high concentration of sodium could be the presence of clay (Chapelle and Knobel, 1983). Somehow, it might be the result of ion exchange as shown by Equation 5.8 from Li *et al.* (2010) as well as Postma and Appelo (2005). Chapelle and Knobel (1983) stated that if ion exchange is one of the processes causing the alteration to the water chemistry, it will also cause a change to the exchange surface composition.



Cation exchange or reverse ion exchange was also assumed to have been taking place in the groundwater system (Equation 5.9). The assumption was made after using Ratio 4.4 to do the calculations, whereby a ratio of <0.5 (Appendix 2) was obtained for samples B50H, B56H, B57H and B62H for spring and summer seasons, B36H for summer and B50H for

autumn. These samples further showed that Cl⁻ was more than Na⁺ in the groundwater as calculated in meq/l.



An explanation behind Equation 5.8 and Equation 5.9 is that X stands for the exchange site which can either be occupied by a divalent or rather two monovalent cations as displayed by the equation (Fisher and Mullican, 1997; Van Camp and Walraevens, 2008).

5.4.1.6 Silica

Lastly, SiO₂ concentrations from the majority of the samples had values of <0.45 mmol/l. The only samples that showed a value of >0.45 mmol/l were B25H, B55H, B58H, B59H and the spring for autumn; whereas B59H and the spring were displayed for summer; and lastly, B58H and the spring for the spring season. Hounslow (1995) explained that if the SiO₂ value in mmol/l is 0.5 or greater, it could be an indication of hydrothermal water. This is because silica can dissolve better in hydrothermal water than in normal groundwater temperatures (Hounslow, 1995). The borehole map (Figure 5.1) shows that all the above-mentioned boreholes were located in such a way that they might be following the same flow path. If this assumption is correct, the hydrothermal water from the spring flowed through these areas, possibly resulting in their increased silica content.

5.4.2 Analysis of the bivariate correlation plots

The bivariate correlation plots were developed for different parameters to determine the correlation between those parameters which can be used to identify the source reactions for the minerals. More correlation plots were developed for the combination of various parameters to identify the hydrogeochemical processes that occurred in the groundwater system. High correlation coefficients were inferred to indicate that the chemistry parameters of the ions evolved from the same or a similarly related hydrogeochemical process. Explanations on what the graphs indicate were done with the correlation coefficients (r) displayed.

Table 5.8 is an indication of Guildford's rule of thumb and shows how these correlation coefficients were interpreted (Kura *et al.*, 2013).

TABLE 5.8: GUILDFORD'S RULE OF THUMB SHOWING VARIATION IN CORRELATION COEFFICIENTS

r-value (correlation coefficient)	Explanation
0.0 to 0.29	Negligible or little correlation
0.3 to 0.49	Low correlation

0.5 to 0.69	Moderate or marked correlation
0.7 to 0.89	High correlation
0.9 to 1.00	Very high correlation

Source: Kura *et al.* (2013).

The bivariate results indicated that there was a very high correlation between Na versus Cl for spring and autumn seasons, whereas the correlation for the summer plot was high. A high correlation was further observed between Ca versus SO₄ and Ca + Mg - SO₄ - HCO₃ versus Na + K - Cl for both spring and autumn. On the other hand, the Ca versus SO₄ and Ca + Mg -SO₄-HCO₃ versus Na + K - Cl plots for the summer season gave a moderate and very high correlation respectively. Furthermore, a moderate correlation was indicated by Ca versus Mg, K versus Cl and Mg versus SO₄ for spring, while summer and autumn gave a high correlation for K versus Cl. Another high correlation was given by the plots of Ca versus Mg for summer and Mg versus SO₄ for autumn. Lastly, a low correlation was displayed for Mg versus SO₄ plot for summer season. These relationships are indicated by the correlation coefficients in Table 5.9.

TABLE 5.9: CORRELATION COEFFICIENTS FOR THE BIVARIATE PLOTS FOR SPRING, SUMMER AND AUTUMN SEASONS

Bivariate plots	Spring	Summer	Autumn
	Correlation coefficient (r-value)		
Na versus Cl	0.93	0.80	0.94
Ca versus SO ₄	0.92	0.64	0.88
Mg versus SO ₄	0.64	0.38	0.76
Ca versus Mg	0.50	0.72	0.37
K versus Cl	0.68	0.72	0.72
Ca + Mg versus HCO ₃ +SO ₄	0.94	0.63	0.95
Ca + Mg - SO ₄ - HCO ₃ versus Na + K - Cl	0.92	0.94	0.86

The comparison among the results pointed out that some correlations between the parameters were very high in the one season, whereas in the other seasons they appeared to be a high positive or moderate. This was controlled by hydrochemical processes such as water-rock interaction, weathering, ion exchange, reverse ion exchange and evaporation taking place in the aquifer system.

5.4.2.1 Calcium + magnesium versus bicarbonate

The scatter plot of Ca + Mg versus HCO₃ (Appendix 3) was done. Nazzal *et al.* (2014) stated that if the calculated ratio of Ca + Mg/HCO₃ is less than 1, it could be a good indication of meteoric groundwater or recharge by fresh water. All the samples that were classified under

the CaHCO₃ water type had a ratio <1 and these were regarded as recently recharged water. Additionally, there were other samples that were classified under the mixed water that also showed a <1 ratio indicating recharge water. These samples were B22H, B36H and B58H for all the seasons, with an addition of B25H for summer and autumn, B54H for summer and B62H for spring season.

The water of sample B36H, although it was classified under mixed water, was enriched in Ca²⁺ and HCO₃⁻. It might be classified under the mixed water type because of the ion exchange or reverse ion exchange and carbonate weathering processes that were deduced to be occurring at this area. Furthermore, B54H and B62H also showed recent recharge water. These samples fell under the mixed water type because they were elevated in other major ions, apart from calcium and bicarbonate. The boreholes were both situated at high elevations (Figure 5.1), explaining that these boreholes get recharged first compared to the ones at lower elevations. The high concentrations in other ions may be the result of mixing of different water types. These samples also showed the occurrence of reverse ion exchange such that freshening of the water at these areas could have happened during recharge, whereby the recent recharge CaHCO₃ water was flushing out other dissolved solids from the water. Hence, the water showed a mixed state.

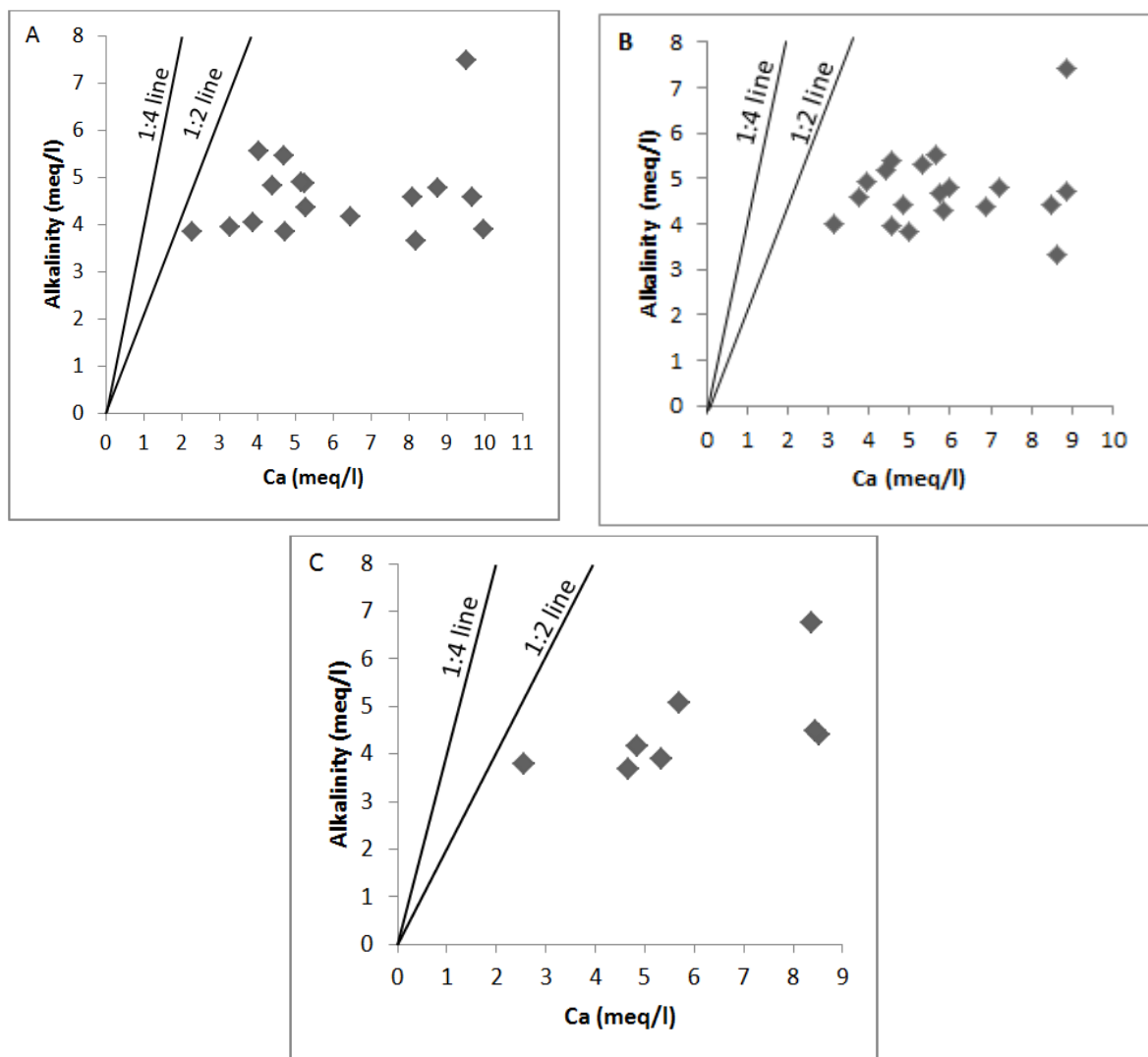
Lastly, samples B22H, B25H and B58H were all located close to each other at the lowest elevation (Figure 5.1). High chances pointed out that these boreholes were receiving their water from the spring through B55H and B10H. The reason was that in Section 5.4.1.6, the samples that showed high silica (>0.45 mmol/l) were B10H, B22H, B25H, B55H, B58H, B59H and the spring that were assumed to be forming the main flow path. Samples B22H, B25H and B58H also showed the occurrence of ion exchange. Mixing might also have been the resulting process; hence, the samples indicated a mixed water type. In addition to mixing, these boreholes have depths of 75 mbgl (B58H) and 62 mbgl (B22H and B25H) as shown in Table 3.3. Their location at low elevations (Figure 5.1) where recharge was less, together with their depths, might suggest that these areas were subject to the influence by other processes or different water types.

According to Jalali (2007), the ratio for Ca + Mg to HCO₃ that is less than 1, show that carbonate weathering is not the only source of HCO₃⁻, but also alternative sources such as silicate weathering, are likely. Furthermore, low concentrations of HCO₃⁻ in some of the water samples showed the absence of carbonates, if not less carbonates. Conversely, the samples that showed a >1 Ca + Mg/HCO₃ ratio were B24H, B44H, B50H, B56H, B57H for all seasons, B25H and B45H for the spring samples, and lastly, B62H for the summer samples. These samples did not receive any recharge by recent water (Zaidi *et al.*, 2015); however, it could also be an indication of very dry climatic areal conditions (Nazzal *et al.*, 2014).

Therefore, since some of these areas were the ones with high Cl^- over Na^+ , they could be receiving their water from connate sources (Zaidi *et al.*, 2015). Additionally, some of these areas were the ones influenced by ion exchange and carbonate weathering.

5.4.2.2 Calcium versus alkalinity

Garrels and Mackenzie (1971) stated that the presence of Ca and HCO_3^- from calcite weathering gives a ratio of 1:2; whereas, if these ions are derived from dolomite weathering, the ratio would be 1:4. Figure 5.5A-C for all the seasons, indicating the plots of Ca versus alkalinity did not show the occurrence of either calcite or dolomite weathering in the aquifer system since the samples plotted below the equilines. However, the sample of the spring water in the spring season results (Figure 5.5A) plotted closest to the 1:2 line, and this could also be an indication of calcite weathering.



Source: Author's own (2016).

Figure 5.5: Linear correlation plots for calcium versus alkalinity for spring (A), summer (B) and autumn (C) seasons

5.4.2.3 Calcium versus magnesium

The plots of Ca versus Mg (Appendix 3) gave the correlation coefficients of 0.50, 0.72 and 0.37 for spring, summer and autumn results, respectively. Maya and Loucks (1995) explained that the dissolution of pure dolomite in water is shown by a Ca/Mg ratio of 1, whereas a ratio >1 is an indication of calcite dissolution (Appendix 2). On the other hand, Jalali (2007) stated that a low Mg/Ca ratio tells that there is weathering of carbonates leading to the release of Ca^{2+} . Additionally, the high Mg/Ca ratio showed Mg^{2+} added as a result of mineral exchange. Either way, the attained results indicated no sample with a ratio equal to 1. However, when using the Ca/Mg ratio, the ratios of 1.33 for the spring sample from the spring season, 1.34 for B25H from summer, and both B25H and the spring for autumn results were accumulated and these were closest to 1. Consequently, the occurrence of dolomite dissolution in the system was not inferred until further analyses were made on the processes that took place.

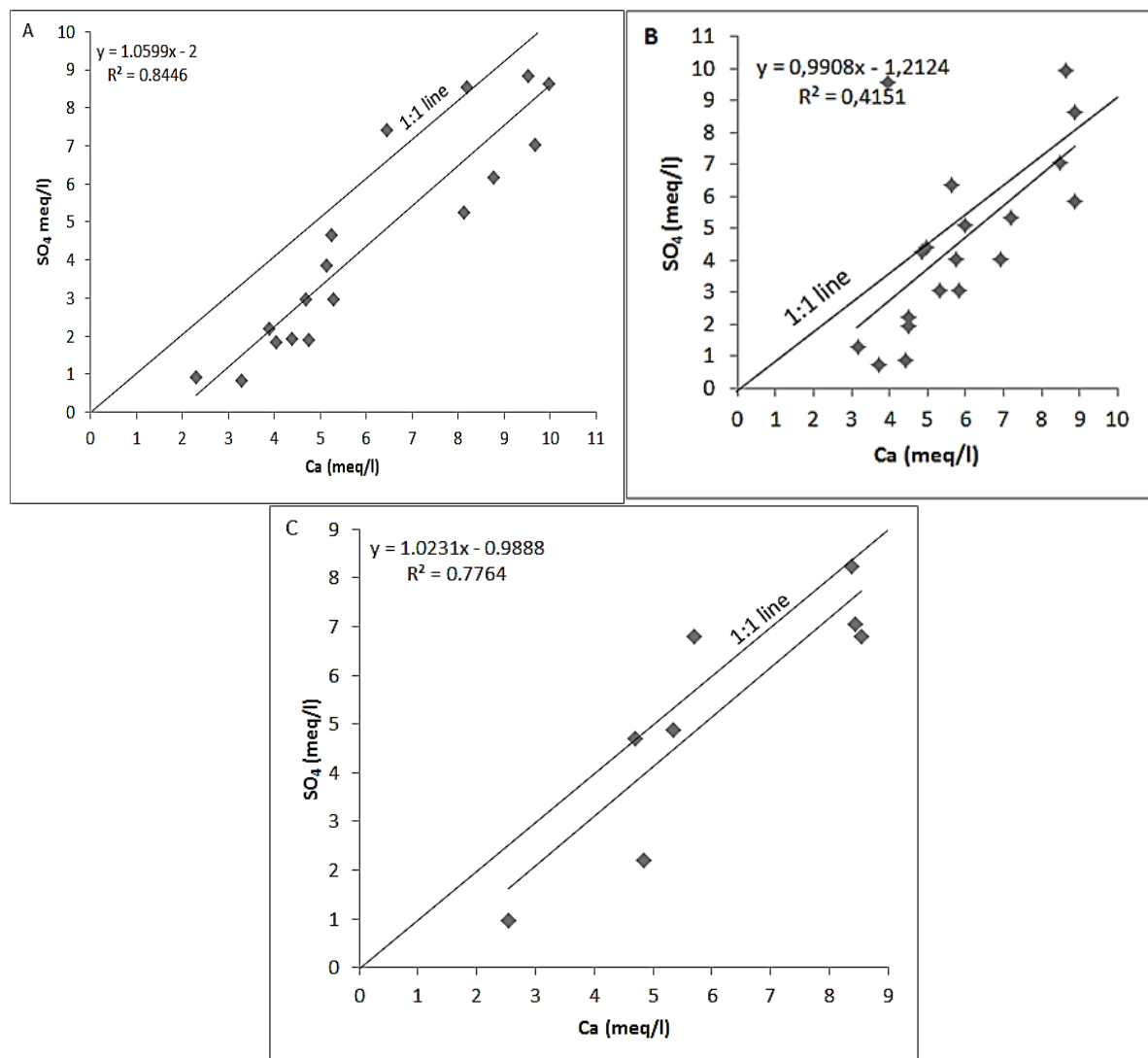
On the other hand, all the samples that gave a value of $>1 <2$, when using the Ca/Mg ratio, indicated dissolution of calcite from weathering. Kozłowski and Komisarek (2016) stated that if the Ca/Mg ratio is more than 2, dissolution of silicate minerals releasing calcium is taking place. Therefore, the only samples that showed the occurrence of calcite dissolution were B22H, B24H, B25H, B36H, B58H, B61H and B62H for the spring season; B36H, B58H, B61H and B62H for the summer season; and B24H and B58H for the autumn season, while the rest of the samples showed silicate dissolution.

The occurrence of carbonate weathering was also pointed out in Section 5.4.1.2. Although the procedure did not specify whether it was calcite or dolomite weathering, the bivariate plots clarified this finding.

5.4.2.4 Calcium versus sulphate

The Ca versus SO_4 plot (Figure 5.6A-C) indicated the correlation coefficients of 0.92, 0.64 and 0.88 from spring, summer and autumn results, respectively. It was presented on the correlation plots that most of the samples plotted below the 1:1 equiline, showing more calcium over sulphate, indicating that there were other sources of Ca^{2+} besides gypsum dissolution (Jalali, 2007). Additionally, gypsum dissolution was not the major source of Ca^{2+} . The only samples that indicated a source of gypsum dissolution plotted on the 1:1 line, and these were B44H for spring; B53H and B55H for summer and B25H for autumn results (Figure 5.6A-C). Nevertheless, there were other samples that plotted closer to the 1:1 line and might also indicate the occurrence of gypsum dissolution. These samples are B22H and B25H for spring (Figure 5.6A), B54H and B58H for summer (Figure 5.6B) and B55H for autumn (Figure 5.6C). More sulphate over calcium might be indicating the removal of

calcium from solution mostly by calcite precipitation (Kozłowski and Komisarek, 2016). These results corresponded with the obtained results in Section 5.4.1.4 that gypsum dissolution was assumed along the same areas using Ratio 4.3.



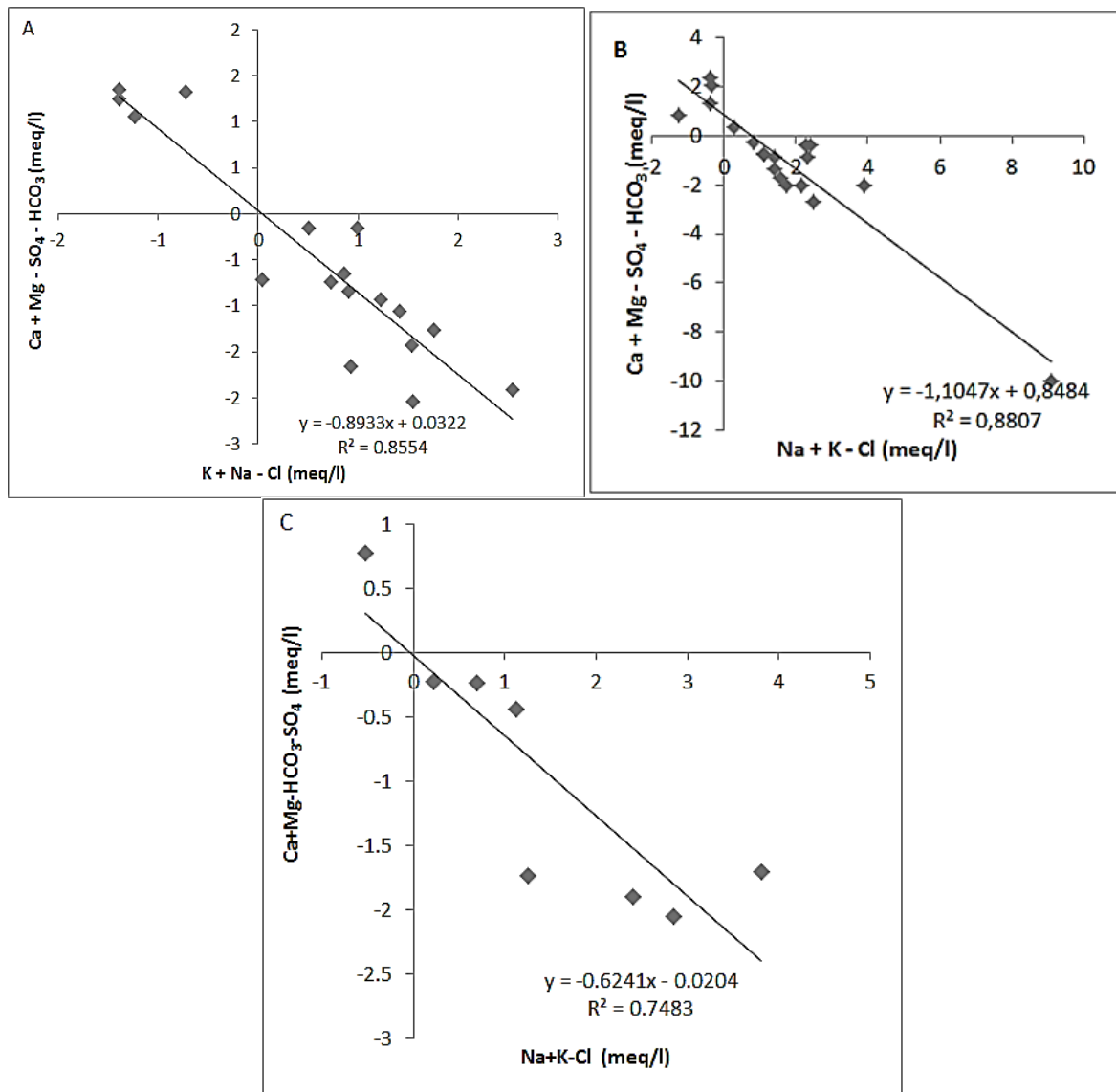
Source: Author's own (2016).

Figure 5.6: Linear correlation plots for calcium versus sulphate for spring (A), summer (B) and autumn (C)

5.4.2.5 Calcium + magnesium-sulphate-bicarbonate versus sodium + potassium-chloride

The Ca + Mg - SO₄ - HCO₃ versus Na + K - Cl plots indicated whether or not the chemistry of the water was highly influenced by ion exchange. As described by Jalali (2007), Na + K - Cl show the quantity added or removed for Na + K in relation to the amount added by dissolved chloride salts such as halite, while Ca + Mg - SO₄ - HCO₃ show the quantity for Ca + Mg added or removed, relative to the amount added by dissolution of gypsum, calcite and dolomite. Figure 5.7A-C indicates slopes of -0.89, -1.10 and -0.62, and the correlation

coefficients of 0.92, 0.94 and 0.86, respectively. Jalali (2007) explained that if calcite, dolomite, gypsum and halite dissolution are the important processes involved in the water chemistry change, a linear plot with a -1 slope should be accumulated. Figure 5.7A-C indicate this relationship by the calculated slopes. Therefore, it was assumed that these were amongst the significant processes that resulted in the various water types. Additionally, Jalali (2005) described that the slope of -1 also confirms cation exchange in the system.



Source: Author's own (2016).

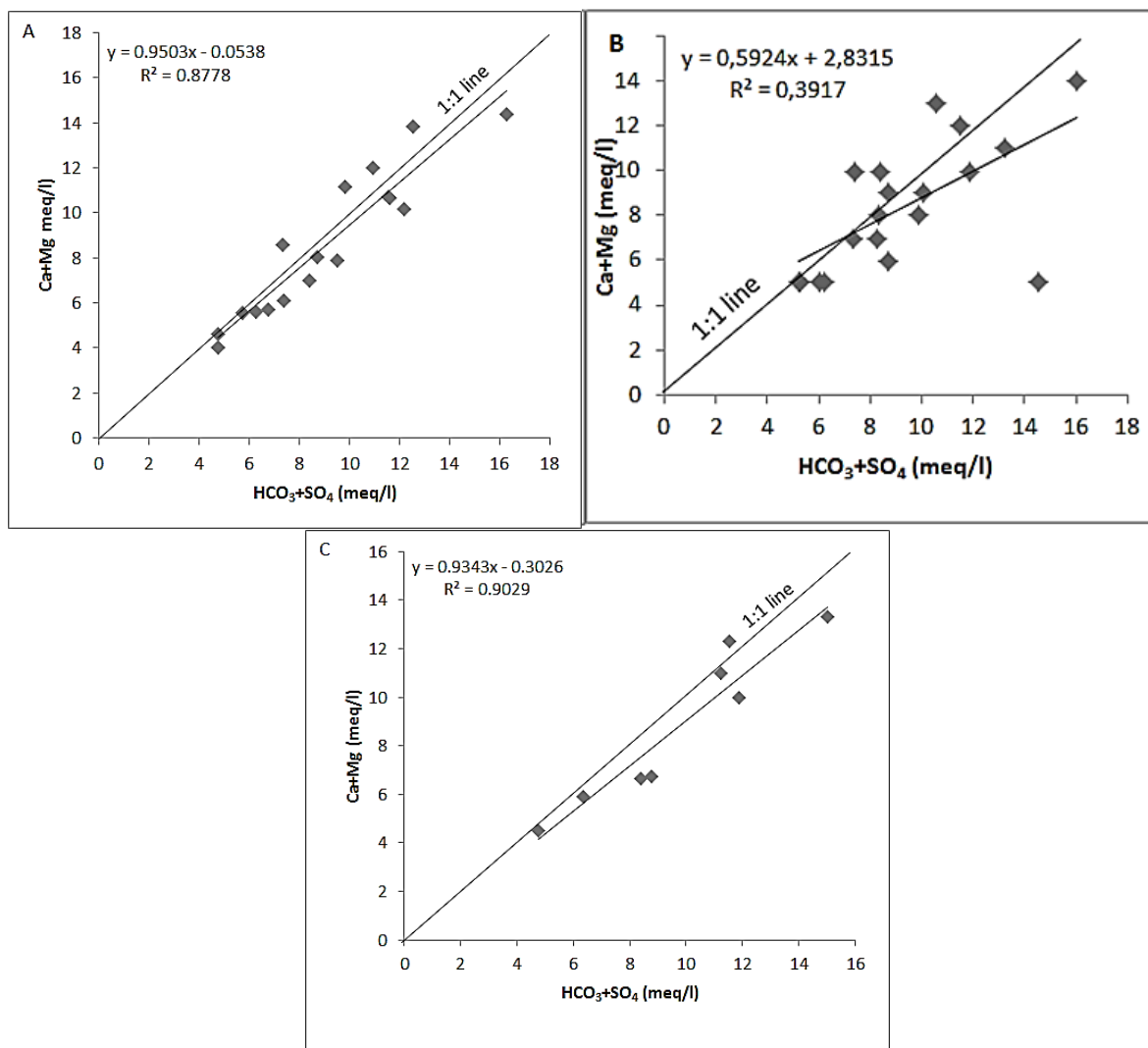
Figure 5.7: Linear correlation plot for calcium + magnesium + sulphate + bicarbonate versus sodium + potassium - chlorine for spring (A), summer (B) and autumn (C)

5.4.2.6 Potassium versus chlorine

Moderate ($r=0.68$) and high ($r=0.72$ and $r=0.72$) correlations were developed for the K versus Cl plots for spring, summer and autumn. Based on this study, this could have been sylvite weathering that contributed to the presence of Cl^- and K^+ in the solution (Jalali, 2007).

5.4.2.7 Calcium + magnesium versus bicarbonate + sulphate

The plot of Ca + Mg versus HCO₃ + SO₄ indicates the relationship between ion exchange and reverse ion exchange. Samples plotted above the 1:1 line showed reverse ion exchange, whereas samples plotted below the line showed ion exchange as indicated in Figure 5.8A-C. The 1:1 equiline may display a simple dissolution of calcite, gypsum and dolomite, showing charge balance between the cations and anions, while the lower side of the 1:1 equiline may also indicate carbonate or silicate weathering apart from ion exchange (Fisher and Mullican, 1997). Belkhiri *et al.* (2010) explained that if carbonate or silicate weathering and ion exchange are the dominant processes, the samples will plot below the 1:1 line showing abundance in HCO₃ + SO₄ over Ca + Mg (Figure 5.8A-C). The opposite (reverse ion exchange) will be observed when there is more Ca + Mg in the system as compared to HCO₃ + SO₄ (Kozlowski and Komisarek, 2016; Rajmohan and Elango, 2004).



Source: Author's own (2016).

Figure 5.8: Linear correlation plots for calcium + magnesium versus bicarbonate + sulphate for spring (A), summer (B) and autumn (C) seasons

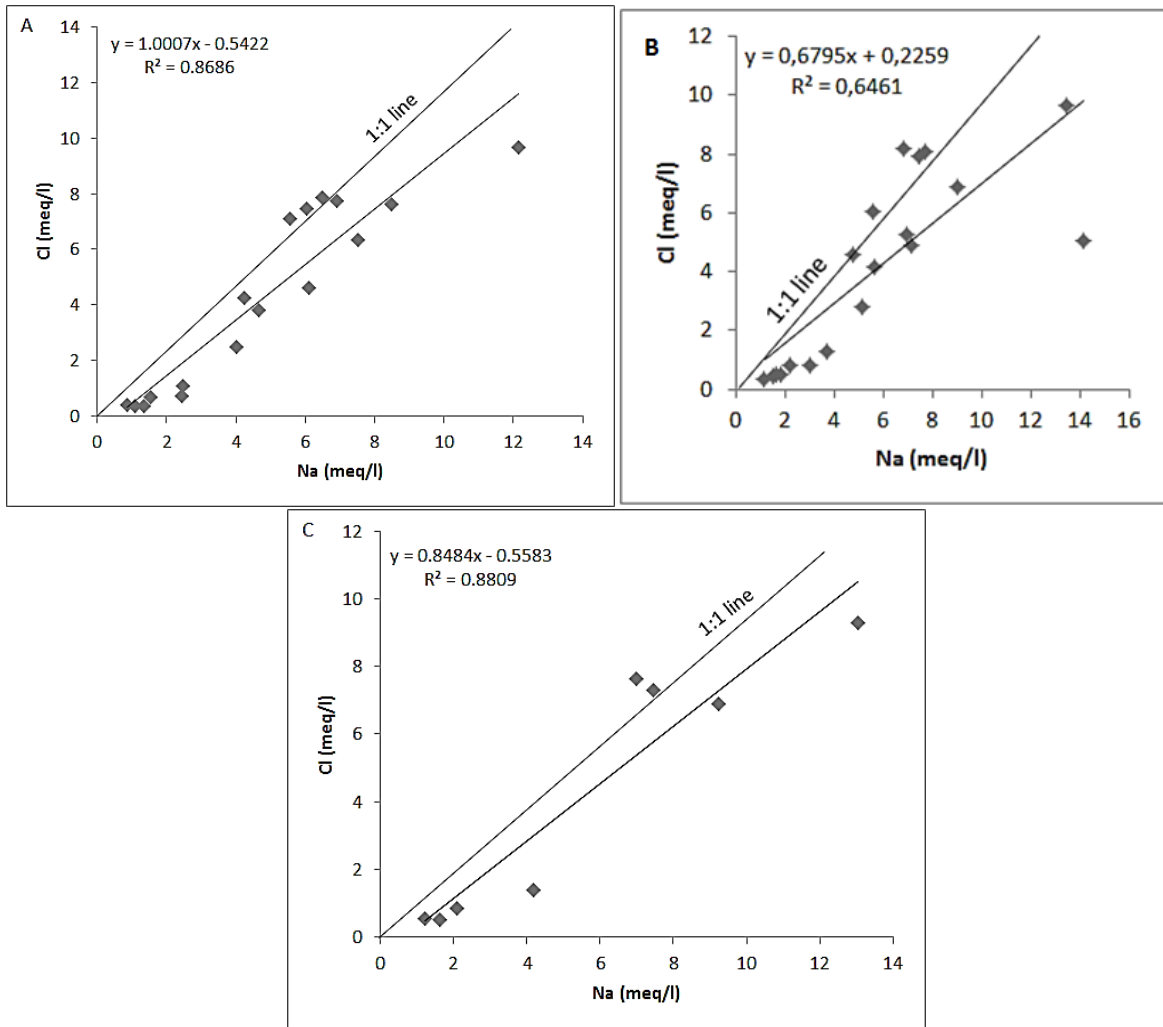
The plots of Ca + Mg versus $\text{HCO}_3 + \text{SO}_4$ for all seasons show the dominance in ion exchange and carbonate or silicate weathering processes over reverse ion exchange, as shown by Figure 5.8A-C. This may explain that there was excess of $\text{HCO}_3 + \text{SO}_4$ in this system as a result of the processes taking place in comparison to Ca + Mg. According to Kozłowski and Komisarek (2016), if the sources of Ca^{2+} and Mg^{2+} are carbonate and silicate weathering only, alkalinity should be the only ion to balance their presence.

Samples B50H, B56H, B57H and B62H indicated the process of reverse ion exchange for spring and summer seasons (Figure 5.8A-B). Contrariwise, samples B11H, B22H, B25H, B44H, B45H, B53H, B54H, B58H, B59H, B60H, B61H and the spring displayed either ion exchange, carbonate or silicate weathering for all seasons, whereas B10H and B55H showed ion exchange in the spring results. A change from ion exchange to reverse ion exchange explains a decrease of $\text{HCO}_3 + \text{SO}_4$ in solution with an increase of Ca + Mg. Furthermore, a change from reverse ion exchange to ion exchange could be the result of dissolution of gypsum with the removal of Ca^{2+} during exchange or rather silicate weathering dominating in the system (Zaidi *et al.*, 2015).

5.4.2.8 Sodium versus chloride

The Na versus Cl plots indicated enrichment for both Na^+ and Cl^- (Figure 5.9A-C). The samples enriched in Na^+ plots below the 1:1 equiline, whereas the samples enriched in Cl^- plots above the line. There were two samples, B36H from the spring season and B45H from the autumn season (Figure 5.9A and C) that plotted on the line, and from these samples halite dissolution in the system could be assumed (Fisher and Mullican, 1997; Zaidi *et al.*, 2015). The samples enriched in Na^+ represented ion exchange or silicate weathering to have been occurring in the system. The samples that showed Na^+ enrichment were B10H, B11H, B22H, B25H, B44H, B45H, B53H, B55H, B58H, B59H, B60H, B61H and spring.

Furthermore, the high Cl^- over Na^+ in the water could be the result of Na^+ removal from solution during cation exchange (Jalali, 2009); it could also be the result of connate water mixing with the aquifer water (Zaidi *et al.*, 2015). The samples that showed high Cl^- enrichment were B50H, B56H, B57H and B62H for all seasons.



Source: Author's own (2016).

Figure 5.9: Linear correlation plot for sodium versus chlorine for spring (A), summer (B) and autumn (C)

The Na versus Cl plots further indicates silicate weathering. Thus, for all samples with a Na/Cl of >1 (Appendix 2), a release of Na⁺ from silicate weathering could be assumed (Meyback, 1987), instead of halite dissolution which gives a ratio equal to 1 (Rajmohan and Elango, 2004). Therefore, albite plagioclase may be one of the significant minerals adding Na⁺ in solution because of a Na/Cl >1 (Appendix 2) showing a release of Na⁺ (Jalali, 2009). The samples were found to be B10H, B11H, B53H, B55H, B59H, B60H, B61H and spring for all three seasons. These were the samples that were classified under the CaHCO₃ water type, meaning that Ca²⁺ and HCO₃⁻ were the most abundant cation and anion, respectively. Rogers (1989) and Jalali (2007) indicated that HCO₃⁻ ion will be excess in samples where silicate weathering is one of the Na⁺ sources because in water HCO₃⁻ is released as the carbonic acid interacts with feldspars (Equation 5.6). Furthermore, HCO₃⁻ and Ca²⁺ may come from carbonate weathering as shown by Equation 5.2 and Equation 5.3 (Jalali, 2007).

Therefore, the release of sodium in these areas is assumed to result from silicate weathering process.

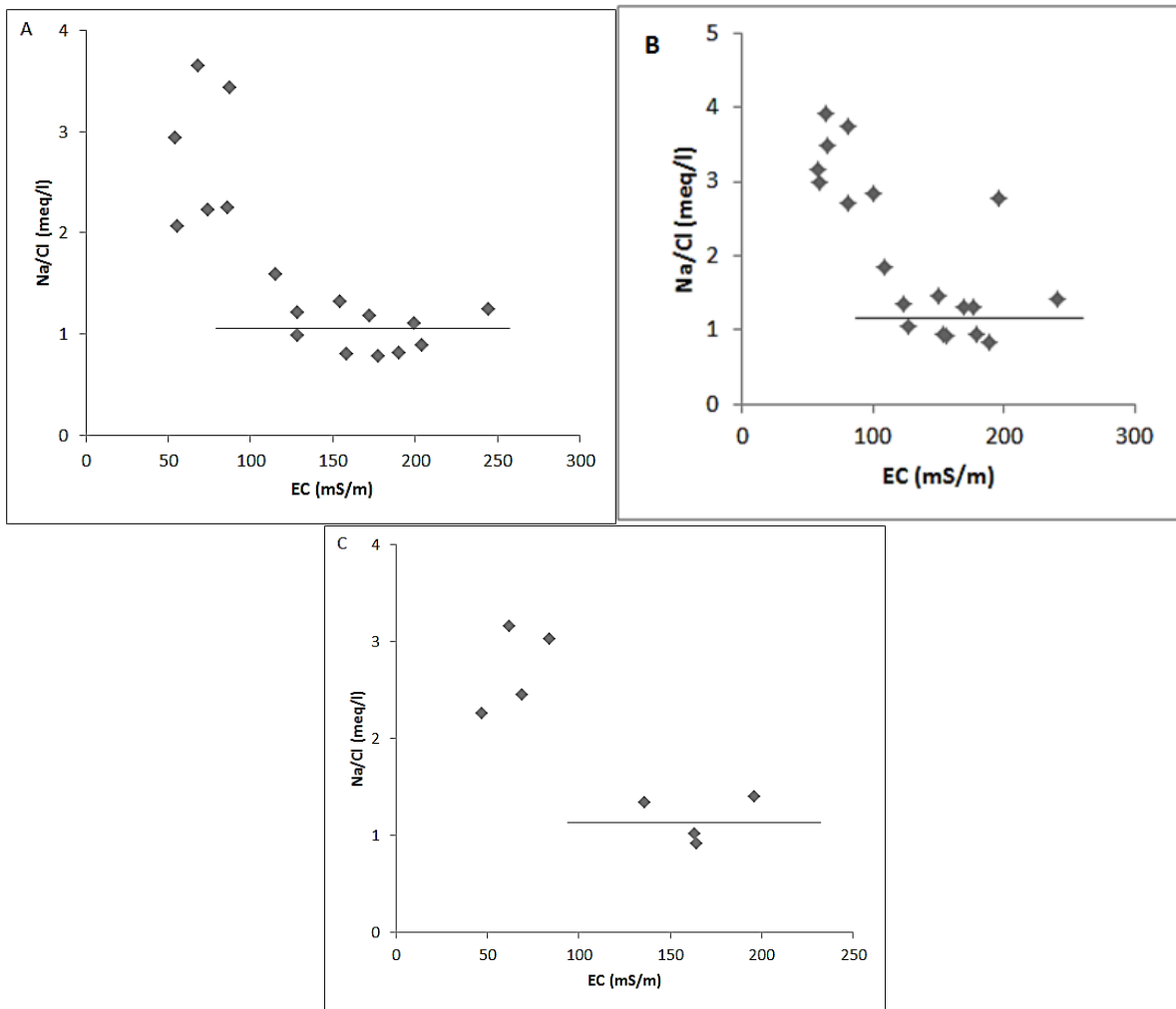
Silicate weathering was already inferred to be occurring in Section 5.4.1.3, although it was not shown by all the samples that indicated its occurrence in this section. Silicate weathering of either calcic or sodic minerals was shown to have taken place at high elevated areas where recharge occurred. This process was also assumed to have taken place at moderate elevations around B44H, B45H and B50H; and also at areas around B56H and B57H.

Contrariwise, Rajmohan and Elango (2004) stated that if the Na/Cl ratio is <1 , processes such as ion exchange and carbonate weathering can be assumed. Ion exchange and reverse ion exchange were also assumed by the use of Ratio 4.4. The results that were attained after the use of Ratio 4.4, correlated with the findings obtained from the bivariate plots. Additionally, ion exchange was shown to have been taking place at lower elevated areas as shown on Figure 5.1. It was occurring at locations where the samples showed mixed to NaCl water types.

5.4.2.9 Sodium/chlorine versus electrical conductivity

Figure 5.10A-C indicates the scatter plots of Na/Cl versus EC. Saini *et al.* (2014) stated that the ratio of Na versus Cl is used to determine evaporation processes in the groundwater. The process of evaporation as explained by Saini *et al.* (2014) as well as Kozłowski and Komisarek (2016), increases the concentration of TDS in the groundwater, although this happens when the Na/Cl ratio is constant with an increase in EC. This variation is indicated by Figure 5.10A-C that shows a horizontal line for some samples that are indicating ion concentration as a result of evaporation.

Figure 5.10A-C further shows that samples B22H, B25H, B36H, B44H, B45H, B50H, B54H, B56H, B57H, B58H and B62H for all three seasons showed high ion concentrations in the groundwater as a result of evaporation. These results indicated that evaporation at Beaufort West was one of the major contributing hydrogeochemical processes that led to the groundwater chemistry evolution. Figure 5.10A-C further indicates that the decrease of the Na/Cl ratio with increasing EC, especially in the samples that did not show a horizontal line, could be an indication of Na^+ removal by ion exchange (Kozłowski and Komisarek, 2016).



Source: Author's own (2016).

Figure 5.10: Scatter plot of sodium/chlorine versus electrical conductivity for spring (A), summer (B) and autumn (C)

5.4.2.10 Summary on water-rock interaction

The following deductions were made from the stoichiometric analysis and bivariate plots analysis. Both the approaches confirmed assumptions on the hydrogeochemical processes that were taking place in the groundwater system. Thus, the same samples that indicated a particular process in the stoichiometric analysis, also explained the same process under bivariate plots. The major processes that were indicated by these approaches were weathering of silicates and carbonates, gypsum dissolution, evaporation, ion exchange and reverse ion exchange. Silicate weathering of both calcic and sodic minerals was assumed to be dominant at areas where recharge by recent water occurred, while ion exchange was assumed to be taking place at lower elevated locations. Additionally, reverse ion exchange took place at locations where two or more water types were mixed. Evaporation was assumed to be dominating low elevated areas that were dominated by ion exchange, reverse ion exchange and/or carbonate weathering. Carbonate weathering and gypsum dissolution

on the other hand, were inferred to be happening at random locations especially at lower elevated areas. Although not appearing as major processes, sylvite and halite dissolution were also inferred to be taking place. Lastly, dolomite dissolution, even though has been inferred by this approach to be one of the processes, still needed to be clarified by more tools.

5.5 Hierarchical cluster analysis

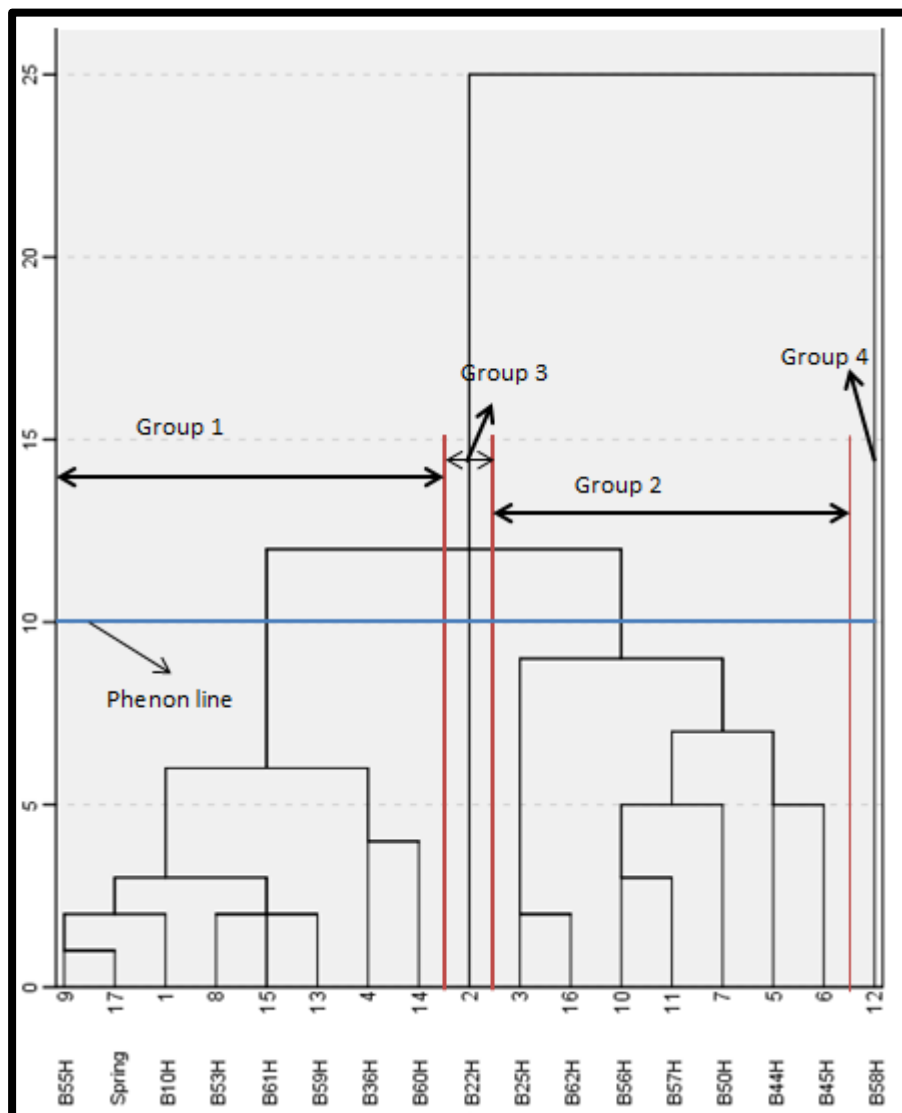
Major ions that greatly influenced the water classification on the dendrogram are Ca^{2+} , Na^+ , HCO_3^- , Cl^- and SO_4^{2-} . They were considered the major influence, because out of all the ions, they were the ones that were dominant in the water and they influenced the main hydrogeochemical processes that took place. Furthermore, these were the ions that resulted in the naming of the main water types found in the study area. Thus, processes such as dissolution of calcite and gypsum, silicate weathering, ion exchange, reverse ion exchange and evaporation led to high concentrations of these ions in the water. Therefore, an addition or removal in one of these ions from solution will alter the water chemistry (Peikam and Jalali, 2016). The TDS as influenced by the number of ions dissolved in the water was also acting as one of the main distinguishing parameters of the groups. Table 5.5, Table 5.6 and Table 5.7 present the results on how the concentrations for parameters vary, whereas Figure 5.11 to Figure 5.13 displays the clustering of the variables and groundwater samples. Sample B24H was not plotted on the dendrogram due to it giving odd results as already explained.

5.5.1 Spring season

Figure 5.11 is a dendrogram indicating a total of four groups as labelled. The hierarchical clustering was done automatically by IBM SPSS software program. The grouping of these clusters showed the close relationship between the water samples relative to the parameters in these samples.

Group 1 comprised of boreholes B10H, B36H, B53H, B55H, B59H, B60H, B61H and the spring. This was the recharged water because of its low TDS showing less mineralisation, and was therefore classified as CaHCO_3 water (see Section 5.3.1.1). Additionally, the results explained in Section 5.4.2.1 stated that these were recharge samples by fresh water. This water was more concentrated in Ca^{2+} and HCO_3^- ions (Table 5.5) as compared to other ions. All the group 1 samples, except B36H, showed the occurrence of silicate weathering (Section 5.4.2.8). Sample B36H, although they appeared in the first group, was classified under mixed water type in the Piper diagram (Figure 5.2). These samples were represented as recharged fresh water (Section 5.4.2.1) in the bivariate plots analysis. Although they

showed recharge by fresh water, the process of reverse ion exchange that took place along these areas led to their classification as mixed water type (Figure 5.2). However, these water samples indicated a closer relationship with the CaHCO₃ classified samples.



Source: Author's own (2016).

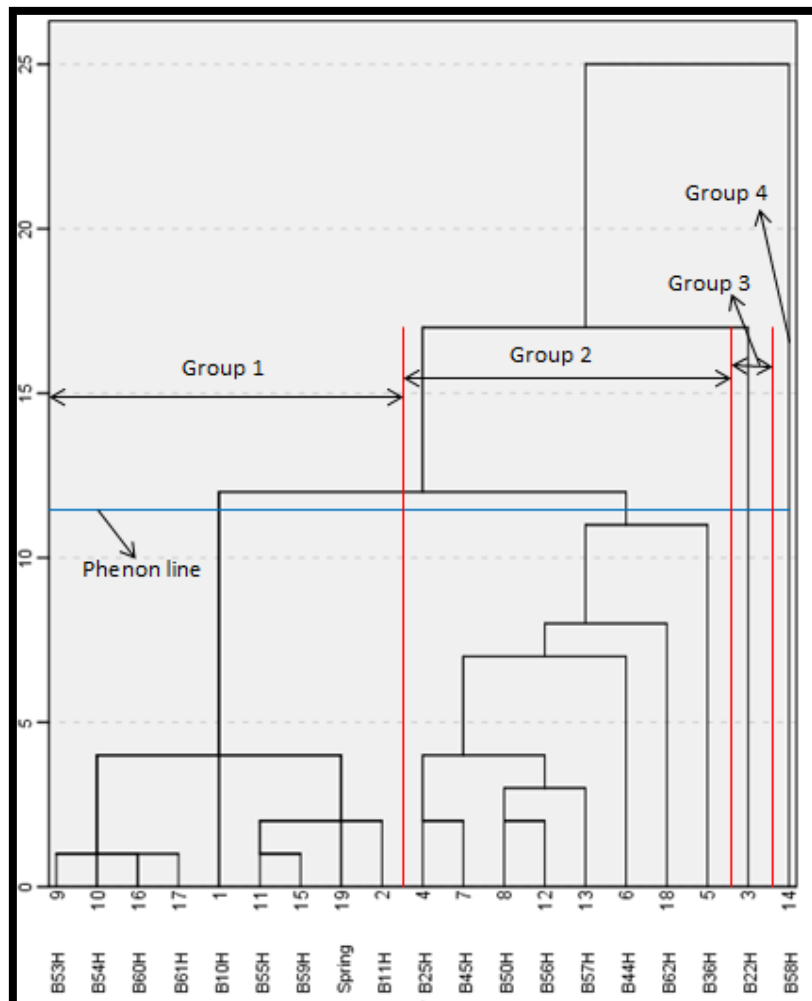
Figure 5.11: Dendrogram indicating the relationship between water samples in groups for spring data

Group 2 encompassed B25H, B44H, B45H, B50H, B56H, B57H and B62H whereas Group 3 contained B22H and Group 4 was B58H alone. These samples were all classified under the mixed water type in the Piper diagram (Figure 5.2) for the spring season. All the Group 2 samples showed either ion or reverse ion exchange in Sections 5.4.1.4 and 5.4.2.8. The separation of B22H and B58H from Group 2 and from each other indicates how these samples were unrelated to others. The groundwater chemistry data (Section 5.3.1.1) also indicated how these water samples were enriched in specific major ions, more especially B58H that had the highest TDS after B24H. Group 3 and 4 similar to the Group 1 samples,

showed recharge by recent water (Section 5.4.2.1). Nevertheless, due to processes such as ion exchange, carbonate weathering, evaporation and mixing taking place as explained in Sections 5.4.1 and 5.4.2, this water changed its composition making it enriched in most of the ions.

5.5.2 Summer season

The dendrogram in Figure 5.12 was generated using the summer hydrochemistry results and it displayed a total of four groups according to the relationship between the water samples. A slight difference was indicated by the results in Figure 5.12 from the results in Figure 5.11.



Source: Author's own (2016).

Figure 5.12: Dendrogram indicating the relationship between water samples in groups for summer data

Four groups were generated with Group 1 represented by B10H, B11H, B53H, B54H, B55H, B59H, B60H, B61H, and the spring that were classified as the CaHCO₃ water in Section 5.3.2.2, with B55H, B54H and B53H classified as mixed water (Figure 5.3). The same explanation for B54H as in Section 5.5.1 still applied. The shifting of B55H could be related to the process of gypsum dissolution (Section 5.4.1.4) that took place prior to sample

collection in the summer season. Furthermore, silicate weathering (Section 5.4.2.7) at both B53H and B55H locations could have resulted in a different water type as collected during the summer season. Nevertheless, the HCA showed that all the Group 1 samples were related in terms of their ions and processes taking place along these locations.

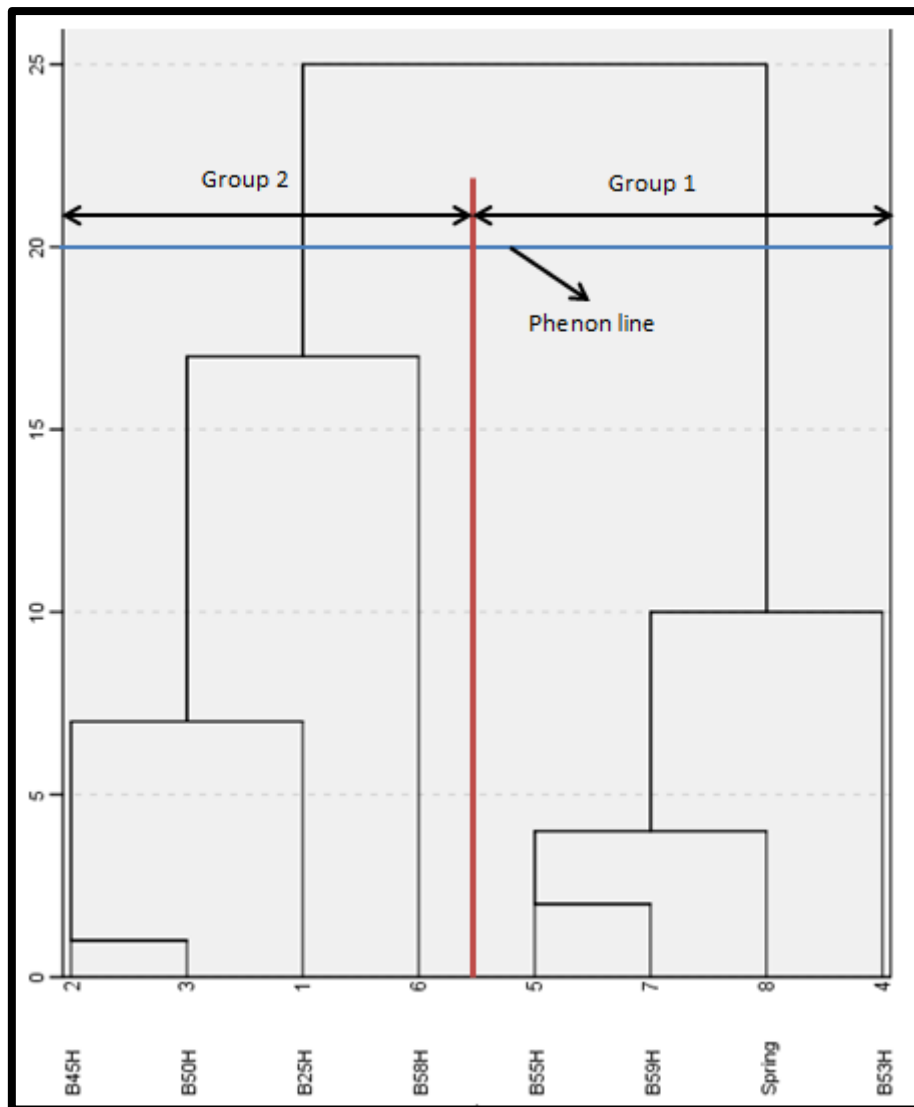
Group 2, 3 and 4, on the other hand, contained the same samples as presented by the groups in the spring season. The only difference in these results was that B22H was classified under mixed water type for the sample that was collected in the spring season and then represented NaClSO_4 water in summer (Figure 5.3). Sample B22H underwent gypsum dissolution and ion exchange prior to collecting the sample in summer, adding more SO_4^{2-} and Na^+ to the groundwater, respectively. These processes were identified under Section 5.4.1 and 5.4.2.

5.5.3 Autumn season

The following cluster (Figure 5.13) indicates how related the samples were to each other and how unrelated they were to samples in the other group. This is shown by the groupings whereby two groups are indicated by this data.

The same approach used in Sections 5.5.1 and 5.5.2 was followed in this section. However, only two groups were generated. The difference displayed by the autumn season in comparison to the other seasons, was that fewer samples were collected for autumn, hence fewer groups. The grouping of the samples indicated a difference from the spring and summer results. Group 1 consisted of B53H, B55H, B59H and the spring, whereas Group 2 was represented by B25H, B45H, B50H and B58H. All the Group 2 samples were classified under the mixed water type in the Piper diagram (Figure 5.4) and the explanations as in Sections 5.5.1 and 5.5.2 also applied here. Additionally, these were the samples that displayed the occurrence of gypsum dissolution as shown in Sections 5.4.1.4 and 5.4.2.2.

Conversely, the samples in Group 1 were all classified in the CaHCO_3 water type. There was no gypsum dissolution taking place (5.4.2.2) before the collection of samples in autumn, and instead of ion exchange, there was cation exchange leading to high Ca^{2+} and Cl^- over Na^+ (Table 5.4) in the solution.



Source: Author's own (2016).

Figure 5.13: Dendrogram indicating the relationship between water samples in groups for autumn data

5.5.4 Summary on cluster analysis

The relationship between the samples on the HCA was indicated by different groups after drawing the phenon line. The HCA represented four main groups for spring and summer seasons and two groups for autumn. The results showed that the grouping was mostly influenced by the hydrogeochemical processes that were taking place along the groundwater system. Furthermore, the grouping was related to the hydrochemical classification as developed by the Piper diagrams. The main findings displayed by the HCA were that the majority of the samples clustered in Group 1, represented the CaHCO_3 water type in the Piper diagrams. Again, the samples clustered as Group 2, 3 and 4 represented the mixed water type in the Piper diagrams. However, the HCA separated the mixed water samples by grouping them according to how closely they were to each other.

Silicate weathering was concluded to have been taking place mostly in the samples that were classified as Group 1, while ion exchange, reverse ion exchange and evaporation were assumed in samples clustered as Group 2, 3 and 4. Gypsum and carbonate dissolutions were also indicated by some samples in these groups, although not in a specific order. The reason that there was less variation in cluster analysis for different seasons could have been because groundwater flow paths were the same, and the similar hydrogeochemical processes took place in this groundwater system. Furthermore, the climatic conditions at Beaufort West followed the same pattern such that during high recharge in the aquifer as a result of increased rainfall, mineralisation to the groundwater was low. Equally, when rainfall was less during dry seasons, there was less recharge with increased residence time of the water leading to high mineralisation in the system.

5.6 Geochemical modelling

5.6.1 Mineral saturation indices

Table 5.10 and Appendix 4 show the saturation indices that were calculated by PHREEQC hydrogeochemical program (Parkhurst and Appelo, 1999), making use of the spring, summer and autumn groundwater chemistry data. The SI was calculated to determine how saturated the solution at a certain point was, relative to specific minerals. The possible minerals found in the study area were described in Section 5.4.1. Variations in processes that took place within the groundwater system leading to the alteration of the chemistry were indicated by SI (Peikam and Jalali, 2016) as presented for each borehole (Table 5.10 and Appendix 4).

5.6.1.1 Spring season

The spring season SI results showed an undersaturation in albite, anorthite, Ca-montmorillonite, gypsum, halite, fluorite, chlorite and sylvite. Contrariwise, K-mica (clay minerals such as muscovite and illite) (Manning, 2009) and quartz appeared oversaturated in solution. Undersaturation of groundwater in these minerals showed that this water has not evolved enough. However, an undersaturation of albite and anorthite throughout all seasons could be that the weathering of these minerals formed clay minerals such as kaolinite and montmorillonite. An explanation for undersaturation is that if there could have been more of these minerals in the aquifer along the flow path, they could still be dissolved if they came in contact with the groundwater, only if the conditions would allow. Quartz showed slightly positive SI values, indicating that it could potentially have been precipitated from the groundwater (Runnells, 1993). However, for this to happen, elevated temperature conditions had to be reached first (Jalali, 2007).

TABLE 5.10: SATURATION INDICES FOR ALL THE BOREHOLES IN THE SPRING SEASON

Phases	Albite	Anorthite	Ca-montmorillonite	Calcite	Chlorite	Dolomite	Fluorite	Gypsum	Halite	K-mica	Kaolinite	Quartz	Rhodochrosite	Sylvite
B10H	-4.55	-7.2	-1.53	-0.69	-14.93	-1.65	-1.55	-2.01	-8.09	1.61	0.78	0.24	-2.97	-8.91
B11H	-	-	-	-	-	-	-	-	-	-	-	-	-	-
B22H	-3.72	-6.88	-1.56	-0.36	-12.54	-0.9	-1.09	-1.24	-6.38	2.14	0.71	0.25	-2.97	-7.41
B24H	-2.77	-6.01	-2.09	0.78	-5.46	1.55	-0.82	-0.5	-4.63	1.96	0.2	0.11	0.35	-6.55
B25H	-3.08	-6.22	-0.75	-0.04	-11.17	0.02	-1.23	-1.07	-5.9	2.91	1.35	0.28	-2.41	-7.38
B36H	-3.61	-6.57	-1.72	-0.1	-9.89	-0.33	-1.09	-1.32	-6.43	2.02	0.49	0.24	-1.93	-7.49
B44H	-4.5	-7.71	-2.82	-0.41	-15.08	-1.32	-0.87	-0.85	-6.25	0.62	-0.15	0.05	-2.09	-7.57
B45H	-3.36	-5.54	-1.23	0.19	-11.01	-0.49	-0.97	-0.87	-6.02	2.8	1.07	0.05	-1.63	-7.52
B50H	-3.41	-5.81	-0.52	-0.35	-12.09	-1.0	-0.98	-0.82	-5.98	3.68	1.75	0.11	-1.51	-7.11
B53H	-3.48	-5.71	-0.38	-0.3	-12.02	-1.0	-1.33	-1.58	-7.23	3.38	1.75	0.2	-3.44	-8.1
B54H	-	-	-	-	-	-	-	-	-	-	-	-	-	-
B55H	-3.81	-6.33	-0.42	-0.68	-13.97	-1.59	-2.18	-1.57	-7.65	2.8	1.7	0.28	-2.39	-8.86
B56H	-3.91	-6.89	-1.65	-0.33	-13.38	-0.96	-0.85	-1.06	-6.1	2.26	0.73	0.16	-3.71	-7.02
B57H	-3.76	-6.68	-1.49	-0.26	-12.91	-0.84	-0.87	-0.98	-6.0	2.49	0.86	0.16	-3.68	-6.97
B58H	-2.72	-5.78	-0.66	0.13	-9.42	0.09	-0.92	-0.87	-5.65	3.12	1.32	0.32	-0.22	-7.19
B59H	-3.78	-5.91	-0.9	-0.2	-11.97	-1.04	-1.81	-1.53	-7.96	2.31	1.21	0.24	-1.31	-9.28
B60H	-3.18	-5.52	-0.12	-0.27	-10.85	-0.72	-1.31	-1.44	-6.68	3.8	1.97	0.2	-3.44	-7.95
B61H	-3.5	-6.1	-0.58	-0.33	-11.72	-0.83	-1.63	-1.66	-7.43	2.81	1.5	0.28	-2.85	-8.74
B62H	-3.22	-6.08	-0.76	-0.34	-10.7	-0.75	-1.51	-1.43	-6.03	2.87	1.37	0.25	-2.9	-7.51
Spring	-3.69	-6.25	-0.17	-0.83	-12.95	-1.65	-2.39	-2.11	-8.05	2.8	1.85	0.35	-3.67	-9.4

Note: (-) = Samples with high IBE

Minerals such as calcite, dolomite, kaolinite and rhodochrosite showed undersaturation at some areas and supersaturation at other areas. Oversaturation of calcite, dolomite and rhodochrosite was shown by samples B24H and B58H; however, B58H did not show oversaturation in rhodochrosite. Oversaturation of calcite and dolomite was also displayed by samples B45H and B25H, respectively. The supersaturation in calcite, dolomite and rhodochrosite in this water might have been the result of carbonate dissolution (see Section 5.4.1.4) since these minerals are easily dissolved in solution. Furthermore, samples B25H, B44H and B58H showed gypsum dissolution (see 5.4.1.4 and 5.4.2.2). The occurrence of carbonate and gypsum dissolution led to the addition of Ca^{2+} , HCO_3^- and SO_4^{2-} in the water, making these ions dominant such that they had to precipitate. Lastly, kaolinite was supersaturated in all the samples, except for B44H, that was undersaturated in this phase.

5.6.1.2 Summer season

Similar to the spring season, the summer season showed undersaturation in albite, anorthite, gypsum, halite, fluorite, chlorite and sylvite, with an exception of Ca-montmorillonite that indicated undersaturation for the summer season. On the other hand, quartz was the only one that showed oversaturation in all the water samples. The rest of the mineral phases such as calcite, dolomite, rhodochrosite, kaolinite, K-mica and Ca-montmorillonite, indicated undersaturation in some samples and oversaturation in others (Appendix 4).

Calcite, dolomite and rhodochrosite appeared oversaturated in sample B24H, whereas in the rest of the samples they showed undersaturation. This might be due to high mineralisation at B24H, since carbonates are easily dissolved as explained in Section 5.6.1.1. The supersaturation of more minerals in the B24H groundwater showed how the solution was evolved. This was the sample that indicated a NaCl water type in the Piper diagram (Figure 5.3). The only difference to be pointed out was in the water chemistry such that the solution in this group was more evolved as compared to the rest of the solutions (Appendix 4).

Furthermore, Ca-montmorillonite that showed undersaturation in all the spring season samples appeared oversaturated in samples B36H and B60H in summer (Appendix 4). These samples both indicated recharge by recent water and the release of Ca-montmorillonite could have occurred during anorthite weathering (Section 5.4.1.3). Kaolinite and K-mica, although they showed supersaturation in the majority of the samples, appeared to be undersaturated in samples B11H and B50H, with an addition of B24H and B56H for kaolinite

5.6.1.3 Autumn season

The same mineral phases that showed undersaturation in all samples for the spring and summer seasons, also appeared undersaturated for the autumn season, except chlorite and Ca-montmorillonite. Again, quartz was the only one that showed oversaturation in all the samples (Appendix 4).

Calcite showed supersaturation in, B24H, B45H, B50H, B59H and the spring, whereas dolomite showed supersaturation in B24H, B45H, B50H, B59H and the spring. Additionally, rhodochrosite only appeared oversaturated in sample B24H (Appendix 4). Supersaturation of these mineral phases in solution might be as a result of carbonate dissolution as stated for spring and summer (Section 5.6.1.1 and 5.6.1.2). As a result of increased rainfall during the wet season, recharge into the aquifer also increased. During recharge, the water enriched in carbonic acid interacted with the carbonate minerals and dissolved them. These led to increased Ca^{2+} , Mg^{2+} and HCO_3^- concentrations in the groundwater (as indicated in Table 5.4) which gave the highest concentrations of Ca^{2+} , Mg^{2+} , HCO_3^- and TDS for all seasons. This explained the supersaturation of the carbonates in these samples.

Mineral chlorite showed oversaturation in B24H. Chlorite has been appearing undersaturated in all the seasons for all the samples (Section 5.4.2.3). Consequently, kaolinite was undersaturated in samples B24H, B25H, B45H, B50H, B59H and the spring. The undersaturation of kaolinite from these samples could be an indication that silicate weathering which normally leads to the release of this mineral phase, was absent at these areas (Section 5.4.2.3). Lastly, K-mica showed oversaturation in all the samples, except B25H and B53H.

5.6.1.4 Summary on saturation indices

The SI results showed a change of calcite, dolomite, rhodochrosite, Ca-montmorillonite, kaolinite, K-mica and chlorite from being undersaturated to oversaturated at some areas for the different seasons. All the evaporites and plagioclase minerals were undersaturated in all samples for different seasons. On the other hand, quartz appeared to be supersaturated in all the samples. The undersaturation of evaporites might have been the result of fewer occurrences of these minerals along certain flow paths.

A seasonal variation was indicated between the results. Most of the samples appeared to be supersaturated in carbonates during autumn, whereby ions, Ca^{2+} , Mg^{2+} and HCO_3^- , were abundant in solution. This was explained to be the result of high recharge to the aquifer that dissolves the carbonates. Another variation was also indicated by the results that in the

majority of the samples, carbonates and Ca-montmorillonite were undersaturated with oversaturation in kaolinite. This could be showing that carbonate weathering took place in the absence of silicate weathering and *vice versa*. However, there were a few samples that showed oversaturation of both kaolinite and Ca-montmorillonite at the same time. This could be an indication of plagioclase (both albite and anorthite) weathering taking place.

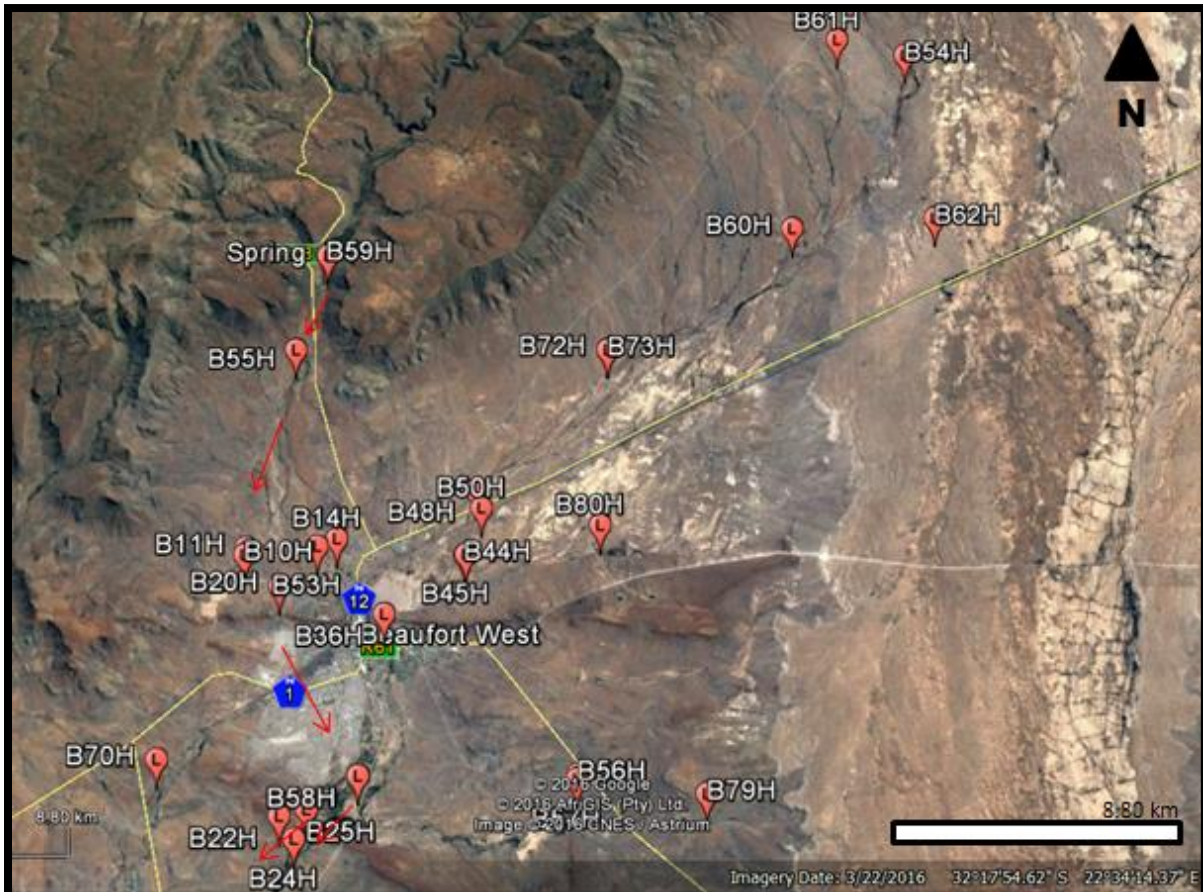
5.6.2 Mass-balance modelling

To conduct mass-balance modelling, sampling points along one general groundwater flow direction (pointing down gradient) was considered. It has been shown that groundwater flow follows topography at the site (Section 3.8). Figure 5.14 indicates what was assumed to be one of the main groundwater flow path that was used in understanding the hydrogeochemical processes that alter the groundwater chemistry. The selected flow path is indicated by red arrows on Figure 5.14. The reason for the selection of one flow path was because of data shortage from the autumn season, since not all the boreholes that were sampled during spring and summer were sampled again during autumn.

The change in the water chemistry along the inferred flow paths was clearly indicated by an increasing TDS from a high elevation to a low elevation. The TDS increase was a reflection of mineralisation that occurred along the flow path as the groundwater continuously interacts with the formation resulting in groundwater evolution. However, a decrease in TDS at some points was seen and this was related to mineral precipitation from a supersaturated solution. Table 5.11 to Table 5.14 displays the change in the water chemistry from the initial to the final solution.

5.6.2.1 Mole transfer between Period 1 (spring to summer) and Period 2 (summer to autumn)

The mass-balance models were developed between two linked boreholes as shown in Figure 5.14, whereby water samples in those boreholes were collected for all three seasons. The phase transfer was done for two periods (Period 1: spring to summer and Period 2: summer to autumn) along the selected boreholes. Thus, a model for Period 1 and Period 2 were generated for one point (for example, transfer from spring to B55H) as indicated in Table 5.11 to Table 5.14. These tables also show the TDS of the up-gradient (inflow) and down-gradient (outflow) modelling boreholes. The TDS was high up-gradient and low on the down-gradient, which reflected the highlighted mineralisation of the groundwater along the inferred flow paths. Modelling uncertainty values used are also displayed in Table 5.11 to Table 5.14.



Source: Author's own (2016).

Figure 5.14: Google Earth map displaying the selection of the flow paths considered for mass transfer

5.6.2.1.1 Evolution from Solution 1 (spring) to Solution 2 (B55H)

Table 5.11 indicates the mass-balance modelling results that were generated for flow path from the spring to B55H. Model simulations were obtained for the periods spring to summer and summer to autumn.

Uncertainty values of 5% were used to conduct the simulation. The spring sample for all the seasons indicated a CaHCO_3 water composition, whereas B55H for summer and autumn samples appeared in the mixed water type as displayed in the Piper diagrams (Figure 5.2, Figure 5.3 and Figure 5.4).

The results indicated by these simulations showed that for Period 1 there was dissolution of gypsum, plagioclase, dolomite, rhodochrosite and sylvite, whereas biotite, calcite, halite and Ca-montmorillonite were precipitating (Table 5.11). On the other hand, the results obtained for Period 2 (summer to autumn), as indicated in Table 5.11, showed that there was dissolution of gypsum, calcite, halite, biotite, rhodochrosite and kaolinite, whereas

plagioclase, dolomite and sylvite were precipitation. The dissolution of gypsum for both periods has been inferred to having taken place at this area (Section 5.4.1.4 and 5.4.2.4).

TABLE 5.11: INVERSE MODELLING RESULTS OBTAINED FROM PHREEQC SHOWING THE MOLE TRANSFER FROM ONE WATER TYPE TO THE NEXT (SPRINGTOB55H)

Months:	November to February	February to May
Period:	Spring to summer	Summer to autumn
Water compositions:	CaHO ₃ - mixed	CaHO ₃ - mixed
TDS (mg/l) between the inflow and outflow points:	260-528	358-523
Phase mole transfer	Spring to B55H	
Elevation (mamsl)	947-911	
Quartz	0.00e+0	0.00e+0
Gypsum	1.74e-03	1.64e-03
Plagioclase	3.15e-03	-4.19e-03
Calcite	-4.50e-03	8.32e-03
Dolomite	3.19e-03	-7.44e-03
Halite	-6.57e-04	2.90e-03
Biotite	-1.04e-03	2.58e-03
Sylvite	1.05e-03	-2.56e-03
Ca-Montmorillonite	-1.42e-03	0.00e+0
Kaolinite	0.00e+0	1.61e-03
Fluorite	0.00e+0	0.00e+0
Rhodochrosite	1.74e-07	4.01e-08
NaX	0.00e+0	0.00e+0
CaX ₂	0.00e+0	0.00e+0
Uncertainties (%)	5	5

There was no ion exchange taking place at this area since the values of NaX and CaX₂ were zero. This was also confirmed by other tools that showed the occurrence of either silicate or carbonate weathering at this area (Section 5.4.2.8).

5.6.2.1.2 Evolution from Solution 1 (B55H) to Solution 2 (B10H)

Simulations were conducted for flow path B55H to B10H to identify the hydrogeochemical processes that have led to an evolution of Solution 1 to Solution 2 (Table 5.12). The models also indicated the relationship between the results for Period 1 and Period 2 along the same flow path.

Uncertainty limits of 5% and 14.5% were used to generate the simulations for spring-summer and summer-autumn, respectively (Table 5.12). The results showed that quartz, gypsum, halite, biotite and kaolinite were all precipitating. Only sylvite and Ca-montmorillonite were

dissolving in these phase transfers. As a result of increased mineral dissolution along the flow path spring to B55H, there was precipitation of majority of the minerals. This led to a decrease in the TDS for both periods, and also the water composition changed from mixed to CaHCO₃ (Table 5.12) for Period 2.

TABLE 5.12: INVERSE MODELLING RESULTS OBTAINED FROM PHREEQC SHOWING THE MOLE TRANSFER FROM ONE WATER TYPE TO THE NEXT (B55H TO B10H)

Months:	November to February	February to May
Period:	Spring to summer	Summer to autumn
Water compositions:	CaHCO ₃ to CaHCO ₃	Mixed to CaHCO ₃
TDS (mg/l) between the inflow and outflow points:	382-394	528-415
Phase mole transfer	B55H to B10H	
Elevation (mamsl)	911-873	
Quartz	-4.43e-03	-1.09e-02
Gypsum	-7.34e-04	-2.011e-03
Plagioclase	0.00e+0	0.00e+0
Calcite	0.00e+0	0.00e+0
Dolomite	0.00e+0	0.00e+0
Halite	-3.91e-04	-6.24e-04
Biotite	-7.96e-05	-9.28e-05
Sylvite	1.08e-04	1.16e-04
Ca-Montmorillonite	3.43e-03	8.32e-03
Kaolinite	-3.95e-03	-9.68e-04
Fluorite	0.00e+0	8.16e-06
Rhodochrosite	0.00e+0	-1.33e-07
NaX	0.00e+0	0.00e+0
CaX ₂	0.00e+0	0.00e+0
Uncertainties (%)	5	14.5

The results obtained for this simulation therefore indicated that the same processes took place along flow path B55H to B10H, regardless of the period. Corresponding with the phase mole transfer between spring and B55H, ion exchange did not take place at this area. Silicate weathering was assumed at this area. Ca-montmorillonite and sylvite results corresponded with the results generated for SI, whereby these minerals appeared to be undersaturated in solution. In addition, kaolinite also related since it showed supersaturation in Sections 5.6.1.1 and 5.6.1.2.

5.6.2.1.3 Evolution from Solution 1 (B10H) to Solution 2 (B58H)

Table 5.13 indicates the mole transfer results from Solution 1 (B10H) to Solution 2 (B58H). This was done for the periods spring to summer and summer to autumn, along the same flow path.

TABLE 5.13: INVERSE MODELLING RESULTS OBTAINED FROM PHREEQC SHOWING THE MOLE TRANSFER FROM ONE WATER TYPE TO THE NEXT (B10H TO B58H)

Months:	November to February	February to May
Period:	Spring to summer	Summer to autumn
Water compositions:	CaHCO ₃ to mixed	CaHCO ₃ to mixed
TDS (mg/l) between the inflow and outflow points:	384-1 592	394-1 610
Phase mole transfer	B10H to B58H	
Elevation (mamsl)	873-826	
Quartz	8.25e-02	4.27e-02
Gypsum	3.91e-03	3.98e-03
Plagioclase	3.66e-03	3.44e-03
Calcite	0.00e+0	0.00e+0
Dolomite	1.76e-03	2.47e-03
Halite	9.69e-03	9.11e-03
Biotite	0.00e+0	-2.19e-04
Sylvite	3.34e-05	2.53e-04
Ca-Montmorillonite	-2.76e-02	-3.47e-02
Kaolinite	2.97e-02	3.81e-02
Fluorite	0.00e+0	0.00e+0
Rhodochrosite	-1.71e-05	6.14e-06
NaX	0.00e+0	0.00e+0
CaX ₂	0.00e+0	0.00e+0
Uncertainties (%)	5	5

The uncertainty limits of 5% were used for these simulations. A huge difference between the TDS of B10H (384 mg/l) and B58H (1 592 mg/l) for Period 1, and B10H (394 mg/l) and B58H (1 610 mg/l) for Period 2 samples was indicated by Table 5.13. This variation assumes that mineral dissolution was the most dominant at the area, thus leading to mineralisation. The two samples differed in their water composition, whereby B10H and B58H were classified under CaHCO₃ and mixed water type, respectively. All the minerals, except Ca-montmorillonite for both periods, rhodochrosite for Period 1 and biotite for Period 2, were dissolving in solution. The dissolution of these minerals led to a high TDS in the resulting solution (B58H).

There was no ion exchange taking place at this area; however, silicate and carbonate weathering (Section 5.4.2.8), as well as dissolution of gypsum (Section 5.4.1.4) and evaporation (Section 5.4.2.9) are inferred to be the dominating processes.

5.6.2.1.4 Evolution from Solution 1 (B58H) to Solution 2 (B25H)

Simulations were also generated for the flow path B58H to B25H for spring to summer and summer to autumn. The results attained are presented in Table 5.14.

TABLE 5.14: INVERSE MODELLING RESULTS OBTAINED FROM PHREEQC SHOWING THE MOLE TRANSFER FROM ONE WATER TYPE TO THE NEXT (B58H TO B25H)

Months:	November to February	February to May
Period:	Spring to summer	Summer to autumn
Water compositions:	Mixed to mixed	Mixed to mixed
TDS (mg/l) between the inflow and outflow points:	1 314-1 102	1 592-1 227
Phase mole transfer	B58H to B25H	
Elevation (mamsl)	826-814	
Quartz	1.26e-03	1.55e-03
Gypsum	-1.25e-03	-1.05e-03
Plagioclase	-8.61e-04	-1.01e-03
Calcite	0.00e+0	0.00e+0
Dolomite	0.00e+0	0.00e+0
Halite	-3.14e-03	-3.34e-03
Biotite	-1.10e-04	-1.38e-04
Sylvite	9.49e-05	1.20e-04
Ca-Montmorillonite	0.00e+0	0.00e+0
Kaolinite	6.50e-04	7.64e-04
Fluorite	-6.07e-06	0.00e+0
Rhodochrosite	-6.09e-06	-6.33e-06
NaX	6.89e-04	-9.83e-05
CaX ₂	-3.45e-04	4.92e-05
Uncertainties (%)	2.5	5

Another mole transfer along the flow path was generated between B58H and B25H, where the uncertainty limits of 2.5% and 5% were used. Dissolution of quartz, sylvite and kaolinite was indicated with precipitation of gypsum, plagioclase, biotite, halite, fluorite and rhodochrosite. Ion exchange along this flow path was occurring around this area down-gradient. The occurrence of ion exchange was indicated by a negative CaX₂ value with a positive NaX. During ion exchange, Na⁺ detached from the sediments to replace Ca²⁺ in

solution. On the other hand, Ca^{2+} was removed to fill in the void Na^+ spaces on the rock surface (Li *et al*, 2010). Conversely, the transfer of moles during Period 2 indicated the occurrence of cation exchange instead. This was indicated by a positive value of CaX_2 with a negative value of NaX along the same flow path. The occurrence of cation exchange at the same area during Period 2 was as a result of high recharge during summer such that sodium ions were flushed out of the system as they were replaced by calcium.

Although B58H is located at a higher elevation than B25H, solution B25H appeared to be less evolved as compared to solution B58H for all the seasons (Figure 5.14). This was indicated by the concentrations for different ions and the TDS and EC of these samples (Table 5.2 to Table 5.4). The results obtained for these simulations explained this variation. An assumption was that by the time the water reached B58H, it was highly mineralised such that precipitation of the majority of phases was experienced. Table 5.2 to Table 5.4 showed how the concentrations of ions decreased from solution B58H to solution B25H. This is explained by the precipitation of these phases from the solution. Another possibility for sample B58H to be more evolved than B25H was that B58H received water from different sources or flow paths. Section 5.4.2.1 gave an explanation that both sample B58H and B25H showed recharge by fresh water. Therefore, due to processes such as mixing and evaporation taking place, there was variation in the TDS of these samples.

5.6.2.1.5 Evolution from Solution 1 (B25H) to Solution 2 (B22H)

The last simulation was developed for mole transfer between B25H and B22H for spring to summer and summer to autumn periods. The results and the uncertainty values that were used are presented in Table 5.15.

The phase mole transfer from B25H to B22H was the last one of the flow paths (Figure 5.14), and uncertainty limits of 5% and 18.5% for spring to summer and summer to autumn were used to generate the models. The hydrochemistry results showed that sample B22H was more evolved as compared to sample B25H for the spring to summer period, whereas the opposite was observed for the summer to autumn period (Table 5.2 and Table 5.3). An explanation behind this variation is that there was dissolution of quartz, gypsum, dolomite, sylvite, Ca-montmorillonite and rhodochrosite. Conversely, halite and biotite were precipitating. Precipitation of a few minerals with dissolution of more, leads to mineralisation of the resultant solution. On the other hand, the opposite was observed for the period summer to autumn, where most of the minerals precipitated from solution. There was precipitation of quartz, gypsum, dolomite, sylvite, Ca-montmorillonite and rhodochrosite; whereas calcite and biotite were dissolving. Hence, the resultant solution was less evolved

(Table 5.15) as compared to Solution 1 (B25H). Similar to the phase mole transfer from B58H to B25H, the process of ion exchange and cation exchange were assumed at this area. This was already stated as obtained by other tools (Sections 5.4.1.4 and 5.4.2.8).

TABLE 5.15: INVERSE MODELLING RESULTS OBTAINED FROM PHREEQC, SHOWING THE MOLE TRANSFER FROM ONE WATER TYPE TO THE NEXT (B25H TO B22H)

Months:	November to February	February to May
Period:	Spring to summer	Summer to autumn
Water compositions:	Mixed to NaClSO ₄	Mixed to mixed
TDS (mg/l) between the inflow and outflow points:	888-1 261	1 102 - 859
Phase mole transfer	B25H to B22H	
Elevation (mamsl)	814-810	
Quartz	1.90e-03	-2.17e-03
Gypsum	1.02e-03	-2.57e-03
Plagioclase	0.00e+0	0.00e+0
Calcite	0.00e+0	5.22e-03
Dolomite	2.30e-03	-5.72e-03
Halite	-3.57e-03	0.00e+0
Biotite	-1.39e-03	1.55e-03
Sylvite	1.38e-03	-1.56e-03
Ca-Montmorillonite	5.95e-04	-6.67e-04
Kaolinite	0.00e+0	0.00e+0
Fluorite	0.00e+0	0.00e+0
Rhodochrosite	2.09e-06	-5.83e-08
NaX	9.51e-03	-4.63e-03
CaX ₂	-4.76e-03	2.31e-03
Uncertainties (%)	5	18.5

5.6.2.2 Summary on inverse geochemical modelling

Mole transfers were generated for two periods along the same flow paths. The process of ion exchange and reverse ion exchange happened at low elevations at the same flow path, although during different periods, and this was related to high recharge in summer. Silicate dissolution was also experienced at high elevations along the flow path. The major silicate weathering that took place was either releasing montmorillonite or kaolinite. Carbonate and gypsum dissolutions were also experienced at some areas along the flow paths. Meanwhile, dissolution of other minerals such as sylvite and halite were also experienced at random areas along the flow path. The mass-balance modelling results indicated that if more minerals were precipitated from solution, the resulting solution would have a TDS

concentration smaller than that of the initial solution. This was assumed to be happening in areas where Solution 1 was mineralised or had a higher TDS than Solution 2 (an example is B58H to B25H). However, if more minerals were dissolved, the resultant solution becomes more mineralised and its TDS increased.

5.7 Statistical analysis

The following section presents and discusses statistical analysis results for the data collected during all three seasons. Minimum, maximum, mean and standard deviations for different parameters are displayed in Table 5.16 to Table 5.18. The PCA is applied for all the seasons in this study to investigate the main hydrogeochemical processes that influence the evolution of the groundwater chemistry. Furthermore, this section attempts to identify the relationship between the results obtained by this tool and the rest of the tools.

5.7.1 Statistical data summary

Table 5.16 to Table 5.18 indicates the univariate statistical summary for the groundwater parameters as calculated by the IBM SPSS software program. The statistical summary on these tables displays the maximum, minimum, average and standard deviation of each parameter before standardisation of the variables was done, since the parameters are reported in different units.

5.7.1.1 Spring season

Table 5.16 shows how parameters differed in terms of their concentrations. This is shown in a statistical form where parameters with highest or lowest values are indicated.

High maximum parameters were indicated in some of the major ions such as Ca^{2+} , Na^+ , HCO_3^- , Cl^- and SO_4^{2-} ; however, bicarbonate had the highest value. These were the ions that contributed the most to the composition of the groundwater chemistry. Amongst the traces, Mn^{2+} was the one with the highest maximum value and low minimum value of 339 $\mu\text{g/l}$ and 0.1 $\mu\text{g/l}$, respectively. Major ions, K^+ and NO_3^- , had the lowest maximum values in the entire data set as compared to the rest of the major ions. Their low concentrations in the groundwater suggested less influence to the water chemistry. The minimum TDS was found in samples that indicated recharge by recent water, whereas high TDS was found in samples that had been mineralised along the inferred groundwater principal flow paths. These were the samples that showed an increase in most of the major ions. Among the minimum values, HCO_3^- was characterised by the highest concentration in all the seasons.

TABLE 5.16: HYDROCHEMICAL PARAMETERS INDICATING STATISTICAL CHARACTERISTICS AS CALCULATED FOR SPRING SEASON SAMPLES

Parameter	Units	Minimum	Maximum	Mean	Standard deviation
pH	-	6.54	7.14	6.78	0.17
EC	mS/m	54.00	244.00	130.89	56.96
TDS	mg/l	260.00	1314.00	567.79	299.16
Ca	mg/l	28.00	200.00	112.89	54.19
Mg	mg/l	7.00	59.00	27.89	15.09
Na	mg/l	20.00	279.00	102.32	70.95
K	mg/l	0.40	5.80	2.28	1.64
HCO ₃	mg/l	223.00	456.00	285.26	53.81
Cl	mg/l	13.00	343.00	144.11	114.19
SO ₄	mg/l	40.00	424.00	204.16	133.52
NO ₃ -N	mg/l	0.20	11.00	3.41	2.94
F	mg/l	0.25	0.97	0.68	0.23
Al	µg/l	0.03	2.10	0.78	0.48
Fe	µg/l	0.23	56.00	5.02	12.62
Mn	µg/l	0.01	339.00	26.81	77.24
NH ₃	mg/l	0.10	1.00	0.24	0.24
SiO ₂	mg/l	21.16	28.16	24.58	1.87

5.7.1.2 Summer season

Table 5.17 shows the statistical summary of data that was collected for the summer season. The results varied in terms of the dominance in ions.

There was an increase in TDS for the summer results as compared to those of the spring. Both the maximum and minimum values for this parameter have increased. This could be explained by the processes that were taking place, such as the water-rock interaction leading to the mineralisation of the solution. The same major ions as in Section 5.4.1.2 were the ones that were most dominant and these were the ions contributing more in the water type classifications.

TABLE 5.17: HYDROCHEMICAL PARAMETERS INDICATING STATISTICAL CHARACTERISTICS AS CALCULATED FOR THE SUMMER SEASON SAMPLES

Parameter	Units	Minimum	Maximum	Mean	Standard deviation
pH	-	6.12	6.83	6.40	0.19
EC	mS/m	57.00	241.00	130.47	54.42
TDS	mg/l	358.00	1592.00	831.95	346.46
Ca	mg/l	63.00	178.00	117.79	36.23
Mg	mg/l	7.00	62.00	29.95	15.62
Na	mg/l	27.00	325.00	131.89	85.25
K	mg/l	0.31	6.70	2.55	1.73
HCO ₃	mg/l	202.00	453.00	288.95	52.48
Cl	mg/l	14.00	342.00	146.21	111.13
SO ₄	mg/l	34.00	477.00	221.47	133.52
NO ₃ -N	mg/l	0.20	11.00	3.68	3.34
F	mg/l	0.20	0.92	0.57	0.23
Al	µg/l	0.73	17.00	2.04	3.71
Fe	µg/l	0.88	14.00	3.26	4.45
Mn	µg/l	0.25	362.00	30.31	84.50
NH ₃	mg/l	0.10	0.19	0.11	0.027
SiO ₂	mg/l	21.56	30.16	24.33	2.18

5.7.1.3 Autumn season

The statistical data showed a summary for variables as well as their respective units. These were the results that were generated from the data collected during the autumn sampling.

TABLE 5.18: HYDROCHEMICAL PARAMETERS INDICATING STATISTICAL CHARACTERISTICS AS CALCULATED FOR THE AUTUMN SEASON SAMPLES

Parameter	Units	Minimum	Maximum	Mean	Standard deviation
pH	-	6.18	8.16	7.20	0.75
EC	mS/m	47.00	196.00	104.55	52.78
TDS	mg/l	320.00	1610.00	797.64	427.87
Ca	mg/l	51.00	171.00	113.73	38.97
Mg	mg/l	9.00	60.00	29.64	16.63
Na	mg/l	28.00	300.00	117.18	89.63
K	mg/l	0.48	4.50	2.05	1.32
HCO ₃	mg/l	225.00	414.00	279.73	53.82
Cl	mg/l	11.00	329.00	128.27	125.82
SO ₄	mg/l	18.00	396.00	190.82	144.09
NO ₃ -N	mg/l	0.20	9.20	2.96	3.28
F	mg/l	0.20	0.90	0.53	0.28
Al	µg/l	0.73	5.20	1.22	1.32
Fe	µg/l	0.88	4.10	1.18	0.97
Mn	µg/l	0.25	338.00	37.58	100.10
NH ₃	mg/l	0.10	0.18	0.11	0.02
SiO ₂	mg/l	25.16	34.16	27.80	2.58

Table 5.18 shows autumn results indicating the highest maximum TDS as compared to the rest of the seasons, which reflects the mineralisation effect over time. Besides an elevated TDS, these results also displayed the highest pH and SiO₂ for all the seasons. The high maximum values were still displayed by major ions, except for K⁺, Mg²⁺ and NO₃⁻. Furthermore, Mn²⁺ still showed the highest maximum concentration among the trace elements.

5.7.2 Principal component analysis

Table 5.19, Table 5.20 and Table 5.21 shows the loadings generated for the rotated component matrix, percentage of variance for each component, percentage of variance for eigenvalues as well as the communalities found for each parameter.

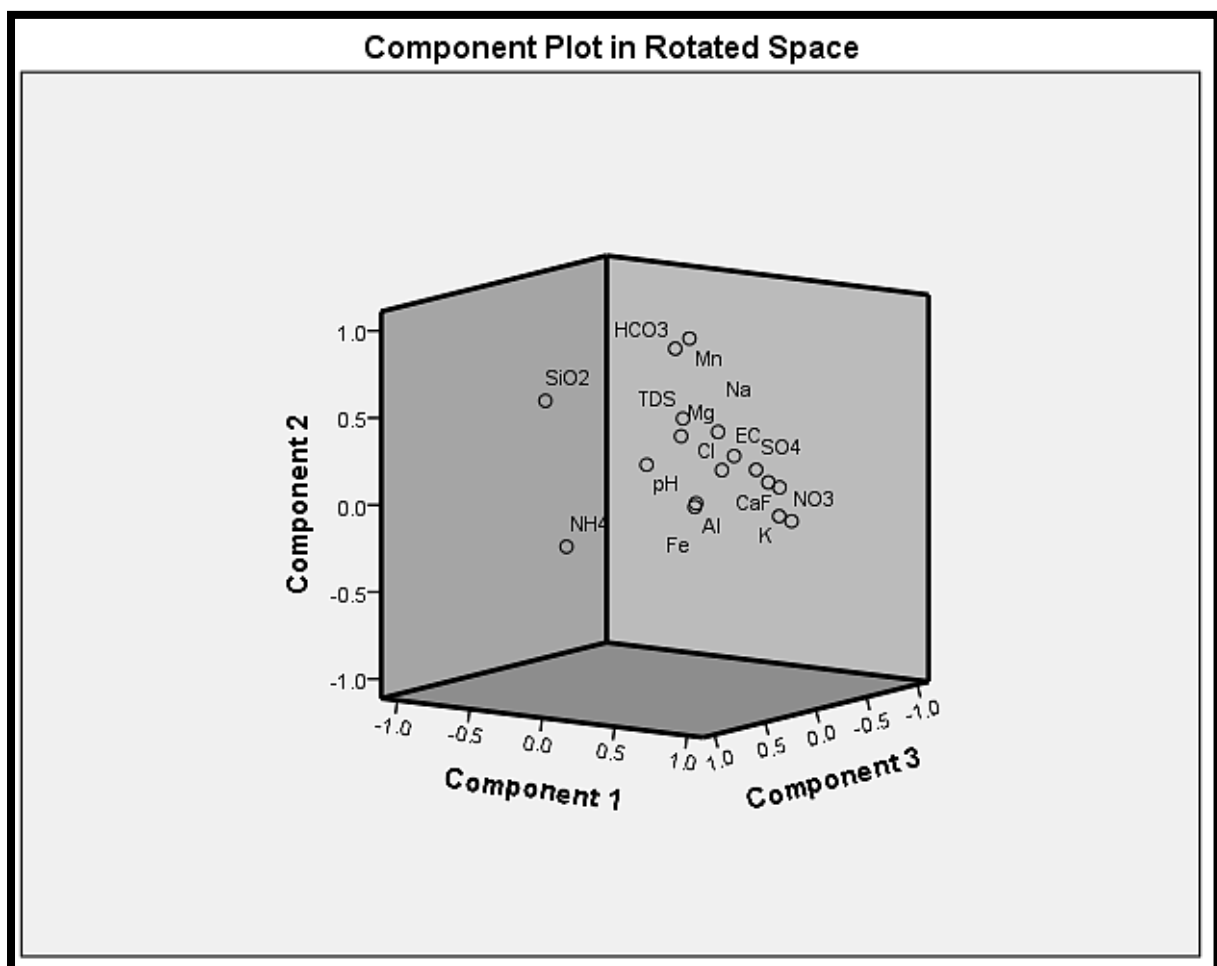
5.7.2.1 Spring season

The data presented in Table 5.19 and Figure 5.15 show the principal component results obtained from the standardised groundwater chemistry data for the spring season. The data was used to generate the results that follow.

TABLE 5.19: PRINCIPAL COMPONENT ANALYSIS RESULTS AFTER VARIMAX ROTATION AS GENERATED FOR SPRING

Parameters	Component					Communalities
	1	2	3	4	5	
pH	-0.07	0.17	-0.02	-0.03	0.92	0.89
EC	0.81	0.37	0.38	0.17	0.04	0.97
TDS	0.53	0.57	0.48	-0.09	-0.03	0.85
Ca	0.87	0.19	0.12	0.26	0.01	0.86
Mg	0.54	0.48	0.52	0.03	-0.38	0.94
Na	0.72	0.50	0.40	0.13	0.09	0.95
K	0.89	-0.01	0.05	-0.14	-0.27	0.89
HCO ₃	0.08	0.85	-0.08	-0.12	0.24	0.80
Cl	0.79	0.30	0.46	0.13	0.01	0.94
SO ₄	0.83	0.27	0.19	0.19	0.07	0.84
NO ₃ -N	0.85	-0.08	-0.14	-0.11	-0.21	0.80
F	0.89	0.15	0.04	-0.23	0.17	0.89
Al	0.29	-0.03	0.02	0.68	0.07	0.55
Fe	0.23	-0.03	-0.08	-0.77	0.09	0.66
Mn	0.21	0.92	-0.04	0.15	0.00	0.92
NH ₃	0.06	-0.14	0.96	0.09	-0.02	0.95
SiO ₂	-0.63	0.51	0.18	-0.22	0.41	0.91
Eigenvalues % of variance	47.41	13.96	9.94	8.53	6.11	
Cumulative % of variance	47.41	61.37	71.31	79.84	85.95	

Five components were extracted for summer results as shown in Table 5.19. The total cumulative variance was calculated to be 85.95%, with the first component contributing 47.41%. The results in Table 5.19 showed the highest loadings for EC, Ca^{2+} , K^+ , SO_4^{2-} , NO_3^- , F^- , Na^+ and Cl^- for Component 1. The rest of the component loadings were considered low and as a result they will be disregarded during the interpretations. Component 1 indicated the most important hydrogeochemical processes that took place in the groundwater system before collection of the samples in the spring season. These are the processes that altered the water chemistry the most. The processes explained by Components 2, 3, 4 and 5 were also important; however, their importance became less from one component to the next, that is, Component 2 is more significant than Component 3, and so forth (Dragon, 2006).



Source: Author's own (2016).

Figure 5.15: Component plot in rotated space for component loadings of spring season

Figure 5.15 indicates how the principal loadings contributed in different components. The component plot in a rotated space shows that EC, Ca^{2+} , K^+ , SO_4^{2-} , NO_3^- , F^- and Cl^- ions were the ones that indicated a strong contribution to Component 1, without having any influence on Component 2. Conversely, Na^+ indicates participation in Component 1 and also Component 2.

The EC increased in the water as a result of dissolution of the ions that showed high positive loadings. Dissolution of gypsum (Section 5.4.1.4, 5.4.2.2 and 5.6.2.1) as already inferred by other tools, had been taking place leading to a high contribution in Ca^{2+} and SO_4^{2-} . Gypsum as an evaporite mineral was formed during evaporation and its interaction with water led to dissolution. Evaporation was also one of the main hydrogeochemical processes that influenced the evolution of the groundwater chemistry (Section 5.4.2.9). Once the precipitated solutes come into contact with water, they are then dissolved until the water is saturated with those ions. Dissolution of halite, sylvite and fluorite was indicated by a strong contribution of Ca^{2+} , Cl^- , Na^+ , K^+ and F^- in the water. The occurrence of these processes have been discussed for other tools (Sections 5.4.2.6, 5.4.2.8 and 5.6.2.1) The presence of Cl^- , Na^+ and Ca^{2+} might also explain the process of ion exchange and reverse ion exchange (5.4.1.4 and 5.4.2.8) at different locations within the groundwater system.

Hu, Luo and Jing (2013) stated that if the presence of fluoride in the groundwater resulted from water-rock interactions, this ion should be associated with the main hydrochemical parameters. The results attained in principal Component 1 indicated high loadings in F^- and other major parameters. An explanation can be that the presence of F^- in the water might be as a result of water interacting with minerals such as fluorite (CaF_2). The occurrence of fluorite may be assumed to be occurring at a slow rate because fluorite dissolves slowly in water. Additionally, dissolution and precipitation of fluorite was also shown in the findings of Section 5.6. Nevertheless, this was not considered as the only source of fluoride in the groundwater. Another possibility as explained by Hu *et al.* (2013) was that if the area has low rainfall leading to low recharge of the groundwater system, F^- concentration will increase. This will happen as a result of long residence time of water in the aquifer. This may be assumed as one of the reasons F^- was present, since Beaufort West is an arid area.

Component 1 also showed a high loading of NO_3^- . Nitrate could have entered the groundwater through leaching as it was used for agricultural purposes. Moreover, Jalali (2007) indicated that NO_3^- in the groundwater may also be linked to high mineralisation within the system. It is therefore highly soluble and mobile in the water since it occurs in an anionic form.

Component 2 was dominated by HCO_3^- and Mn^{2+} as indicated on both the rotated component (Figure 5.15) as well as Table 5.19. Manganese is well known to occur in association with iron in sedimentary rocks such as sandstone and shale or in limestones. In most instances, iron is found to be most abundant as compared to manganese. However, in a study that was conducted by Penrose (1893), it was found that some areas have more iron with little manganese, whereas other areas contain more manganese with less iron, mostly in marine limestone. This can be assumed to be the case for this study whereby the presence of Mn^{2+} can be associated to HCO_3^- in limestone, possibly as rhodochrosite (MnCO_3). The dissolution of this mineral was discussed in Section 5.6. This was also the same case in component loadings, where for spring results, Mn^{2+} fell in Component 2 with Fe^{2+} in Component 4. The bicarbonate could be the one dissolved during the groundwater recharge.

Component 3 showed a high loading of ammonia. Similar to nitrate, ammonia present in the water may have resulted from agricultural and industrial works that takes place around Beaufort West. Since the area also run the municipality's waste water treatment project, chlorine that is used in the disinfection process might also be leaking into the groundwater sources leading to ammonia in the water. Furthermore, it might also be assumed to be ammonia occurring naturally in the soil as indicated by Component 3 in Table 5.19. According to Jalali (2007), ammonium-N can undergo the process of nitrification (microbial oxidation of $\text{NH}_4\text{-N}$ to NO_3^-) leading to the release of NO_3^- mostly in the unsaturated zone.

Component 4 was represented by high aluminium and iron loadings, with magnesium also showing a high positive loading of 0.52; this indicated mica biotite weathering. The National Groundwater Association (NGWA, 1999) explained that as much as Al^{3+} may occur in most of the rocks, its solubility is low and once dissolved, it can easily precipitate. It is indicated in literature that mica, such as biotite, muscovite and sericite, are the minerals that forms part of the geology. Although some of them, like muscovite and biotite, occur as accessory minerals. This explains why they fall under Component 4, showing that they least contribute in the water chemistry change.

Lastly, Component 5 was represented by a high pH component loading. This indicates how least the pH influences the entire groundwater system.

5.7.2.2 Summer season

Table 5.20 and Figure 5.16 show the results that were generated during PCA for the summer results. A total of four components were extracted as shown by Table 5.20, where the components are ordered according to which ones contribute the most and the least in the

evolution of the groundwater chemistry. The communalities were also displayed in the table for each parameter. The component loadings that contributed the most in each component were highlighted and discussed below. The cumulative percentage of variance indicated a total of 79.06%, which is a bit lower than that of the spring results where the variance percentage was 85.95 after the extraction of five components. Component 1 displayed a very high percentage of 46.36, followed by Component 2, showing a percentage of 13.73, Component 3 with 11.34%, and lastly Component 4 showing a variance of 7.63%.

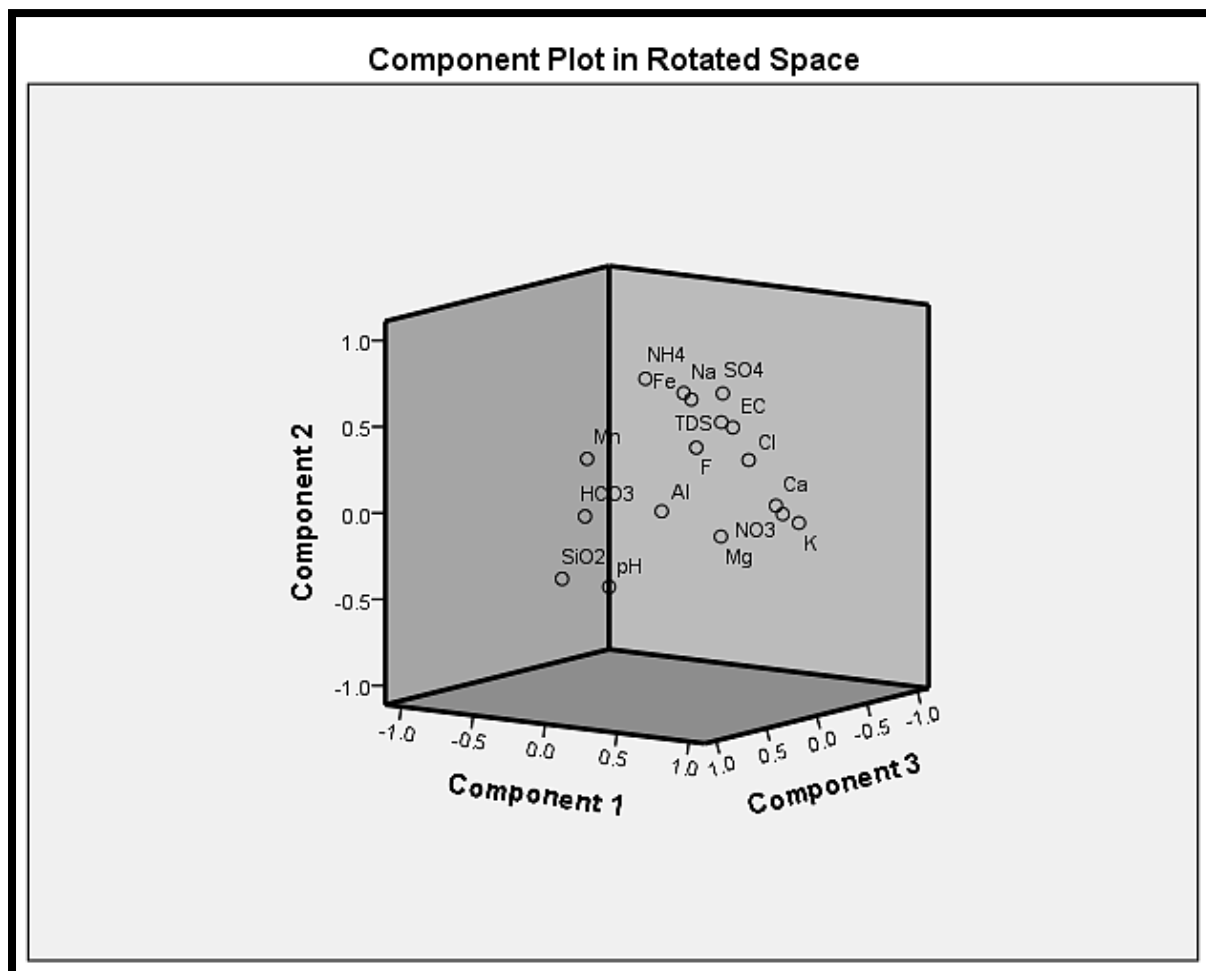
TABLE 5.20: PRINCIPAL COMPONENT ANALYSIS RESULTS AFTER VARIMAX ROTATION AS GENERATED FOR SUMMER

Parameters	Component				Communalities
	1	2	3	4	
pH	0.10	-0.38	0.62	0.11	0.55
EC	0.75	0.57	0.32	0.00	0.99
TDS	0.70	0.60	0.36	-0.01	0.98
Ca	0.90	0.10	0.11	-0.12	0.85
Mg	0.75	-0.05	0.44	0.03	0.76
Na	0.47	0.76	0.41	0.01	0.96
K	0.94	-0.02	-0.07	0.12	0.90
HCO ₃	0.13	0.08	0.90	-0.08	0.83
Cl	0.83	0.38	0.28	-0.02	0.92
SO ₄	0.53	0.71	0.11	0.01	0.80
NO ₃ -N	0.90	0.04	0.04	0.15	0.84
F	0.39	0.39	0.16	0.20	0.37
Al	0.06	-0.03	0.03	0.96	0.92
Fe	0.07	0.58	-0.24	0.70	0.89
Mn	0.08	0.39	0.81	-0.10	0.82
NH ₃	-0.13	0.71	-0.07	0.08	0.53
SiO ₂	-0.54	-0.46	0.17	-0.03	0.53
Eigenvalues % of variance	46.36	13.73	11.34	7.63	
Cumulative % of variance	46.36	60.09	71.43	79.06	

Figure 5.16 is a component plot in a rotated space. The diagram shows how and where the component loadings plotted on the diagram. Variables Ca²⁺, K⁺, Cl⁻ and NO₃⁻ indicated a very strong contribution in Component 1, whereas TDS, EC and Mg²⁺ indicated a contribution, but not very strong such as Ca²⁺, K⁺, Cl⁻ and NO₃⁻. The TDS and EC component loading also contributed in Component 2. Some of these loadings were shown to be high or strong in

Component 1 of the spring results. However, the difference could still be noted in most cases and it is explained below.

TDS showed high values as a result of water-rock interaction, where minerals were dissolved in solution, leading to elevation of total solids in the water. Reverse ion exchange was also considered one of the hydrogeochemical processes since only Ca^{2+} and Cl^- , and not Na^+ , were high or contributed most in Component 1. The same explanation as in the spring results could still be made for a strong contribution of NO_3^- in the groundwater.



Source: Author's own (2016).

Figure 5.16: Component plot in rotated space for component loadings of summer season

Component 2 showed high component loading for TDS, Na^+ , SO_4^{2-} and NH_3 . High TDS in this component was again from the dissolution of ions such as SO_4^{2-} and Na^+ that leads to increased salts in the water. Ion exchange was one of the processes assumed here, where Na^+ indicated a strong contribution, whereas Ca^{2+} was very low, close to zero. NH_3 was one variable that might have entered the water from the soil; an interaction between water and

soil (Dragon, 2006). Furthermore, it might have resulted from anthropogenic sources as already explained in the spring season results (5.7.2.1).

The strongly contributing component loadings in Component 3 are pH, HCO_3^- and Mn^{2+} . Bicarbonate ion was the first one to be added in solution during recharge of the groundwater as the water moved through the aquifer. According to the NGWA (2010) the production of HCO_3^- leads to an environment that is alkaline. That is, the elevation concentration of pH was caused by the addition of more HCO_3^- in the system during the interaction of carbonate rocks and carbonic acid water.

Lastly, Component 4 showed high Al^{3+} and Fe^{2+} loadings; these may be assumed to have resembled from dissolution of micas with the addition of these ions in the system.

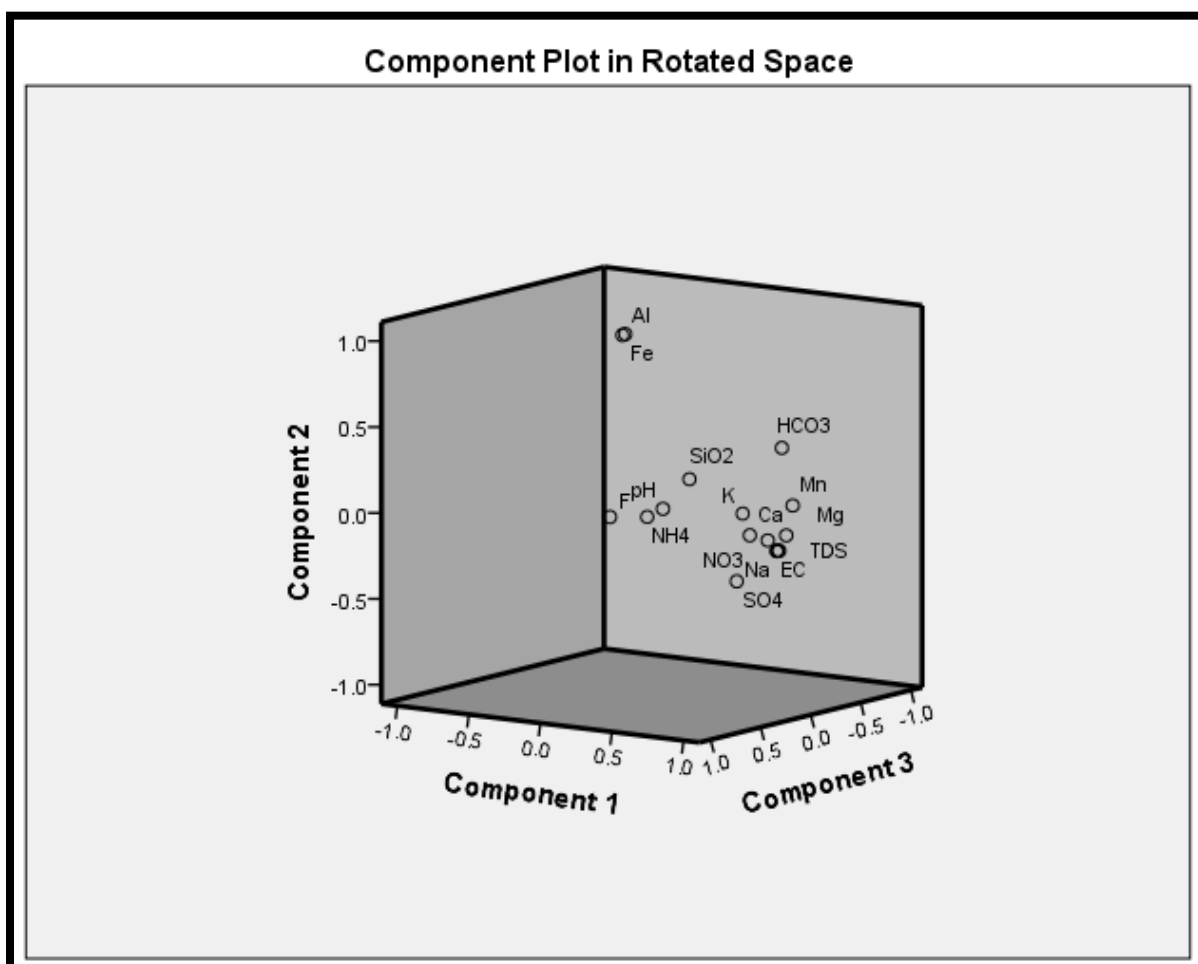
5.7.2.3 Autumn season

The results displayed in Table 5.21 and Figure 5.17 was generated for the autumn season. Most of the results calculated were similar to the ones obtained for spring and summer results. Only the difference in these results will be considered for explanation.

TABLE 5.21: PRINCIPAL COMPONENT ANALYSIS RESULTS AFTER VARIMAX ROTATION AS GENERATED FOR AUTUMN

Parameters	Components					Communalities
	1	2	3	4	5	
pH	-0.04	-0.05	-0.16	-0.97	0.03	0.98
EC	0.97	-0.15	0.14	0.07	-0.01	0.99
TDS	0.95	-0.16	0.10	0.24	-0.02	0.99
Ca	0.88	-0.05	0.27	-0.08	-0.28	0.93
Mg	0.88	-0.10	-0.08	0.22	0.04	0.84
Na	0.91	-0.17	0.05	0.35	0.09	0.99
K	0.90	0.09	0.38	-0.16	-0.06	0.99
HCO_3^-	0.66	0.35	-0.35	0.48	-0.17	0.94
Cl	0.97	-0.15	0.11	0.06	0.03	0.98
SO_4	0.76	-0.34	0.24	0.15	-0.40	0.93
$\text{NO}_3\text{-N}$	0.94	-0.09	0.19	-0.18	0.08	0.97
F	0.32	0.09	0.87	0.01	0.23	0.91
Al	-0.17	0.98	0.05	0.02	-0.04	0.99
Fe	-0.17	0.98	0.03	0.05	-0.01	0.99
Mn	0.60	-0.02	-0.54	0.48	-0.16	0.91
NH_3	-0.00	-0.07	0.04	-0.05	0.96	0.92
SiO_2	-0.28	0.01	-0.78	-0.23	0.26	0.80
Eigenvalues % of variance	53.59	13.57	12.52	7.83	6.95	
Cumulative % of Variance	53.59	67.15	79.67	87.50	94.45	

Table 5.21 is an indication of the component loadings extracted for the autumn results. Equally to the spring results, five components were extracted explaining the processes that influenced the evolution of the water and other processes that might have been taking place within the aquifer system. The communalities were also shown for each variable in relation to the respective components. This was the set of results that displayed the highest percentage of variance that equalled 94.45% with five principal components. The first component displayed the highest correlation with a variation percentage of 53.59, whereas Component 2 had a variance of 13.57%. Component 3 had a variance of 12.52% and Component 4 was characterised by a variance of 6.95%. Component 1 again indicated a high number of strong variables showing contribution and this included EC, TDS, Ca^{2+} , Mg^{2+} , Na^+ , K^+ , Cl^- , SO_4^{2-} and NO_3^- .



Source: Author's own (2016).

Figure 5.17: Component plot in rotated space for component loadings of autumn season

Figure 5.17 is an indication of how the autumn results appear on the rotated space. Variables EC, TDS, Ca^{2+} , Mg^{2+} , Na^+ , K^+ , Cl^- , SO_4^{2-} and NO_3^- all indicated a strong contribution

in Component 1. HCO_3^- and Mn^{2+} also showed a positive contribution, although it was not as high as the other ions. Generally, all the major ions contributed to this component. The high TDS and EC loadings were of no surprise when looking at how the major ions were contributing highly in this component (Kura *et al.*, 2013). Many processes might be assumed here and this included carbonate, halite, sylvite and gypsum dissolutions. The strong contribution of Ca^{2+} and Mg^{2+} in the water increased in the autumn results as compared the other seasons. This explained the occurrence of dolomite dissolution in the system as already inferred in Sections 5.6.1.3 and 5.6.2.1.4.

Component 2 indicated high iron and aluminium. High component loadings were indicated for F^- and SiO_2 in Component 3. This could be an enhanced weathering of silicates such as muscovite as a result of the increase of H_2CO_3 from the interaction of carbon dioxide in the soil zone with water. The hydrogeochemistry results (Table 5.4) indicated that the pH concentration in these samples had increased and this also led to an increase in SiO_2 in the water.

Component 4 was represented by a high pH loading with an addition of HCO_3^- and Mn^{2+} . The same explanation for spring and summer applies. Ammonia had the highest loading in Component 5. It can be assumed that the presence of this ion had a slight impact in altering the groundwater composition in this season.

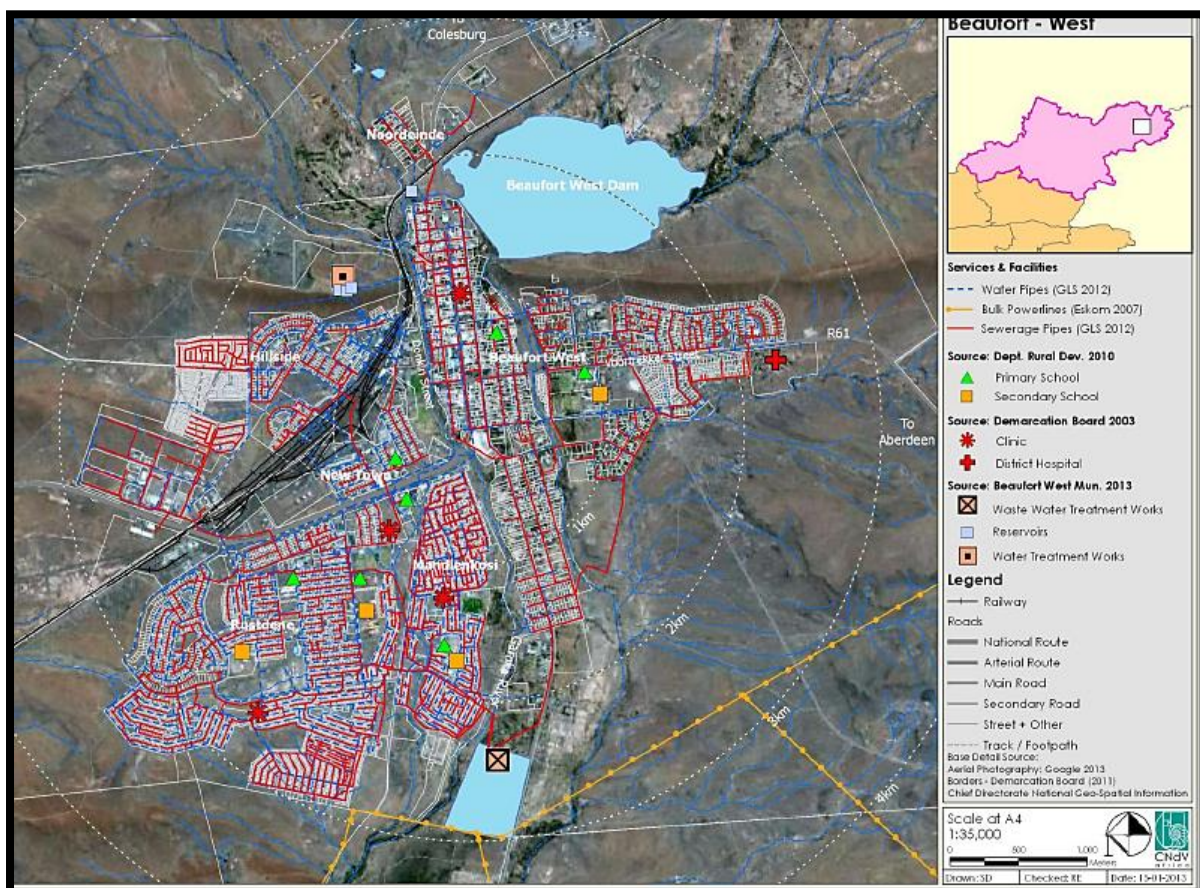
5.7.2.4 Summary on statistical analysis

The results as obtained for PCA improved the understanding of hydrogeochemical processes that have taken place in the groundwater system and influenced the groundwater quality. These processes were being confirmed since they were already discussed in the previous tools. The main processes that were assumed by this tool were ion exchange, reverse ion exchange and dissolution of evaporite minerals. Alteration of the groundwater by anthropogenic sources was also indicated, whereby NO_3^- showed a strong contribution. Although the same hydrogeochemical processes were inferred to have been taking place in all the seasons, different processes dominated at certain areas and in different times as indicated by the other tools. Carbonate dissolution and silicate weathering were not indicated as the principal hydrogeochemical process as displayed by the rest of the tools. However, carbonate weathering was indicated as one of the dominating processes for the autumn season due to increased recharge.

5.8 Groundwater Quality Assessment

The water quality assessment was done to determine the suitability of water for certain uses such as drinking, domestic and agricultural purposes. Thus, the standards of water usage for certain activities are provided in different guideline sources. The SAWQG (1996) as well as the WHO (2011) guidelines were used to assess the fitness of the groundwater at the study site for such uses.

Figure 5.18 shows the different activities that take place at Beaufort West town, as well as where certain man-made facilities that can affect the groundwater quality are situated. The map will be used as a reference in the following sections to point out activities that might be affecting the quality of the groundwater.



Source: Beaufort West annual report (2013).

Figure 5.18: Beaufort West indicating the activities and facilities around town

5.8.1 Groundwater suitability for irrigation purposes

Groundwater suitability for irrigation looks at many aspects like effects of waters' mineral concentration on the soil and plants (Richards, 1954). The quality of the water for irrigation

depends on factors such as high total dissolved solids (TDS) and salt concentrations. TDS may influence the water and nutrients intake by plants resulting in plant growth being disturbed (Bob *et al.*, 2015; Singhal and Gupta, 2010). Therefore, irrigation water may have an influence on the growth of plants (Zaidi *et al.*, 2015). Furthermore, high salt concentrations in the water for irrigation may affect the soil structure together with the permeability rate resulting in growth of the plant being affected (Singh *et al.*, 2015). The number of certain ions may also be toxic to the growth of plants if they are abundant in the water (Singhal and Gupta, 2010).

TABLE 5.22: CRITERIA FOR TESTING THE SUITABILITY OF WATER FOR IRRIGATION PURPOSES AS APPLIED OVER THREE SEASONS

Site Name	Spring				Summer				Autumn			
	SAR	RSC	%Na	Mg/Ca	SAR	RSC	%Na	Mg/Ca	SAR	RSC	%Na	Mg/Ca
B10H	0.57	-0.68	16.64	0.40	0.74	-0.45	19.47	0.35	-	-	-	-
B11H	-	-	-	-	1.16	0.00	26.79	0.17	-	-	-	-
B22H	2.34	-3	37.59	0.50	9.41	0.43	75.85	0.15	-	-	-	-
B24H	11.27	-13.82	61.03	0.76	10.43	-14.71	61.36	0.41	12.29	-11.56	65.34	0.61
B25H	3.66	-6.57	44.34	0.66	4.06	-4.33	47.96	0.74	4.13	-4.91	48.21	0.75
B36H	2.11	-3.14	34.90	0.56	2.22	-4.44	34.66	0.59	ND	ND	ND	ND
B44H	2.7	-6.5	37.73	0.24	2.92	-7.87	38.48	0.30	ND	ND	ND	ND
B45H	3.26	-6.11	41.53	0.10	3.32	-4.46	43.86	0.29	3.17	-6.58	40.64	0.29
B50H	2.63	-9.96	33.67	0.39	2.76	-7.86	36.15	0.45	2.82	-7.81	36.66	0.46
B53H	1.47	-0.88	30.62	0.30	2.15	-1.63	38.35	0.25	2.28	-2.84	38.50	0.26
B54H	-	-	-	-	2.81	-3.39	41.16	0.37	ND	ND	ND	ND
B55H	0.91	-1.56	21.51	0.44	1.20	-3.03	24.57	0.38	1.15	-2.97	24.06	0.42
B56H	2.36	-6.6	33.87	0.37	2.52	-5.37	36.93	0.42	ND	ND	ND	ND
B57H	2.65	-7.21	35.61	0.37	2.97	-7.88	37.68	0.42	ND	ND	ND	ND
B58H	4.53	-6.91	45.94	0.51	5.10	-6.56	49.24	0.57	5.05	-6.53	49.58	0.59
B59H	0.81	-1.73	19.65	0.17	0.95	-1.48	22.52	0.20	0.94	-1.75	21.62	0.22
B60H	2.14	-1.53	36.68	0.49	2.59	-2.68	39.60	0.49	ND	ND	ND	ND
B61H	1.4	-0.56	28.82	0.51	1.64	-1.54	30.75	0.53	ND	ND	ND	ND
B62H	2.92	-4.22	41.51	0.62	3.48	-5.41	44.27	0.66	ND	ND	ND	ND
Spring	0.77	-0.18	21.44	0.75	1.07	-0.56	26.26	0.44	0.81	-0.72	21.43	0.78

Note: ND=No data - data in these boreholes was not collected in autumn; (-) = Samples with high IBE

In order to assess if water is suitable for irrigation use, chemical parameters such as SAR, RSC, total salinity (estimates of the EC), magnesium hazard and sodium percentage (%Na)

can be used (Nazzal *et al.*, 2014; Singh *et al.*, 2015; Wilcox, 1955; Zaidi *et al.*, 2015). The calculations as applied for the above-mentioned approaches are displayed in Table 5.22.

Table 5.23 indicates how the irrigation water is classified with reference to the parameters or criteria that are used to determine the fitness of water for irrigation. The calculations are indicated in Table 5.22 and the classifications are done in Table 5.23. The samples column indicates the number of samples that falls within a specified category from the results calculated for the study area.

TABLE 5.23: GROUNDWATER CLASSIFICATION FOR IRRIGATION PURPOSES BY FOLLOWING THE DIFFERENT CRITERIA

Parameter	Range	Classification	Samples
Alkalinity hazard (SAR) (meq/l)	0 - 10	Excellent	44 (17 Sp, 19 Sm, 8 A)
	10 - 18	Good	3 (1 Sp, 1 Sm, 1 A)
	18 - 26	Fair	0
	>26	Poor	0
RSC (meq/l)	<1.25	Good	50 (18 Sp, 20 Sm, 9 A)
	1.25 - 2.5	Medium	0
	>2.5	Bad	0
Na% (meq/l) (after Wilcox, 1955)	0 - 20	Excellent	3 (2 Sp, 1 Sm)
	20 - 40	Good	27 (10 Sp, 12 Sm, 5 A)
	40 - 60	Permissible	12 (4 Sp, 5 Sm, 3 A)
	60 - 80	Doubtful	4 (1 Sp, 2 Sm, 1 A)
	>80	Unsuitable	0
Salinity hazard (EC) (mS/m) (SAWQG, 1996b)	0 - 40	Excellent	0
	40 - 90	Good	16 (6 Sp, 6 Sm, 4 A)
	90 - 270	Permissible	28 (11 Sp, 13 Sm, 4 A)
	270 - 540	Doubtful	2 (1 Sm, 1 A)
	>540	Unsuitable	1 (Sp)
Residual Mg/Ca ratio (meq/l)	<1.5	Safe	55
	1.5 - 3	Moderate	0
	>3	Unsafe	0

Note: Samples column is symbolised by Sp=spring, Sm=summer and A=autumn

5.8.1.1 Sodium adsorption ratio

Sodium adsorption ratio (SAR) is the significant criteria in determining how fit the water is for irrigation. This parameter is expressed as the ratio of Na^+ to Ca^{2+} and Mg^{2+} (Wilcox, 1955; Singh *et al.*, 2015) as indicated by Ratio 4.5. The concentrations of these ions are presented

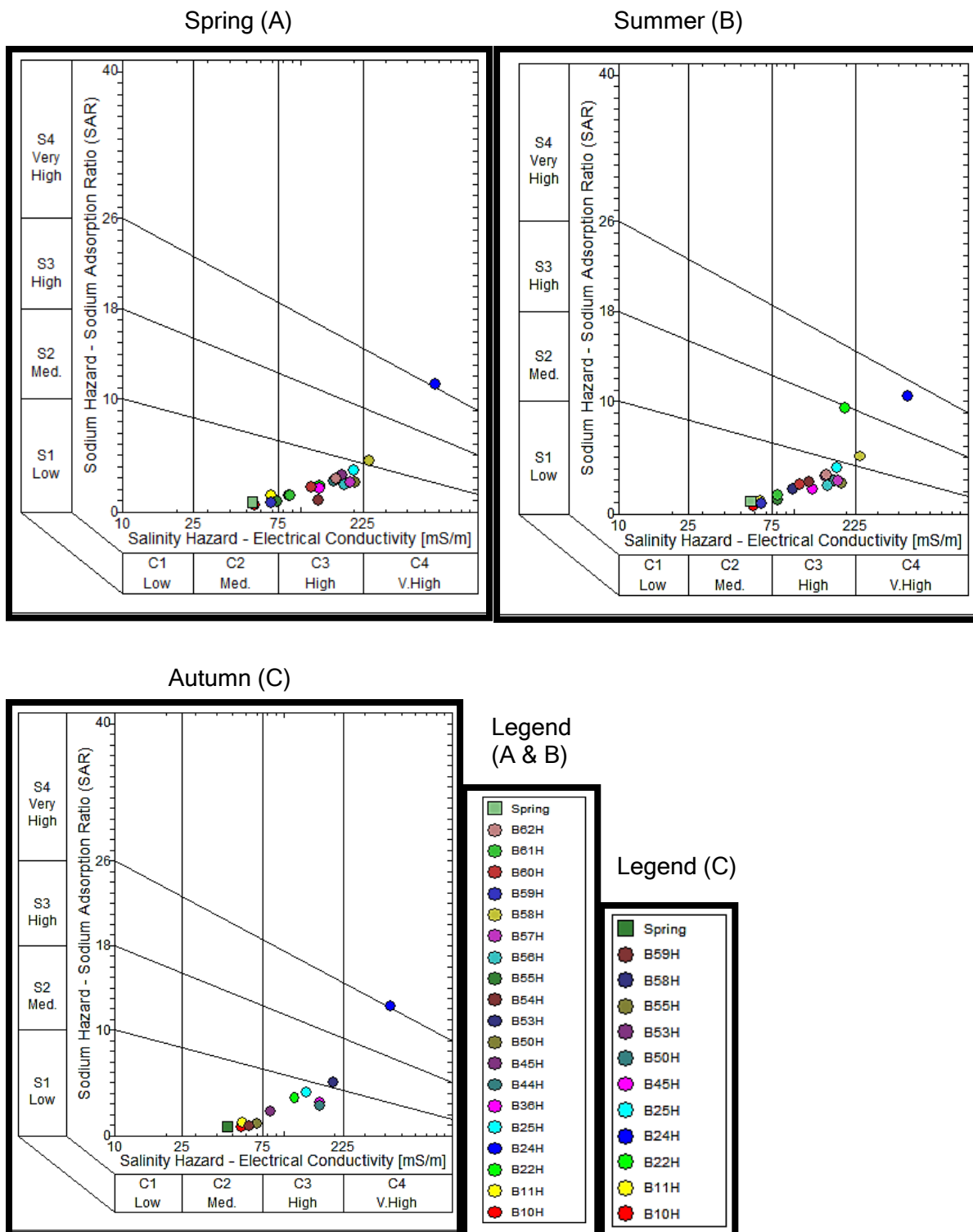
in meq/l (Nazzal *et al.*, 2014; Zaidi *et al.*, 2015) as calculated in Table 5.5 to Table 5.7. The amount of sodium ions in the water may cause the soil particles to scatter as the ions become adsorbed (Pearson, 2003). This leads to soil solidifying or hardening and becoming more like cement after reforming such that its infiltration rate is reduced (Ayers and Westcot, 1976; Hanson *et al.*, 2006). Moreover, as a result, penetration of the plant roots into the soil becomes limited, leading to plants receiving less water and nutrients (Bob *et al.*, 2015). Soil that has high sodium is also hard to cultivate. Singh *et al.* (2015) explained that high SAR may cause the soil to break in its physical structure.

The SAR values as indicated by Table 5.22 were low and fell within the suitable limit. However, SAWQG (1996b) stated that at certain ranges the sodium sensitive crops will uptake sodium toxic levels with their roots since crops differ in sensitivity to sodium. This will therefore affect the growth of those plants. The SAR values calculated, ranged from 0.57 to 11.27, 0.74 to 10.43 and 0.81 to 12.29 for spring, summer and autumn seasons, respectively. Ratio 4.5 was used for calculating SAR in order to determine the suitability of groundwater for the purpose of irrigation.

Figure 5.19 plotted all the samples in the SAR diagram according to the suitability of the water for irrigation purposes. The plotting was done for all three seasons so that the results would indicate the relationship between sodium (SAR) and salinity (EC) hazards.

Diagrams A to C indicate the salinity hazards versus the sodium hazards, whereby the hazards are classified into low, medium, high and very high. Diagrams A and B shows the majority of the samples plotting along the S1C3 class. This class was represented by low SAR and a high salinity hazard. Thus, the water was suitable for irrigation in cases where the drainage of the soil could flush the salts out (Bob *et al.*, 2015; Gomo *et al.*, 2013), and could also be used for crops that are not salt sensitive (Bob *et al.*, 2015).

All the samples classified under the CaHCO₃ water type fell in the S1C2 class, for all three seasons, with the exception of B53H for all the seasons and B61H for the summer season. These samples were therefore characterised by low SAR and moderate salinity. The water was considered good for irrigation (Nazzal *et al.*, 2014).



Source: Author's own (2016).

Figure 5.19: SAR diagrams classifying water for irrigation purposes for spring (A), summer (B) and autumn (C)

Additionally, sample B22H plotted within the S1C3 class for spring and autumn seasons, whereas it plotted in S2C3 for summer. On the other hand, sample B58H plotted on class S2C4 for spring and summer and in S2C3 for the autumn season. Lastly, sample B24H plotted within a very high SAR and salinity for spring and autumn seasons, whereas it fell within S3C4 for summer. Samples B22H and B58H still indicated an acceptable class range for SAR, whereas they indicated a high (B24H and B58H) to very high (B58H) for salinity. Furthermore, B24H indicated unacceptable limits for both SAR and salinity. Therefore, water that was very high in salinity could be considered for irrigation under restricted conditions. The conditions include cultivation of crops that can be grown in high salt conditions and also the application of leaching requirements (Al-Harbi, Hussain and Lafouza, 2009). Moreover, Nazzal *et al.* (2014) stated that if the water samples fall under high salinity and low to medium SAR they can be taken as permissible for irrigation.

The SAR results indicated that all the water samples could be recommended as water suitable for irrigation at normal conditions, except for samples B58H and B24H that had very high salinity. Furthermore, B24H had both very high salinity and high sodium.

5.8.1.2 Total salinity

The increased salinity from high calcium and magnesium in the water can result in the binding of soil particles through flocculation mechanisms (Pearson, 2003). This mechanism is helpful to the plants since it makes soil to be more permeable, whereby plant roots can penetrate well and take up water and nutrients for plant growth (Hanson *et al.*, 2006). The assessment of salinity hazard was done based on the EC values (Wilcox, 1955).

The SAWQG (1996b) explained that if the water has an EC value of <540 mS/m, it can be considered suitable for irrigation. However, this depends on the type of crops since crops differ in the way they tolerate salinity. The EC values (Table 5.5, Table 5.6 and Table 5.7) fell within the suitable range for irrigation use. The values ranged between 53.6 mS/m and 575 mS/m for spring, 57 mS/m and 451 mS/m for summer, and 46.9 mS/m and 431 mS/m for the autumn season. All the values in mS/m were below 540, except for one sample (B24H) that gave an EC of 575 mS/m. According to the SAWQG (1996b), the water can still be used for irrigation under restricted conditions, such as for irrigation of selected crops. Annapoorna and Janardhana (2015) explained that the high EC variation in the water may result from hydrogeochemical processes such as ion and reverse ion exchange, rock-water interaction, silicate weathering, sulphate reduction and oxidation processes as well as evaporation.

5.8.1.3 Residual sodium carbonate

Residual sodium carbonate (RSC) is another sodium hazard indicator that may be used to classify water for irrigation (Nazzal *et al.*, 2014). The concentrations of the ions as displayed by Expression 4.6 are expressed in meq/l. RSC is expressed as the difference between the sum of bicarbonate and carbonate to the sum of calcium and magnesium. Precipitation of calcium and magnesium may result in high Na⁺ content in the soil and this can be seen by RSC values that are positive. High bicarbonate concentration results in high pH values as indicated by the positive RSC; this may cause the dissolution of organic matter (Bob *et al.*, 2015; Nazzal *et al.*, 2014).

Table 5.22 indicates the results found after the application of Expression 4.6 for all seasons. Bob *et al.* (2015), Nazzal *et al.* (2014) and Singh *et al.* (2015) indicated that the RSC value should be less than 2.5 meq/l for water to be regarded as suitable for irrigation purposes. The calculated RSC values ranged from -13.82 meq/l to 2.91 meq/l for spring, -14.71 meq/l to 0.43 meq/l for summer, and -11.56 meq/l to -0.9 meq/l for autumn. Table 5.22 shows that all the water samples had an RSC value of <2.5 meq/l and therefore it can be concluded that this water would be suitable for irrigation. There was only one sample (B54H) from the season spring results that displayed a value of >2.5 meq/l. Few positive RSC values may also indicate that there was very low precipitation of calcium and magnesium. Additionally, this shows that the bicarbonate concentration is not higher than the sum of calcium and magnesium. Contrariwise, negative values indicate that there is more dissolved calcium and magnesium as compared to carbonate and bicarbonate concentrations (Wang, 2013).

5.8.1.4 Sodium percentage

Sodium percentage (Na%) also gives an indication of how suitable the water is for irrigation purposes (Singh *et al.*, 2015). The concentrations of the ions are expressed in meq/l, just like in the other criteria. High sodium amounts in the groundwater are unacceptable since it reacts with soil leading to its low permeability. As a result, the growth of plants is also limited this way (Singh *et al.*, 2015). The sodium percentage is expressed as the sum of sodium and potassium over the sum of all the cations multiplied by 100% (Ratio 4.7).

The results calculated with Ratio 4.7 are shown in Table 5.22. The Na% values as calculated, showed in the range of 16.64% to 61.03%, 19.47% to 75.85% and 20.05% to 65.34% for spring, summer and autumn seasons, respectively. It was stated in Singh *et al.* (2015) that the Na% should not be >60% for the water to be permissible for irrigation. Therefore, sample B24H for all the seasons gave a doubtful to unsuitable percentage for

safe irrigation water; whereas B22H gave doubtful results for the summer season (Bob *et al.*, 2015; Nazzal *et al.*, 2014). Although B58H fell within the permissible limit (Bob *et al.*, 2015; Singh *et al.*, 2015), its Na% had been increasing from spring to autumn. This might be the result of increased mineralisation in the system or the addition of sodium from ion exchange. The increased Na% in the water might be the result of weathering of sodic silicate minerals such as plagioclase albite and also an ion exchange process.

5.8.1.5 Magnesium hazard

Magnesium hazard is calculated from the Mg^{2+} to Ca^{2+} ratio in the water. Like the rest of the approaches, it is also calculated in meq/l concentrations. Nazzal *et al.* (2014) and Zaidi *et al.* (2015) classified the irrigation water as follows after the calculation of the Mg/Ca ratio: A ratio of <1.5 indicates safe water; 1.5 to 3 is moderate; whereas >3 is unsafe water. The Mg/Ca ratio results as shown in Table 5.22 for all the seasons, displayed values of <1.5. Thus, all the samples fell within the safe water classification. The values ranged from 0.10 to 0.76, 0.15 to 0.74 and 0.17 to 0.78 for spring, summer and autumn, respectively.

Generally, the water quality guidelines for irrigation indicated that the water from B24H was not suitable for irrigation purposes. This water sample had the highest salinity as a result of elevated ions and also high sodium in the water. Therefore, the rest of the water can be used for irrigation, although some water like B58H should only be used for irrigation to crops that are not negatively influenced by salt.

5.8.2 Groundwater suitability for domestic purposes

Groundwater may be considered as one of the significant sources of water for drinking and domestic purposes. In most cases, groundwater may be found to be cleaner as compared to surface water, especially when looking at pollution by bacteria (Singhal and Gupta, 2010). Nevertheless, determination of the chemical constituents in the water is important to decide whether water can be used for a particular activity or not. WHO (2011) explained that no drinking water should have a visible colour since that indicates the presence of organic matter, metals or natural impurities. Classifying if water is suitable for drinking, the SANS (2015) and WHO (2011) standards were used for comparison (Table 5.24).

The distribution of ions in the groundwater had been discussed in Section 5.3.1 and will be used as a reference to how the concentration of ions correlates with the standards. Table 5.2 and Table 5.4 will also be used as references in the discussions.

TABLE 5.24: STANDARDS AS DESCRIBED IN THE SOUTH AFRICAN NATIONAL STANDARDS (SANS) AND WORLD HEALTH ORGANIZATION (WHO)

Parameter	Unit	SANS (2015)	WHO (2011)	Effects at higher concentrations
Ca	mg/l	<150	200	Scale formation
Mg	mg/l	<70	150	Scale formation
Na	mg/l	<200	200	High blood pressure
K	mg/l	<50	12	Bitter taste
HCO ₃	mg/l	-	300	Unpleasant taste
Cl	mg/l	<300	250	Salty taste
SO ₄	mg/l	<500	250	Laxative effect
NO ₃ & NO ₂ (N)	mg/l	<11	50	Methemoglobinemia, gastric cancer, goitre
NH ₃ (N)	mg/l	<1.5	0.2	Taste and odour
F	mg/l	<1.5	1.5	Dental fluorosis, deformation of bones
Al	mg/l	<0.3	0.1-0.2	Chronic human health
Fe	mg/l	<0.3	0.3	Turbidity, colour and taste, stains laundry
Mn	mg/l	<0.4	0.1	Undesirable taste, stains sanitary ware and laundry
TH	mg/l	-	500	Scale formations
pH		≥5.0 and ≤9.7	9.2	Unpleasant taste
TDS	mg/l	-	1 500	Gastrointestinal irritation

Table 5.25 shows the calculated TH for calcium and magnesium. The concentrations of fluoride, ammonia, iron and manganese were averaged for all the seasons and the average values are indicated in the table. The averaging was done because most of these samples had more or less equal concentrations. Therefore, averaging them did not make a huge impact on the final concentrations.

The depths of the boreholes as indicated in Table 5.25 did not affect the distribution of ions in the water samples. However, the spatial distribution, as well as the elevation of boreholes indicated, some variations. The variation that is indicated by the borehole locations as well as the elevations will be discussed below.

TABLE 5.25: DEPTH, CALCULATED TOTAL HARDNESS FOR ALL SEASONS, AS WELL AS THE AVERAGE OF FLUORIDE, AMMONIA, IRON AND MANGANESE FOR EACH BOREHOLE

Site name	Total harness			F	NH ₃	Fe	Mn	Depth
	Spring	Summer	Autumn	mg/l		µg/l		mbgl
B10H	230.6	253.1	-	0.53	0.10	1.74	1.63	53.68
B11H	-	259.4	-	0.47	0.12	0.88	34.33	NM
B22H	393.7	226.2	-	0.77	0.15	5.06	40.03	62.01
B24H	1300.1	1085.7	1069.3	1.07	0.32	33.40	548.67	62.01
B25H	535.7	491.6	498.2	0.76	0.30	0.88	7.47	62.20
B36H	401	455.6	ND	0.78	0.16	10.35	3.42	NM
B44H	508.4	462.5	ND	0.86	0.10	8.15	10.10	36.24
B45H	534.2	613.6	550.5	0.82	0.10	4.16	5.97	78.00
B50H	692.7	304	615.2	0.80	0.18	1.25	18.90	59.88
B53H	285.6	410.7	337.2	0.73	0.15	0.88	0.34	NM
B54H	-	344.3	ND	0.62	0.10	1.24	0.96	110.00
B55H	281.1	488.5	333.4	0.28	0.10	1.09	6.27	85.00
B56H	559.2	629.5	ND	0.91	0.12	2.84	0.50	130.00
B57H	599.9	699.2	ND	0.57	0.26	0.88	0.25	108.00
B58H	719.4	272.6	666	0.66	0.10	0.88	346.33	75.00
B59H	278.5	398.7	295.8	0.31	0.11	1.69	19.67	91.44
B60H	349.8	346.4	ND	0.45	0.20	1.79	5.13	56.90
B61H	305	485.2	ND	0.48	0.10	1.70	0.91	85.19
B62H	429	227.2	ND	0.57	0.60	1.19	0.92	88.94
Spring	201.1	227.3	225.9	0.25	0.10	0.88	3.83	N/A

Note: ND=No data, NM=Not measured, N/A=Not applicable; (-) = Samples with high IBE

5.8.2.1 pH

The pH amount in the water does not impact humans directly (WHO, 2011). In order for disinfection processes with chlorine to be accurate, the water pH should be at the most 8. Therefore, pH of the water that is distributed for drinking and other domestic purposes should always be controlled to avoid corrosion to the distribution pipes. Accordingly, corrosion mostly develops once the pH of the water becomes seven or less; as a result, water may be contaminated, changing its taste and colour (WHO, 2008).

The pH for all seasons ranged from 6.5 to 8 (see also Table 5.2, Table 5.3 and Table 5.4), which is an indication of groundwater that is slightly alkaline. This range indicates that the water is suitable for drinking by humans as stated in the WHO guidelines (2011), with recommended standards of 6.5 to 8.5. Mor *et al.* (2006) explained that the reason groundwater might be in a slightly alkaline state is because HCO_3^- enters the aquifers as rainwater infiltrates through the soil zones. Acidic or alkaline water may give the water an unpleasant taste.

5.8.2.2 Total dissolved solids

Total dissolved solid (TDS) is a combination of inorganic salts that can dissolve in the water, dissolved gases and organic matter (Singh *et al.*, 2015). The measured TDS for all the seasons ranged between 260 mg/l and 4 520 mg/l, 358 mg/l and 3 676 mg/l, and 320 mg/l and 3 787 mg/l for spring, summer and autumn, respectively (see also Table 5.2, Table 5.3 and Table 5.4).

TABLE 5.26: WATER QUALITY DESCRIPTION FOR TOTAL DISSOLVED SOLIDS AS WELL AS THE SAMPLES THAT FALL UNDER THE RESPECTIVE CATEGORIES

Quality description	TDS (mg/l)	Samples
Excellent	<300	3 (Spring)
Good	300-600	20 (9 Spring, 6 Summer, 5 Autumn)
Fair	600-900	11 (5 Spring, 4 Summer, 2 Autumn)
Poor	900-1200	11 (2 Spring, 7 Summer, 2 Autumn)
Unacceptable	>1200	7 (1 Spring, 3 Summer, 3 Autumn)

Source: WHO (2011)

The TDS classification indicated that 12 out of 20 samples collected for the spring season, was water that can be used for drinking purposes (Table 5.26). Five of the samples (B22H, B25H, B50H, B60H and B62H) were considered fair for drinking, whereas three (B24H, B57H and B58H) were poor to unacceptable for drinking.

The summer results, on the other hand, indicated a total of 10 samples that were poor to unacceptable for drinking. These were B25H, B44H, B45H, B50H, B54H, B57H and B62H (poor); B24H, B22H and B58H (unacceptable). The six samples that were categorised to be good were B10H, B11H, B55H, B59H, B61H and the spring. This is the water that can be used for drinking purposes.

Lastly, the autumn results showed that samples B24H, B25H and B58H were classified as unacceptable, whereas B45H and B50H were poor for drinking. The samples that indicated water that was good for drinking, were B10H, B11H, B55H, B59H and the spring.

The samples that were classified under excellent or good for drinking in summer and autumn were classified under the CaHCO_3 in the piper diagrams. Furthermore, the ones classified as good for spring, fell under CaHCO_3 and mixed water type. These samples were from the boreholes located at high elevations where recharge to the aquifer with recent water occurs. The unacceptable and poor water fell within the NaCl and mixed water type, showing the occurrence of hydrogeochemical processes that altered the groundwater chemistry. This variation was seen in boreholes situated at low elevations such that the recharge was not from recent water.

Freeze and Cherry (1979) explained that water that has a TDS of $<1\ 000\ \text{mg/l}$ is considered fresh, whereas water with a TDS of $>1\ 000\ \text{mg/l}$ is brackish. All the samples that were classified under excellent, good and fair TDS, with the addition of B45H, B54H and B62H from the autumn results, met these criteria. This water had a TDS of $<1\ 000\ \text{mg/l}$ and therefore it was considered fresh. The rest of the water that was classified as poor or unacceptable with a TDS of $>1\ 000\ \text{mg/l}$ was classified as brackish. The samples that had brackish water were B24H, B57H and B58H (spring), B22H, B24H, B25H, B44H, B50H, B57H and B58H (summer) and lastly B24H, B25H, B45H, B50H and B58H (autumn).

All the boreholes that had brackish water were located at low elevations. However, B36H and B56H were also located at low elevations, but their water was fresh. High TDS in the water samples was the result of mineralisation during water-rock interactions in the flow path, weathering and dissolution of carbonates, silicates, gypsum, sylvite and halite and also evaporation.

5.8.2.3 Total hardness

Drinking water may be classified as hard or soft depending on the number of chemical constituents in the water. This depends on which standards are used per country. Hardness in the water is mainly caused by the presence of calcium and magnesium. However, other metals such as zinc, iron, manganese and aluminium may also cause hardness to the water, though at a very low rate as compared to Ca^{2+} and Mg^{2+} . TH is expressed as CaCO_3 in mg/l and Expression 4.8 was used.

The TH values showed a range of $106.9\ \text{mg/l}$ to $1\ 300.1\ \text{mg/l}$ for summer, $226.2\ \text{mg/l}$ to $1\ 085.7\ \text{mg/l}$ for autumn, and $225.9\ \text{mg/l}$ to $1\ 069.3\ \text{mg/l}$ for autumn. The results in Table

5.27 show that only two samples had slightly hard water. The rest of the samples for all seasons had hard to very hard water. Therefore, the study area did not show any soft water. Hard water along the study area was caused by the presence of Ca^{2+} and Mg^{2+} (Annapoorna and Janardhana, 2015). The high Ca^{2+} and Mg^{2+} in the water might have resulted from processes such as carbonate dissolution cation exchange and evaporation that are assumed to have been taking place. Again, the addition of more calcium could have been from dissolution of gypsum.

TABLE 5.27: HARDNESS OF WATER EXPRESSED AS CALCIUM CARBONATE

Hardness range (CaCO_3 mg/l)	Description of hardness	Samples
0 to 50	Soft	0
50 to 100	Moderately soft	0
100 to 150	Slightly hard	2 (Spring)
150 to 200	Moderately hard	0
200 to 300	Hard	13 (5 Spring, 5 Summer, 3 Autumn)
>300	Very hard	37 (13 Spring, 15 Summer, 9 Autumn)

Source: SAWQG (1996a).

Depending on the pH and alkalinity, hard to very hard water (200 mg/l) may result in scale deposition in water heaters, boilers, cooking utensils, distribution pipe systems, pipe works and treatment works. Hard water also consumes much soap during cleaning and washing of clothes (Singh *et al.*, 2015; WHO, 2011). Although Annapoorna and Janardhana (2015) indicated that hard water is not a health hazard, Agrawal and Jagetia (1997) explained that this water may cause health effects such as cardiovascular disorders, parental mortality, and even some types of cancer. Conversely, soft water with a hardness of <100 mg/l may corrode the pipe systems due to its low buffering capacity (WHO, 2008).

5.8.2.4 Sodium

Sodium concentrations in drinking water should not exceed the permissible limit of 200 mg/l, since high concentrations may give an unacceptable taste to the water (WHO, 2008). The ranges of sodium among the results accumulated for this study were as follows. There was a range between 20 mg/l and 934 mg/l, 27 mg/l and 790 mg/l, and 28 mg/l and 924 mg/l for spring, summer and autumn, respectively. Since the sodium limit for drinking water is 200 mg/l, there were samples that exceed this limit. These were two samples (B24H and B58H) for spring, four samples (B24H, B58H, B22H and B25H) for summer, and three samples (B24H, B58H and B25H) for autumn. High concentrations of sodium in drinking

water may result in health effects such as kidney failure, nervous disorders and hypertension (Annapoorna and Janardhana, 2015).

5.8.2.5 Potassium

The concentration of potassium in the groundwater was very low and would therefore not have any effect on the drinking water. All the values were less than the maximum permissible concentration, such that the range was between 0.3 mg/l and 6.7 mg/l for all the seasons. Therefore, this ion would not have any impact on the drinking water quality.

5.8.2.6 Bicarbonate

The WHO (2004) described the maximum permissible limit of HCO_3 in drinking water to be 300 mg/l. The bicarbonate concentrations ranged from 223 mg/l to 744 mg/l, 202 mg/l to 427 mg/l, and 225 mg/l to 599 mg/l for spring, summer and autumn, respectively. Therefore, water with exceeding limits of bicarbonate would be considered unfit from drinking. Four water samples for spring were considered unfit for drinking due to high bicarbonate (B24H, B58H, B60H and B61H); five for autumn (B24H, B25H, B58H, B60H and B61H); and four for summer (B10H, B24H, B25H and B58H).

5.8.2.7 Chloride

The presence of chloride (Cl) in drinking water may come from natural sources, sewage and industrial processes, as well as urban run-off (WHO, 2008). High (250 mg/l) Cl concentrations result in water being saline or having a salty taste (WHO, 2011). The range for chloride concentrations in the groundwater samples was 13-1 248 mg/l (spring), 14-872 mg/l (summer) and 11-1 019 mg/l (autumn). The samples that had concentrations that exceeded the limit of 250 mg/l were B24H, B50H and B58H for all the seasons, whereas B57H represented spring and summer and B25H spring and autumn. Samples B53H and B56H (spring), B62H (summer) and B45H (autumn) also had a Cl⁻ concentration >250 mg/l. Both Annapoorna and Janardhana (2015) and Singhal and Gupta (2010) stated that high chloride concentrations may cause heart problems and high blood pressure.

5.8.2.8 Sulphate

The maximum permissible limit of sulphate in drinking water as described by WHO (2011) is 250 mg/l. Thus, high SO_4 concentrations in the water might cause laxative effects (Annapoorna and Janardhana, 2015). Sulphate concentrations ranged from 40 mg/l to 1 193 mg/l for spring, 34 mg/l to 1 399 mg/l for summer and 18 mg/l to 1 148 mg/l for autumn.

Twenty-one samples in total exceeded the 250 mg/l limit. These were B24H, B25H, B44H, B45H, B50H, B57H and B58H for all the seasons. Also, B22H (summer) and B56H (spring) exceeded this limit. High sulphate concentrations in this study area could be the result of gypsum dissolution.

More or less the same boreholes indicated high concentrations of chloride and sulphate. These boreholes are situated around the town of Beaufort West and they are at low elevations as compared to the boreholes at mountainous areas where recharge by recent water occurred. An assumption was made that since the town is surrounded by sewerage systems that dump at the waste water treatment works, there could have been some damaged sewerage pipes. Therefore, these pipes might have been leaking waste water into the soil and then to the groundwater (Eiswirth and Hotzl, 1994). Furthermore, it could be leakage of contaminants from the waste dump site. This might be resulting in high Cl, SO₄ and Na concentrations that exceeded the maximum limit per WHO (2011) standards. The variation was seen only in the boreholes at and around town.

5.8.2.9 Nitrate

Nitrate may also be toxic if present in higher concentrations in the groundwater. The presence of this contaminant in the water may be caused by waste from sewage and animals and also agricultural fertilisers (Chapman, 1996; WHO, 2008). The acceptable concentration of nitrate in the water is 11 mg/l (SANS, 2015). Nitrate, amongst all the major anions, had the lowest concentrations of all the samples. None of the samples had a concentration that exceeded the acceptable limit as described by SANS (2011), since the range was between 0.2 mg/l and 11 mg/l. Therefore, nitrate was not considered as a threat in this drinking water.

Although nitrate found in the groundwater of the study area was not risky, discussions on the elevated concentrations were deemed necessary. Nitrate was noticed to be increasing in other samples from spring to summer and then autumn. These samples were B50H, B56H and B57H for all seasons, as well as B36H from spring to summer and B45H from summer to autumn. These boreholes were located at a distance within 6 km from the centre of Beaufort West town. Nitrate concentrations that were increasing in the water might have been leaching from sewerage pipes (Figure 5.18) and also from agricultural activities.

Since B56H and B57H were situated a few metres from the dump site, nitrate from some dumped material might have been leaching into the groundwater. The concentration of nitrate in B57H increased from spring to summer. This could be an indication that the groundwater was vulnerable to contamination by nitrate, especially B56H that had a

concentration of 11 mg/l. Furthermore, B58H was also facing an increase from one season to the next, as indicated above. This borehole was not situated far from the sewage system, so this was where the nitrate might have been leaking into the groundwater. Although the boreholes explained above indicated >5 mg/l of nitrate, this did not indicate any kind of pollution since the drinking water standards fell within the acceptable limit. Meanwhile, B56H had a nitrate-N concentration of >10 mg/l; this could lead to contamination of groundwater by nitrate seeping underground through run-off. Therefore, quick measures need to be taken to prevent the increasing nitrate concentration in the groundwater.

Nitrate in the water may cause human health risks such as blue baby syndrome in infants (Singhal and Gupta, 2010), hypertension, goitre, gastric cancer and methemoglobinemia (Annapoorna and Janardhana, 2015).

5.8.2.10 Ammonia

The presence of ammonia in groundwater may be from disinfections with chloramine or from agricultural and industrial processes (WHO, 2008). The levels of ammonia in groundwater should be below 0.2 mg/l for drinking water (WHO, 2011). Therefore, concentrations >1.5 mg/l may change the taste and odour of the water (SAWQG, 1996a). The presence of ammonia in drinking water may not cause immediate health effects.

There were samples that indicated an ammonia concentration that was >0.2 mg/l, which is considered as the maximum limit for drinking water. The following samples were above the limit: B24H, B25H, B36H, B50H, B53H, B57H and B60H for spring season, and none for the other seasons. The reason for this could be that ammonia present in the water was converted to nitrates through nitrification.

The same variation that was explained for chloride and sulphate could also be assumed for nitrate (N) and ammonia (NH₃), namely that waste could have been leaking from sewerage pipes that might have been damaged. These contaminants could be leading to the presence of nitrogen compounds (Eiswirth and Hotzl, 1994), with the addition of nitrogen from the soil.

5.8.2.11 Fluoride

Fluoride is described as one of the most important element for humans (WHO, 2011). Its presence in the groundwater may be as a result of long residence time of the groundwater, semiarid climate, irrigation processes and mainly leaching from fluoride-rich rocks (Annapoorna and Janardhana, 2015). The allowed concentration of fluoride in drinking water should be 1.0 mg/l (SANS, 2006). The fluoride values (Table 5.27) ranged from 0.25 mg/l to

1.07 mg/l. These values fell within the permissible limit of drinking water. Therefore, fluoride was not a threat in the groundwater. If fluoride is present in high concentrations in groundwater it may cause some health effects such as skeletal and dental fluorosis (Singhal and Gupta, 2010).

5.8.2.12 Iron

Iron cannot impact human health directly, but may be considered for aesthetic importance. This is seen where iron present in the groundwater promotes the growth of iron bacteria that produce a slimy coating in the water, leading to plugging of water pipes and also clogging the well screen (Singhal and Gupta, 2010). Iron gives the water a bad taste and odour and it stains laundry; these may be experienced in instances whereby the iron concentration is >0.3 mg/l as indicated by the SANS (2006) and WHO (2011) standards. The results indicated that the presence of iron in the groundwater was not a hazard because its concentration ranged between 0.0008 mg/l and 0.0334 mg/l, which were within the permissible limit of 0.3 mg/l.

5.8.2.13 Manganese

Manganese, like iron, cannot impact human health directly. However, it may give an unwanted taste to the water if its concentration exceeds 0.1 mg/l such that the concentrations below 0.1 mg/l are acceptable (SANS, 2006; WHO, 2011). Like iron present in the water, manganese may also stain laundry at concentrations of >0.1 mg/l, and may form coatings on pipes at concentrations of >0.2 mg/l. Manganese ranged from 0.0002 mg/l to 0.5487 mg/l in the water. Thus, the amount of manganese in the water was higher than that of iron. Other samples had a manganese concentration that was above the limit of 0.1 mg/l. These samples were B24H and B58H for all the seasons, as well as B22H for the autumn season. The presence of a high manganese concentration is related to the presence of limestone in the study area. Manganese occurs in association with bicarbonate in the limestones at this area.

5.8.3 Groundwater suitability for use by livestock

Water standards for usage by livestock depends on the type and age of the livestock, as well as their food and habits (Lloyd and Heathcote, 1985; SAWQG, 1996c). However, the standards that are used for human consumption can still be considered for livestock, even though livestock can tolerate as much TDS in the water as 1 000 mg/l (Deshmukh, 2013; Singhal and Gupta, 2010). Livestock cannot use water with an EC concentration as high as 1 000 mS/m for drinking since this water may cause diarrhoea and weight loss.

Table 5.28 indicates the maximum permissible limits for livestock use. However, these limits do not apply to all livestock since some livestock can tolerate higher concentrations.

TABLE 5.28: PARAMETERS AND THEIR RESPECTIVE RANGE FOR SUITABILITY FOR LIVESTOCK WATERING

Parameters	General permissible limits for livestock watering (mg/l)	Samples
Ca	1 000	All
Cl	1 500	All
Mg	500	All
Na	2 000	All
SO ₄	1 000	All
F	4	All
Fe	10	All
Mn	10	All
NO ₃	100	All

The permissible limits of certain ions for use by livestock depend on several factors as described above. There are livestock that can consume water containing concentrations far above the ones indicated by Table 5.28.

The results obtained for this study indicated that the water was suitable for consumption by livestock. Although the TDS for some samples highly exceeded 1 000 mg/l, this water could still be permitted for use by livestock such as sheep, cattle and pigs (SAWQG, 1996c).

5.9 Conclusion

This chapter focused on examining the raw groundwater data using various complementary hydrogeochemical tools. Classification of water types was performed using the hydrochemical data. The grouping of the water samples on the Piper diagrams and on the hierarchical cluster plots corresponded with one another, and this led to the conclusion of the main groundwater types. Additional to the water types, the hydrogeochemical processes that were involved in changing the groundwater chemistry were also described. The complementary tools gave corresponding results such that similar processes were indicated to be taking place at the study area to change the groundwater chemistry regardless of the season. This showed the importance of applying various tools for data analysis.

Chapter 6

Conclusions and Recommendations

6.1 Conclusions

The study was conducted at Beaufort West town in Quaternary Catchment J21A to characterise the groundwater hydrogeochemical processes and assess the groundwater quality for domestic and agricultural uses. Multiple tools were used as complementary techniques to interpret the data. The findings have improved the understanding of hydrogeochemical processes that control the evolution of groundwater chemistry and their influence on groundwater quality in the town. Sample collection was conducted throughout the period of three seasons (spring, summer and autumn). Specific findings from the study are presented in the subsequent sections.

6.1.1 Main water types

The findings indicated the main water types to be calcium bicarbonate, sodium chloride and mixed water types. These water types resulted from water-rock interaction and the geochemical reactions that took place in the groundwater system of Beaufort West.

6.1.2 Main hydrogeochemical processes and their influence on groundwater chemistry

Various tools were used to identify the hydrogeochemical processes controlling the evolution of the groundwater chemistry and quality at Beaufort West. These tools were utilised after identification of various groundwater types in the study area. The knowledge on the hydrogeochemical processes that control the groundwater chemistry and quality contributed to understand the variation in water compositions in the same area and also the chemistry changes from one season to the next.

The following hydrogeochemical processes were concluded to be the main ones as inferred from various tools:

❖ Ion exchange

Ion exchange resulted in increased sodium in the groundwater system, whereby calcium ions were removed from solution to fill up the exchange sites in the sediments. Ion exchange as indicated by the tools, was dominating the low elevated areas where the groundwater was highly mineralised.

❖ **Reverse ion exchange**

Reverse ion exchange indicated more chloride and/or calcium than sodium in the groundwater. The occurrence of reverse ion exchange resulted in (1) an increase in chloride over sodium in the water through mixing of groundwater with another source of water such as connate water; and (2) cation exchange where calcium ions replaced sodium ions in solution through freshening of the aquifer by CaHCO_3 water flushing out the salt in the water. This process was concluded to be occurring at areas where there was mixing of water.

❖ **Weathering and dissolution of silicates, carbonates and evaporites**

Dissolution took place as a result of water-rock interaction, whereby minerals were dissolved in solution. These minerals included carbonate, silicates and evaporites such as gypsum, halite and sylvite. Dissolution of evaporites occurred at random areas, although gypsum dissolution dominated the dissolution of other evaporites.

Silicate weathering occurrence was inferred by all the tools that were used. This processes contributed to increased Ca^{2+} , Na^+ and SiO_2 in the groundwater. Silicate weathering was also concluded to be dominating the areas of recharge by recent water. Although this process dominated areas of high elevation, it was also experienced at other areas along the flow paths down-gradient.

Carbonate weathering was also estimated by all the tools, and this was concluded to be more of calcite dissolution than dolomite dissolution. Carbonate weathering; although it occurred at some areas at high elevations, it was dominant at low elevated areas where ion exchange and reverse ion exchange were dominating.

❖ **Evaporation**

Evaporation was also inferred to be taking place due to the hot and dry climatic conditions of the area. This process was concluded to dominate areas where processes such as ion exchange, reverse ion exchange, carbonate and gypsum dissolution were dominating. These are the areas that did not receive recharge by recent water. Evaporation led to increased TDS at these areas.

❖ **Mixing**

Mixing also occurred in the groundwater system whereby water from different sources mixed, changing the chemistry and the quality of the initial water. The processes of mixing took place at various areas along the flow paths.

The major findings on the main hydrogeochemical processes that played a role in evolving the groundwater chemistry and quality showed that silicate weathering was the most dominating process. This was followed by evaporation, ion exchange, carbonate weathering, reverse ion exchange and gypsum dissolution.

6.1.3 Anthropogenic sources

Although anthropogenic sources did not form part of the hydrogeochemical processes, they played a role in altering the groundwater chemistry and quality. Nitrate, as one of the major ions, indicated its occurrence in the groundwater from anthropogenic sources such as industrial, sewage and agricultural works. Ammonia was also concluded to come from these anthropogenic sources.

6.1.4 Seasonal variations

There were slight variations in the results obtained for different seasons. The main water types and hydrogeochemical processes inferred were the same throughout the groundwater system for all seasons. The only difference was that hydrogeochemical processes such as dissolution of evaporites, were occurring at random locations with the result that their occurrence in the system was different seasonally. Meanwhile, processes such as ion exchange, reverse ion exchange, silicate weathering and evaporation were dominating at the same areas throughout the seasons. Consequently, as a result of high rainfall and recharge, ion exchange was dominated by cation exchange during autumn.

The concentrations of TDS in the groundwater also increased from spring to summer and then to autumn. The increased TDS resulted from increased Ca^{2+} , Mg^{2+} and HCO_3^- levels in the groundwater as a result of high recharge, since the collection of the samples during the summer and autumn seasons was done after periods of rainfall. Rainfall water interacted with carbon dioxide to form carbonic acid that reacted with carbonates, leading to their dissolution. Additionally, increased HCO_3^- as a result of interaction of carbonates with carbonic acid, led to increased pH (more alkaline) in autumn. The presence of fluoride in the groundwater was indicated for the spring season, showing long residence times due to low recharge during this season. On the other hand, summer and autumn did not show the presence of fluoride because the samples were collected in these seasons after periods of rainfall.

6.1.5 Groundwater quality characteristics

Water quality for irrigation, drinking, domestic and livestock purposes were assessed by the application of various criteria.

❖ Irrigation purposes

Sample B24H was the only sample that indicated water that was not suitable for irrigation. This water had the highest sodium and salinity as a result of elevated ions in the water. The rest of the groundwater can be used for irrigation, although some water such as that from B58H needs to be used for irrigation to crops that are not sensitive to salt.

❖ Domestic purposes

The pH of the water was good for domestic purposes, since the water appeared to be slightly alkaline. Conversely, the TDS was not approved for all samples. Some samples showed water that can be used for drinking and this appeared to be water classified as recent water from recharge at high elevations. There was water that was categorised to be fair for drinking and thus needs to be treated first before it can be distributed. On the other hand, water with a TDS >900 mg/l was classified as poor for drinking purposes. This was water from boreholes at low elevations which were categorised as mixed water.

Total hardness of the water showed only two samples to be slightly hard, whereas the rest of the samples in all seasons displayed hard to very hard water. The high concentrations of other major ions such as sodium, chloride, bicarbonate and sulphate may cause health effects to humans if they should drink this water. Nitrate, iron and fluoride, though present, did not exceed the permissible limit for drinking water.

Ammonia was one ion that was present in the water; however, this was only identified in spring season samples. A conclusion was made that during sampling for other seasons the ammonia that was present was already converted to nitrates by nitrification, hence an increase in NO_3 in the groundwater. Manganese also exceeded the limit at some areas. Water with high manganese may stain laundry and may form coatings on pipes. Thus, this water is not suitable for domestic purposes.

❖ Livestock purposes

The groundwater chemistry results indicated water suitable for use by livestock. Although some of the water was disregarded for human use, the water could still be used by livestock since livestock can appreciate higher concentrations of different constituents in the water.

6.2 Recommendations

The following are recommended for further studies that could be conducted at Beaufort West town:

- ❖ Sample collection may be done for at least four seasons of the year or more in order to make better comparisons of the data; also to determine any variations in the hydrochemistry of the area.
- ❖ Sampling should cover a larger area for further studies; thus, more boreholes should be sampled so that there would not be data shortage during the interpretation of results. This will also assist in determining any link on the hydraulic behaviour for different catchments around the area.
- ❖ Arrangement of the Beaufort West Municipality personnel who should be available at all times to assist with unlocking of the municipality production boreholes. This way consistency in data collection is maintained; that is, sampling the same boreholes during the rest of the seasons.
- ❖ Further sampling should be done to test for nitrate in the water, especially from boreholes that indicated an increase in this ion from one season to the next, more specifically because they are production boreholes.
- ❖ Water levels should be measured in all the accessible boreholes; this would assist in determining the groundwater flow direction.
- ❖ If there would be an opportunity that a borehole or two can be drilled, this should be done in order to obtain borehole logs that will be used to study the geology visually, unlike relying on literature.
- ❖ Conducting pump tests would also be helpful since this will provide more knowledge on the types of aquifers that one is working on; this will also help to conclude on the behaviour of certain water samples from different boreholes. Pump tests would also give better insight on the aquifer parameters.

References

- Acock, A.C. 2008. *A gentle introduction to Stata*. (2nd edition). Texas: Stata Press.
- Adams, S., Titus, R., Pietersen, K., Tredoux, G. and Harris, C. 2001. Hydrochemical characteristics of aquifers near Sutherland in the Western Karoo, South Africa, *Journal of Hydrology*, 241(1-2):94-101.
- Agrawal, V. and Jagetia, M. 1997. Hydrogeochemical assessment of groundwater quality in Udaipur city, Rajasthan, India. *Proceedings of the National Conference on Dimensions of Environmental Stress in India Baroda*: 51-154.
- Al-Harbi, O., Hussain, G. and Lafouza, O. 2009. Irrigation water quality evaluation of Al-Mendasah groundwater and drainage water, Al-Medainah Al-Monwarah region, Saudi Arabia. *International Journal of Soil Science*, 4:123-141. DOI: [10.3923/ijss.2009.123.141](https://doi.org/10.3923/ijss.2009.123.141)
- Alizadeh, M.T.H., Ghaneian, M.T. and Motedayen, A. 2011. Efficiency evaluation of rainwater quality modification by utilizing mixing method with surface water and groundwater. In: Brebbia, C.A. and Popov, V. (Eds.) 2011. *Water resources management VI*. Sixth International Conference on Sustainable Resources Management. Southampton Boston: WIT Press, 395-402.
- Annapoorna, H. and Janardhana, M.R. 2015. *Assessment of groundwater quality for drinking purpose in rural areas surrounding a defunct copper mine*. *Aquatic Procedia*, 4:685-692. <http://dx.doi.org/10.1016/j.aqpro.2015.02.088>
- Appelo, C.A.J. and Willemsen, A. 1987. Geochemical calculations and observations on saltwater intrusions, I. A combined geochemical/mixing cell model. *Journal of Hydrology*, 94(3-4):313-330. [http://dx.doi.org/10.1016/0022-1694\(87\)90058-8](http://dx.doi.org/10.1016/0022-1694(87)90058-8)
- Appelo, C.A.J. and Postma, D. 1996. *Geochemistry, groundwater and pollution*. Rotterdam: Balkema.
- Appelo, C.A.J. and Postma, D. 2005. *Geochemistry, groundwater and pollution*. (2nd edition). Rotterdam: Balkema.
- Arslan, H. 2013. Application of multivariate statistical techniques in the assessment of groundwater quality in seawater intrusion area in Bafra Plain, Turkey. *Environmental Monitoring and Assessment*, 185(3):2439-2452. DOI: [10.1007/s10661-012-2722-x](https://doi.org/10.1007/s10661-012-2722-x)
- Ayers, R.S. and Westcot, D.W. 1976. Water quality for agriculture. *FAO Irrigation and Drainage Paper*, 29, Rev. 1. Rome: Food and Agriculture Organization (FAO).

Beaufort West Municipality Annual Review. 2013. *Integrated Development Plan*. Beaufort West.

Belkhiri, L., Boudoukha, A., Mouni, L. and Baouz, T. 2010. Application of multivariate statistical methods and inverse geochemical modelling for characterization of groundwater - A case study: Ain Azel plain (Algeria). *Geoderma*, 159(3-4):390-398.

Bethke, C.M. and Yeakel, S. 2013. *Reactive transport modelling guide: The geochemist's workbench*, Release 9.0. Illinois: Aqueous Solutions. Available from: <https://www.gwb.com/pdf/GWB9/GWBtransport.pdf>

Black, K. 2009. *Business statistics: Contemporary decision making*. New York: John Wiley and Sons.

Bob, M., Rahman, N. A., Elamin, A. and Taher, S. 2015. Assessment of groundwater suitability for irrigation in Madinah City, Saudi Arabia. *Arabian Journal of Geoscience*, 9(38):5-9. DOI: 10.1007/s12517-015-2024-z

Bowen, N.L. 1922. The reaction principle in petrogenesis. *The Journal of Geology*, 30(3):177-198.

Bredenhann, L. and Hodgson, F.D.I. 1998. Minimum requirements for water monitoring at waste management facilities: Waste management series. (2nd edition). Pretoria: Department of Water Affairs and Forestry. Available from: <http://sawic.environment.gov.za/documents/267.PDF>

Campbell, G.D.M. 1980. Beaufort West groundwater investigation (1975-1977). Unpublished Technical Report GH3155. Pretoria: Department of Water Affairs, South Africa.

Chapelle, F.H. and Knobel, L.L. 1983. Aqueous geochemistry and the exchangeable cation composition of glauconite in the Aquia aquifer, Maryland. *Groundwater*, 21(3):343-352 DOI: 10.1111/j.1745-6584.1983.tb00734.x

Chapman, D.V. 1996. *Water quality assessment: A guide to use biota, sediments and water*. (2nd edition). UNESCO, WHO, London.

Chidambaram, S., Anandhan, P., Prasanna, M.V., Srinivasamoorthy, K. and Vasanthavigar, M. 2013. Major ion chemistry and identification of hydrogeochemical processes controlling groundwater in and around Neyveli lignite mines, Tamil Nadu, South India, *Arabian Journal of Geosciences*, 6(9):3451-3467.

Clark, I. 2015. *Groundwater geochemistry and isotopes*. Boca Raton, FL: CRC Press.

ClimateData.org. <http://www.en.climate-data.org/location/8470/> (Accessed 01 August 2016).

David, R. and Pyne, G. 1995. *Groundwater recharge and wells: A guide to aquifer storage recovery*. Boca Raton, Florida: CRC Press.

Davis, J C. 1973. *Statistics and data analysis in geology*. New York: John Wiley and Sons.

De Moel, P.J., Van Derk, J.C. and Van der Meer, W.G.J. 2013. Aquatic chemistry for engineers: Self-study course on PHREEQXEL for modelling water quality and water treatment. Volume 1. *Starting with PHREEQC for water treatment*. Delft University of Technology. Available from: http://ac4e.omnisys.nl/wp-content/uploads/2015/09/AC4E_Vol_1.pdf. (Accessed: 15 September 2016).

Department of Environmental Affairs and Development Planning (DEADP), Western Cape Government. 2011. The Gouritz WMA, Chapter 10:263-286. *Western Cape Integrated Water Resources Management Action Plan. Executive Summary: Status Quo Report Final Draft*. Available form:

https://www.westerncape.gov.za/other/2011/8/chapter_10_the_gouritz_wma.pdf

Deshmukh, K.K. 2013. Evaluation of groundwater quality with regard to livestock use from Sangamner area, Ahmednagar district, Maharashtra, India. *Rasayan Journal of Chemistry*, 6(3):245-257.

Deutsch, W.J. 1997. *Groundwater geochemistry: Fundamentals and applications to contamination*. Florida: CRC Press.

Domenico, P.A. and Schwartz, F.W. 1990. *Physical and chemical hydrogeology*. New York: John Wiley and Sons.

Dragon, K. 2006. Application of factor analysis to study contamination of a semi-confined aquifer (Wielkopolska Buried Valley aquifer, Poland). *Journal of Hydrology*, 331(1-2):272-279. <http://dx.doi.org/10.1016/j.jhydrol.2006.05.032>

Earle, S. 2015. *Physical geology. Chapter 5.2: Chemical weathering*. BC Open Textbook Project, BC Campus: OpenEd.

Einax, J.W., Zwanziger, H.W. and Geib, S. 1997. *Chemometrics in environmental analysis*. New York: John Wiley and Sons.

Eiswirth, M. and Hotzl, H. 1994. Groundwater contamination by leaky sewerage systems: The impact of leaking sewers on urban groundwater:399-404. <http://search.informit.com.au/documentSummary;dn=748001404936685;res=IELENG>

El-Manharawy, S. and Hafez, A. 2003. A new chemical classification system of natural waters for desalination and other industrial uses. *Desalination* 156(1-3):163-180. [http://dx.doi.org/10.1016/S0011-9164\(03\)00339-4](http://dx.doi.org/10.1016/S0011-9164(03)00339-4)

- Fisher, R.S. and Mullican, W.F. 1997. Hydrochemical evolution of sodium-sulfate and sodium-chloride groundwater beneath the Northern Chihuahuan Desert, Trans-Pecos, Texas, USA. *Hydrogeology Journal*, 5(2):4-16. DOI: 10.1007/s100400050102
- Freeze, R.A. and Cherry, J.A. 1979. *Groundwater*. Englewood Cliffs, New Jersey: Prentice Hall.
- Gajbhiye, S., Sharma, S K. and Awashi, M.K. 2015. Application of principal components analysis for interpretation and grouping of water quality parameters. *International Journal of Hybrid Information Technology*, 8(4):89-93. <http://dx.doi.org/10.14257/ijhit.2015.8.4.11>
- Garrels, R.M. and MacKenzie, F.T. 1971. *Evolution of sedimentary rocks: A new approach to the study of material transfer and change through time*. New York: W.W. Norton & Co.
- Goldich, S.S. 1938. A study in rock weathering. *The Journal of Geology*, 46(1):17-58.
- Gomo, M. 2009. *Site characterisation of LNAPL - Contaminated fractured-rock aquifer*. MSc dissertation, University of the Free State, Bloemfontein.
- Gomo, M., Van Tonder, G.J. and Steyl, G. 2013. Investigation of the hydrogeochemical process in an alluvial channel aquifer located in a typical Karoo Basin of Southern Africa. *Environmental Earth Sciences*, 70(1):227-238. DOI: 10.1007/s12665-012-2118-9
- Google Earth AfriGIS 2016. Beaufort West -32°18'27.87"S, 22°40'00"E, elevation 893 m. CNES/Astrium. <http://www.google.com/earth/index.html> (Accessed 03 March 2016).
- Hanson, B., Grattan, S.R. and Fulton, A. 2006. *Agricultural salinity and drainage*. University of California Irrigation Program Division of Agriculture and Natural Resources, Publication 3375.
- Hounslow, A.W. 1995. *Water quality data: Analysis and interpretation*. New York: Lewis Publishers.
- Hu, S., Luo, T. and Jing, C. 2013. Principal component analysis of fluoride geochemistry of groundwater in Shanxi and inner Mongolia, China. *Journal of Geochemical Exploration*, 135:124-129. <http://dx.doi.org/10.1016/j.gexplo.2012.08.013>
- Jalali, M. 2005. Major ion chemistry of groundwater in the Bahar area, Hamadan, western Iran. *Environmental Geology*, 47(6):763-772. DOI: 10.1007/s00254-004-1200-3
- Jalali, M. 2007. Assessment of the chemical components of Famenin groundwater, Western Iran. *Environmental Geochemistry and Health*, 29(5):357-374. DOI: [10.1007/s10653-006-9080-y](https://doi.org/10.1007/s10653-006-9080-y)

Jalali, M. 2009. Geochemistry characterization of groundwater in an agricultural area of Razan, Hamadan, Iran. *Environmental Geology*, 56(7):1479-1488. DOI: 10.1007/s00254-008-1245-9

Jenn, F., Kofahl C., Müller, M., Radschinski, J. and Voigt, H.J. 2007. Interpretation of geological, hydrogeological and geochemical results. In: Knödel, K., Lange, G. and Voigt, H.J. (Eds.), *Environmental geology: Handbook of field methods and case studies*. New York: Springer, pp. 941-1051.

Karoo Groundwater Expert Group (Woodford, A.C., Van Tonder, G., Talma, A.S., Tredoux, G., Rosewarne, P.N., Goes, M., O'Brien, R., Visser, D. and Esterhuysen, C. 2013. *Karoo groundwater atlas*, Volume 2. Kimberley: SRK Consulting.

Knödel, K., Lange, G. and Voigt, H. J. (2007). *Environmental Geology: Handbook of field methods and case studies*. Springer Science & Business Media.

Kozłowski, M. and Komisarek, J. 2016. Identification of the hydrogeochemical processes in the groundwater of gleysols and retisols top sequence of the Opalenica plain. *Journal of Ecological Engineering*, 17(2):113-120. <https://doi.org/10.12911/22998993/62302>

Kumar, P.J.S., Jegathambal, P. and James, E.J. 2011. Multivariate and geostatistical analysis of groundwater quality in Palar river basin. *International Journal of Geology*, 5(4):108-119.

Kura, N.U., Ramli, M.F., Sulaiman, W.N.A., Ibrahim, S., Aris, Z. and Mustapha, A. 2013. Evaluation of factors influencing the groundwater chemistry in a small tropical island of Malaysia. *International Journal of Environmental Research and Public Health*, 10(5):1861-1881. DOI: [10.3390/ijerph10051861](https://doi.org/10.3390/ijerph10051861)

Li, P., Qian, H., Wu, J. and Ding, J. 2010. Geochemical modelling of groundwater in southern plain area of Pengyang country, Ningxia, China. *Water Science and Engineering*, 3(3):282-291. <http://dx.doi.org/10.3882/j.issn.1674-2370.2010.03.004>

Lloyd, J.W. and Heathcote, J.A. 1985. *Natural inorganic hydrochemistry in relation to groundwater*. New York: Oxford University Press.

Lollar, B.S. (Ed.) 2005. *Environmental geochemistry*, Volume 9. Elsevier.

Manning, D.A.C. 2009. Experimental studies of clay mineral occurrence. In: Worden, R.H. and Morad, S. (Eds.) 2009. *Clay mineral cements in sandstones*. Special Publication Number 34 of the International Association of Sedimentologists. Oxford, UK: Blackwell Publishing, pp. 177-190.

Maya, A.L. and Loucks, M.D. 1995. Solute and isotopic geochemistry and ground water flow in the Central Wasatch Range, Utah, *Journal of Hydrology*, 172(4):31-59 [http://dx.doi.org/10.1016/0022-1694\(95\)02748-E](http://dx.doi.org/10.1016/0022-1694(95)02748-E)

Merkel, B.J. and Planer-Friedrich, B. 2008. *Groundwater geochemistry: A practical guide to modelling of natural and contaminated aquatic systems*. Nordstrom, D. K (Ed), Springer.

Meyback, M. 1987. Global chemical weathering of surficial rocks estimated from river dissolved loads. *American Journal of Science*, 287(5):417-421. DOI: 10.2475/ajs.287.5.401

Mor, S., Ravindra, K., De Vissher, A., Dahiya, R.P. and Chandra, A. 2006. Municipal solid waste characterization and its assessment for potential methane generation: A case study. *Science of the Total Environment*, 371(1-3):1-20. <http://dx.doi.org/10.1016/j.scitotenv.2006.04.014>

Murray, K. and Wade, P. 1996. Checking anion-cation charge balance of water quality analyses: Limitations of the traditional method for non-potable waters. *Water SA*, 22(1):27-32.

Nazzal, Y., Ahmed, I., Al-Arifi, N. S.N., Ghrefat, H., Zaidi, F.K., El-Waheidi, M.M., Batayneh, A. and Zumlot, T. 2014. A pragmatic approach to study the groundwater quality suitability for domestic and agricultural usage, Saq aquifer, Northwest of Saudi Arabia. *Environmental Monitoring and Assessment*, 186:8:4655-4667. DOI: [10.1007/s10661-014-3728-3](https://doi.org/10.1007/s10661-014-3728-3)

NGWA (The National Groundwater Association). 2010. *Dissolved mineral sources and significance*. [Online]. Excerpt from Chapter 23 of the 1999 NGWA publication, *Ground water hydrology for water well contractors*. Available from: <http://www.ngwa.org/Fundamentals/studying/Pages/Dissolved-mineral-sources-and-significance.aspx> (Accessed: 09 September 2016).

Norman, G.R. and Streiner, D.L. 2008. *Biostatistics: The bare essentials*. (3rd edition). Hamilton: BC Decker Inc.

Norris, G., Qureshi, F., Howitt, D. and Cramer, D. 2014. *Introduction to statistics with SPSS for social science*. New York: Routledge.

Okiongbo, K.S. and Douglas, R.K. 2014. Evaluation of major factors influencing the geochemistry of groundwater using graphical and multivariate statistical methods in Yenagoa city, Southern Nigeria. *Applied Water Science*, 5(1):27-37. DOI: 10.1007/s13201-014-0166-x.

- Olmez, I., Beal, J. W. and Villaume, J.F. 1994. A new approach to understanding multiple-source groundwater contamination: Factor analysis and chemical mass balances, *Water Research* 28(5):1095-1101. [http://dx.doi.org/10.1016/0043-1354\(94\)90195-3](http://dx.doi.org/10.1016/0043-1354(94)90195-3)
- Parkhurst, D.L. and Appelo, C.A.J. 1999. *User's guide to PHREEQC (Version 2) - A computer program for speciation, batch-reaction, one-dimensional transport, and inverse geochemical calculations*. U.S. Department of the Interior.
- Parkhurst, D.L. and Appelo, C.A.J. 2012. *Description of input and examples for PHREEQC (Version 3): A Computer program for speciation, batch-Reaction, one-dimensional transport, and inverse geochemical calculations*. Water-Resources Investigations Report 99-4259. Denver. Colorado: U.S. Department of the interior & U.S. Geological Survey.
- Parkhurst, D.L. and Plummer, L.N. 1993. Geochemical modelling. In: Alley, WM. (Ed.), *Regional groundwater quality*. New York: Van Nostrand Reinhold: 199-222.
- Parkhurst, D.L., Thorstenson, D.C. and Plummer, N.L. 1980. *PHREEQE- A computer program for geochemical calculations: water resource investigations*, US Geological Survey.
- Pearson, K.E. 2003. Basics of salinity and sodicity effects on soil physical properties. [Online]. Available from: <http://waterquality.montana.edu/energy/cbm/background/soil-prop.html>(Accessed: 03 July 2016).
- Peikam, E.N. and Jalali, M. 2016. Application of inverse geochemical modelling for predicting surface water chemistry in Ekbatan watershed, Hamedan, western Iran. *Hydrological Sciences Journal*, 61(6):1124-1134. <http://dx.doi.org/10.1080/02626667.2015.1016947>
- Penrose, R.A.F. Jr. 1893. The chemical relation of iron and manganese in sedimentary rocks. *The Journal of Geology*, 1(4):356-370.
- Petrucci, R.H., Harwood, W.S., Herring, G.E. and Madura, J.D. 2007. *General chemistry: Principles and modern applications*. (9th edition). New Jersey: Prentice Hall.
- Plummer, L.N. and Back, W. 1980. The mass balance approach: Application to interpreting the chemical evolution of hydrologic systems. *American Journal of Science*, 280(2):130-142. DOI: 10.2475/ajs.280.2.130
- Plummer, L.N., Prestemon, E.C. and Parkhurst, D.L. 1994. *An interactive code (NETPATH) for modelling net geochemical reactions along a flow path version 2.0*. Water Resources Investigation Report 94-4169. Denver, Colorado: US Geological Survey.
- Praekelt, H.E. and Nel, L. 2011. *Excursion guide for the field school in the Barkly East-Elliot-Ugie area*. Guide book, Department of Geology, University of the Free State, Bloemfontein.

- Rajmohan, N. and Elango, L. 2004. Identification and evolution of hydrogeochemical processes in the groundwater environment in an area of the Palar and Cheyyar River basins, Southern India. *Environmental Geology*, 46(1):47-61. DOI: 10.1007/s00254-004-1012-5
- Richards, L.A. (Ed.) 1954. *Diagnosis and improvement of saline and alkali soils*. Agriculture Handbook No. 60. Washington: United States Department of Agriculture. Available from: https://www.ars.usda.gov/ARSUserFiles/20360500/hb60_pdf/hb60complete.pdf(Accessed: 05 July 2016).
- Rogers, R.J. 1989. Geochemical comparison of groundwater in areas of New England, New York and Pennsylvania. *Groundwater*, 27(5):690-712. DOI: 10.1111/j.1745-6584.1989.tb00483.x
- Rose, R. and Conrad, J. 2007. *A regional reconnaissance to identify areas for groundwater development in Beaufort West*. GEOSS Report No. G2007/05-03. Cape Town: Geohydrological and Spatial Solutions International (Pty.) Ltd.
- Runnells, D.D. 1993. Inorganic chemical processes and reactions. In: Alley, W.M. (Ed.), *Regional ground-water quality*. New York: Van Nostrand Reinhold, pp. 131-154.
- Saini, R., Tuli, N.K., Kaur, G. and Krishan, G. 2014. Assessment of groundwater quality in Baddi catchment, Solan, Himachal Pradesh, India. *Water and Energy International*, 59(2):53-57.
- SANS. 2006. South African National Standards (SANS 241). *Drinking water: Quality requirements* (6th edition). Available from: http://www.alabbott.co.za/docs/2985_SANS-241_spec.pdf
- SAWQG. 1996a. *South African Water Quality Guidelines, Volume 1. Domestic Use*. (2nd edition). Pretoria: Department of Water Affairs and Forestry. Available from: https://www.dwa.gov.za/iwqs/wq_guide/Pol_saWQguideFRESH_vol1_Domesticuse.PDF
- SAWQG. 1996b. *South African Water Quality Guidelines, Volume 4. Agricultural Use: Irrigation*. (2nd edition). Pretoria: Department of Water Affairs and Forestry. Available from: http://www.iwa-network.org/filemanager-uploads/WQ_Compendium/Database/Future_analysis/080.pdf
- SAWQG. 1996c. *South African Water Quality Guidelines, Volume 5. Agricultural Use: Livestock watering*. (2nd edition). Pretoria: Department of Water Affairs and Forestry. Available from: https://www.dwa.gov.za/iwqs/wq_guide/Pol_saWQguideFRESHLivestockwateringvol5.pdf

- Schreiber, B.C. and El Tabakh, M. 2000. Deposition and early alteration of evaporites, sedimentology. *Sedimentology*, 47(1):215-238. Available from: http://www.umanitoba.ca/faculties/science/geological_sciences/faculty/last/Courses/evap/se d47.pdf (Accessed: 28 August 2016).
- Sharif, M.U., Davis, R.K., Steele, K.F., Kim, B., Kresse, T.M. and Fazio, J.A. 2008. Inverse geochemical modelling of groundwater evolution with emphasis on arsenic in the Mississippi River Valley alluvial aquifer, Arkansas (USA). *Journal of Hydrology*, 350:41-55. DOI: 10.1016/j.jhydrol.2007.11.027
- Sharma, A.K. 2005. *Text book of elementary statistics*. New Delhi, India: Discovery Publishing House.
- Sharma, K.K., Kumar, A. and Chaudhary, A. 2009. *Statistics in management sciences, India* Krishna Prakashan Media, pp. 55-76.
- Singh, S., Janardhana, R. and Ramakrishna, C. 2015. Evaluation of groundwater quality and its suitability for domestic and irrigation use in parts of the Chandauli-Varanasi region, Uttar Pradesh, India. *Journal of Water Resource and Protection*, 7(7):572-587. DOI: [10.4236/jwarp.2015.77046](https://doi.org/10.4236/jwarp.2015.77046)
- Singhal, B.B.S. and Gupta, R.P. 2010. Groundwater quality. In: Singhal, B.B.S. and Gupta, R.P. (Eds.), *Applied hydrogeology of fractured rocks*. (2nd edition). New York: Springer Publishers, pp. 205-219.
- Suk, H. and Lee, K.K. 1999. Characterization of water hydrochemical system through multivariate analysis: Clustering into groundwater zones. *Groundwater*, 37(3):358-366. DOI: 10.1111/j.1745-6584.1999.tb01112.x
- Turner, B.R. 1981. *Revised stratigraphy of the Beaufort Group in the Southern Karoo basin*, Department of Geology. *Palaeontologia Africana*, 24:87-98. The University, Newcastle Tyne, England. <http://hdl.handle.net/10539/16302>
- US EPA. (United States. Environmental Protection Agency). 2006. *Data quality assessment: Statistical methods for practitioners*. EPA QA/G-9S, Washington DC.
- Van Camp, M. and Walraevens, K. 2008. Identifying and interpreting baseline trends. In: Edmunds, W.M. and Shand, P. (Eds.), *Natural groundwater quality*. Massachusetts: Wiley-Blackwell Publishing. pp. 131-154.
- Van Wyk, Y. and Witthueser, K. 2011. A forced-gradient tracer test on the Hansrivier dyke: Beaufort West, South Africa. *Water SA*, 37(4):437-443.

- Villegas, P., Paredes, V., Betancur, T. and Ribeiro, L. 2013. Assessing the hydrochemistry of the Urabá aquifer, Colombia by principal component analysis. *Journal of Geochemical Exploration*, 134:120-129. <http://dx.doi.org/10.1016/j.gexplo.2013.08.011>
- Wang, S. 2013. Groundwater quality and its suitability for drinking and agricultural use in the Yandi Basin of Xinjiang Province, Northwest China. *Environmental Monitoring Assessment*, 185:7469-7484. DOI: 10.1007/s10661-013-3113-7
- Wasserman, S. and Faust, K. 1994. *Social network analysis: Methods and applications*, Cambridge: Cambridge University.
- Weaver, J.M.C., Cave, L. and Talma, A.S. 2007. *Groundwater sampling: A comprehensive guide for sampling methods*. WRC Report No TT 303/07. (2nd edition). Gezina: Water Research Commission. Available from: <http://www.wrc.org.za/Knowledge%20Hub%20Documents/Research%20Reports/TT303-07.pdf>
- Wendland, F., Hannappel, S., Kunkel, R., Schenk, R., Voigt, H.J. and Wolter, R. 2005. A procedure to define natural groundwater conditions of groundwater bodies in Germany. *Water Science & Technology*, 51(3-4):249-257.
- WHO (World Health Organisation). 2004. *Guidelines for drinking-water quality*. Geneva, Switzerland.
- WHO (World Health Organisation). 2008. *Guidelines for drinking-water quality*. (3rd edition). Geneva Switzerland.
- WHO (World Health Organisation). 2011. *Guidelines for drinking-water quality*. (4th edition). (NLM classification: WA 675). Geneva, Switzerland.
- Wilcox, L.V. 1955. *Classification and use of irrigation waters*. Circular No. 969. Washington, D.C: United States Department of Agriculture.
- Wolery, T.J. and Daveler, S.A. 1992. EQ6, A computer program for reaction path modelling of aqueous geochemical systems: Theoretical manual, user's guide and related documentation (Version 7.0). California: Lawrence Liverpool National Laboratory. Available from: http://wipp.energy.gov/information_repository/cra/2009_cra/references/Others/Wolery_Daveler_1992_EQ36_A_Computer_Program_for_Reaction_Path_Modeling_of_Aqueous_Geochemical_Systems_ERMS241379.pdf

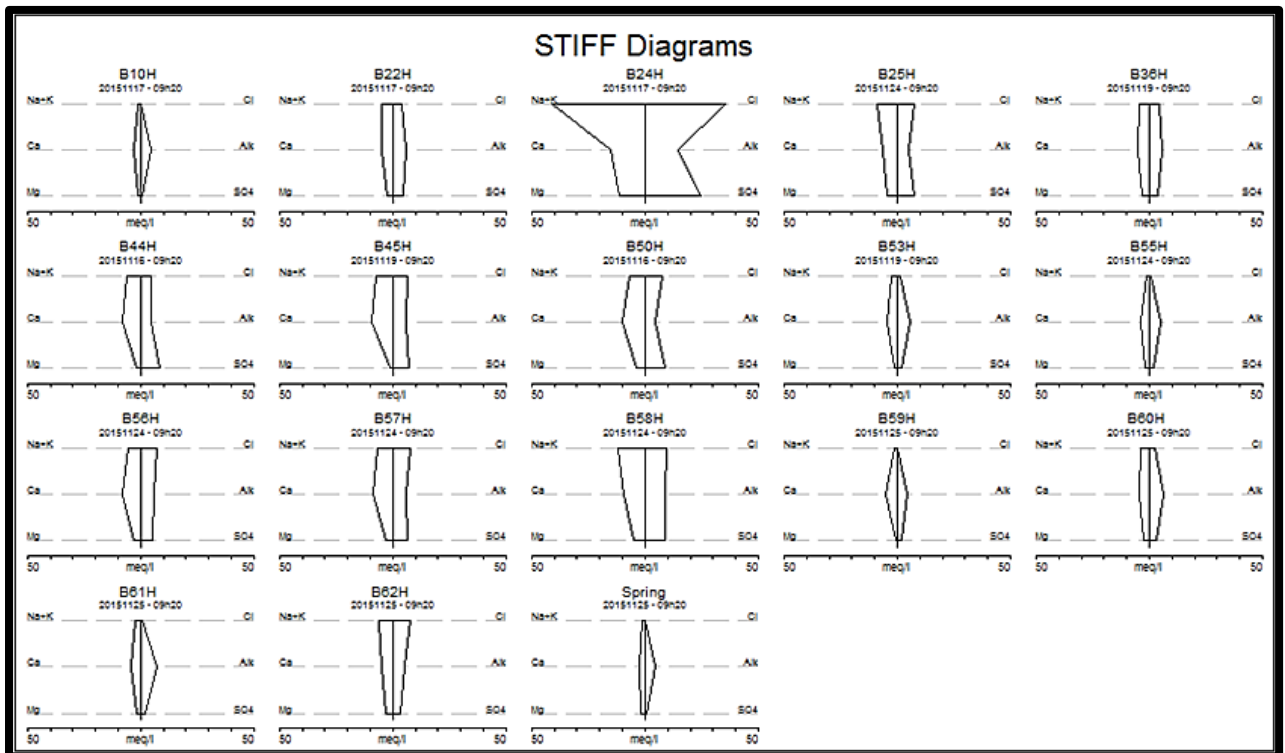
- Woodford, A. and Chevallier, L. 2002. *Hydrogeology of the main Karoo Basin: Current knowledge and research needs*. Water Research Commission, Report No TT 179/02, pp. 30-41.
- Younger, P.L. 2007. *Groundwater in the environment: An introduction*. Massachusetts: Blackwell Publishing.
- Zaidi, F.K., Nazzal, Y., Jafri, M. K., Naeem, M. and Ahmed, I. 2015. Reverse ion exchange as a major process controlling the groundwater chemistry in an arid environment: A case study from Northwestern Saudi Arabia. *Environmental Monitoring and Assessment*, 187(607):1-18. DOI: 10.1007/s10661-015-4828-4
- Zaporozec, A. 1972. Graphical interpretation of water-quality data *Groundwater*, 10(2):32-43. DOI: 10.1111/j.1745-6584.1972.tb02912.x
- Zhang, R., Hu, S., Zhang, X. and Yu, W. 2007. Dissolution kinetics of dolomite in water at elevated temperatures. *Aquatic Geochemistry*, 13(4):309-338. DOI: 10.1007/s10498-007-9022-z
- Zhu, C. and Anderson, G. 2002. *Environmental applications of geochemical modelling*. Cambridge: Cambridge University Press.

Appendix 1

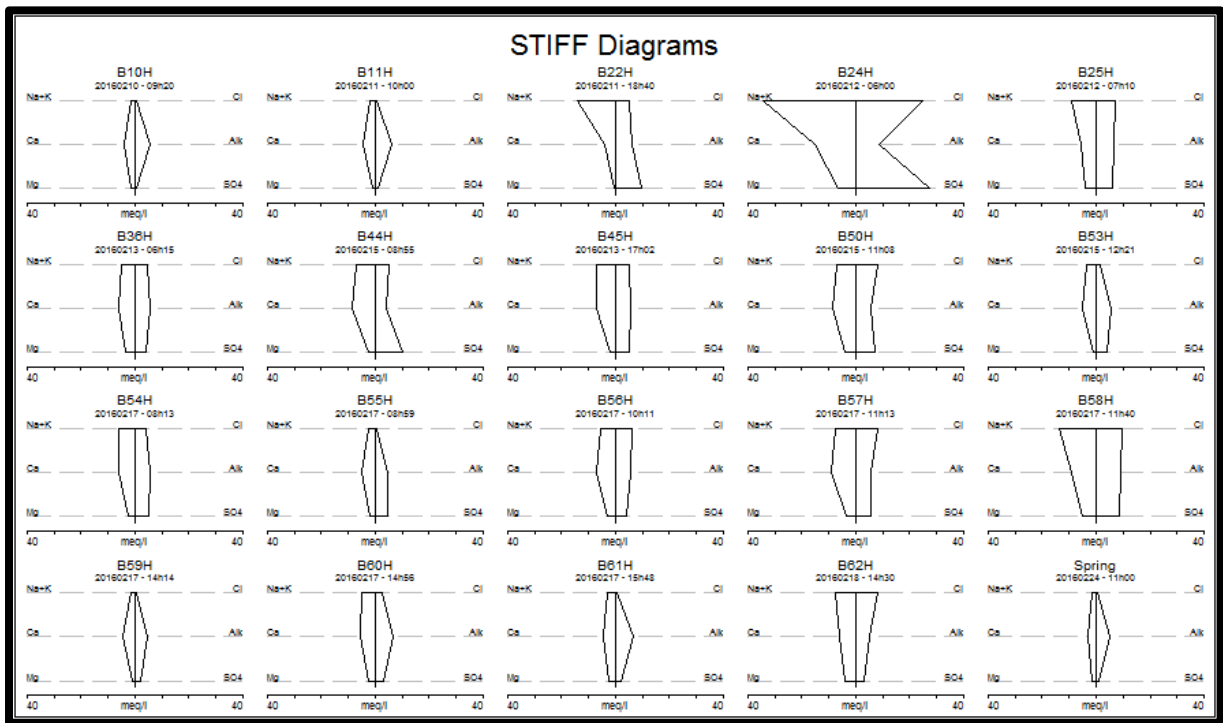
Hydrochemical Classification (Stiff Diagrams)

The stiff diagrams were generated for spring, summer and autumn seasons. These diagrams were done for all the boreholes that were sampled including the spring.

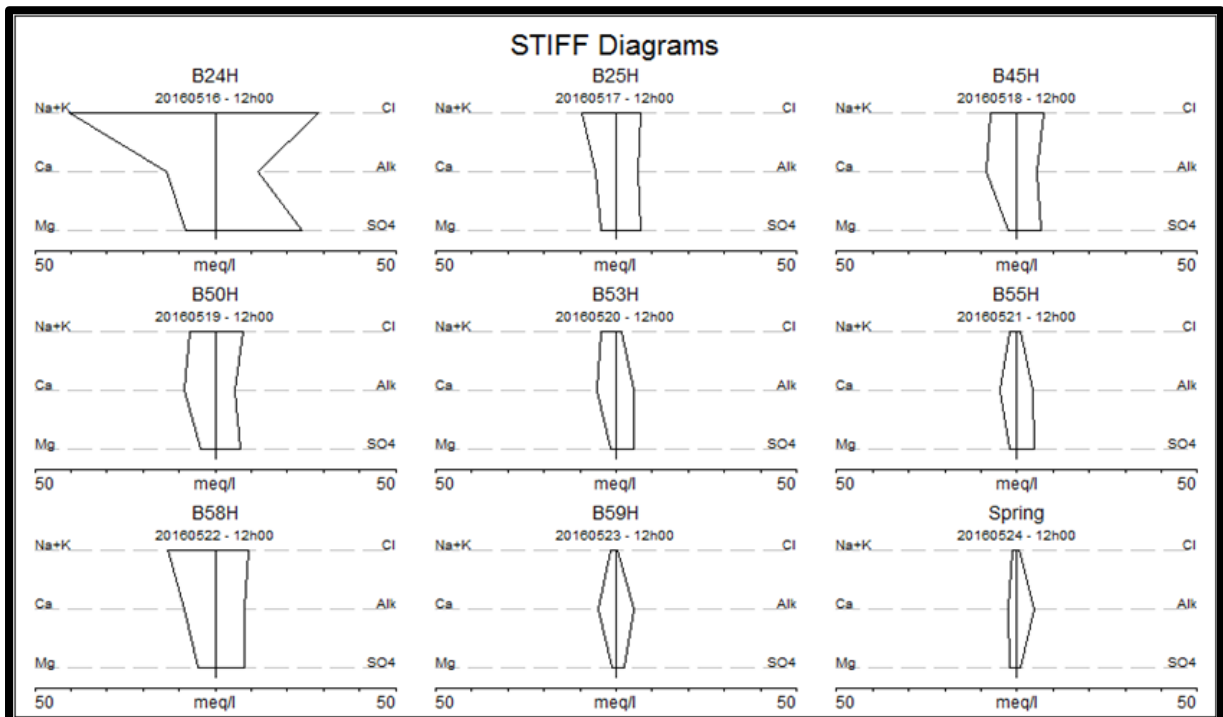
Spring season



Summer season



Autumn season



Appendix 2

Water-Rock Interaction Calculations

The following tables display ratios that were calculated prior to prediction of the possible hydrogeochemical processes that were involved in evolving the groundwater quality. These ratios were therefore used to infer the dominant processes for both stoichiometric analysis and bivariate correlation plots. The following ratios were used for calculations:

$$\frac{\text{HCO}_3^-}{\text{SiO}_2} \quad (4.1)$$

$$\frac{\text{Na}^+ + \text{K}^+ - \text{Cl}^-}{\text{Na}^+ + \text{K}^+ - \text{Cl}^- + \text{Ca}^{2+}} \quad (4.2)$$

$$\frac{\text{Ca}^{2+}}{\text{Ca}^{2+} + \text{SO}_4^{2-}} \quad (4.3)$$

$$\frac{\text{Na}^+}{\text{Na}^+ + \text{Cl}^-} \quad (4.4)$$

$$\frac{\text{Na}^+}{\text{Cl}^-} \quad (5.10)$$

$$\frac{\text{Ca}^{2+}}{\text{Mg}^{2+}} \quad (5.11)$$

$$\frac{\text{Ca}^{2+} + \text{Mg}^{2+}}{\text{HCO}_3^-} \quad (5.12)$$

The results are displayed for all the three seasons such that concentrations in meq/l were substituted in the ratios.

Spring season

Site name	Na/Cl	Ca/Mg	Ca+Mg/HCO ₃	HCO ₃ /SiO ₂	Ca/Ca+SO ₄	Na/Na+Cl	Na+K-Cl/Na+K-Cl+Ca
Units	meq/l						
B10H	2.07	2.49	1.17	9.36	0.80	0.67	0.13
B11H	-	-	-	-	-	-	-
B22H	1.22	1.99	1.62	11.60	0.53	0.55	0.15
B24H	1.15	1.32	2.13	32.95	0.37	0.54	3.68
B25H	1.11	1.50	2.58	9.43	0.46	0.53	0.12
B36H	0.99	1.78	1.64	11.62	0.57	0.50	0.01
B44H	1.32	4.15	2.78	10.43	0.49	0.57	0.16
B45H	1.19	9.78	2.34	13.03	0.58	0.54	0.11
B50H	0.89	2.58	3.56	10.51	0.54	0.47	-0.08
B53H	2.25	3.33	1.18	12.08	0.69	0.69	0.24
B54H	-	-	-	-	-	-	-
B55H	2.24	2.25	1.38	9.23	0.64	0.69	0.18
B56H	0.78	2.67	2.44	11.72	0.61	0.44	-0.21
B57H	0.82	2.74	2.51	12.26	0.59	0.45	-0.16
B58H	1.25	1.96	1.93	16.60	0.52	0.56	0.21
B59H	3.65	5.78	1.45	9.12	0.71	0.78	0.17
B60H	1.59	2.04	1.28	13.65	0.61	0.61	0.25
B61H	3.44	1.96	1.10	12.59	0.69	0.77	0.30
B62H	0.81	1.61	1.97	10.38	0.64	0.45	-0.36
Spring	2.95	1.33	1.05	8.19	0.71	0.75	0.24

Summer season

Site name	Na/Cl	Ca/Mg	Ca+Mg/HCO ₃	HCO ₃ /SiO ₂	Ca/Ca+SO ₄	Na/Na+Cl	Na+K-Cl/Na+K-Cl+Ca
Units	meq/l						
B10H	2.97	2.84	9.61	10.57	0.84	0.75	0.18
B11H	3.90	6.00	10.18	12.36	0.83	0.80	0.24
B22H	2.78	6.85	9.95	13.79	0.29	0.74	0.70
B24H	1.44	2.43	3.10	20.55	0.36	0.58	0.39
B25H	1.31	1.34	15.51	13.15	0.47	0.57	0.28
B36H	1.04	1.70	13.67	11.15	0.59	0.51	0.05
B44H	1.31	3.38	14.31	8.78	0.47	0.57	0.17
B45H	1.46	3.49	13.79	13.15	0.58	0.59	0.25
B50H	0.83	2.24	16.41	10.96	0.55	0.45	-0.17
B53H	2.82	3.92	10.44	11.04	0.53	0.74	0.34
B54H	1.36	2.70	12.82	12.44	0.54	0.58	0.21
B55H	2.71	2.64	10.85	9.19	0.53	0.73	0.22

B56H	0.91	2.39	14.39	11.69	0.63	0.48	-0.06
B57H	0.94	2.40	17.70	12.64	0.60	0.48	-0.04
B58H	1.40	1.74	21.42	17.72	0.51	0.58	0.31
B59H	3.47	5.02	8.97	8.46	0.67	0.78	0.20
B60H	1.85	2.03	13.29	14.03	0.64	0.65	0.31
B61H	372	1.90	12.39	13.41	0.70	0.79	0.33
B62H	0.95	1.51	14.29	11.38	0.66	0.49	-0.07
Spring	3.17	2.25	8.98	7.93	0.72	0.76	0.26

Autumn season

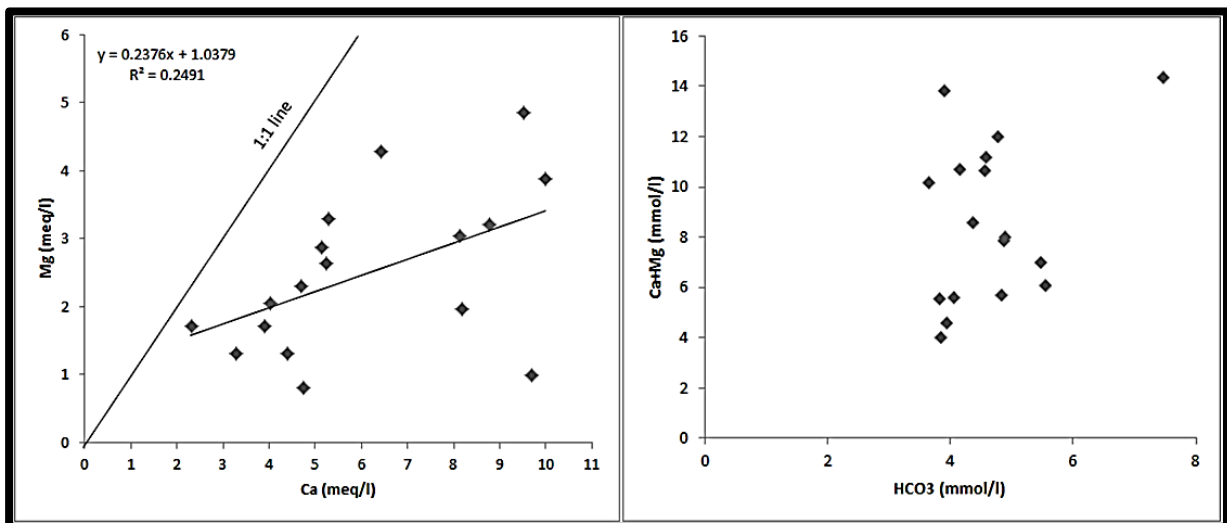
Site Name	Na/Cl	Ca/Mg	Ca+Mg/HCO ₃	HCO ₃ /SiO ₂	Ca/Ca+SO ₄	Na/Na+Cl	Na+K-Cl/Na+K - Cl+Ca
Units	meq/l						
B10H	-	-	-	-	-	-	-
B11H	-	-	-	-	-	-	-
B22H	-	-	-	-	-	-	-
B24H	1.40	1.65	2.17	23.38	0.36	0.58	0.47
B25H	1.34	1.33	0.98	11.24	0.46	0.57	0.30
B45H	1.02	3.45	1.24	10.52	0.56	0.50	0.03
B50H	0.92	2.18	1.37	10.20	0.54	0.48	-0.07
B53H	3.03	3.81	0.86	9.29	0.52	0.75	0.35
B55H	2.46	2.38	0.91	8.20	0.50	0.71	0.21
B58H	1.41	1.70	0.98	14.43	0.50	0.58	0.31
B59H	3.16	4.52	0.71	8.32	0.69	0.76	0.19
Spring	2.26	1.29	0.60	6.65	0.73	0.69	0.21

Appendix 3

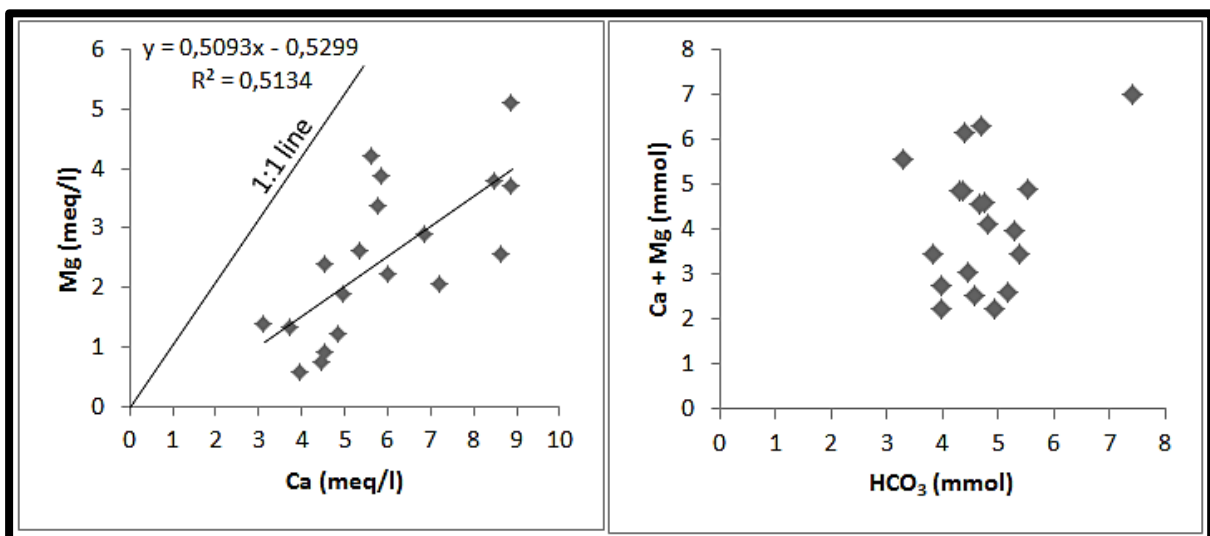
Bivariate Correlation Plots

The bivariate correlation plots displayed below show the correlation between Ca versus Mg and Ca + Mg versus HCO₃. These were also plotted for all the seasons to identify the variations.

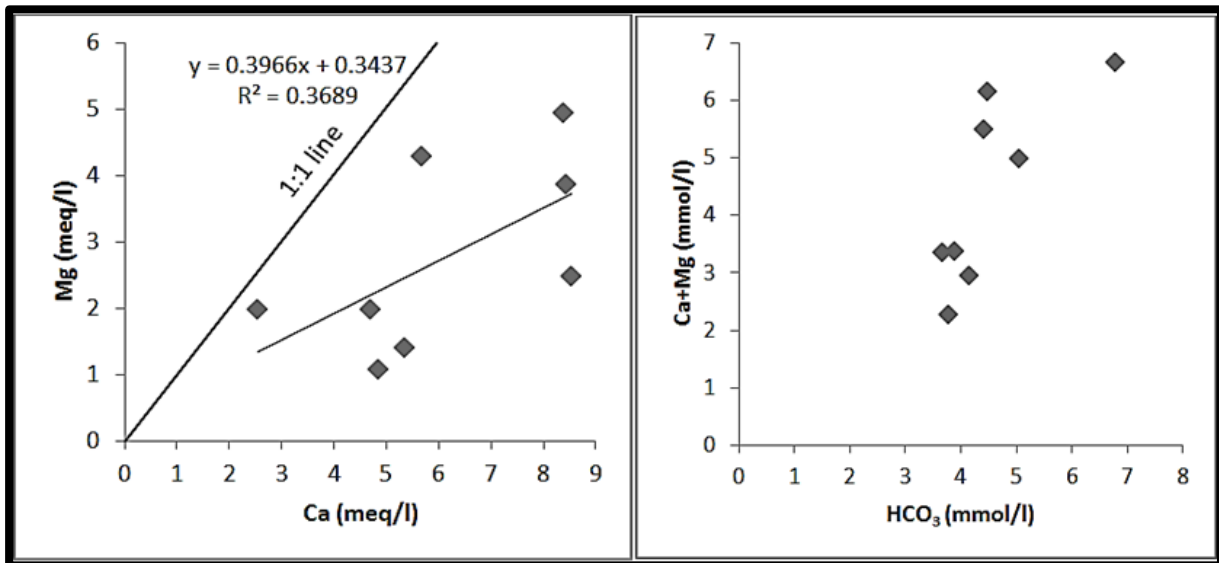
Spring season



Summer season



Autumn season



Appendix 4

Mineral Saturation Indices

The presented mineral saturation indices were generated for summer and autumn seasons as shown by the following tables.

Summer season

Phases	Albite	Anorthite	Ca-montmorillonite	Calcite	Chlorite	Dolomite	Fluorite	Gypsum	Halite	K-mica	Kaolinite	Quartz	Rhodochrosite	Sylvite
B10H	-3.76	-5.99	-0.62	-0.32	-11.75	-0.97	-1.64	-2.04	-7.99	3.09	1.44	0.28	-2.75	-8.7
B11H	-5.41	-9.48	-3.46	-0.88	-22.01	-2.41	-1.33	-1.88	-7.71	-1.17	-0.76	0.24	-2.11	-8.9
B22H	-4.35	-8.59	-2.53	-1.08	-22.17	-2.89	-1.49	-1.11	-5.85	0.7	0.25	0.07	-1.47	-7.58
B24H	-3.13	-6.17	-2.49	0.6	-6.75	0.92	-0.83	-0.4	-4.84	1.59	-0.04	0.02	0.35	-6.73
B25H	-3.65	-7.29	-1.53	-0.57	-14.11	-1.15	-1.33	-1.15	5.91	1.85	0.8	0.25	-2.47	-7.41
B36H	-2.53	-4.46	1.72	-0.59	-11.58	-1.28	-1.3	-1.27	-6.36	6.21	3.58	0.25	-3.25	-6.63
B44H	-4.75	-8.65	-2.85	-0.92	-19.31	-2.26	-1.06	-0.79	-6.14	0.25	0.14	0.13	-2.78	-7.42
B45H	-4.3	-7.66	-2.37	-0.46	-15.89	-1.35	-0.93	-1.08	-6.15	1.18	0.23	0.09	-3.08	-7.4
B50H	-4.87	-9.15	-3.38	-0.77	-18.61	-1.77	-1.05	-0.95	-5.96	-0.38	-0.69	0.21	-2.92	-7.06
B53H	-3.95	-7	-1.36	-0.6	-15.76	-1.67	-1.36	-1.25	-6.98	1.99	0.98	0.2	-3.43	-8.3
B54H	-4.03	-7.28	-1.65	-0.59	-15.64	-1.48	-1.43	-1.15	-6.31	1.67	0.79	0.16	-2.96	-7.76
B55H	-4.48	-7.75	-1.56	-0.96	-18.1	-2.23	-2.09	-1.23	-7.41	1.25	0.85	0.24	-2.52	-8.73
B56H	-4.58	-8.16	-2.69	-0.61	-16.41	-1.48	-1.02	-1.21	-6.16	0.89	-0.06	0.13	-3.44	-7.06
B57H	-3.75	-6.61	-1.01	-0.5	-14.41	-1.25	-2.21	-1.01	-5.94	3.11	1.38	0.12	-3.91	-6.91
B58H	-3.03	-6.25	-0.87	-0.1	-11.41	-0.32	-1.1	-0.91	-5.61	2.89	1.29	0.25	-0.39	-7.16
B59H	-3.7	-6.32	-0.27	-0.68	-15.85	-1.94	-2.03	-1.49	-7.81	2.75	1.76	0.35	-1.91	-9.11
B60H	-3.34	-5.73	0.3	-0.65	-14.2	-1.47	-2.35	-1.39	-6.52	4.26	2.52	0.13	-2.25	-7.86

B61H	-3.77	-6.46	-0.59	-0.58	-14.15	-1.32	-1.63	-1.61	-7.27	2.85	1.66	0.2	-3.21	-8.6
B62H	-2.95	-6.51	-0.66	-0.73	-14.05	-1.51	-1.48	-1.49	-5.32	3.05	1.68	0.14	-3.49	-7.42
Spring	-4.54	-8.4	-1.75	-1.14	-19.54	-2.51	-2.12	-1.86	-7.74	0.24	0.54	0.41	-3.47	-9.38

Autumn season

Phases	Albite	Anorthite	Ca-montmorillonite	Calcite	Chlorite	Dolomite	Fluorite	Gypsum	Halite	K-mica	Kaolinite	Quartz	Rhodochrosite	Sylvite
B10H	-	-	-	-	-	-	-	-	-	-	-	-	-	-
B11H	-	-	-	-	-	-	-	-	-	-	-	-	-	-
B22H	-	-	-	-	-	-	-	-	-	-	-	-	-	-
B24H	-2.37	-5.76	-3.06	1.37	0.2	2.64	-0.83	-0.53	-4.71	0.93	-0.99	0.24	0.76	-6.62
B25H	-4.48	-9.27	-3.2	-0.88	-18.16	-1.76	-1.21	-1.12	-5.9	-0.57	-0.64	0.32	-2.32	-7.39
B45H	-2.87	-5.37	-2.5	1	-1.48	1.57	-1.05	-0.95	-5.97	1.63	-0.48	0.24	-1.22	-7.2
B50H	-2.97	-5.67	-2.96	1.07	-0.05	1.93	-1.03	-0.96	-5.98	1.1	-0.94	0.28	-1.53	-7.1
B53H	-5.32	-9.96	-4.07	-0.98	-21.37	-2.43	-1.02	-1.17	-6.92	-1.76	-1.3	0.25	-4.17	-8.26
B55H	-3.25	-5.56	-0.62	-0.14	-8.77	-0.54	-2.03	-1.22	-7.43	2.83	1.33	0.38	-2.17	-8.72
B58H	-3.01	-6.62	-0.5	-0.48	-14.26	-1.06	-2.04	-0.94	-5.64	3.01	1.58	0.35	-0.75	-7.17
B59H	-3.2	-5.52	-2.65	1.01	-1.25	1.5	-1.99	-1.49	-7.75	0.56	-0.82	0.4	-0.78	-9.06
Spring	-3.01	-5.55	-1.73	0.46	-1.73	0.94	-2.56	-2.06	-7.84	1.32	-0.03	0.5	-0.94	-9.16

